Improved Interference Management Techniques for Multi-Cell Multi-User MIMO Systems

Chinazo Onyinye Unachukwu

Submitted in accordance with the requirements for the degree of Doctor of Philosophy

The University of Leeds

School of Electronic and Electrical Engineering

September 2014

Declaration

The candidate confirms that the work submitted is her own and that appropriate credit has been given where reference has been made to the work of others. The material contained in the chapters of this thesis has been previously published in research articles written entirely by the author of this thesis (Chinazo Onyinye Unachukwu) who also appears as the lead author in all published papers. The research has been supervised and guided by Dr. Li Zhang, Dr. Des McLernon and Prof. Mounir Ghogho, who appear as the co-authors in all published articles. All the materials included in this document is of the author's intellectual ownership.

The work in Chapter 2 of the thesis has appeared in publication as follows:

- Chinazo Unachukwu, Li Zhang, Des McLernon and Mounir Ghogho, 'Downlink CoMP Transmission with Multiple Cooperating Sets', 9th International Symposium on Wireless Communication Systems (ISWCS), 2012.

The work in Chapter 3 of the thesis has appeared in publication as follows:

- Chinazo Unachukwu, Li Zhang, Des McLernon and Mounir Ghogho, 'Cooperating Set Selection for Reduced Power Consumption and Data Overhead in Downlink CoMP', 10th International Symposium on Wireless Communication Systems (ISWCS), 2013.

The work in Chapter 4 of the thesis has appeared in publication as follows:

- Chinazo Unachukwu, Li Zhang, Des McLernon and Mounir Ghogho, 'Joint and Adaptive Cooperating Set Selection for max-min SINR in Downlink CoMP', to be submitted to IEEE Wireless Communication Letters, 2015.

This thesis is dedicated to my LORD and to the Unachukwus'

- Oliver, Bene, Ada, Uzo, Nkechi, Kenechi, Chioma,

Daniel & David.

“But you, be strong and do not lose courage, for there is reward for your work.” - 2 Chronicles 15:7

Acknowledgements

This thesis would have remained a dream had it not been for Dr. Li Zhang, who mentored me from the beginning of my master's program at the University of Leeds. Dr. Li was very instrumental in beginning my 4-year PhD journey at the University of Leeds. She has been very supportive and professional while guiding me through my research and thesis write up, for which I am mostly grateful.

I relay my immense gratitude to Dr. Des McLernon for his unwavering guidance and professional support from the beginning of my journey as a master's student at the University of Leeds. I also express my heartfelt gratitude to Professor Mounir Ghogho for his direction and encouragement during my PhD studies. Thanks to Dr. Des and Prof. Mounir, the social part of our research group has always been fun and my stay in Leeds has been very memorable.

Obtaining quality education, especially from an internationally recognised university, requires a lot of financial backing. So I would like to acknowledge and thank the Faculty of Engineering, University of Leeds for granting me a tuition waiver to pursue my PhD program. I also acknowledge and thank the Schlumberger Foundation Faculty for the Future, for granting me bursary to support my PhD program.

To my colleagues in Lab 352: Jinlin, Raul, Edmond, Yen and Nabil who made my time here very memorable especially with Yusuf who ensured the office was always vibrant. Also to my friends: Chinelo, Kokomma, Ikem, Deji, Akinola, Lara, Bridget, Dr. Jude and Omon and the members of Leeds Cathedral Afro Caribbean Choir, who have made my stay in Leeds very interesting and memorable. I thank you all.

Finally, I want to thank my dad and mum for their unwavering sacrifice and support towards my ambitions and goals in life. Also my gratitude goes to my lovely sisters and brothers who have been very patient, understanding and loving, even during long times of no communication. Most importantly, I am so grateful to God who has brought me thus far and blessed me with life and good health to successfully complete my PhD program.

Acronyms

ABS	Almost Blank Subframe
AMPS	Advanced Mobile Phone System
AP	Access Point
BER	Bit Error Rate
BS	Base Station
CA	Cooperating Area
CAT	Cooperating-Set Allocation Time
CB	Cordinated Beamforming
CCI	Co-channel Interference
CCU	Central Control Unit
CDMA	Code Division Multiple Access
CEPC	Cell Edge Pico Cell
CEPCU	Cell Edge Pico Cell User
CnS	Conventional Solution
CoMP	Coordinated Multi-Point Transmission
CS	Cooperating Set
CSI	Channel State Information
CSIR	Channel State Information at the Receiver
CSIT	Channel State Information at the Transmitter
CU	Central Unit
CQI	Channel Quality Information
DCS	Dynamic Cell Selection
D-ICIC	Dynamic Inter Cell Interference Coordination
DoF	Degree of Freedom
e-ICIC	enhanced Inter Cell Interference Coordination
eNB	eNodeB

EME	Electromagnetic Energy
FDD	Frequency Division Duplex
FDMA	Frequency Division Multiple Access
FFR	Fractional Frequency Reuse
4G	Fourth Generation
GSM	Global System Mobile
HetNet	Heterogeneous Network
HomoNet	Homogeneous Network
HSPC	Hotspot Pico Cell
HSPCU	Hotspot Pico Cell User
IA	Interferernce Alignment
IC	Interference Cancellation
IaCI	Intra Cell Interference
ICI	Inter Cell Interference
ICIC	Inter Cell Interference Coordination
ISD	Inter Site Distance
ITU	International Telecommunications Union
IUI	Inter User Interference
JP	Joint Processing
JT	Joint Transmission
LMMSE	Linear Minimum Mean Square Error
LOS	Line of Sight
LSMCS	Left Side Macro Cell Sector
LTMCS	Left Top Macro Cell Sector
LTE	Long Term Evolution
LTE-A	Long Term Evolution Advanced
MAC	Multi Access Channel
MC	Macro Cell
MCU	Macro Cell User

MIMO	Multiple Input Multiple Output
MME	Mobility Management Entity
nMCUs	number of Macro Cell Users
NMT	Nordic Mobile Telephone
nPCUs	number of Pico Cell Users
NP	Non-deterministic Polynomial-time
OCI	Other Cell Interference
OCR	Output to Cost Ratio
OFDMA	Orthogonal Frequency Division Multiple Access
OS	Optimum Solution
PAPC	Per Antenna Power Constraint
PBPC	Per Base-Station Power Constraint
PCU	Pico Cell User
PFR	Partial Frequency Reuse
PS	Proposed Solution
QoS	Quality of Service
Rx	Receiver
RB	Resource Block
RBA	Resource Block Allocation
RBAU	Resource Block Allocation Unit
RHS	Right Hand Side
RNC	Radio Network Controller
RRM	Radio Resource Management
RSMCS	Right Side Macro Cell Sector
RTMCS	Right Top Macro Cell Sector
Rel-8	Release 8
Rel-11	Release 11
SFR	Soft Frequency Reuse
SerFR	Softer Frequency Reuse

SINR	Signal to Interference plus Noise Ratio
SLINR	Signal to Leakage plus Interference and Noise Ratio
SLR	Signal to Leakage Ratio
SNR	Signal to Noise Ratio
SON	Self Organising Network
Tx	Transmitter
TACS	Total Access Communication Systems
TDD	Time Division Duplex
TDMA	Time Division Multiple Access
3G	Third Generation
3GPP	Third Generation Patnership Project
TPC	Total Power Constraint
UE	User Equipment
UMTS	Universal Mobile Telecommunications Systems
WCDMA	Wideband Code Division Multiple Access

Notations

M_t	number of transmit antennas
N_r	number of receive antennas
K	number of BS-user pairs
$\mathbf{H}$	wireless channel characteristics between a transmitter and receiver
$\mathbf{s}$	transmitted signal vector
$\mathbf{n}$	the additive white Gaussian noise vector
σ_n^2	the noise variance
T_c	Coherence time
W_c	Coherence bandwidth
D_c	Coherence distance
Δt	Time lag
Δf	Frequency lag
Δd	Distance lag
B	Bandwidth
C	Capacity
P_T	Total transmit power
$\mathbf{I}$	Identity matrix
$\mathbf{v}$	precoding vector
$\mathbf{V}$	precoding matrix
$\mathbf{u}$	receive beamforming vector
$\mathbf{U}$	receive beamforming matrix
ρ	power allocation to transmit signal data
y_k	received signal at user k
M_{max}	maximum number of allowed transmit BS per user
P_m	Power allocation to BS m
$\mathbb{E}[\mathbf{A}]$	Expectation of matrix $\mathbf{A}$
J	number of clusters

R_k	Rate of user *k*
R_T	Sum rate
$\|\|\mathbf{A}\|\|_2$	*l*-2 norm of matrix **A**
$\|\|\mathbf{A}\|\|_F$	Frobenius norm of matrix **A**
Δ	CS Selection matrix
D_o	Reference distance
p^{TOT}	total power constraint
p^{PBPC}	per base-station power constraint
p^{PAPC}	per antenna power constraint
γ_k	SINR at receiver *k*
O	Overhead factor

Abstract

One major limiting factor for wireless communication systems is the limited available bandwidth for cellular networks. Current technologies like Long Term Evolution (LTE) and LTE-Advanced (LTE-A) have standardised a frequency reuse factor of 1 to enable more channel resources in each cell. Also multi-layer networks that consist of overlapping macro cells and small cells like pico cells, micro cells and femto cells have also been used to improve the capacity of the cellular network system. These multi-layer networks are known as heterogeneous networks or HetNets while the single layer, traditional cellular systems are referred to as homogeneous networks or HomoNets.

Several interference management systems and techniques have been proposed in the past to deal with the effect of inter-cell interference (ICI) (i.e., the interference from a macro cell base station (BS) to a macro cell user in another macro cell) and inter-user interference (IUI) (i.e., the interference of another user's data signal to a given user within the same cell on the same time and frequency slot). Interference cancellation techniques such as beamforming, uses transmit pre-coders and receive beam-formers to limit the effect of interference. The interference alignment strategy ensures that the interference is aligned into a given subspace and leaves a residual subspace free for the desired signal. Coordinated scheduling/beamforming and coordinated multi-point transmission (CoMP) have also been used to limit the interference within the cellular network. For HetNets, interference avoidance techniques based on radio resource management (RRM) have been used to limit the effect of interference within the network and improve the attainable system capacity. This thesis investigates the challenges of two main interference management techniques and proposes methods to alleviate these issues without impeding the expected performance already attained. The main techniques considered for HomoNets and HetNets are: CoMP transmission under the interference cancellation technique and resource block allocation (RBA) under the interference avoidance technique. The setbacks for the well known CoMP transmission strategy are high data overhead, energy consumption and other associated costs to the network

provider. Further investigations were carried out and a joint selection of transmit antennas for the users was proposed with the main aim of preserving or exceeding the already achieved gains but obtaining a further reduction in the data overhead.

Fully distributed RBA solutions are required, especially since future networks tend to become self-organising networks (SON). Another major consideration in choosing the resource blocks (RBs) for the users in each cell is the RBA metric. Since the capacity of the cell is dependent on the sum-rate of the users, it is important to consider the maximisation of the sum-rate or sum-SINR (i.e the sum signal to interference and noise ratio) when assigning RBs to users. The RBA technique aims to choose the RBs such that the interference within the cell is avoided. To achieve this, a RBA metric is required to obtain the qualification matrix before allocating RBs to the users. Many authors in the past have proposed several metrics for RBA but avoided any RBA metric that required a direct estimation of the interference power on each RB for each user's allocation. This is because the SINR or interference power on each RB for any user can only be obtained with pre-knowledge of already occupied RBs in neighbouring cells. In this thesis, two distributed RBA solutions based on a direct interference estimation was proposed to obtain the required qualification matrix for the RBA under the HomoNet and HetNet system models. The gains and advantages obtained are shown and analysed using the obtained simulation results.

The issue of interference coupled with limited available channels remains a major limiting factor for HetNets. Therefore, it is very important to develop techniques that maximise the utilisation of available bandwidth for each cell while minimising possible interference from neighbouring cells. Finally, this thesis considers and investigates a possible joint solution using both interference avoidance and interference mitigation techniques. Hence two solutions are proposed: joint RBA plus beamforming and joint RBA plus CoMP transmission, to further mitigate the high interference in HetNets. The simulation results have shown significantly improved system performance especially for a highly dense HetNet.

Contents

List of figures

List of tables

Chapter 1

Introduction

1.1 Evolution of the Wireless Communication System

The mobile cellular system, as we know it today, has come a long way from the first generation (1G), analog system using frequency division multiple access (FDMA) (such as Advanced Mobile Phone System (AMPS), Total Access Communication System (TACS) and Nordic Mobile Telephone (NMT)) to digital systems using time division multiple access (TDMA), code division multiple access (CDMA) or orthogonal frequency division multiple access (OFDMA) (such as Global System for Mobile Communication (GSM) - a 2G system, Universal Mobile Telecommunications System (UMTS) - a 3G system, Long-Term Evolution (LTE) - a 3.9G system and LTE-Advanced (LTE-A) - a 4G system [2]). Some of the capabilities of the various types of systems are summarised in Table 1.1. The third generation (3G) system is based on the packet switched network and was developed by the International Telecommunications Union (ITU) under IMT-2000 and UMTS. UMTS uses Wideband Code Division Multiple Access (W-CDMA) to establish 3G wireless networks with high spectral efficiency for both voice and data users.

Release 8 (Rel-8) [6] defined the LTE standards for wireless communication and provided data rates of 300 Mbps and 75Mbps in the downlink and uplink respectively. The LTE system which evolved from the UMTS network, was standardised to provide better data

rates compared to the previous standards. LTE uses multiple bandwidths with both frequency division duplex (FDD) and time division duplex (TDD).

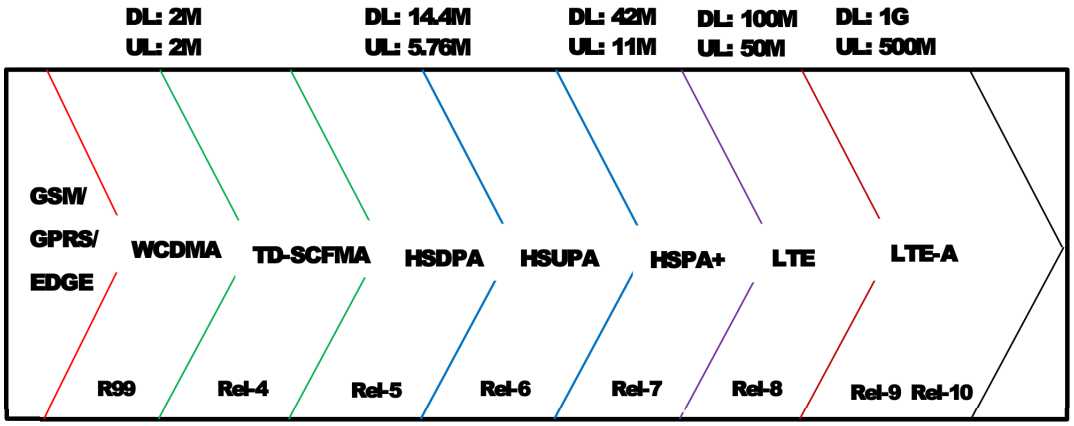

Figure 1.1: Mobile network evolution [1].

LTE-A has been shown to improve the cell-edge performance and spectral efficiency per unit area, provide better bandwidth scalability and decrease latency [1]. Some network features considered under LTE-A include: improved power efficiency to ensure a greener cellular network, reduced cost of infrastructure, intelligent resource allocation, further interference avoidance and mitigation, self-organising capabilities in cellular networks, and aggregation of several frequency bands. To achieve these targets, some well-known technologies have been proposed such as multiple-input and multiple-output (MIMO) systems, coordinated multipoint transmission (CoMP) and heterogeneous networks (HetNets). These techniques will be further investigated in this thesis.

System	Channel Spacing	Access	Comments
AMPS (1G)	30 KHz	FDMA	Advanced Mobile Phone System, first developed in the US.
NAMPS (1G)	10 kHz	FDMA	Narrowband AMPS, having 10 kHz carrier spacing and used in US and Israel.
TACS (1G)	25 kHz	FDMA	Based on 900 MHz, used worldwide, Extended-TACS was to improve the channel by adding more channels to reduce congestion.
NMT (1G)	25 kHz	FDMA	Based on the 450 MHz and then 900 MHz frequency band. First system to be widely used commercially.
NTT (1G)	25 kHz	FDMA	Nippon Telegraph and Telephone. Used in Japan, operating at 900 MHz.
C450 (1G)	20 kHz	FDMA	Operating on 450 MHz, used in Germany.
GSM (2G)	200 kHz	TDMA	Developed in Europe, originally called Groupe Speciale Mobile then Global Systems for Mobile communication. Operates on 900 MHz and some 850 MHz exists in USA.
DCS 1800 (2G)	200 kHz	TDMA	Digital Cellular Service also known as GSM 1800, operates on 1800 MHz.
PCS 1900 (2G)	200 kHz	TDMA	Personal Communication Service also known as GSM 1900, operates on 1800 MHz.
US-TDMA (2G)	30 kHz	TDMA	United States TDMA was designed to operate alongside the AMPS. Also known by its standard IS-54 and then updated to IS-136.

PDC (2G)	30 kHz	TDMA	Pacific Digital Cellular similar to North America TDMA. Only used in Japan.
GPRS (2.5G)	200 kHz	TDMA	General Packet Radio Service. It is a packet switched network and provides data up to 114 kbps.
EDGE (2.5/ 3G)	200 kHz	TDMA	Enhanced Data rates for GSM Evolution. Based on packet switching and 8 PSK.
CDMA One (2G)	1.25 MHz	CDMA	Also known as IS-95, this system had a widespread use with data rates up to 115 kbps.
CDMA 2000 1X (2.5G)	1.25 MHz	CDMA	Supports high-speed data services. Peak data rates of 153 kbps are currently obtainable and up to 614 kbps are expected with two channels.
CDMA 2000 1xEV-DO (3G)	1.25 MHz	CDMA	EV-DO stands for Evolution Data Optimised. Designed for only data use to provide data rates up to 2.45 Mbps on the downlink. Aimed to reduce cost per megabyte capability. Also allows charges based on actual download rather than connection time.
CDMA 2000 1xEV-DV (3G)	1.25 MHz	CDMA	EV-DV means Evolution Data and Voice. Able to simultaneously transmit data and voice and achieves up to 3.1 Mbps on the downlink.
UMTS (3G)	5 MHz	CDMA/ TDMA	Uses W-CDMA with one 5 MHz on the downlink for both data and voice. Achieves up to 2 Mbps.

TD-SCDMA (3G)	1.6 MHz	CDMA	Time Division Synchronous CDMA. Developed in China and uses TDD systems. Uses the same band to transmit and receive. Allows different time slots to be allocated for base stations and mobiles to communicate.
LTE (3.9G)	1.4 MHz-20 MHz	OFDMA	High speed downlink data transmission up to 100 Mbps. LTE supports both FDD and TDD systems.The packet-switched approach in LTE allows support for all services including voice through packet only connections.
LTE-A (4G)	40 MHz-100 MHz	OFDMA	High speed downlink data transmission up to 1 Gbps. LTE-A supports both FDD and TDD systems. LTE-A significantly enhances the existing LTE and supports much higher peak rates, higher throughput and coverage, and lower latencies, resulting in a better user experience.

Table 1.1: Main capabilities of the evolved cellular network system [2].

1.2 MIMO Systems

A MIMO system refers to a communication system which transmits and receives information using multiple antennas at both ends of the communication system. MIMO systems can be used for beamforming, spatial multiplexing and diversity combining. The signal from a transmitter to a receiver travels through a wireless channel which undergoes multipath fading. The wireless channel can be modelled as a Rician fading channel if there exists a dominant line-of-sight (LOS) component from the transmitter to the receiver, hence the mean of the random process will no longer be zero [7]. A Rayleigh fading

channel occurs if no LOS component exists, hence the mean of the random process will be zero[7]. Assuming the number of antennas at the transmitter is M_t and the number of antennas at the receiver is N_r, then the input/output relationship, assuming a flat-fading channel, is given as:

$$\mathbf{y} = \mathbf{Hs} + \mathbf{n}, \tag{1.2.1}$$

where $\mathbf{H}$ is the $N_r \times M_t$ matrix whose elements are complex Gaussian random variables, with zero-mean Gaussian real and imaginary parts, $\mathbf{s}$ is the transmitted signal vector with dimension $M_t \times 1$, $\mathbf{n}$ is the additive white Gaussian noise, whose elements are complex random variables with zero mean and variance σ_n^2 and $\mathbf{y}$ is the received signal vector with dimensions $N_r \times 1$.

MIMO technology achieves an increase in the capacity and performance of the wireless communication system, thus enhancing reliability. The capacity of a MIMO network increases as the number of antennas increases, when compared to a single antenna system. MIMO systems can be used to offer increased diversity and/or multiplexing gains. Through spatial multiplexing, different multiple signals can be transmitted on multiple antennas simultaneously, leading to an increase in capacity.

1.2.1 Channel State Information (CSI)

In wireless systems there are two types of channel state information:

- Channel State Information at the Receiver (CSIR)
- Channel State Information at the Transmitter (CSIT).

CSIR can be obtained at the receiver by using a training sequence or pilot bits known at both the transmitter and receiver. The pilot bits are sent from the transmitter to the receiver, and from the received information the receiver calculates the CSI [8]. CSIT can be obtained at the transmitter using the feedback and reciprocity principle. The time

varying channel makes it difficult and often costly to obtain CSIT. Mobile users with a small coherence time suffer much degradation of CSIT due to scheduling lag, limited feedback resources and feedback delays in a closed-loop method; antenna calibration errors and turn-around time lags in an open-loop method. In MIMO systems, knowledge of the CSIT can be used in adapting the modulation rate, power control and beamforming to provide significant performance gain to the system.

Feedback Method

As shown in Fig. 1.2, CSI is estimated at the receiver using the pilot bits and then sent back to the transmitter using a feedback channel. This is also called a closed-loop system and is found mostly in FDD channels.

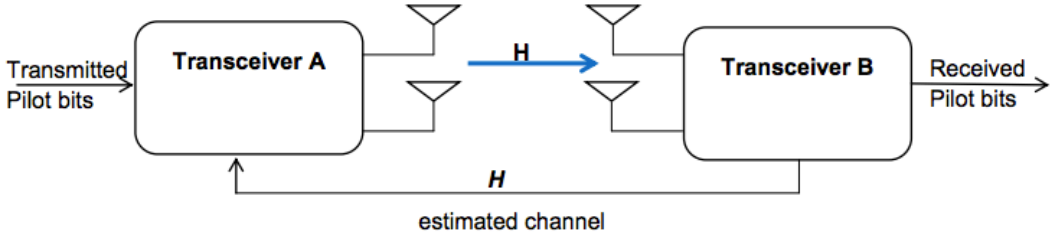

Figure 1.2: CSIT in a closed-loop system.

Due to the time lag (Δt) between acquiring the CSI at the receiver and transmitting it back to the transmitter, the CSIT is not perfect. Although estimation and correction factors can be used, it is desired that the coherence time $T_c >> \Delta t$. For mobile links, feedback methods are effective up to a certain mobile speed depending on the carrier frequency, transmission frame length and feedback turn-around time. High feedback overhead results from a fast changing channel. The feedback overhead can be reduced by sending a partial channel information such as the channel quality indicator (CQI) [9, 10].

Reciprocity Theorem

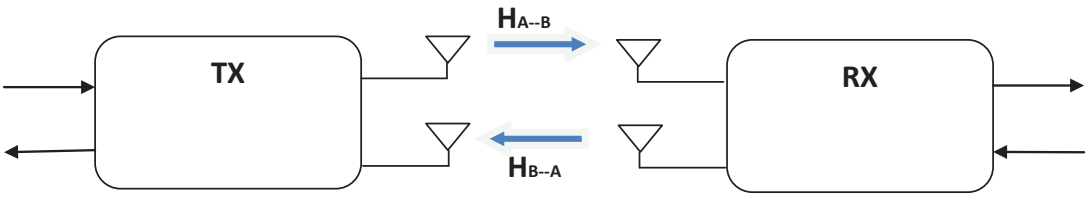

Figure 1.3: CSIT in an open-loop system.

The reciprocity principle states that the channel $\mathbf{H}_{A-B}$ is identical to the transpose of channel $\mathbf{H}_{B-A}$. Reciprocity approximately holds if between the transmitter and the receiver [8]:

- The time lag is less than the coherence time (i.e. $\Delta t << T_c$).
- The frequency lag is less than the coherence bandwidth (i.e. $\Delta f << W_c$).
- The distance lag is less than the coherence distance (i.e. $\Delta d << D_c$).

1.2.2 Capacity of MIMO Systems

Consider a MIMO system with M_t transmit antennas, N_r receive antennas and a flat fading channel (**H**) with CSI at the receiver, the capacity can be written as:

$$\mathrm{C} = B \log_2 \left| \mathrm{I}_{N_r} + \frac{1}{\sigma_n^2} \mathbf{HPH}^H \right| \; bps, \tag{1.2.2}$$

where the total transmit power P_T = tr(**P**), $\mathbf{P} = \frac{P_T}{M_t}\mathbf{I}_{M_t}$ is the covariance matrix of **s**, $\mathbf{I}_j$ is a $j \times j$ identity matrix, σ_n^2 is the noise variance and $|\mathbf{A}|$ is the determinant of **A**. The capacity of the MIMO system can then be re-written as:

$$\mathrm{C} = B \sum_{i=1}^{r} \log_2 \left(1 + \left(\frac{P_i}{\sigma_n^2} \right) \lambda_i \right) \; bps, \tag{1.2.3}$$

where B is the channel bandwidth, r is the rank of **H**, λ_i are the eigenvalues of $\mathbf{HH}^H$ and P_i is the power equally allocated to the i-th eigenmode, $P_i = P_T/M_t$ [2].

1.3 Multi-Cell MIMO Systems

Multi-cell MIMO systems are groups of multiple base stations (BSs) in a cellular system, each serving a group of users. The cellular system has many cells and the frequency channel on each cell can be reused at other cells, separated by sufficient distance to avoid inter-cell interference (ICI). But due to the properties of wireless communication systems, there are bound to be some inter-cell interference as transmissions from the BSs are not limited to the cell. CoMP transmission is an interference mitigation technique that improves the system performance by transforming the interference channel into a desired channel. This is achieved by coordinating multiple transmit BSs from different multi-cells to transmit the same data signal to a given user. The user then receives useful signal from neighbouring BSs thereby improving the user's performance. Currently, there exists two main types of multi-cellular networks: Homogeneous Networks (HomoNets) and heterogeneous networks. HomoNets are traditional cellular networks with each cell having the same capabilities while HetNets are multi-layer cellular networks with different cell types and capabilities. The HomoNets are transformed into HetNets by overlaying the traditional cellular network with smaller cells to improve the system performance in terms of coverage and capacity[1]. Both cell structures are prone to high interference if the frequency re-use is 1, especially HetNets.

1.4 Research Objectives

This thesis is aimed at investigating current interference management techniques and proposing new algorithms and techniques to solve existing issues. Two major forms of interference management techniques are considered in this thesis.

1. Interference mitigation technique: The CoMP transmission in the multi-cell multi-user MIMO systems is analysed for the homogeneous network which consists of macro cells using the same antenna type and having the same capabilities. The

macro cells cover long distances and transmit data signals with very high power. However, at the cell-edge, users suffer high interference from neighbouring macro cell BSs and also low signal power from the paired transmit BS. This causes low signal-to-interference and noise ratio (SINR) and poor system performance. So CoMP transmission was proposed to allow the neighbouring BSs to cooperate and transmit data to a given user to improve its received signal power. The user's data signals are made available to the cooperating BSs at each macro cell, thereby resulting in very high data signalling overhead in the backhaul link. This thesis addresses and proposes solutions to the following challenges:

(a) The high data overhead in the backhaul link, which results in high latency, poor synchronisation, backhaul bottleneck and high cost for the network provider [11].

(b) Minimising the power consumption in the network, which would result in a greener cellular network [12].

(c) Obtaining the best number of allowed transmit BSs per user for CoMP transmission in a given communication system [13].

2. Interference avoidance technique: the radio resource management (RRM) technique is analysed under homogeneous and heterogeneous networks. Several resource block allocation (RBA) techniques under the homogeneous networks have been proposed to avoid interference and improve the system performance. However, several challenges still exist such as selecting the RBA metric and the RBA mode (i.e. the mode of allocating the resource blocks (RBs) in the network). The HetNet was proposed in order to expand netowrk coverage and increase capacity. The interference in a heterogeneous network is a major setback and better forms of RBA are required to manage the interference. Under heterogeneous networks, very few solutions have been shown to effectively manage interference and more research is currently being carried out. This thesis will address the following challenges:

(a) Obtaining a distributed RBA strategy such that each macro cell sector is responsible for allocating RBs as opposed to a centralised or semi-centralised approach which is unsuitable for current generation systems including 4G and beyond.

(b) Obtaining a distributed RBA strategy for HetNets such that each macro cell sector and each small cell sector are responsible for allocating RBs to their users.

(c) Choosing an effective RBA metric that allows the interference within the HomoNets and HetNets to be evaluated and used to implement a solution leading to a better system performance.

(d) High interference remains a major setback especially for HetNets. For this reason, this thesis investigates two joint interference management techniques that will improve the performance obtained with only the proposed interference avoidance (i.e. the RBA) technique.

1.5 Thesis Organisation

The rest of this thesis is organised as follows:

In Chapter 2, the interference mitigation techniques based on interference cancellation using beamformers for multi-cell multi-user systems are presented. These techniques paved way for the introduction of CoMP transmission in multi-cell multi-user networks. A trade-off of system performance for a reduced data overhead reduction is investigated in Chapter 2 and simulation results are used to analyse the obtained system performance. Chapters 3 and 4 continue the study of the challenges faced in CoMP transmission. Both chapters focus on obtaining a further reduction in the data overhead, power consumption and improved performance under different optimisation strategies. A joint and adaptive cooperating set (CS) selection algorithm is proposed to achieve the CSs for all users,

where the minimum number of BS transmission can range from 1 to a pre-set maximum value.

The interference avoidance strategy based on the RBA selection for homogeneous and heterogeneous networks will be studied in Chapter 5. Two novel, distributed RBA strategies are proposed for the homogeneous and heterogeneous cellular networks.

Chapter 6 continues to study the interference in heterogeneous networks and a joint interference avoidance and mitigation strategy is proposed to further combat the high interference in HetNets and obtain an increased system performance. Simulation results show performance gains using the proposed interference avoidance strategy with different interference mitigation strategies.

Finally, conclusions are drawn in Chapter 7, and future work for consideration is presented.

1.6 List of Publications

Published Papers

- Chinazo Unachukwu, Li Zhang, Des McLernon and Mounir Ghogho, 'Downlink CoMP Transmission with Multiple Cooperating Sets', 9th International Symposium on Wireless Communication Systems (ISWCS), 2012.
- Chinazo Unachukwu, Li Zhang, Des McLernon and Mounir Ghogho, 'Cooperating Set Selection for Reduced Power Consumption and Data Overhead in Downlink CoM', 10th International Symposium on Wireless Communication Systems (ISWCS), 2013.

Chapter 2

Coordinated Multi-Point Transmission

The major focus in this chapter is on LTE downlink CoMP transmission for cell-edge users in multi-cell networks. LTE downlink CoMP transmission is a technique used to transmit data signals from multiple BSs to a given user, such that the cell-edge user's performance is optimised and improved. At the cell-edge, users experience low signal strength and high interference from neighbouring cells. By transforming the ICI into desired signals, LTE CoMP transmission can improve the cell-edge user's performance. LTE downlink CoMP requires cooperation and coordination between BSs to achieve almost perfect synchronised transmission from all transmitting BSs to the desired users.

CoMP transmission requires the exchange of user's data over the backhaul network. This means a linear increase in backhaul demand as the number of transmit BSs per user increases. This problem is a huge drawback for LTE CoMP transmission and a major challenge for the network operators. Issues such as high latency, poor synchronisation, backhaul congestion and high data overhead are currently being investigated by researchers [11].

The contributions of this chapter are as follows: Firstly, to reduce the data overhead required for CoMP transmission in the backhaul link. Secondly, two solutions based on the network-centric and user-centric approach are proposed using a reduced number of transmit BSs. Thirdly, simulation results are used to analyse the system performance

and trade-off of performance to data overhead when using a lower number or size of clusters/CoMP sets for data transmission.

The remaining parts of this chapter are organised as follows: Section 2.1 presents the interference mitigation techniques. The introduction of CoMP transmission into the wireless communication system is presented in Section 2.2. Sections 2.3 and 2.4 present the proposed data overhead reduction under the network-centric and user-centric approach. The system performance is evaluated when a limited number of transmit BSs per user is utilised for CoMP transmission and the effect on the performance is analysed. This chapter concludes in Section 2.5.

2.1 Overview of Interference Mitigation Techniques

The major setback in LTE and beyond is ICI, especially for the cell-edge user, as neighbouring BSs cause huge interference and reduction in the system performance. CoMP transmission has been standardised in the Third Generation Partnership Project (3GPP) LTE Release 11 (Rel-11) [14], as a key technology in improving the system throughput. Some strategies used in CoMP transmission include: joint processing (CoMP JP) and coordinated scheduling or beamforming. Users experiencing interference from other cells are assigned the same RBs in time and frequency and a set of BSs that coordinate to mitigate ICI is defined as a cooperating set or CoMP set. Joint processing is further grouped into dynamic cell selection and joint transmission (JT). Fig. 2.1(a) shows the operating principle of downlink joint transmission, where multiple coordinating BSs are scheduled to transmit data to the same user simultaneously [15]. Fig. 2.1(b) shows the operating principle behind dynamic cell selection (DCS), the cell with the minimum path loss among the coordinating cells is scheduled for transmission to the user, while muting transmission to the neighbouring users. The selection of the transmit BS is done through fast scheduling at the centralised BS and fast switching. This allows the user to achieve its maximum receive power and also prevents any interference from the neighbouring cells.

Fig. 2.1(c) shows the transmit principle behind coordinated beamforming. Coordinated beamforming allows the BSs to transmit data to the paired users at the same time, while using precoding techniques to minimise interference to other users in neighbouring cells. This thesis will focus on CoMP JT which requires both the sharing of data, CSIT and precoding information. Under CoMP JT, the users' data can be stored at all transmission points, where the slave cells receive the scheduling information via the X2 interface from the master cell. The X2 is a logical interface between neighbouring BSs (eNodeBs) that enables the transfer or sharing of information [16, 17].

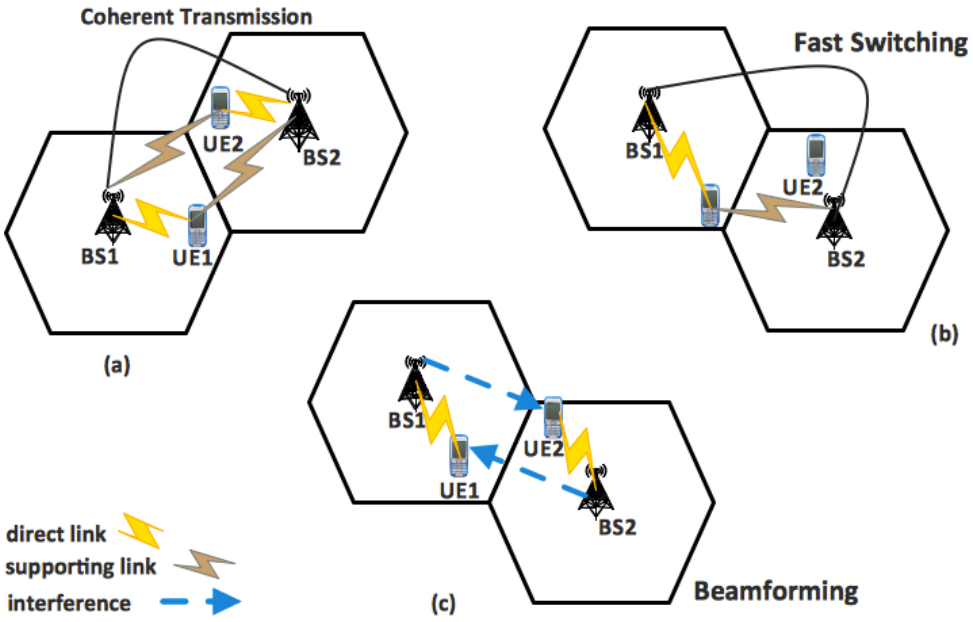

Figure 2.1: CoMP transmission in downlink: (a) CoMP joint transmission, (b) dynamic cell selection and (c) coordinated beamforming.

.

Alternatively, the master cell centrally performs the precoding design, and then forwards the data, scheduling and precoding information to the slave cells. While for coordinated

scheduling, the BSs take turns at different time slots to transmit data to their paired users. Coordinated scheduling does not require CSIT but only the channel information of the direct link, while coordinated beamforming requires the CSIT for the pre-coder design.

CoMP JT has been shown to outperform other described techniques in terms of user performance, but requires both CSIT and data sharing over the backhaul network, which causes severe bottlenecks in a backhaul capacity-limited network [15, 18, 19]. This setback reduces the potential for utilising CoMP transmission effectively and limits the significant advantage of CoMP transmission.

2.1.1 Interference Mitigation for Multi-Cell Multi-User MIMO System

One of the most critical issues of the multi-cell multi-user MIMO system is the large amount of interference. In [20], a suboptimal precoding scheme was proposed to mitigate interference for a multi-cell, multi-user MIMO system where the time and frequency resources are shared between the users. In [21], a leakage based precoding scheme was proposed for the multi-user MIMO downlink systems to mitigate other cell interference (OCI) within the system. These strategies are used to cancel or mitigate the received interference by the users from neighbouring BSs. Consider the multi-cell multi-user MIMO system as shown in Fig. 2.2. Each user suffers inter-user interference (IUI) (interference from transmitting multiple user's data) and OCI (interference from other neighbouring cells due to the broadcast nature of the wireless channel).

Interference mitigation can also be achieved using cooperation between the BSs. Multi-cell cooperation between all the BSs in the cellular system was found to combat ICI and improve the system performance especially at the cell-edge. Transmit and receive beamforming techniques are used to improve the multi-cell network sum-rate with cooperation between the BSs [22]. The use of an iterative algorithm to construct the transmit pre-coders and receive beam-formers was shown to achieve improved sum-

capacity in an interference channel [22].

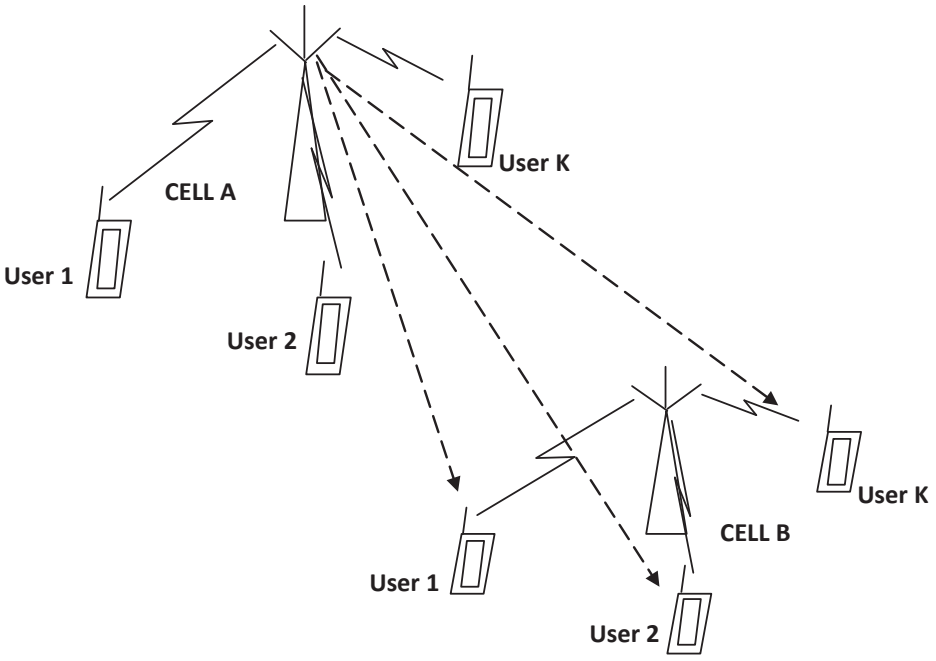

Figure 2.2: A multi-cell multi-user system.

2.1.2 Beamformer Design Approach

This section presents the well-known interference mitigation technique using both the transmit and receive beam-formers in the multi-cell multi-user MIMO system. Assuming M macro cells and K users in each macro cell, the received signal at the k-th user within the m-th macro cell is given by:

$$\mathbf{y}_{k,m} = \underbrace{\mathbf{H}_{k,m}^{(m)}\mathbf{v}_{m,k}\sqrt{\rho_{m,k}}\boldsymbol{s}_{m,k}}_{\text{desired signal}} + \underbrace{\sum_{\substack{p=1\\p\neq k}}^{K}\mathbf{H}_{k,m}^{(m)}\mathbf{v}_{m,p}\sqrt{\rho_{m,p}}\boldsymbol{s}_{m,p}}_{\text{IUI}} + \underbrace{\sum_{\substack{n=1\\n\neq m}}^{M}\sum_{p=1}^{K}\mathbf{H}_{k,m}^{(n)}\mathbf{v}_{n,p}\sqrt{\rho_{n,p}}\boldsymbol{s}_{n,p}}_{\text{OCI}}$$
$$+ \mathbf{n}_{k,m}, \forall m \in [1,2,\cdots,M],\ \forall k \in [1,2,\cdots,K], \qquad (2.1.1)$$

where $s_{m,k}$ is the data signal from the *m*-th BS to the *k*-th user and $\mathrm{E}\{|s_{m,k}|^2\} = 1$. The channel matrix between the *k*-th user in the *m*-th cell and the *n*-th BS is denoted by $\mathbf{H}_{k,m}^{(n)}$. $\mathbf{v}_{m,k}$ with dimension $M_t \times 1$, is the vector used to precode the *k*-th user data signal at the *m*-th BS, $\rho_{m,k}$ the power allocated to transmit the *k*-th user data signal at the *m*-th BS and $\mathbf{n}_k$ is additive, zero-mean, white, complex Gaussian noise vector with variance σ_k^2 for each element. At the receiver, the received signal ($\mathbf{y}_{k,m}$) is post-processed ($\mathbf{u}_{m,k}$) as shown below [23]:

$$\mathbf{u}_{m,k}^H \mathbf{y}_{k,m} = \mathbf{u}_{m,k}^H \mathbf{H}_{k,m}^{(m)} \mathbf{v}_{m,k} \sqrt{\rho_{m,k}} s_{m,k} + \sum_{\substack{p=1 \\ p \neq k}}^{K} \mathbf{u}_{m,k}^H \mathbf{H}_{k,m}^{(m)} \mathbf{v}_{m,p} \sqrt{\rho_{m,p}} s_{m,p}$$
$$+ \sum_{\substack{n=1 \\ n \neq m}}^{M} \sum_{p=1}^{K} \mathbf{u}_{m,k}^H \mathbf{H}_{k,m}^{(n)} \mathbf{v}_{n,p} \sqrt{\rho_{n,p}} s_{n,p} + \mathbf{u}_{m,k}^H \mathbf{n}_{k,m}, \forall m \in [1, 2, \cdots, M],\ \forall k \in [1, 2, \cdots, K], \tag{2.1.2}$$

where $\mathbf{u}_{m,k}$ is the $N_r \times 1$ receive beamforming vector used to cancel the received interference at the the *k*-th user in the *m*-th macro cell.

Beam-former Design based on SLNR maximisation

The signal to leakage plus noise ratio (SLNR) maximisation technique aims to maximise the SLNR at each BS by minimising the leakage caused by that BS to other users in the system. This technique is iterative and uses both transmit and receive beam-formers on the BSs and user equipment (UEs) respectively. Assuming the transmit beamforming vectors $\left\{ \{\mathbf{v}_{m,k}\}_{k=1}^{K},\ m = 1, \cdots, M \right\}$ with dimensions $M_t \times 1$ are randomly selected for each user *k* in the *m*-th macro cell. The receive beamforming vector $\mathbf{u}_{m,k}$ is selected such that it zero-forces the received IUI and OCI from all the BSs as shown in (2.1.3). So what we seek to achieve at the *k*-th user is:

$$\sum_{n=1}^{M} \sum_{\substack{p=1 \\ p \neq k, \text{if } n=m}}^{K} |\mathbf{u}_{m,k}^H \mathbf{H}_{k,m}^{(n)} \mathbf{v}_{n,p}|^2 = 0,\ \forall m \in [1, 2, \cdots, M], \forall\, k \in [1, 2, \cdots, K]. \tag{2.1.3}$$

This is done by choosing $\mathbf{u}_{m,k}$ as the eigenvector corresponding to the minimum eigenvalue of:

$$\sum_{n=1}^{M} \sum_{\substack{p=1 \\ p\neq k, \text{if } n=m}}^{K} \mathbf{H}_{k,m}^{(n)} \mathbf{v}_{n,p} \mathbf{v}_{n,p}^{H} \mathbf{H}_{k,m}^{(n)H}. \tag{2.1.4}$$

Subsequently, the transmit pre-coding vectors $\left\{ \{\mathbf{v}_{m,k}\}_{k=1}^{K}, m = 1, \cdots, M \right\}$ are selected such that the undesired signal leakage power to the users are zero-forced after post-processing with the vector $\mathbf{u}_{m,k}$ as shown below [23]:

$$\sum_{n=1}^{M} \sum_{\substack{p=1 \\ p\neq k, \text{if } n=m}}^{K} |\mathbf{u}_{n,p}^{H} \mathbf{H}_{p,n}^{(m)} \mathbf{v}_{m,k}|^2 = 0, \forall m \in [1, 2, \cdots, M],\ \forall k \in [1, 2, \cdots, K]. \tag{2.1.5}$$

From (2.1.6) it is easy to see that $\mathbf{v}_{m,k}$ is chosen to be the eigenvector corresponding to the minimum eigenvalue of [23]:

$$\sum_{n=1}^{M} \sum_{\substack{p=1 \\ p\neq k, \text{if } n=m}}^{K} \mathbf{H}_{p,n}^{(m)H} \mathbf{u}_{n,p} \mathbf{u}_{n,p}^{H} \mathbf{H}_{p,n}^{(m)}. \tag{2.1.6}$$

Pre-coder Design with SNR maximisation

For signal to noise ratio (SNR) maximisation, if only the CSIR is available, then the precoding vectors and receive beam-formers can be designed at the receiver side and only the pre-coder information are transmitted to the BSs. But if the CSI and receive beam-formers are available at the transmitter, then the pre-coders can be designed at the transmitter. Under the SNR maximisation strategy, the precoding vectors $\left\{ \{\mathbf{v}_{m,k}\}_{k=1}^{K}, m = 1, 2, \cdots, M \right\}$, required to transmit the *k*-th user's data from the *m*-th BS, are designed such that the SNR at each user is maximized as shown in (2.1.7):

$$\mathbf{v}_{m,k} = \arg\max_{\mathbf{v}_{m,k}} |\mathbf{u}_{m,k}^{H} \mathbf{H}_{k,m}^{(m)} \mathbf{v}_{m,k}|^2,\ \forall m \in [1, 2, \cdots, M],\ \forall k \in [1, 2, \cdots, K]. \tag{2.1.7}$$

If $\mathbf{u}_{m,k}$ is known or given, the pre-coder $\mathbf{v}_{m,k}$, can be found as [24]:

$$\mathbf{v}_{m,k} \propto \max \text{eigenvector}\ \ (\mathbf{H}_{k,m}^{(m)H} \mathbf{u}_{m,k} \mathbf{u}_{m,k}^{H} \mathbf{H}_{k,m}^{(m)}). \tag{2.1.8}$$

Now the receive beam-formers $\left\{\{\mathbf{u}_{m,k}\}_{k=1}^{K},\ m = 1, 2, \cdots, M\right\}$, are designed such that the SNR is maximised as shown in (2.1.9):

$$\mathbf{u}_{m,k} = \arg\max_{\mathbf{u}_{m,k}} |\mathbf{u}_{m,k}^{H}\mathbf{H}_{k,m}^{(m)}\mathbf{v}_{m,k}|^2,\ \forall m \in [1, 2, \cdots, M],\ \forall k \in [1, 2, \cdots, K], \tag{2.1.9}$$

so $\mathbf{u}_{m,k}$ can be chosen as [24]:

$$\mathbf{u}_{m,k} \propto \max \text{eigenvector}\ \ (\mathbf{H}_{k,m}^{(m)}\mathbf{v}_{m,k}\mathbf{v}_{m,k}^{H}\mathbf{H}_{k,m}^{(m)H}). \tag{2.1.10}$$

2.2 Existing CoMP transmission

CoMP transmission requires a group of BSs to transmit user information simultaneously to a given user, such that the user's performance is enhanced, especially for the cell-edge users. The cooperation between the BSs was deemed practical since the BSs are fixed in location and are interconnected through optical fibres or have very fast point-to-point communication links. With cooperation, the network can be viewed as a single cell BS with distributed antenna arrays. The downlink channel of a multi-cell MIMO system with cooperation can then be treated as a single cell multi-user MIMO system and the only drawback is that the average transmit power across all antennas is bounded [25]. Pre-specified BS clusters that do not change with time and channel conditions are known as static clustering. Dynamic clustering adapts to the changing channel conditions and system conditions and gives a better performance than static clustering [18, 26]. However the gain which can be obtained by adaptive clustering is yet to be fully harnessed. In 3GPP LTE, there are three main types of cooperating area (CA): 1) Network centric CA: the cells in a network are divided statistically into different clusters for all users in the network. 2) User centric CA: CSs are assigned to users based on the strong channel links to each user. 3) Network-centric user assisted CA: this is a hybrid of both CAs previously stated, highlighting the benefits of both techniques [15].

2.3 CoMP Transmission in a Network Centric Cooperating Area

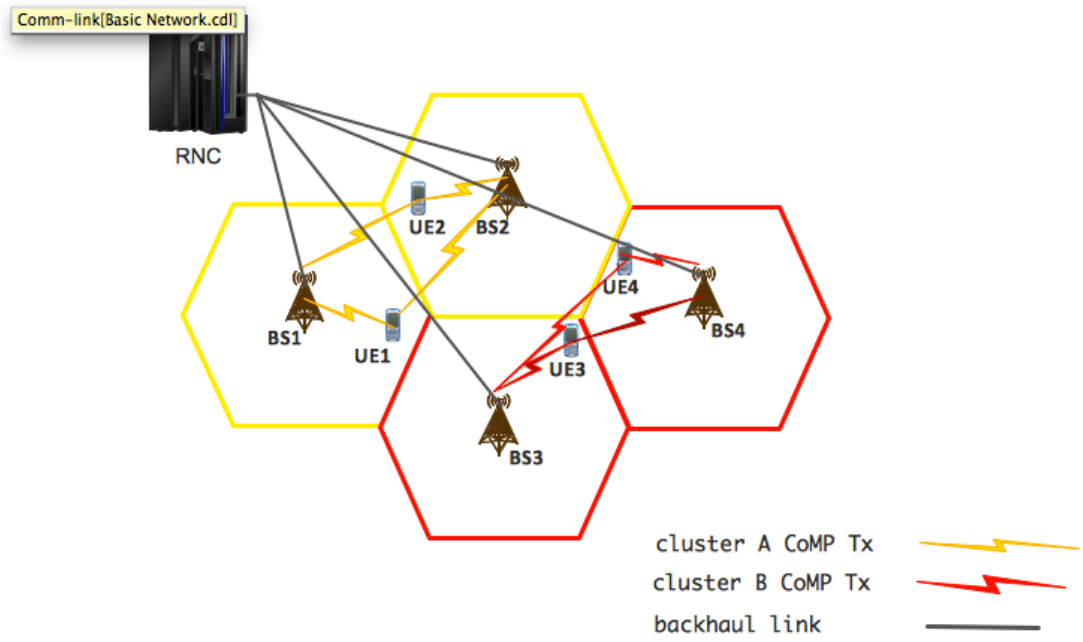

Figure 2.3: CoMP transmission within clusters, $K = 4$ BS-UE pairs and $M_{max} = 2$ BS-UE pairs per cluster.

The network centric CoMP transmission allows multiple transmission from BSs within a cluster to the user equipments (UEs) within the same cluster. In Figs. 2.3 and 2.4, the system models show a given set of four macro cells partitioned into two clusters, where $M_{max} = 2$ BSs are cooperating within a given cluster and all users share the same RB. In Fig. 2.5, full coordination or full CoMP transmission exists within each cluster and all the BSs in each cluster require the signal information of the user(s) for CoMP transmission. The size of each cluster is pre-set by the network, and a large cluster size is known to cause high data overhead in the backhaul [18]. However, this can be used as an advantage for interference cancellation if the BSs act as a super BS with distributed antennas, thereby

increasing the available degrees of freedom (DoF) for interference cancellation [19]. The DoF is defined as the number of independent channels exploited by the transmitter which can also be defined as the ratio of the sum capacity of the network to the log of the total transmit power, in the limit that $P \rightarrow \infty$, i.e. $\lim_{P \longrightarrow \infty} \frac{C(\mathrm{P})}{\log_2 \mathrm{P}}$ [27]. In [15], the authors selected the CSs of the users based on the available backhaul capacity. In [26], the authors suggested that the clusters performing CoMP transmission can be selected based on a cost function, where the cost is proportional to the cluster cardinality and inversely proportional to the channel characteristics.

The network is divided into different clusters and members of each cluster can be static or dynamic. The cluster size and the selection of macro cells for each cluster can be pre-set by the network or varied depending on the network conditions. Under dynamic clustering, BSs are grouped into clusters based on the channel conditions of the users, the proximity of users to the neighbouring BSs, or other factors. The BSs coordinate only within the cluster to transmit data to the users served by that cluster. Each user receives IUI and ICI from its supporting cluster and OCI from other clusters within the network. The conventional clusterisation allowed large number of BSs to transmit data to users within each cluster, thereby causing high data overhead in the backhaul links.

To alleviate the data overhead problem, this chapter analyses the possible trade-off in performance to achieve a reduced data overhead. Intuitively, having a large number of clusters within a network would lead to a reduced data overhead in exchanging user's signals and precoding information to each serving BS. In the following section, a reduction in the cluster size is proposed using the proposed algorithm and the effect of this strategy is analysed and discussed through simulation results.

2.3.1 System Model

As shown in Fig. 2.3, the downlink cell deployment considers only the cell-edge users. The BS and UE pair are equipped with M_t transmit and N_r receive antennas respectively. Assuming equal base station power ($P_m, \forall m$) across all the BSs, let the power allocated

tp the m-th BS for each user's data within a cluster be $\rho_{m,k} = P_m/M_{max}$. Note that M_{max} is the number of BS-UE pairs in a given cluster and for the full CoMP transmission M_{max} = K BS-UE pairs. Under full CoMP transmission as shown in Fig. 2.5, the direct and interfering channels carry the desired and undesired signals to each UE. Each user receives its desired signal and the undesired signals are cancelled using both transmit precoders and receive beamformers.

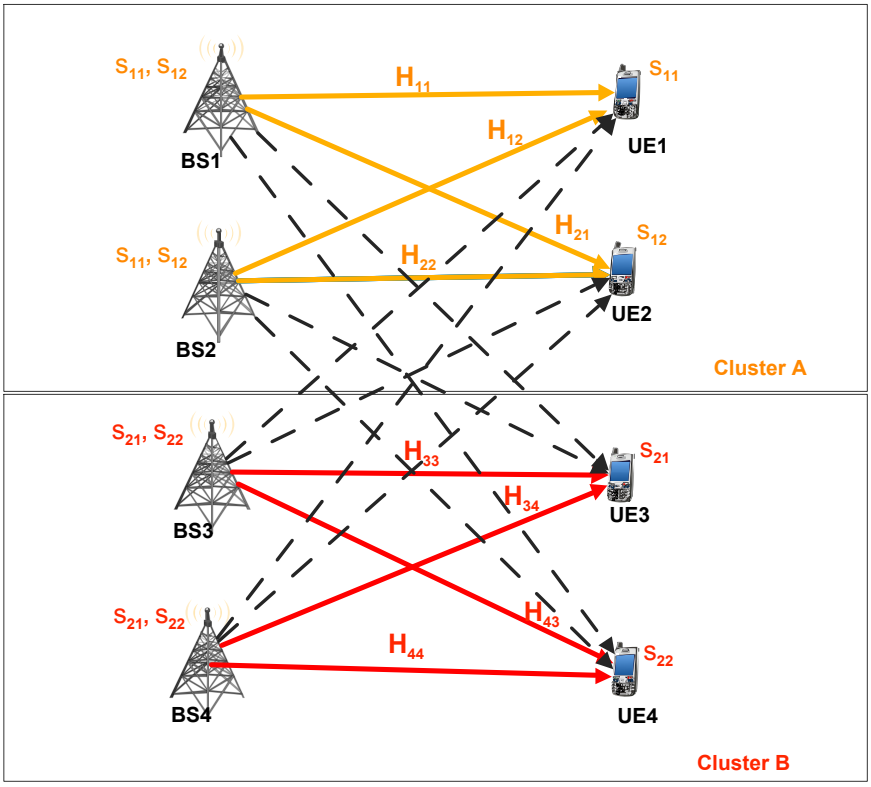

Figure 2.4: CoMP transmission links with $K = 4$ BS-UE pairs and $M_{max} = 2$ BS-UE pairs in the cluster.

The dashed lines represent the interference channels as shown in Fig. 2.4 while the solid lines represent the direct channel links as shown in Figs. 2.4 and 2.5. The channel matrix between the k-th user and the m-th BS is a flat-fading channel, denoted by $\mathbf{H}_{k,m} \in \mathbb{C}^{N_r \times M_t}$. The coefficients of $\mathbf{H}_{k,m}$ are complex random variables, with zero-mean Gaussian real and imaginary parts. The channel links experience large scale fading, with path loss exponent

(α) and log-normal shadowing having zero-mean and variance σ_s^2.

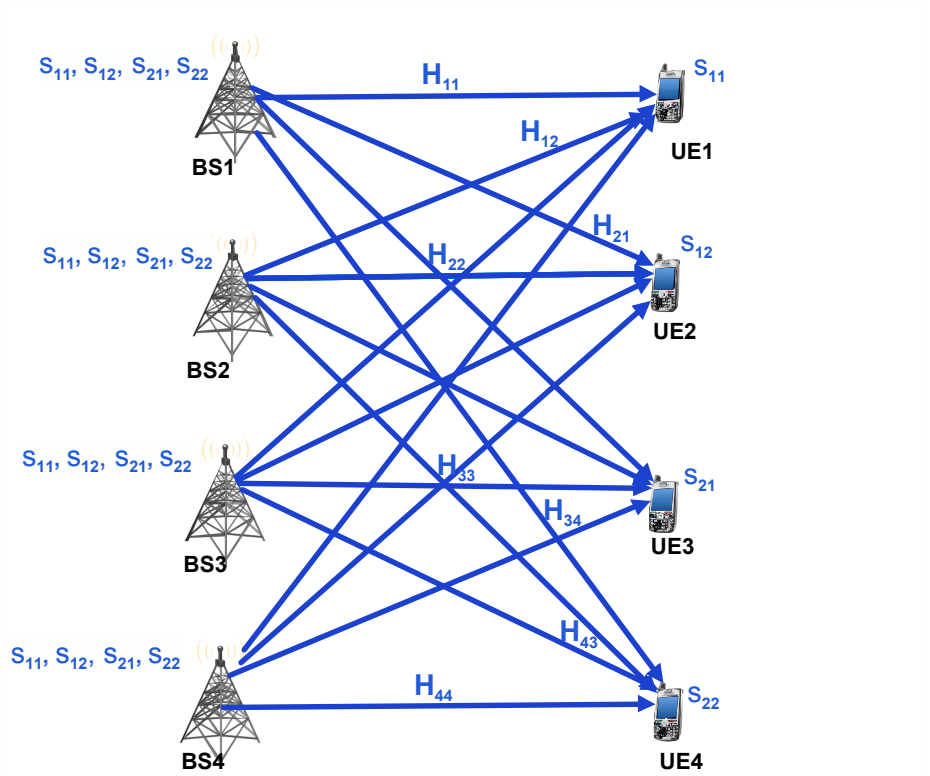

Figure 2.5: Full CoMP transmission links with K = 4 BS-UE pairs and M_{max} = 4 BS-UE pairs in the cluster.

Assuming a single user is paired to a given BS and a single data stream is transmitted from each BS to each user or groups of users. Let $\mathbf{H}_k = [\mathbf{H}_{k,1}, \mathbf{H}_{k,2}, ..., \mathbf{H}_{k,K}]$, be the channel matrix between the user k and all K transmit BSs. Let $\mathbf{U} = [\mathbf{u}_1, ..., \mathbf{u}_K]$, be the matrix containing all the receive beamforming column vectors ($\mathbf{u}_k$) of user k. Let $\mathbf{V} = [\mathbf{v}_1, \mathbf{v}_2, ..., \mathbf{v}_K]$, be the matrix containing all the unitary precoding vectors of user data k, where $\mathbf{v}_k = [\mathbf{v}_{1k}^T, \mathbf{v}_{2k}^T, ..., \mathbf{v}_{K,k}^T]^T$ and $\mathbf{v}_{m,k}$ is used to precode the data of the k-th user from the m-th BS. In addition, $\rho_{m,k}$ is the power allocated to the k-th user data at the selected m-th BS in the j-th cluster. s_k is the complex (scalar) data signal destined for the k-th user ($\mathrm{E}\{|s_k|^2\}$ = 1) and $\mathbf{n}_k$ is an additive, zero-mean, white, complex Gaussian noise vector

with a variance of σ_k^2.

Each cluster *j*, has M_{max} BS-UE pairs and each BS in each cluster transmits multiple streams of data containing a single data stream to each user in the cluster. The received signal at the *k*-th user in the *j*-th cluster is given by (2.3.11):

$$\begin{aligned}\mathbf{y}_k^{(j)} = &\sum_{\substack{m=1\\ m\in T_j}}^{K} \mathbf{H}_{k,m}\mathbf{v}_{m,k}\sqrt{\rho_{m,k}}s_k + \sum_{\substack{m=1\\ m\in T_j}}^{K}\sum_{\substack{p=1,p\neq k\\ p\in T_j}}^{K} \mathbf{H}_{k,m}\mathbf{v}_{m,p}\sqrt{\rho_{m,p}}s_p \\ &+ \sum_{\substack{i=1\\ i\neq j}}^{J}\sum_{\substack{m=1\\ m\in T_i}}^{K}\sum_{\substack{p=1\\ p\in T_i}}^{K} \mathbf{H}_{km}\mathbf{v}_{m,p}\sqrt{\rho_{m,p}}s_p + \mathbf{n}_k, \\ &\forall j \in [1,2,\cdots,J],\ \forall k \in [1,2,\cdots,K], k \in T_j, \end{aligned} \tag{2.3.11}$$

where T_j is the set of all BS-user pairs in cluster *j* and *J* is the total number of clusters. In (2.3.11), the second and third components respectively, are the IUI and ICI received within the same CS and the OCI received from other CSs in the CoMP system. The SINR of the *k*-th user is given by:

$$\text{SINR}_k = \frac{\sum\limits_{\substack{m=1\\ m\in T_j}}^{K} \left|\mathbf{u}_k^H\mathbf{H}_{km}\mathbf{v}_{mk}\right|^2 \rho_{m,k}}{\sum\limits_{\substack{m=1\\ m\in T_j}}^{K}\sum\limits_{\substack{p=1,p\neq k\\ p\in T_j}}^{K} \left|\mathbf{u}_k^H\mathbf{H}_{k,m}\mathbf{v}_{m,p}\right|^2 \rho_{m,p} + \sum\limits_{\substack{i=1\\ i\neq j}}^{J}\sum\limits_{\substack{m=1\\ m\in T_i}}^{K}\sum\limits_{\substack{p=1,p\neq k\\ p\in T_j}}^{K} \left|\mathbf{u}_k^H\mathbf{H}_{k,m}\mathbf{v}_{m,p}\right|^2 \rho_{m,p} + \sigma_k^2}, \tag{2.3.12}$$

R_k is the rate of user *k* and the sum-rate (R_T) is expressed as:

$$R_T = \sum_{k=1}^{K} \underbrace{\log_2\left(1+\text{SINR}_k\right)}_{\text{R}_k} \tag{2.3.13}$$

2.3.2 Proposed Clusterisation Algorithm

In this section, a new method is proposed to divide the given network into smaller cluster in order to analyse the possible trade-off in performance when the number of transmit

BSs are further limited. From the cell topology in Figs. 2.3 and 2.4, assuming a cluster size of M_{max} = 2. For easier clustering, BS#1 and BS#4 are not allowed to cooperate within the CoMP system since they are further apart. Therefore BS#1 and BS#4 can only cooperate with BS#2 or BS#3. The clusters of BS-UE pairs are selected based on the channel conditions as shown below:

Step 1: Using the obtained CSIT, the channel norms from UE#1 and UE#4 are obtained relative to BS#2 and BS#3 (i.e. $\|\mathbf{H}_{12}\|_F, \|\mathbf{H}_{13}\|_F$ and $\|\mathbf{H}_{42}\|_F, \|\mathbf{H}_{43}\|_F$) while the channel norms for UE#2 and UE#3 are also obtained relative to BS#1 and BS#4 (i.e $\|\mathbf{H}_{21}\|_F, \|\mathbf{H}_{24}\|_F$ and $\|\mathbf{H}_{31}\|_F, \|\mathbf{H}_{34}\|_F$).

Step 2: Let $\mathcal{X}$ be defined as the set of values obtained from the sum of all interfering channel norms in each possible cluster. The number and members of all possible clusters is a combinatorial problem which can be easily obtained for small sizes of clusters. For the given set-up in Figs. 2.4 and 2.5, $\mathcal{X}$ can be obtained as:

$$\mathcal{X} = [\mathcal{X}(1),\ \mathcal{X}(2),\ \mathcal{X}(3),\ \mathcal{X}(4)] \tag{2.3.14}$$

where

$$\mathcal{X}(1) = \|\mathbf{H}_{12}\|_F + \|\mathbf{H}_{21}\|_F$$
$$\mathcal{X}(2) = \|\mathbf{H}_{13}\|_F + \|\mathbf{H}_{31}\|_F$$
$$\mathcal{X}(3) = \|\mathbf{H}_{42}\|_F + \|\mathbf{H}_{24}\|_F$$
$$\mathcal{X}(4) = \|\mathbf{H}_{43}\|_F + \|\mathbf{H}_{34}\|_F$$

.

Step 3: Using the information obtained in Step 2, in a successive manner, the cluster with the best interfering channel links is chosen. Each subsequent cluster chosen must be exclusive and should not contain BSs already chosen for previous clusters.

For instance, if $\max(\mathcal{X})$ = $\mathcal{X}(1)$ or $\mathcal{X}(4)$ then the scheduled cooperating sets will be (BS#1, BS#2) and (BS#3, BS#4) otherwise the cooperating sets will be (BS#1, BS#3) and (BS#2, BS#4).

2.3.3 Simulation Results and Evaluation

In this section, simulation results are obtained for the network centric clusterisation approach using the proposed algorithm. The performance metric used are the sum-rate and bit error rate (BER). The BER performance is used to measure the number of errored received bits transmitted through a given communication medium [28]. Consider the system setup in Fig. 2.3, Fig. 2.4 (showing a cluster size of M_{max} = 2) and Fig. 2.5 (showing a cluster size of M_{max} = 4). The performance of the algorithm is evaluated for K BS-UE pairs where each user k is served by $M_k = M_{max}$ number of BSs in each cluster. The value of M_{max} is varied to analyse the effect of the system performance against the number of transmit BSs allowed for CoMP transmission. In this section the non-CoMP system, which is based on a single downlink transmission between each BS-UE pair, would be compared to the proposed (small size of clusters) and existing strategies (large size of clusters). Also a random clusterisation, which randomly selects each clusters without taking any network factors into consideration is evaluated and compared with the static clusterisation method (where the clusters are fixed regardless of the changing network conditions).

For the analysis required in this section, the following parameters are defined:

- 'bernc' and 'rtnc' represents the BER and sum-rate performance respectively under non-CoMP transmission and $\{M_k\}_{k=1}^{K} = M_{max}$ = 1.
- 'berrc', and 'rtrc' represent the BER and sum-rate performance respectively under a random clusterisation of the BS-UE pairs and $\{M_k\}_{k=1}^{K} = M_{max}$ = 2.
- 'bersc' and 'rtsc' represent the BER and sum-rate performance respectively under a network preset clusterisation for the given BS-UE pairs and $\{M_k\}_{k=1}^{K} = M_{max}$ = 2.
- 'berdc' and 'rtdc' represent the BER and sum-rate performance respectively under the proposed dynamic clusterisation of the BS-UE pairs based using the algorithm

presented in Section 2.3.2 for K = 4 BS-UE pairs. The clusterisation is dynamic and changes with the given channel conditions and $\{M_k\}_{k=1}^{K} = M_{max}$ = 2.

- 'berfc' and 'rtfc' represent the BER and sum-rate performance respectively under full CoMP transmission. The users receive data from all K BSs and $\{M_k\}_{k=1}^{K} = M_{max}$ = K = 4.

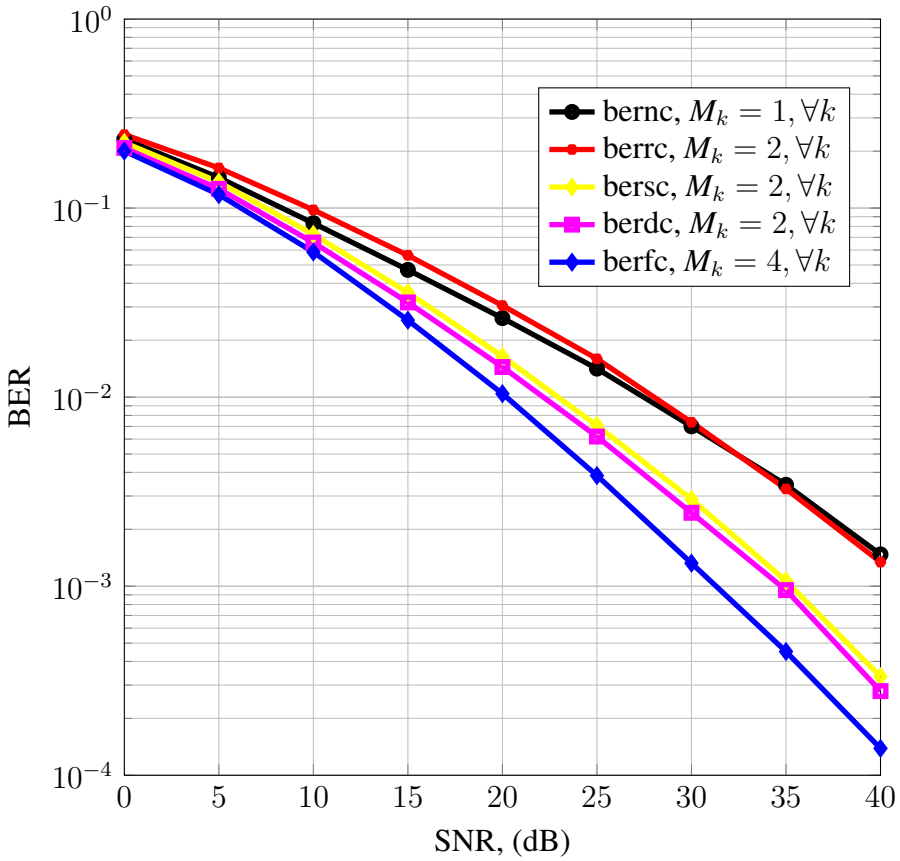

Figure 2.6: BER performance with M_t = 4, N_r = 2 and K = 4 BS-UE pairs in a network centric CA.

Figs. 2.6 and 2.7 show the BER performance and the sum-rate performance of the given system, under the different clustering strategies. It can be observed from Fig. 2.6 that 'bernc' and 'berrc' achieve poor BER performance when compared to 'bersc', 'berdc' and 'berfc'. It can also be observed from Fig. 2.7 that 'rtnc' and 'rtrc' achieve poor

BER performance when compared to 'rtsc', 'rtdc' and 'rtfc'. However the sum-rate performance obtained with 'rtnc' exceeds that obtained with 'rtrc' as the SNR increases. This shows that a random clusterisation approach does not provide any gain even with CoMP transmission as compared to a non-CoMP transmission with a single BS-UE pair.

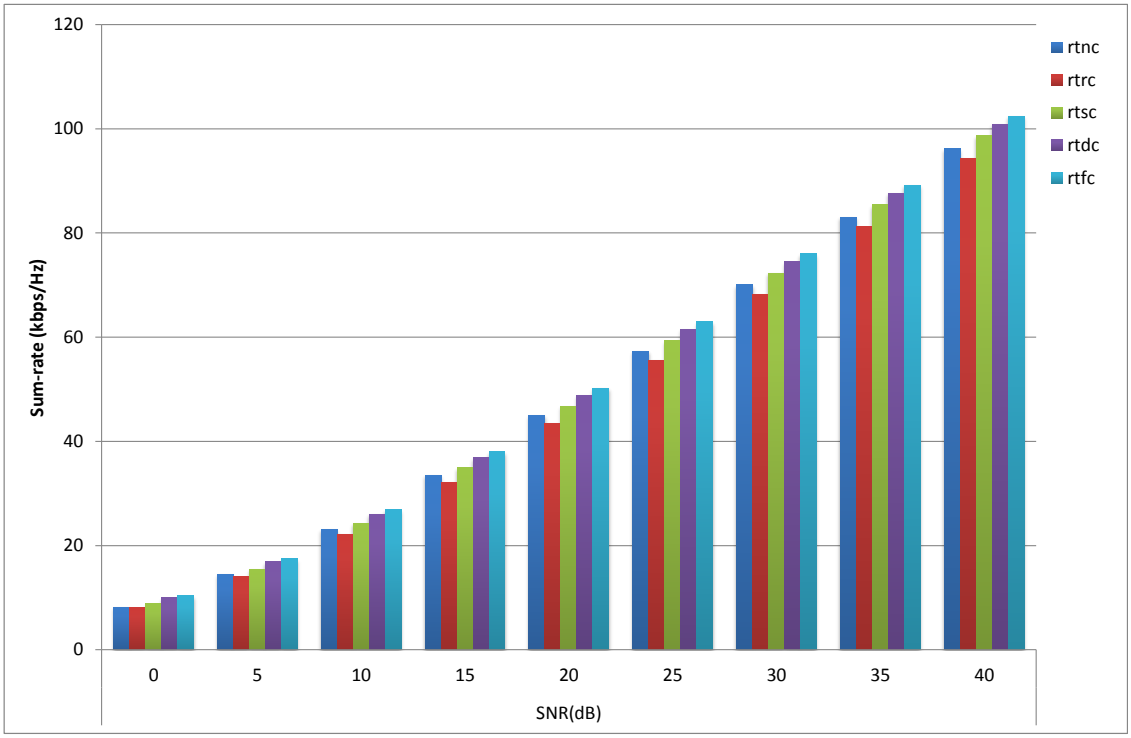

Figure 2.7: Sum-rate performance with $M_t = 4$, $N_r = 2$ and $K = 4$ BS-UE pairs in a network centric CA.

The proposed 'rtdc' is seen to achieve a higher sum-rate than 'rtsc', while 'rtfc' is seen to have the best performance when compared to all other four strategies. The channel characteristics of the wireless channel changes with time and the dynamic clusterisation takes advantage of this unique characteristics unlike the static clustering approach. As expected, the performance obtained under the dynamic method is seen to outperform the static approach. This is because unlike static clustering, dynamic cluster takes into account the changing channel conditions of the network during clustering. Dynamic clustering approach re-clusters the users using the given strategy such that the best BSs

are clustered together at every given time. This result validates the need for a dynamic cluster selection as opposed to a static or random clusterisation of BS-UE pairs as well as non-CoMP transmission.

The best BER and sum-rate performance is achieved under 'berfc' and 'rtfc' with M_k = 4 transmit BSs for the *k*-th user. However when compared to 'berdc' and 'rtdc' with only M_k = 2 transmit BSs for the *k*-th user, a 50% reduction is expected in the backhaul overhead using the proposed solution for only a slight decrease in the performance. For instance to obtain a BER performance of 10^{-2}, 'berfc' and 'berdc' requires an SNR of 20 dB and 22 dB. Also when the SNR is 25 dB, 'rtfc' and 'rtdc' obtains a sum-rate performance of 63 kbps/Hz and 61 kbps/Hz respectively. As observed, a considerable gain is not achieved with full CoMP transmission when M_{max} = 4 when compared to $M_{max} = 2$, even though the resulting data overhead is doubled. The backhaul link is limited and could potentially cause poor synchronisation and high latency, if congested. It is therefore important to avoid full CoMP transmission with a large number of transmit BSs per user. Hence, the cluster size needs to be reduced and the members of each cluster needs to be properly selected such that the system performance is maximised with limited backhaul overhead.

Using the same number of transmit and receive antennas, for K = 6 BS-UE pairs, the simulation results show the BER and sum-rate performance in Figs. 2.8 and 2.9 respectively. The proposed dynamic clusterisation presented earlier in Section 2.3.2 is applied for K = 6 BS-UE pairs. Note that to completely cancel the interference using precoding and/or beamforming at the transmitter and/or receiver respectively, there has to be available DoF at the transmitter and/or receiver. And so for the given set-up, the constraints on the transmit and/or receive antennas respectively are $M_t > (K-1)$ and/or $N_r > (K-1)M_{max}$, which means either constraint or both constraints needs to be satisfied for complete interference cancellation. If the number of transmit antennas do not meet the constraint required to completely null the transmitted leakage to the users, the DoF at the receive antennas can be used to also mitigate the received interference.

Now one can observe that 'berfc' and 'rtfc' achieve a better performance compared to all

other four strategies when SNR $\leq$ 10 dB. But at higher SNR values, 'berfc' and 'rtfc' are seen to achieve the worst performance. This is because for the given system set-up with M_t = 4, N_r = 2, $M_{max} = 6$ and K = 6 BS-UE, the condition for complete interference zero-forcing is not met, thereby causing very poor mitigation of the received interference.

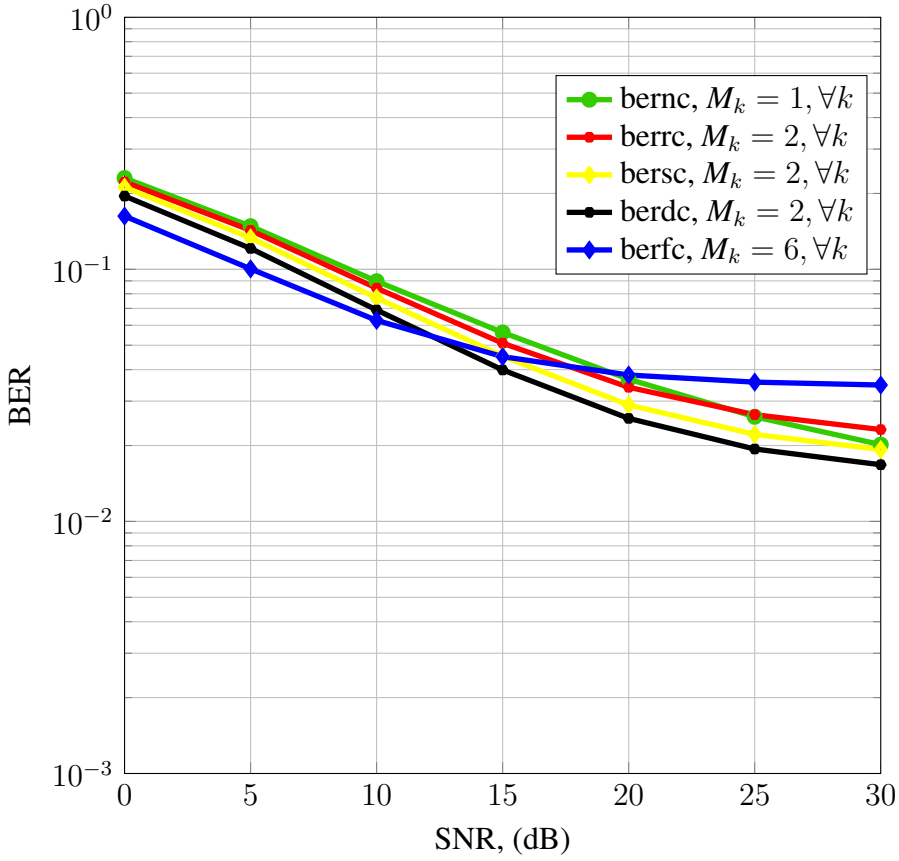

Figure 2.8: BER performance with M_t = 4, N_r = 2 and K = 6 BS-UE pairs in a network centric CA.

It can be seen from Fig. 2.8, that the BER performance flattens out at higher SNR values due to unavailable DoF for complete interference cancellation. Again 'berdc' is seen to exceed the BER performance obtained by 'bernc','berrc' and 'bersc'. Also from Fig. 2.9, 'rtdc' is seen to achieve a better sum-rate performance over 15 dB to 20 dB and 'rtnc' achieves a better performance from 30 dB upwards. This happens because under the given system conditions, none of the solutions meet the transmit antenna constraints.

However, 'rtnc' (with M_{max} = 1) would obtain a less dominant interference since the receive antenna conditions are less stringent as opposed to 'rtdc' (with M_{max} = 2) and 'rtfc' (with M_{max} = 6). So at higher SNR values 'rtnc' would experience a better SINR and system performance due to lower level of interference compared to 'rtdc' and 'rtfc'.

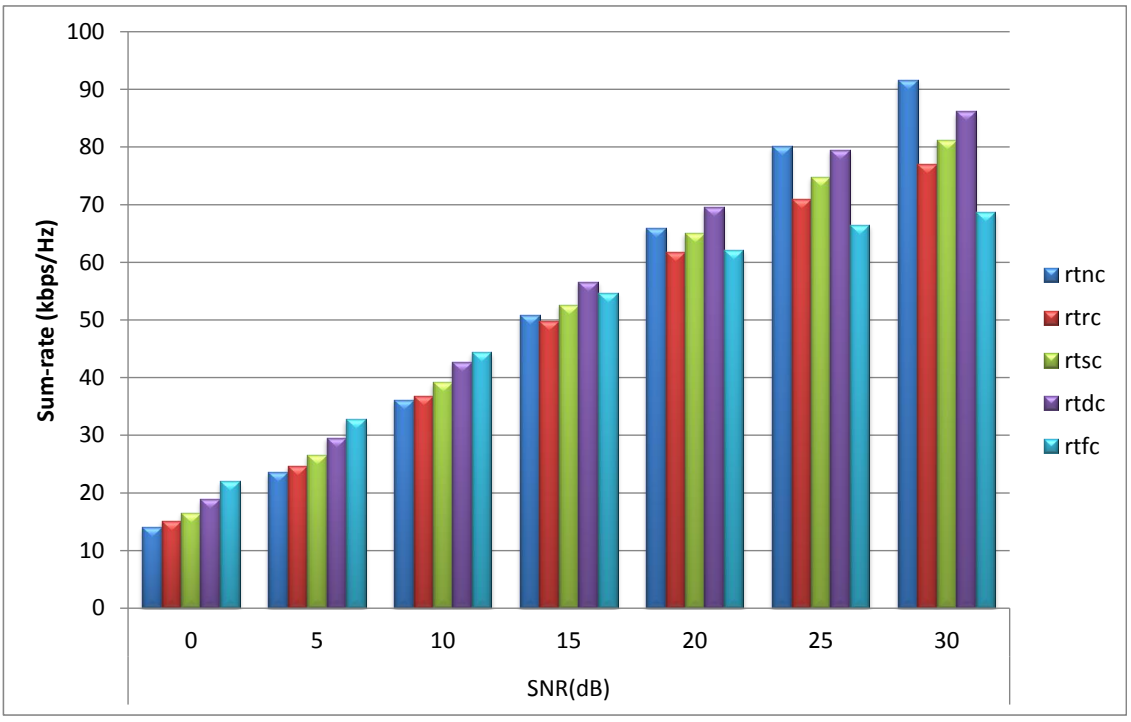

Figure 2.9: Sum-rate performance with $M_t = 4$, $N_r = 2$ and $K = 6$ BS-UE pairs in a network centric CA.

From these observations, one can see that the number of available transmit and receive antennas can affect the performance of CoMP transmission with a large cluster size under certain condition. In addition, the data overhead experienced in this case is three times more than the data overhead required under the proposed clustering approach. Even at low SNR values, the increase in performance is very trivial compared to the required increase in the data overhead. For instance at 0 dB, 'rtfc' and 'rtdc' achieve a sum-rate performance of 22 kbps/Hz with M_{max} = 6 and 19 kbps/Hz with M_{max} = 2.

2.4 CoMP Transmission in a User Centric Cooperating Area

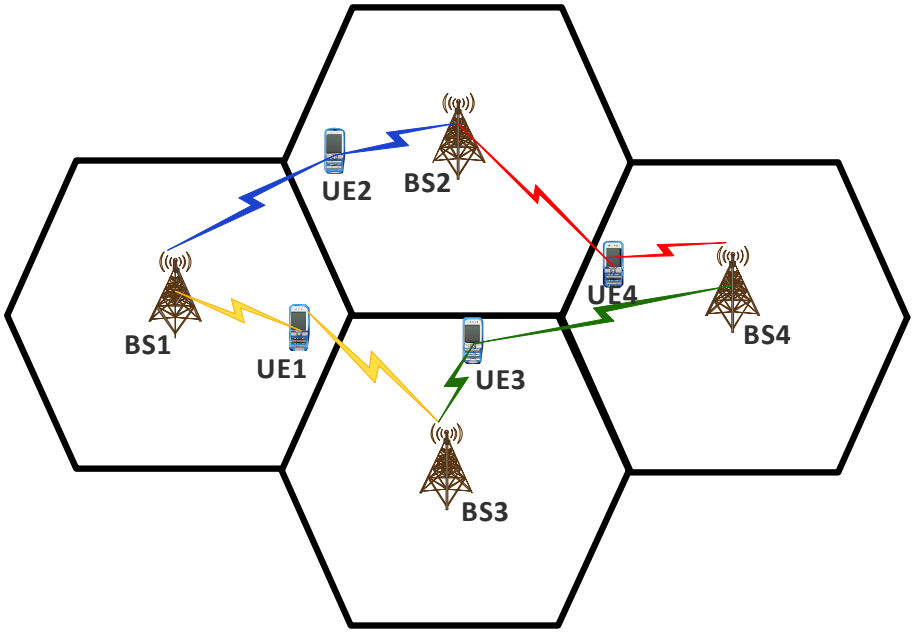

Figure 2.10: CoMP transmission in a user centric CA, with $K = 4$, $M_{max} = 2$.

The CS of a given user is defined as the set of BSs transmitting data to that given user. The user centric approach shown in Fig. 2.10 allows a fixed number of BSs to be selected for each user, based on the channel quality to that user. Therefore, the resulting CSs are not exclusive unlike the network centric clusters. Network centric CS is defined as exclusive since a BS-UE pair can only belong to one cluster. The clusters can also be said to be symmetric since each BS in each cluster supports the same users. However for user centric clustering, the clusters can be said to be asymmetric, since each BS can support different number of users at a given time. The user centric approach aims to limit the backhaul overhead by setting a fixed number of transmit BSs per user (M_{max}). The advantage of the asymmetric CS is that the users have more flexibility in choosing BSs with good channel quality as opposed to the network centric clusterisation. The

BSs selected for each user can be static or dynamic. Under the dynamic CS allocation, BSs with good channel quality are assigned to users for CoMP transmission. Each user receives IUI, ICI and OCI from other BSs within the network. Full coordination or full CoMP transmission also exists where $M_{max} = K$ BSs are selected for CoMP transmission as shown in Fig. 2.5. The disadvantages of using a large number of BSs for CoMP transmission is the high data overhead which has already been highlighted in Section 2.3.

2.4.1 System Model

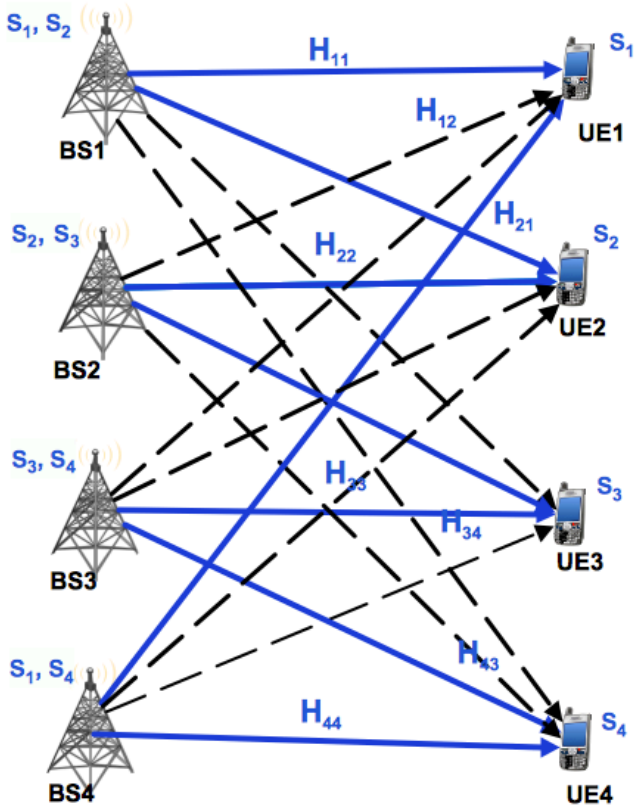

Figure 2.11: CoMP transmission links with $K = 4$ BS-UE pairs and $M_{max} = 2$ BSs per user, the dashed lines and solid lines represents the undesired and desired channel links respectively.

Consider the cell deployment in Fig. 2.11 where each BS-UE pair is equipped with M_t and N_r transmit and receive antennas respectively and an equal base station power ($P_m, \forall m$) is assumed across the network. Let the power allocated on the *m*-th BS to each user's data within a cluster be $\rho_{m,k}$. Assuming equal power across all data signals from each BS, then the power assigned to each user's data signal is the total BS power divided equally across all users' data signals. Note that M_{max} is the maximum number of allowed transmit BSs per user and for the full CoMP transmission M_{max} = K BS-UE pairs.

As shown in Fig. 2.11, the dashed black line represents the interference channel while the blue solid line represents the direct channel. Also the users share the same RB, and the channel matrix between the *k*-th user and the *m*-th BS is a flat-fading channel, denoted by $\mathbf{H}_{k,m} \in \mathbb{C}^{N_r \times M_t}$. The coefficients of $\mathbf{H}_{k,m}$ are complex random variables, with zero-mean Gaussian real and imaginary parts. The channel links experience large scale fading, with path loss exponent (α) and log-normal shadowing having zero-mean and variance σ_s^2.

Let $\mathbf{H}_k = [\mathbf{H}_{k,1}, \mathbf{H}_{k,2}, ..., \mathbf{H}_{k,K}]$, be the channel matrix between the user *k* and all *K* transmit BSs. Let $\mathbf{U} = [\mathbf{u}_1, ..., \mathbf{u}_K]$, be the matrix containing all the receive beamforming column vectors ($\mathbf{u}_k$) of user *k*. Let $\mathbf{V} = [\mathbf{v}_1, \mathbf{v}_2, ..., \mathbf{v}_K]$, be the matrix containing all the unitary precoding vectors of user data *k*, where $\mathbf{v}_k = [\mathbf{v}_{1k}^T, \mathbf{v}_{2k}^T, ..., \mathbf{v}_{K,k}^T]^T$ and $\mathbf{v}_{m,k}$ is used to precode the data of the *k*-th user from the *m*-th BS. In addition, $\rho_{m,k}$ is the power allocated to the *k*-th user data at the selected *m*-th BS in the *j*-th cluster. s_k is the complex (scalar) data signal destined for the *k*-th user ($\mathrm{E}\{|s_k|^2\}$ = 1) and $\mathbf{n}_k$ is an additive, zero-mean, white, complex Gaussian noise vector with a variance of σ_k^2. Each BS transmits multiple streams of data containing a single data stream to each user in the cluster. The received signal at the *k*-th user is given by (2.4.15):

$$\mathbf{y}_k = \sum_{\substack{m=1 \\ m \in L_k}}^{K} \mathbf{H}_{k,m}\mathbf{v}_{m,k}\sqrt{\rho_{m,k}}s_k + \sum_{\substack{p=1 \\ p \neq k}}^{K} \sum_{\substack{m=1 \\ m \in L_p}}^{K} \mathbf{H}_{k,m}\mathbf{v}_{m,p}\sqrt{\rho_{m,p}}s_p + \mathbf{n}_k$$
$$\forall k \in [1, 2, \cdots, K], \tag{2.4.15}$$

where L_j is the set of all BSs transmitting to user *j*. In (2.4.15), the first and second components respectively, are the desired received signal and the IUI plus OCI received

within the system.

From (2.4.15), after post-processing with $\mathbf{u}_k$ at the receiver, the SINR at the k-th UE is given by:

$$\text{SINR}_k = \frac{\sum\limits_{\substack{m=1 \\ m\in L_k}}^{K} \left|\mathbf{u}_k^H \mathbf{H}_{km} \mathbf{v}_{mk}\right|^2 \rho_{m,k}}{\sum\limits_{\substack{m=1 \\ m\in L_p}}^{K} \sum\limits_{\substack{p=1 \\ p\neq k}}^{K} \left|\mathbf{u}_k^H \mathbf{H}_{k,m} \mathbf{v}_{m,p}\right|^2 \rho_{m,p} + \sigma_k^2} \tag{2.4.16}$$

R_k for the k-th user and sum-rate (R_T) can be obtained using (2.3.13).

2.4.2 Proposed User Centric CS Algorithm

To limit the data overhead of the system under the user centric approach, the number of allowed transmit BSs per user is reduced and the resulting BER and sum-rate performance is obtained and analysed. For the purpose of analysing the objectives of this chapter, only the channel gain would be considered in the proposed CS algorithm. However, this is not optimal since the rate of the user is based on the SINR metric. In Chapters 3 and 4, the interference within the network would be taken into account and the SINR would be the ultimate metric used in the proposed CS selection algorithm.

The CSs of the UEs are selected as shown below:

Step 1: The CSIT of the network is obtained, and the channel norms from the available neighbouring BSs (m) to each user (k) are calculated (i.e. $\|\mathbf{H}_{k,m}\|_F, \forall k, m, \in [1, 2, \cdots, K]$).

Step 2: Using the information obtained in Step 1, the CSs for the users are obtained by assigning M_{max} transmit BSs for each user. The BSs assigned to each user are BSs with the best channel quality. These BSs perform CoMP transmission to the user.

Since the CS selection is user based, the number of users assigned to each BS at a given time varies based on the changing channel conditions from each BS to each user.

2.4.3 Simulation Results and Evaluation

In this section, the simulation results are obtained for the user centric clustering approach using the proposed algorithm in Section 2.4.2 for dynamic clusterisation. Considering the system set-up in Fig. 2.11 (showing a CS size of M_{max} = 2) and Fig. 2.5 (showing a CS size of M_{max} = 4). The performance of the algorithm is evaluated for K BS-UE pairs where each user k is served by $M_k = M_{max}$ BSs in each cluster. The value of M_{max} is further reduced and the trade-off between system performance and data overhead is analysed. Also for the purpose of this work, the static approach to user centric clusterisation is analysed. The users are assigned pre-set BSs depending on the allowed BS size by the network. The obtained results are compared with the static user centric clusterisation ('berasc'), dynamic user centric clusterisation ('beradc'), non-CoMP transmission ('bernc'), dynamic network centric clusterisation ('berdc') and full CoMP transmission ('berfc').

For the analysis required in this section, the following additional parameters are defined:

- 'berasc' and 'rtasc' represent the BER and sum-rate performance respectively under static pre-set CS selection for the users and $\{M_k\}_{k=1}^{K} = M_{max}$ = 2.
- 'beradc' and 'rtadc' represent the BER and sum-rate performance respectively using the proposed dynamic user centric CS selection and $\{M_k\}_{k=1}^{K} = M_{max}$ = 2.

Figs. 2.12 and 2.13 show the BER performance and the sum-rate performance of the given system, under the different clusterisation strategies. From Fig. 2.12, one can observe that the use of multiple BSs improves the system performance. Now 'berasc' achieves a similar BER performance with 'berdc', however the sum-rate performance for 'rtdc' is slightly better than 'rtasc' as shown in Fig. 2.13. This shows that even with a static user centric CS selection, the performance obtained is comparable to the performance achieved with a dynamic network centric clusterisation. It also shows that the user centric

approach used to obtain the CSs for each user, allows more flexibility in choosing a better interference channel for CoMP transmission using neighbouring BSs as opposed to the network centric clusterisation, where the BSs in the clusters may not always have the best channel link to all the users in the given cluster.

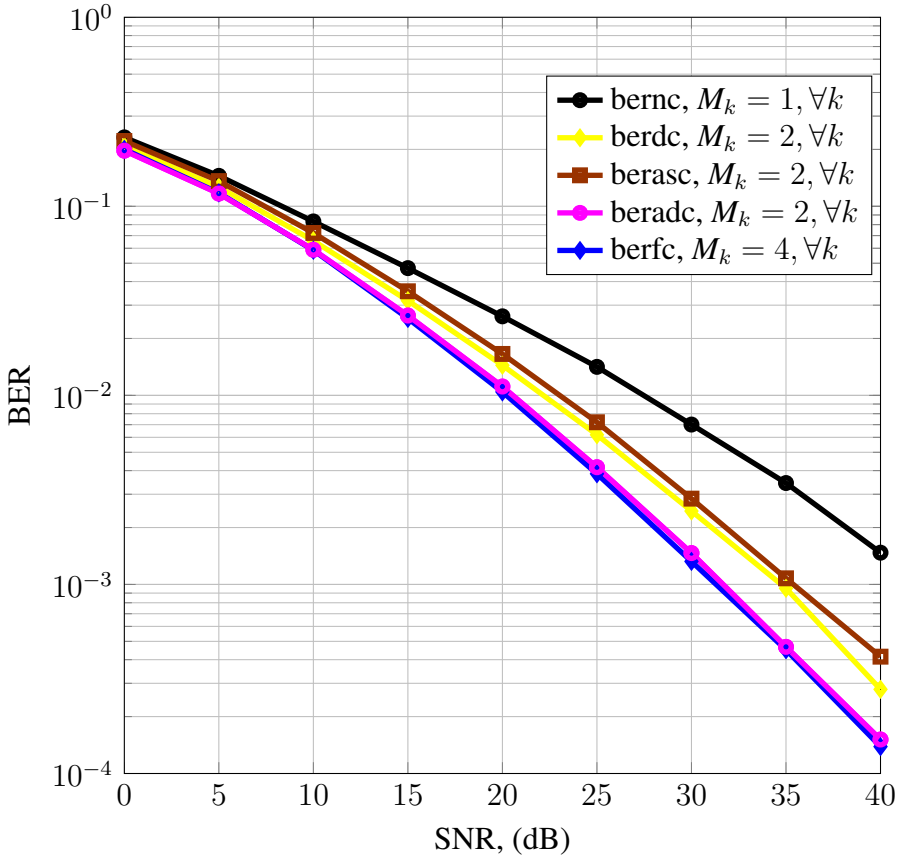

Figure 2.12: BER performance with $M_t = 4$, $N_r = 2$ and $K = 4$ BS-UE pairs in a user centric CA.

Again in Fig. 2.12, 'beradc' is seen to achieve a gain of 3 dB when compared to the network centric clusterisation approach, 'berdc'. Also the sum-rate performance of 'rtadc' slightly exceeds 'rtdc' as seen in Fig. 2.13. Now comparing 'beradc' to 'berfc', the BER performance achieved is similar but 'beradc' uses only 2 transmit BSs per user as opposed to 4 transmit BSs per user. This proves that CoMP transmission using a large CS size may offer little or no considerable advantage when compared to a smaller CS

size if the CSs with a smaller size are chosen to maximise the signal strength to each user. However, the data overhead required for full CoMP transmission is twice the data overhead required using the proposed user centric solution. In this case only the channel gain was considered without the effect of interference and noise, but in Chapter 4 the SINR would be considered in choosing the BSs of each user's CS.

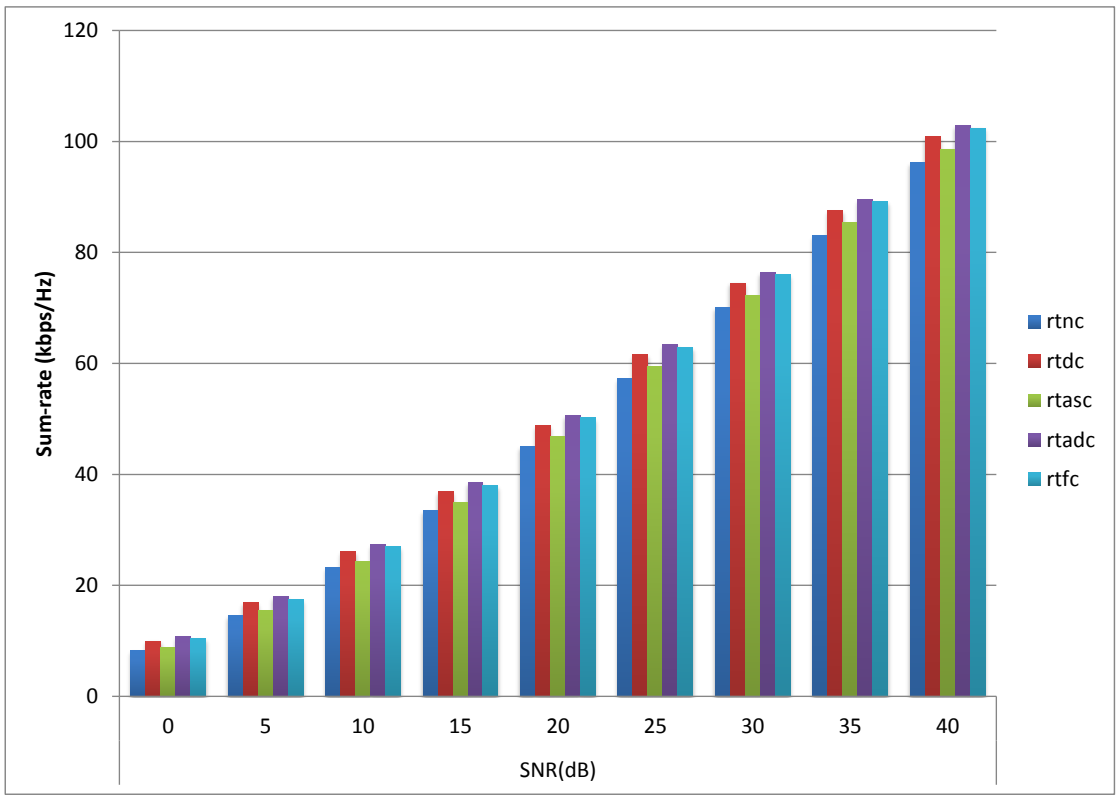

Figure 2.13: Sum-rate performance with $M_t = 4$, $N_r = 2$ and $K = 4$ BS-UE pairs in a user centric CA.

The observed advantage in the sum-rate is expected and can be explained intuitively. For the given set-up in Fig. 2.10, let the number of transmit BSs per user equal to the number of served users per BS for any given value of M_{max}. Assuming an equal total transmit power for each BS, an equal power allocation on each user's data transmission from each BS, zero interference, unit noise power and different channel gains from each BSs to each

user. Then the received signal power when M_{max} = 2 transmit BSs per user would be higher than the received signal power for M_{max} = 4 transmit BSs per user, since more power is allocated to the channel gains with greater strength when M_{max} = 2 and less transmit powers are allocated to both the strong and weaker channel gains when M_{max} = 4.

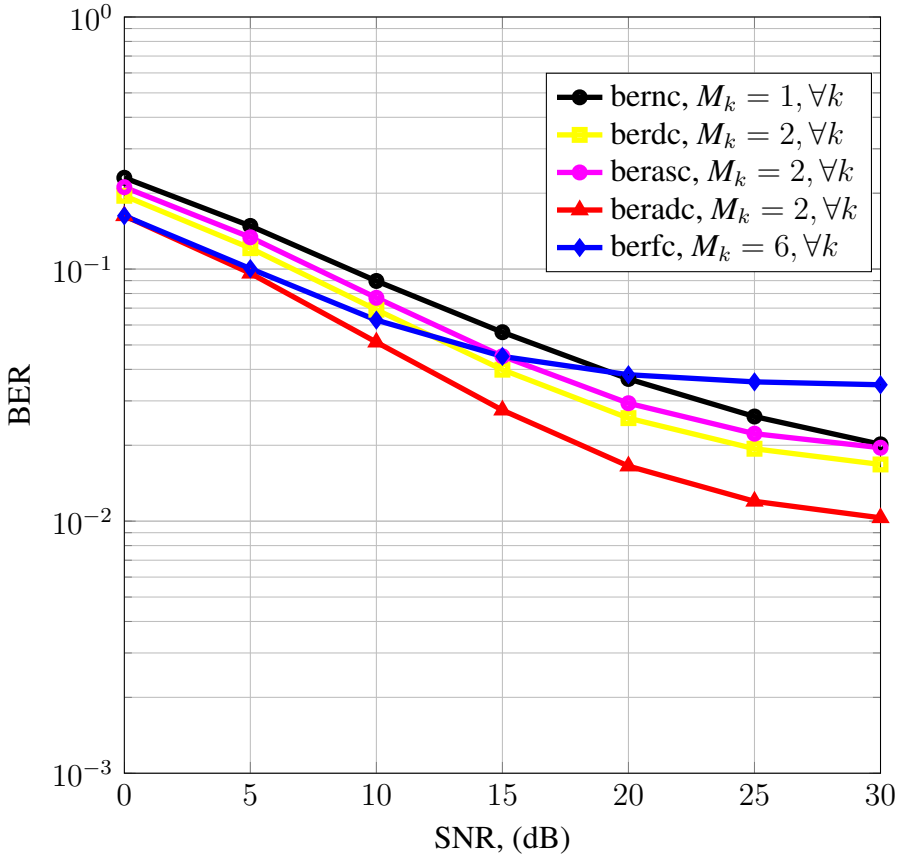

Figure 2.14: BER performance with M_t = 4, N_r = 2 and K = 6 BS-UE pairs in a user centric CA.

This validation can be seen again in Figs. 2.14 and 2.15 when K = 6, as 'beradc' and 'rtadc' offers better performance compared to all other strategies including the network centric approach, non-CoMP transmission and full CoMP transmission. The BER is seen to flatten out at higher SNR values because of unavailable DoF at the transmitter and/or receiver to null the interference within the system. At 30 dB, the achieved sum-rates

for ‘rtnc’, ‘rtdc’, ‘rtasc’, ‘rtadc’ and ‘rtfc’ respectively are 91 kbps/Hz, 86 kbps/Hz, 81 kbps/Hz, 97.5 kbps/Hz and 69 kbps/Hz.

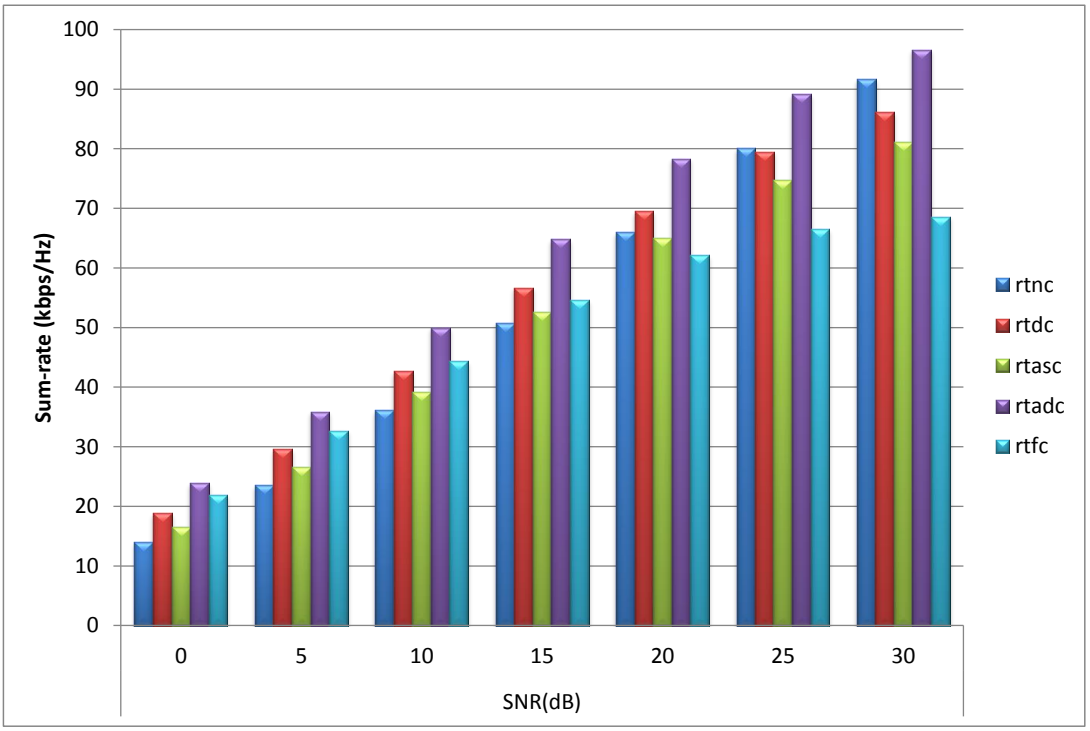

Figure 2.15: Sum-rate performance with $M_t = 4$, $N_r = 2$ and $K = 6$ BS-UE pairs in a user centric CA.

Using a large number of CSs introduces more interference, especially when a limited number of transmit and receive antennas are available for interference cancellation. This can explain why full CoMP transmission is unable to achieve the required gains but rather causes a huge data overhead in the backhaul. As seen in the previous section, ‘rtnc’ (non-CoMP transmission, $M_{max} = 1$) achieved a better sum-rate than ‘rtdc’ (proposed network centric solution, $M_{max} = 2$). But ‘rtadc’ can be seen to achieve a greater sum-rate than ‘rtnc’, using the proposed user centric CS selection for $M_{max} = 2$. Therefore, a reduced size of the CS for each user and a unique selection of the BSs in each user’s CS, allow the users attain a better signal power in severe interference conditions such that the resulting

performance surpasses that obtained with the non-CoMP solution or full CoMP solution.

2.5 Summary

Chapter 2 analysed the standard CoMP transmission technique which required all neighbouring cells to perform CoMP transmission to the users. However, the gains obtained by CoMP transmission is known to be limited by the huge amount of data signalling overhead transfer required in the backhaul, low latency time and tight synchronisation. To obtain a reduction in the data overhead, the number of cluster size (under the network centric approach) and allowed transmit BSs per user (under the user centric approach) was further reduced. Using the proposed clusterisation strategies the size of the clusters or CSs was analysed for M_{max} = 2. The results were compared with the full CoMP transmission for M_{max} = K.

The user centric clustering method allowed more flexibility in choosing the transmit BSs for each user and was shown to outperform the network centric clusterisation method. A significant data overhead reduction was obtained using the proposed user centric CS selection and the sum-rate performance exceeded the performance obtained using full CoMP transmission. The results show that certain conditions like the channel conditions, number of transmit and receive antennas and the power constraints are important factors that need to be considered when choosing the number of transmit BSs per user. This result is significant, but due to the ever increasing growth in wireless devices, higher data rates, real time streaming, amongst others, additional data overhead reduction will be desirable especially if performance can be preserved or exceeded. The possibility of obtaining a further reduction is presented and analysed in Chapter 3 and 4.

Chapter 3

Joint and Adaptive Cooperating Set Selection

CoMP transmission is a fairly recent technology proposed to improve interference mitigation and increase spectral efficiency in the wireless network. In this chapter, the downlink CoMP JT is considered in a multi-cell, multi-user system where multiple BSs transmit data streams to each user. CoMP JT is known to be accompanied by huge requirements on the backhaul network architecture such as low latency, unlimited backhaul capacity, perfect synchronization and low energy consumption. But satisfying all of these conditions seems impossible as the number of BSs transmitting to each user increases, and so the number of transmit BSs per user has to be limited in order to achieve reduced overhead and affordable backhaul capability.

3.1 Introduction

CoMP transmission/reception has been proposed to increase cell-edge and average cell throughputs in cellular network like LTE-A [29, 30, 31]. This technique has been considered as an effective approach for inter-cell interference coordination (ICIC) in LTE-A. The throughput gain promised by CoMP transmission is achieved by serving each

user with a cluster or CS of BSs. A central unit (CU) performs the CS selection and may be co-located with any BS within the network. As shown in the previous chapter, CoMP JT uses multiple BSs simultaneously to transmit data to multiple users in the network while performing IC to eliminate unwanted data signals to other users [32], whereas coordinated beamforming/scheduling transmission uses beam-formers to avoid interference or schedules transmission to only a single user at a given time hence requiring no IC [33]. The selection of the CSs for each user in CoMP JT is mainly dependent on the wireless channel characteristics and can be either static or dynamic [34, 18, 35]. In the case of static CS selection, a pre-set CS for each user is saved into the network and does not adapt to the time-varying channel while in dynamic CS selection, the CS for each user is selected based on the channel characteristics of the entire network and automatically adapts using the configured scheduling algorithm as the channel varies with time. To achieve the aforementioned gains using dynamic CSs for CoMP transmission, the CSI, precoding information, coordination information, user signalling has to be exchanged thereby causing an increased backhaul capacity requirement and a stringent latency constraint which is almost impossible to attain with an increased number of serving BSs per user. As shown in Chapter 2, as the number of BSs transmitting to a given user increases, the system performance does not always improve in a linear fashion, but the overhead does increase linearly. The trade-off of performance gain to increased data overhead is very costly and so choosing an appropriate number of BSs to perform CoMP transmission is necessary to reduce the overhead in the CoMP system [36]. But finding the optimal maximum number of transmitting BSs in a CS, that would preserve the performance advantage of CoMP transmission still remains a challenge [13].

The contributions of this chapter are as follows: Firstly, a joint and adaptive solution that considers the dynamic nature of the channel conditions, QoS constraints and the location of all users within the system, while simultaneously assigning CSs of different sizes to each user and also limiting the maximum number of possible transmit BSs per user to (M_{max}) is proposed [37]. Secondly, the CS selection is obtained by optimising one of the two criteria i.e., either a) maximization of sum rate with a total power constraint or

b) minimization of total transmit power with a given target rate. Thirdly, by increasing the maximum number of allowed BSs/user in a step-wise manner, from $M_{max} = 1$ to $M_{max} = K$ (i.e. non-CoMP transmission to full CoMP transmission), the total increase in energy consumption and data overhead is analysed and the best value of M_{max} that can satisfy both optimization problems with lower cost implication is deduced, based on the given system set-up.

The remaining parts of this chapter are organised as follows: The system model is shown in Section 3.2. The beam-former design, power allocation and corresponding network costs are presented in Section 3.3. The proposed joint and adaptive CS selection is presented in Section 3.4 using two different optimisation strategies and the simulation results are evaluated in Section 3.5. Finally this chapter is concluded in Section 3.6.

3.2 System Model

Consider a multi-cell, multi-user network with K BS-UE pairs as shown in Figs. 3.1 and 3.2. Each BS and cell-edge UE are equipped with M_t and N_r transmit and receive antennas respectively and the number of BSs scheduled to transmit to user k is $1 \leq M_k \leq M_{max}$, where M_{max} is the maximum number of serving BS allowed per user and M_k is the number of transmit BSs to user k.

Let $\mathbf{H}_k = [\mathbf{H}_{k,1}, \mathbf{H}_{k,2}, ..., \mathbf{H}_{k,K}]$, be the flat-fading channel matrix between the user k and all K transmit BSs. The coefficients of $\mathbf{H}_{k,m}, m = 1, \cdots K, \in \mathbb{C}^{N_r \times M_t}$ are complex random variables, with zero-mean Gaussian real and imaginary parts. The channel links experience large scale fading, with path loss exponent (α). Let $\mathbf{U} = [\mathbf{u}_1, ..., \mathbf{u}_K]$ be the matrix containing all the beamforming column vectors $\mathbf{u}_k$ of user k. Let $\mathbf{V} = [\mathbf{V}_1^T, ..., \mathbf{V}_K^T]^T$ be the matrix containing all the precoding matrices $\mathbf{V}_m = [\mathbf{v}_{m,1}, ..., \mathbf{v}_{m,K}]$ of BS m where the column vector $\mathbf{v}_{m,k}$ is used to precode the data of the k-th user from the m-th BS. Also $\mathbf{P} = [\mathbf{p}_1^T, ..., \mathbf{p}_K^T]^T$ is the power allocation matrix where $\mathbf{p}_m = [\rho_{m,1}, ..., \rho_{m,K}]^T$ and $\rho_{m,k}$ is the power allocated to the k-th user's data at the m-th BS.

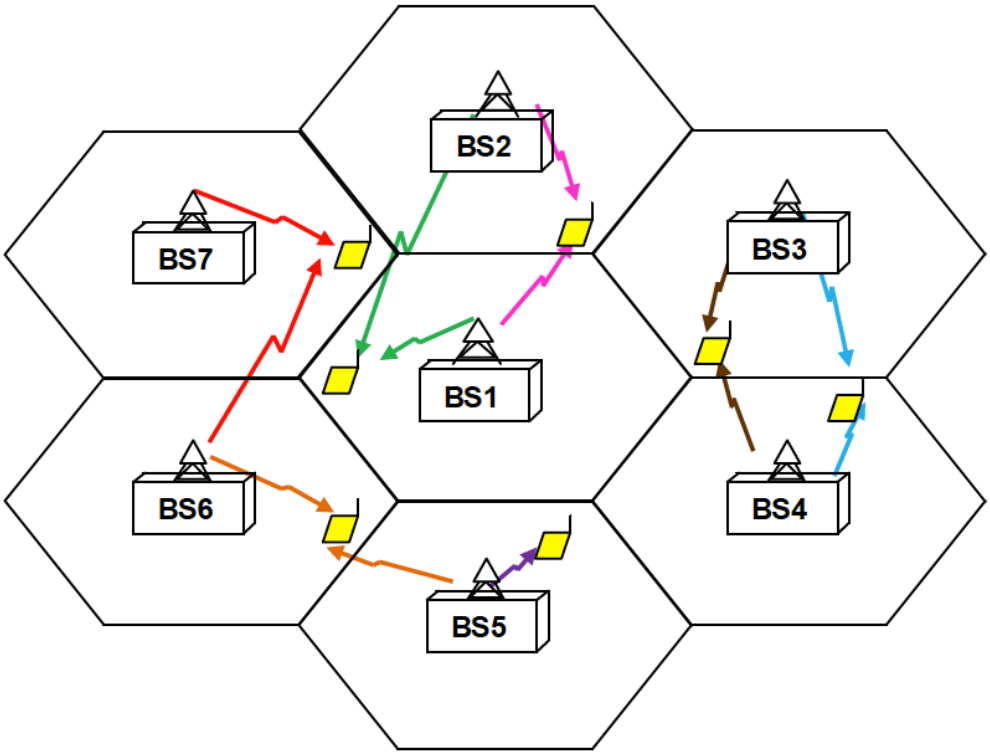

Figure 3.1: CoMP transmission in a multi-cell multi-user network on a shared RB, $K = 7$ BS-UE pairs with $M_{max} = 2$.

The optimisation problems considered in this chapter are based separately on two major cost functions: i.) the sum-rate of the network and ii.) the power consumption of the network. These two cost functions are important as they separately focus on the ouput function (user focused) and the input function (network focused). In both cases, the major aim is to find the CS selection matrix (Δ) that meet the objectives of the optimisation problems. The two optimisation problems considered in this chapter are: i) the sum-rate maximisation problem as shown in (3.2.1) and ii) the total power minimisation with given target rates as shown in (3.2.2). Considering the two optimisation problems separately, the aim of the proposed CS selection strategy is to jointly obtain the CS of all users as well as the corresponding beamforming, precoding and power allocation matrices that satisfy either of the optimization problems:

$$\max_{\Delta,\mathbf{U},\mathbf{V},\mathbf{P}} \sum_{k=1}^{K} R_k \quad s.t., \sum_{k=1}^{K}\sum_{m=1}^{K} \rho_{k,m} = P_{max} \quad \text{or} \tag{3.2.1}$$

$$\min_{\Delta,\mathbf{U},\mathbf{V},\mathbf{P}} \sum_{k=1}^{K}\sum_{m=1}^{K} \rho_{k,m} \; s.t., \; R_k \geq \phi_k, \; \forall k \in [1,2,\cdots,K]. \tag{3.2.2}$$

where R_k is the rate of user k and R_T is the sum-rate (see (2.3.13)), P_{max} is the total power constraint and ϕ_k is the k-th user's target rate.

So at user k, the received signal y_k after post-processing by the receive beamforming vector $\mathbf{u}_k$ is given by:

$$\mathbf{u}_k^H \mathbf{y}_k = \sum_{m=1}^{K} \mathbf{u}_k^H \mathbf{H}_{k,m} \mathbf{v}_{m,k} \sqrt{\rho_{m,k}} \delta_{m,k} s_k + \sum_{m=1}^{K} \sum_{\substack{p=1 \\ p \neq k}}^{K} \mathbf{u}_k^H \mathbf{H}_{k,m} \mathbf{v}_{m,p} \sqrt{\rho_{m,p}} \delta_{m,p} s_p$$

$$+ \mathbf{u}_k^H \mathbf{n}_k, \quad \forall k \in [1,2,\cdots,K]. \tag{3.2.3}$$

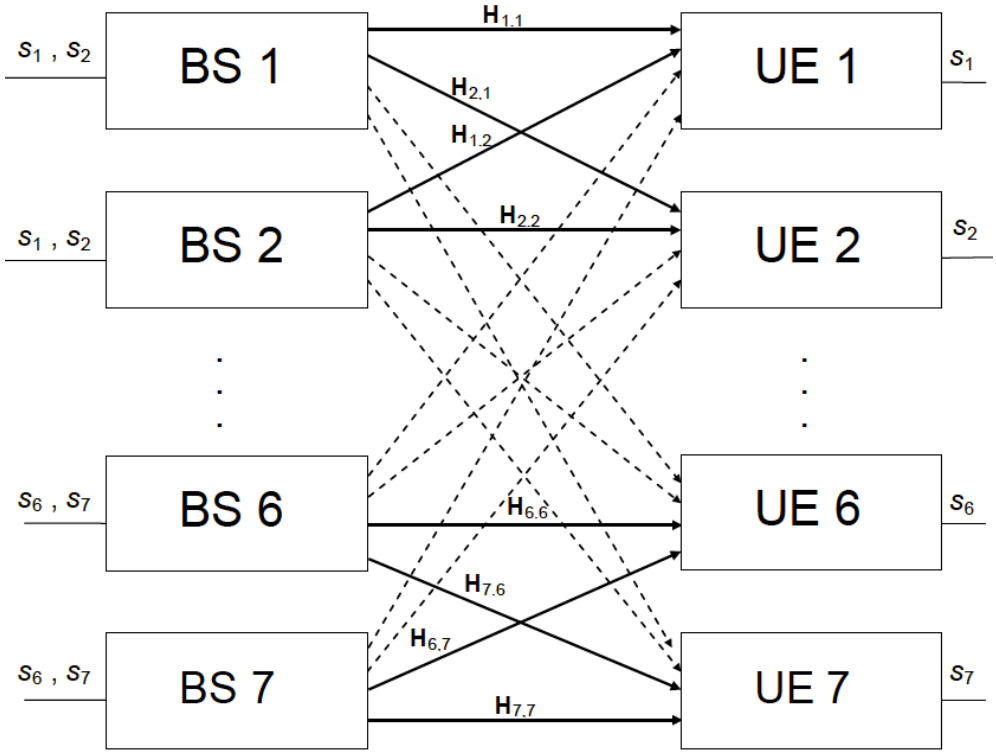

Figure 3.2: The MIMO CoMP transmission system with $K = 7$ BS-UE pairs and $M_{max} = 2$ (i.e., each user receives "wanted data" from a max. of 2 BSs).

where s_k is the complex (scalar) data signal destined for the k-th user and $\mathrm{E}\{|s_k|^2\} = 1$

and $\mathbf{n}_k$ is an additive, zero-mean, white, complex Gaussian noise vector with a variance of σ_k^2 for each element. The CS of a user is defined as the subset of BSs scheduled to simultaneously transmit data to that user. Finally, the "BS serving factor" ($\delta_{m,k}$) and the "CS selection matrix" (Δ) are respectively defined as:

$$\delta_{m,k} = \begin{cases} 1, & \text{if BS } m \text{ serves user } k \\ 0, & \text{otherwise.} \end{cases} \tag{3.2.4}$$

$$\text{and } \Delta = \begin{bmatrix} \delta_{1,1} & \delta_{1,2} & \cdots & \delta_{1,K} \\ \vdots & \ddots & \ldots & \vdots \\ \delta_{K,1} & \delta_{K,2} & \cdots & \delta_{K,K} \end{bmatrix}. \tag{3.2.5}$$

In (3.2.3), the first term on the right hand side (RHS) is the useful signal while the second term is the received co-channel interference (CCI) which needs to be eliminated by using appropriate precoders and receive beamformer. The SINR at the k-th UE is derived as:

$$\text{SINR}_k = \frac{\sum_{m=1}^{K} \left|\mathbf{u}_k^H \mathbf{H}_{k,m} \mathbf{v}_{m,k}\right|^2 \rho_{m,k} \delta_{m,k}}{\sum_{m=1}^{K} \sum_{\substack{p=1 \\ p \neq k}}^{K} \left|\mathbf{u}_k^H \mathbf{H}_{k,m} \mathbf{v}_{m,p}\right|^2 \rho_{m,p} \delta_{m,p} + \sigma_k^2}. \tag{3.2.6}$$

3.3 Beam-former Design, Power Allocation, Energy Consumption and System Overhead

The main focus of this chapter is to obtain the CSs that meets the objectives as stated in Section 3.1 and then analyse the obtained results. However to achieve this, the beam-former design and power allocation are required. Firstly, a simple pre-coder design and power allocation strategy are reviewed and then the energy consumption and system overhead needed for analysis are defined.

3.3.1 Beam-former Design

In (3.2.6), it can be observed that the SINR of each user k depends on all the precoding vectors. Therefore using the SINR as an optimisation metric to obtain the precoding vectors would lead to a coupled, complex, joint optimisation problem. This can be avoided by selecting the precoding vectors based on the SLNR [38, 23, 39]. To obtain the pre-coders and receive beam-formers required to maximise the SLNR, the leakage power to other users needs to be minimised (refer to Section 2.1.2). Using the same idea in Section 2.1.2, $\mathbf{v}_{m,k}$ is chosen to be the eigenvector corresponding to the minimum eigenvalue of:

$$\sum_{\substack{p=1 \\ p\neq k}}^{K} \mathbf{H}_{p,m}^{H}\mathbf{u}_p\mathbf{u}_p^{H}\mathbf{H}_{p,m}, \forall\, m,\, k \in [1, 2, \cdots, K],\ \text{if } \delta_{m,k} = 1, \tag{3.3.7}$$

and $\mathbf{u}_k$ is chosen to be the eigenvector corresponding to the minimum eigenvalue of:

$$\sum_{m=1}^{K}\sum_{\substack{p=1 \\ p\neq k}}^{K} \mathbf{H}_{k,m}\mathbf{v}_{m,p}\delta_{m,p}\mathbf{v}_{m,p}^{H}\mathbf{H}_{k,m}^{H}, \forall\, k \in [1, 2, \cdots, K]. \tag{3.3.8}$$

3.3.2 Power Allocation

The power allocation shown below is obtained separately based on one of the two optimisation problems.

- find $\{\rho_{m,k}\}_{m,\,k=1}^{K}$ that maximises $\sum_{k=1}^{K} R_k$, s.t. $\sum_{m=1}^{K}\sum_{k=1}^{K} \rho_{m,k} = P_{max}$
- find $\{\rho_{m,k}\}_{m,\,k=1}^{K}$ that minimises $\sum_{m=1}^{K}\sum_{k=1}^{K} \rho_{m,k}$ s.t $R_k \geq \phi_k$, where ϕ_k is the target rate of user k.

Power allocation based on the sum-rate maximisation with power constraints

Consider the system model as described in Section 3.2, while assuming perfect CSI and complete nulling of interference using the precoder design described in Section 3.3.1.

From (3.2.6), let σ_k^2 = 1 and $\beta_{m,k} = \left|\mathbf{u}_k^H \mathbf{H}_{k,m} \mathbf{v}_{m,k}\right|^2$. The optimisation problem is to find the power allocation matrix **P**, given a total power constraint, P_{max} such that the sum rate is maximised [40]. That is,

$$\max_{\mathbf{P}} \sum_{k=1}^{K} \log_2 \left(1 + \sum_{m=1}^{K} \beta_{m,k}\rho_{m,k}\right) \; s.t., \; \sum_{m=1}^{K}\sum_{k=1}^{K} \rho_{m,k} \leq P_{max}, \\ \rho_{m,k} \neq 0 \text{ if } \delta_{m,k} = 1. \tag{3.3.9}$$

Finding the optimum **P** to solve (3.3.9) is complex. A simple, suboptimal approach is to maximise the total sum rate as follows. Intuitively, assuming the total power (P_{max}) is used for transmission, then the individual power allocation can be obtained by allocating P_{max} across all the user data streams in proportion to the "effective gain" ($\beta_{m,k}$) in (3.2.6) to maximise the sum-rate (R_T) in (2.3.13). Following this approach, it is not difficult to show that [41]:

$$\rho_{m,k} = P_{max} \left(\beta_{m,k} / \sum_{k=1}^{K}\sum_{m=1}^{K} \beta_{m,k}\right), \forall \; m, \; k \in [1, 2, \cdots, K]. \tag{3.3.10}$$

Power allocation based on total power minimisation with constraint on user rate

Here, the optimisation problem is to minimise the total transmit power subject to achieving the target rate, (ϕ_k) for user k [40], where the target rate depends on the QoS requirement of the given user. That is,

$$\min_{\mathbf{P}} \sum_{m=1}^{K}\sum_{k=1}^{K} \rho_{m,k} \;\; s.t., \; R_k \geq \phi_k \; \forall k \in [1, 2, \cdots, K]. \tag{3.3.11}$$

To achieve the user target rate in (3.3.11), then $\text{SINR}_k \geq \bar{\gamma}_k$ where $\bar{\gamma}_k = (2^{\phi_k} - 1)$ becomes the target SINR for user k. Again assuming complete interference zero-forcing, σ_k^2 = 1 and $\beta_{m,k} = \left|\mathbf{u}_k^H \mathbf{H}_{k,m} \mathbf{v}_{m,k}\right|^2$, the optimisation problem can be re-written as:

$$\min_{\mathbf{P}} \sum_{m=1}^{K}\sum_{k=1}^{K} \rho_{m,k} \; s.t., \; \sum_{m=1}^{K} \beta_{m,k}\rho_{m,k} \geq \bar{\gamma}_k \text{ and } \rho_{m,k} > 0 \tag{3.3.12}$$

Since this is a linear programming problem, interior point methods [40] can be used to obtain $\{\rho_{m,k}\}_{m,\,k=1}^{K}$ that satisfy (3.3.11) and (3.3.12). Note that other linear optimisation

solvers such as the dual-simplex, simplex and active-set methods can be used. However, the interior point method was chosen since it is faster and uses less memory than the simplex and active-set methods [42].

3.3.3 Energy Consumption

This section highlights the model used to estimate the energy consumption required to transmit the user data signal using CoMP transmission. It takes into account the power consumed by the BS (P_{BS}), the power consumed in the backhaul through fiber optic data transmission (P_{bh}) and the total transmit power in the given network (P_T). The power consumption of a BS, (P_{BS}) is given as [43]:

$$P_{BS} = a_p P_r + b_p + c_p. \tag{3.3.13}$$

Here P_r is the average radiated power of a BS, a_p is the power consumption that scales with the BS transmit power due to the radio frequency amplifiers and feeder losses, b_p is the power due to signal processing and cooling while c_p is the power consumption of the small-form factor pluggable (SFP) used to transmit over the backhaul fiber [43]. The total power consumed in the backhaul (P_{bh}) while transmitting data at a given rate R_{bh} is proportionally dependent on the number of users served at each BS k. As the backhaul traffic increases the backhaul power increases. In this chapter, for ease of analysis, P_{bh} in [43] is simplified with:

$$P_{bh} = \sum_{k=1}^{K} \sum_{m=1}^{K} \delta_{m,k} P_{sw}. \tag{3.3.14}$$

where P_{sw} is the maximum power consumption of the communication switch. Hence the total energy consumption per BS, (E_T) in a unit of time is:

$$E_T = \frac{1}{K} \left(K P_{BS} + P_{bh} + P_T \right), \tag{3.3.15}$$

where P_T can be obtained from finding $\mathbf{P}$ in (3.3.10) and (3.3.12):

$$P_T = \sum_{k=1}^{K} \sum_{m=1}^{K} \rho_{m,k}. \tag{3.3.16}$$

3.3.4 System Overhead

For the purpose of this work, the backhaul overhead is defined as the associated data or backhaul load required in the backhaul network when performing data transmission within a given network at a given time. This includes the data load required when sharing users' data signals and precoding information. Since the overhead increases linearly as the number of transmit BSs per user increases, the overhead factor, (O), is a measure of the observed backhaul load during CoMP transmission, which is dependent on the average number of transmit BSs per user at a given time. The overhead factor is represented as the following ratio:

$$O = \frac{1}{K}\sum_{k=1}^{K} M_k. \tag{3.3.17}$$

For non-CoMP transmission, the overhead factor obtained is 1, since each user is served by one BS ($M_k = 1, \forall k$).

3.4 Cooperating Set Selection

From Chapter 2, it was shown under the user centric approach that reducing the number of M_{max} from 4 BSs/user to 2 BSs/user, with the proposed CS selection strategy, achieved a 50% reduction in data overhead under the given system model, yet the obtained overall performance was better than using M_{max} = 4 BSs/user. Since the user's location and channel conditions are dynamic, this means that the user may experience good channel conditions at different times and the QoS constraint may still be achieved with a single data transmission (i.e. non-CoMP transmission). How can the size and BSs for each user's CS be identified, such that the optimisation problem or QoS constraints are met? With this in mind, the objectives of this section are motivated and the proposed CS selection is user centric. The CS of a user is defined as the subset of BSs scheduled to simultaneously transmit data to that user. The proposed CS selection strategy allows any BS to be included in as many CSs as possible while noting that each user is allowed

a maximum of M_{max} BSs in its CS. The two optimisation problems considered for the purpose of this work are given in 3.2.1 and 3.2.2. This section proposes the CS selection algorithm that would obtain a joint CS selection for all users; and using the beamforming and power allocation solutions presented in Section 3.3, the corresponding transmit and receive beam-formers as well as the power allocation solution would be obtained.

To obtain the optimum solution would require using a search algorithm over the total number of possible solutions (N_{TS}), where N_{TS} is:

$$N_{TS} = \left(\sum_{m=1}^{M_{max}} \left(\frac{K!}{m!\,(K-m)!} \right) \right)^{K}. \tag{3.4.18}$$

This search is NP-hard and therefore not solvable with practical complexity although it can still be solved for smaller values of M_{max} and K. For instance, if K = 7 and M_{max} = 4, 5, 6 and 7 respectively, $N_{TS} = [8.68, 33.8, 50.4, 53.3] \times 10^{13}$ respectively. In this chapter, the main focus is obtaining a joint CS selection for all the users' data transmission. It is important to measure the proposed algorithm against the hard search algorithm to determine how effective and efficient the proposed solution is. Therefore, the proposed solution which is heuristic and sub-optimal would be compared to the "optimum CS selection" in Chapter 4. The proposed CS selection algorithm as summarised in Table 3.1, performs the CS selection to the optimisation problems in (3.2.1) and (3.2.2) with much lower complexity and faster convergence. The optimum solution to the optimisation problem in (3.2.1) and (3.2.2) requires a joint solution for Δ (the CS selection matrix), **U** and **V** (the receive and transmit beam-formers) and the power allocation matrix **P**. To reduce the complexity, the proposed solution decouples the problems in (3.2.1) and (3.2.2) into sub-problems to allow disjoint solutions to **U, V** and **P** to be obtained as shown previously in Section 3.3. The proposed CS selection is presented in Section 3.4.1.

3.4.1 Proposed CS Selection Algorithm

The sub-optimal joint solution to Δ, that solves the given optimisation problem is obtained by searching through a significantly reduced set of possible solutions. The proposed

algorithm begins the search by assigning a single transmit BS with the best channel quality to each user. Then the iterative algorithm aims to improve the obtained performance by assigning more BSs to the users with lower performance than the given QoS constraint (users' sum-rate) or network set threshold (maximum power consumption threshold).

Table 3.1: CS selection algorithm (based on sum-rate maximization or total power minimization).

Initialization: $i = 0$, $R_T^{(i)} = 0\,(P_T^{(i)} = \infty)$, $\left\{g_k^{(i)}\right\}_{k=1}^{K} = -1$, $g_{avg}^{(i)} = 0$, $\left\{f_k^{(i)}\right\}_{k=1}^{K} = 0$, $x^{(i)} = 1$.

while any $(g_k^{(i)} < g_{avg}^{(i)})$

if $x^{(i)} \neq 0$

1. Find $\Delta^{(i+1)}$

for $k = 1 : K$

if $g_k^{(i)} < g_{avg}^{(i)}$ and $f_k^{(i)} < M_{max}$

$f_k^{(i+1)} = f_k^{(i)} + 1$,

$\delta_{m,k}^{(i+1)} = 1$, if BS m has the best channel quality to user k and $\delta_{m,k}^{(i)} = 0$.

end if, **end for**

2. Find $\mathbf{U}^{(i+1)}$, $\mathbf{V}^{(i+1)}$ and $\mathbf{P}^{(i+1)}$ using algorithms introduced in Section 3.3.

3. Find $g_k^{(i+1)} = \sum_{m=1}^{K} \beta_{m,k}^{(i+1)}$ and $R_T^{(i+1)}(P_T^{(i+1)})$ from (2.3.13)/(3.3.16).

if $R_T^{(i+1)}(-P_T^{(i+1)}) > R_T^{(i)}(-P_T^{(i)})$

$\Delta \leftarrow \Delta^{(i+1)}$, $\mathbf{U} \leftarrow \mathbf{U}^{(i+1)}$, $\mathbf{V} \leftarrow \mathbf{V}^{(i+1)}$, $\mathbf{P} \leftarrow \mathbf{P}^{(i+1)}$, $R_T(P_T) \leftarrow R_T^{(i+1)}(P_T^{(i+1)})$

end if

$g_{avg}^{(i+1)} = \frac{1}{K}(\sum_{k=1}^{K} g_k^{(i+1)})$, $x^{(i+1)} = \sum_{k=1}^{K}(f_k^{(i+1)} - f_k^{(i)})$, $f_k^{(i+1)} = f_k^{(i)}\ \forall k$, i++.

end if

end while.

4. Repeat steps 1-3 till convergence.

The variables are initialised as shown in Table 3.1, where *i* is the iteration count, $x^{(i)}$ is the convergence variable of the algorithm, f_k is the number of assigned BSs to user *k* and g_{avg} is the average "effective gain". Assign the BS with the best channel quality to each user to obtain $\Delta^{(i+1)}$ and find the corresponding solutions $\mathbf{U}^{(i+1)}$, $\mathbf{V}^{(i+1)}$ and $\mathbf{P}^{(i+1)}$. At each iteration, using the proposed scheduling algorithm, BSs are assigned to each user to maximise the "effective gain" ($g_k = \sum_{m=1}^{K} \beta_{m,k}$). The "effective gain" of each user *k* (i.e. g_k) is maximised by assigning another BS to user *k* when $g_k < g_{avg}$. This can be explained intuitively. In other to achieve a total power minimisation, the required transmit power needed to achieve a given target rate reduces as the "effective gain" increases. Also, for sum-rate maximisation, given a total power constraint, the achieved sum-rate increases as the "effective gain" increases. This process is done iteratively until the maximum number of transmit BSs per user is reached and no BS assignment is possible. The Δ and corresponding **U, V** and **P** that best solve each optimisation problem is selected as the CS for the users required for CoMP transmission.

3.5 Simulation Results and Evaluation

Table 3.2: Summary of simulation parameters.

Parameters	**Value**
Antenna layout	Omnidirectional
Inter site distance (ISD)[3]	500m
Users per cell	1, distributed randomly
Reference distance (D_o)	260 m
Distance of UE to BS pair	$D_{k,k} > D_o$
Path loss coefficient (α)[4]	2
Number of antennas (M_t, N_r)	(7,2)
Transmission scheme	CoMP (M_{max} =1:*K*)
$\bar{P}_{sw}$[43]	300W

$\bar{P}_r$[43]	43dBm (20W)
a_p[43]	21.45W
b_p[43]	354.44W
c_p [43]	1W

In this section, a range of simulation results are used to evaluate the reduction achieved in the data overhead and energy consumption under the given optimisation problems, while taking into account the attained sum-rate performance or target user rate. This is done by considering different maximum number of BSs per user (M_{max}), i.e. M_{max} = [1, 2, $\cdots$, K]. Using the assumed parameters in Table 3.2, for K = 7, M_t = 7 and N_r = 2, the obtained results are shown in Figs. 3.3 - 3.7. The CSs are obtained for all users and each user is served with a maximum of M_{max} BSs (i.e. $M \leq M_{max}$, $M = \{M_1, \cdots, M_K\}$), using the proposed CS scheduling algorithm in Table 3.1. The proposed CS scheduling algorithm is compared to a system which uses the conventional CoMP transmission, where all users are served with M_{max} BSs at any given time (i.e. $M = M_{max}$). The following parameters: sum-rate (R_T), average energy consumption (E_T) and the average overhead (O) are used to present the simulation results.

For the optimization problem in (3.2.1), the following values of P_{max} are considered for simulation: 0.07 kW, 0.7 kW and 7 kW. The results obtained for sum-rate performance, energy consumption and data overhead are shown in Figs. 3.3, 3.4 and 3.5 respectively. The results are obtained under the sum-rate maximisation problem with given total power constraint. In Fig. 3.3, one can observe that the sum-rate performance of the proposed strategy slightly exceeds the conventional solution for different values of P_{max}, as the number of M_{max} increases. Although the maximum number of BSs is used for data transmission, a better sum-rate performance under the conventional solution is not

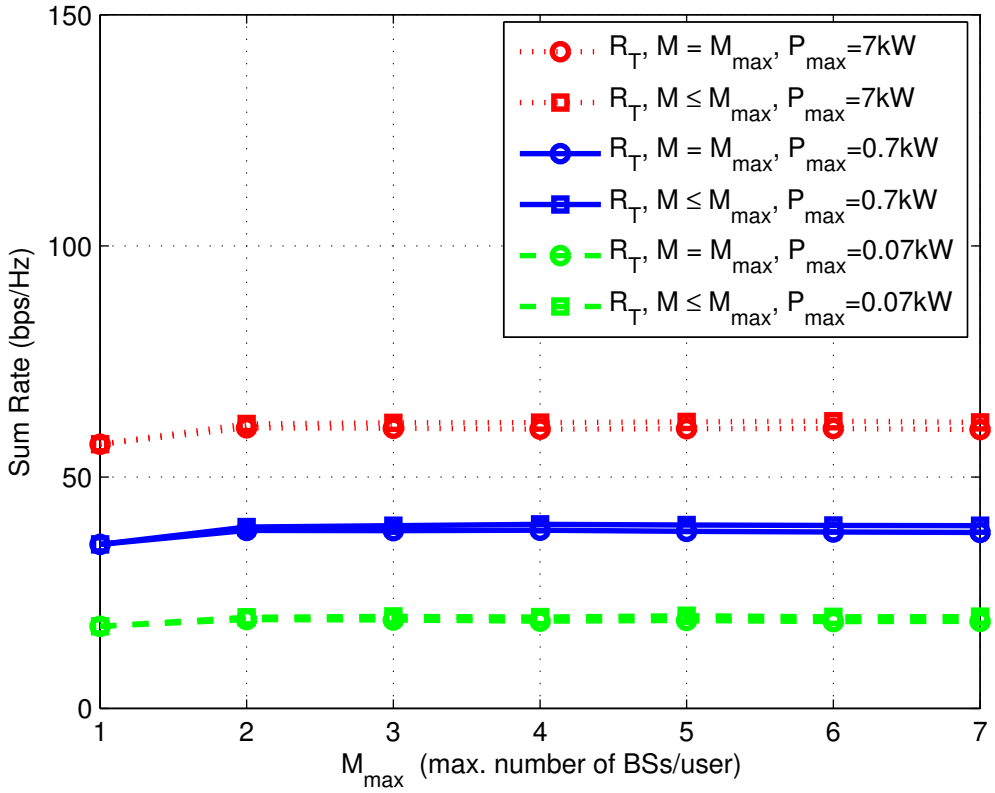

Figure 3.3: Sum-rate performance with $K = 7$, $M_t = 7$ and $N_r = 2$, under the sum-rate maximisation problem.

guaranteed. This is because under the total power constraint, more power is given to less number of BSs with larger "effective gain" as opposed to less power allocation to a greater number of BSs with decreasing "effective gain". Also, as seen in Fig. 3.4 for different values of P_{max}, as M_{max} increases the energy consumption under the conventional solution ('$M = M_{max}$'), is seen to increase linearly. However the energy consumption using the proposed strategy ('$M \leq M_{max}$') is seen to have an almost constant value even for high values of M_{max}.

In Fig. 3.5, the required data overhead can be analysed using the results obtained. As the value of M_{max} increases, the data overhead increases linearly under the conventional solution for all values of P_{max}. However, the data overhead results obtained using

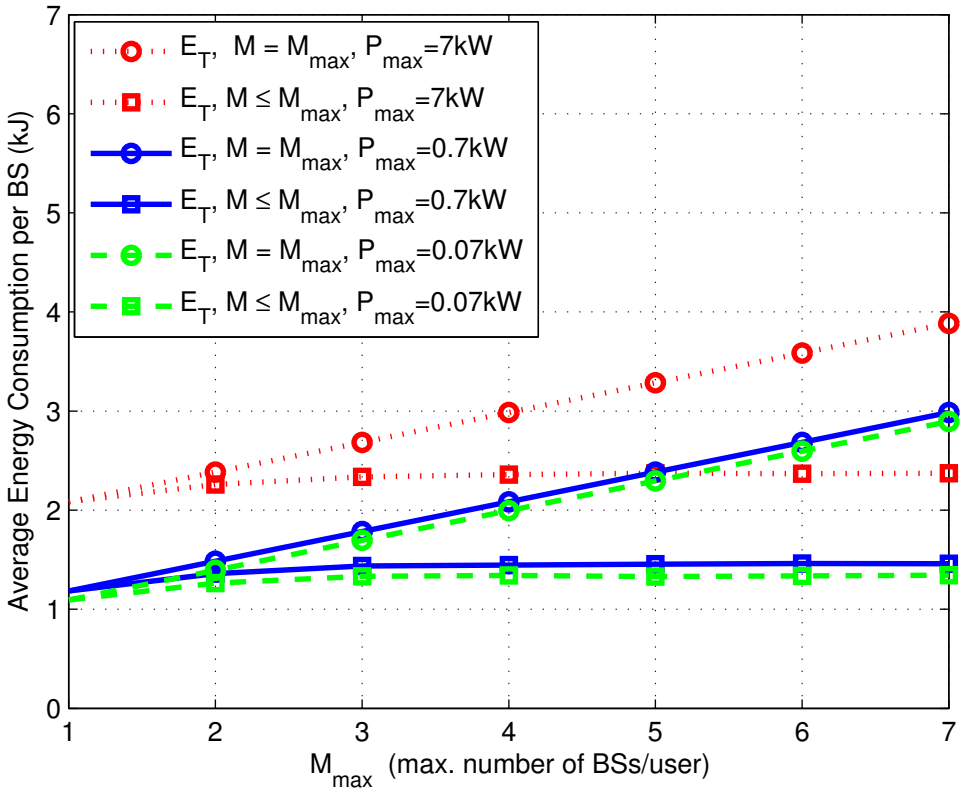

Figure 3.4: Average energy consumption with $K = 7$, $M_t = 7$ and $N_r = 2$, under the sum-rate maximisation problem.

the proposed solution for different values of P_{max}, is seen to increase then peak at approximately 200% from $M_{max} = 3$ to 7. For instance when $M_{max} = 3$ and $P_{max} =$ 0.07 kW, the sum-rate performance obtained for a given RB is about 20 bps/Hz for both the conventional and proposed strategy, however the data overhead required is 300% and 200% respectively and the corresponding energy consumed is 1.7 kJ and 1.3 kJ respectively.

Considering the total power minimisation problem with a given target user in (3.2.2), the following values of ϕ are considered for simulation: 2 bps/Hz, 7 bps/Hz and 10 bps/Hz. The same target rate ($\phi_k = \phi$, $\forall k$) is assumed for all users. The energy consumption and data overhead are shown in Fig. 3.6 and Fig. 3.7 respectively.

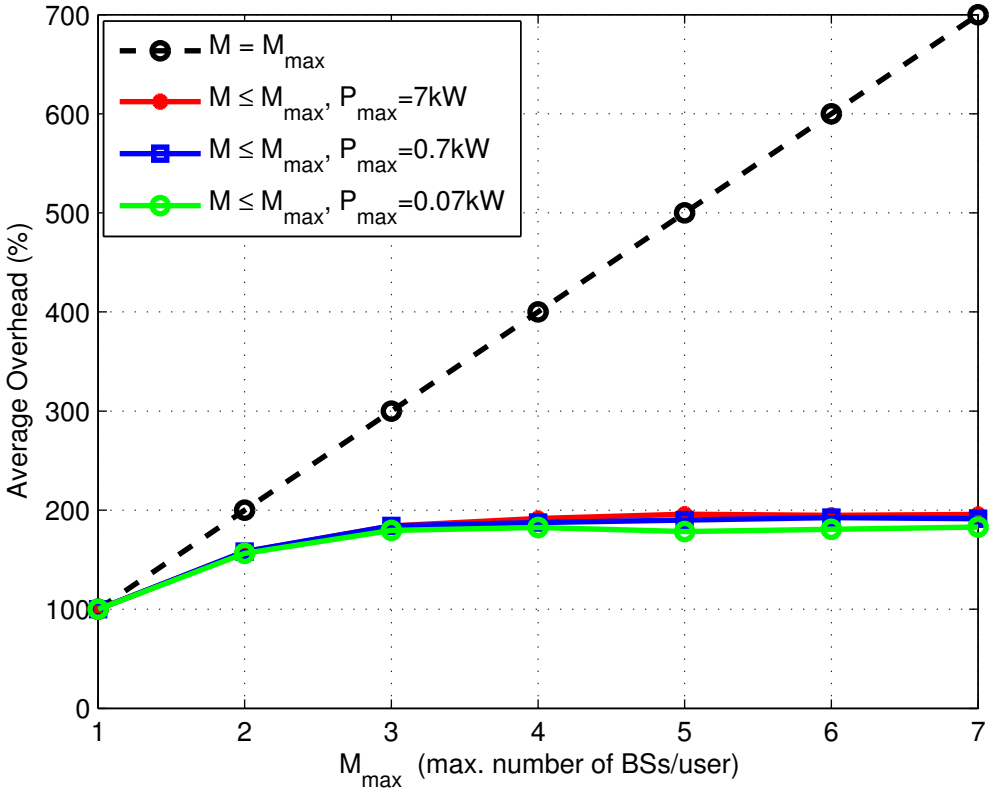

Figure 3.5: Average overhead with $K = 7$, $M_t = 7$ and $N_r = 2$, under the sum-rate maximisation problem.

Now comparing the proposed solution ('$M \leq M_{max}$') to the conventional solution ('$M = M_{max}$'), for different target rates one can observe an almost constant energy consumption and data overhead for '$M \leq M_{max}$' as opposed to a linear increase achieved with '$M = M_{max}$'. But when ϕ = 10 bps/Hz and $M_{max} = 1$, a high energy consumption per BS is observed and E_T = 13kJ. This is because for the given target rate, the required transmission power P_T needed to achieve the desired rate is very high while using a single transmitting BS to each user and since $P_T >> P_{BS} + P_{sw}$ the energy spike occurs for $M_{max} = 1$. However for $M_{max} \geq 2$, the average energy consumed per BS increases linearly for '$M_k = M_{max}$', but the average energy flattens out for '$M_k \leq M_{max}$'.

For example to achieve a given target rate of ϕ= 10 bps/Hz on a given RB, when M_{max} = 3, a data overhead of 300% is required using the conventional solution as opposed to 150% using the proposed CS selection. Also the corresponding energy consumption per BS is 8 kJ as opposed to 5.4 kJ. This shows that under certain QoS constraints, the users may not require full CoMP transmission to achieve the required targets even for a low value of M_{max}. Also if the CSs are chosen jointly, the best CS selection for each user can be obtained such that the lowest cost to the network is required to achieve the best performance.

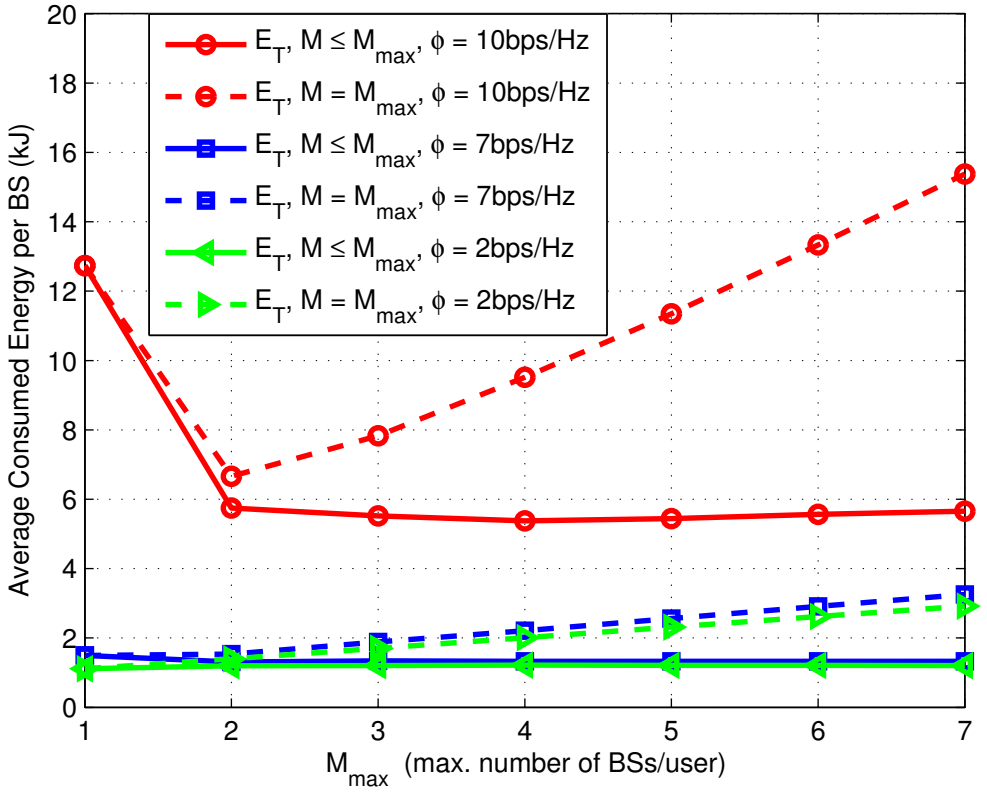

Figure 3.6: Average energy consumption with K = 7, M_t = 7 and N_r = 2, under the total power minimisation problem.

Based on the results obtained under both optimisation problems, the best value of M_{max} that generally satisfies both optimisation problems presented in this chapter, with minimum cost to the network operator is when M_{max} is 2. At M_{max} = 2, a better output

sum-rate is achieved with a reduced input cost (i.e. the energy consumed and the overhead required) compared to other values of M_{max}.

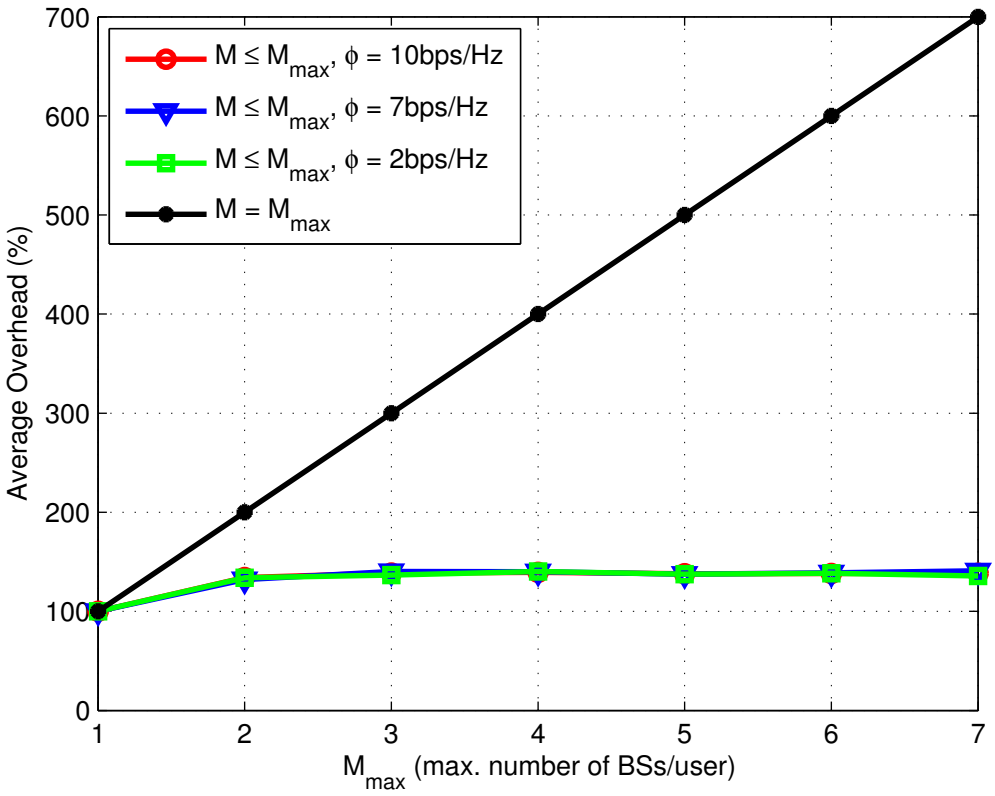

Figure 3.7: Average overhead with $K = 7$, $M_t = 7$ and $N_r = 2$, under the total power minimisation problem.

3.6 Summary

This chapter has proposed a heuristic CS selection algorithm that achieves the joint CS selection with a significant reduction in the complexity since the optimum joint solution is known to be very complex and highly computational. In this chapter, a further reduction in the overhead has been achieved in the backhaul network and this reduction has led to a corresponding decrease in the consumed energy required for data transmission. The achieved reduction obtained in the associated network costs is significant, it shows that

a joint and adaptive CS selection for CoMP transmission enables different numbers of transmit BSs to be allocated to each user based on the system conditions and the users' demands.

Obtaining a green cellular network is very important for current and future wireless communication networks, and this can be achieved by improving the power efficiency of the cellular network. Also perfect synchronisation, low latency and improved performance are all important factors for current and future wireless network systems. This chapter has shown that the proposed technique under CoMP transmission is capable of alleviating the problem of high data overhead in the network as well as energy consumption without sacrificing the expected performance using full CoMP transmission, but achieving an improved system performance. And as a result possible congestions in the backhaul that could lead to poor synchronisation and high latency are mitigated.

Chapter 4

Improved Cooperating Set Selection for CoMP Transmission

The backhaul overhead still remains a challenge since the number of wireless devices keeps growing exponentially, thereby increasing the high demand placed on the backhaul network architecture which is very costly for the network provider. In addition to these challenges caused by CoMP JT (i.e. adaptive CoMP clustering and high backhaul requirements), achieving a green cellular network has become paramount. It is important to the user and the environment, that the carbon emitted from operating a cellular network is kept at its minimum. Therefore it is important to consider energy efficiency as a factor during CoMP transmission. A reduction in the data overhead in CoMP transmission, would bring about a reduction in the network power consumption, since less transmit BSs per user would lead to an overall reduction in the power consumption. In Chapter 3, it was shown that a fixed number of BS or full CoMP transmission for all users may not always yield the best system performance at every given system condition. This is because less power is given to more channels which may not all have good quality as opposed to giving more power to less channels with good channel quality. So being able to determine if and when CoMP transmission is needed, would lead to reduced data overhead.

4.1 Introduction

CoMP transmission has been shown to boost the peak data rates by mitigating the ICI from neighbouring cells [44, 45]. This is achieved by allowing neighbouring cells to coordinate and transmit signals to the same user. In Chapter 2, the benefits of CoMP as well as the associated challenge of high data overhead was presented. A reduced number of BSs per user was proposed to limit the problem of high data overhead in the backhaul as opposed to using full CoMP transmission from all neighbouring BSs.

In this chapter, the proposed work presented in Chapter 3 is extended and improved. In Chapter 3, the idea of a joint CS selection was first conceived and was shown to obtain a further reduction in the data overhead, by allowing a variable number of transmit BSs per user but setting a maximum on the number of allowed transmit BS per user for CoMP transmission, such that the number of transmit BSs for the k-th user's data transmission is $M_k \leq M_{max}$. To also effectively analyse the system performance of the proposed method, and obtain a validation for the need of a variable number of transmit BSs due to the changing system conditions as opposed to a fixed number of transmit BSs for all users, $M_{max} = [1, 2, \cdots, K]$ was considered for $K = 7$ BS-UE pairs. The result under the sum-rate maximisation problem showed that with $M_{max} = [3, 4, \cdots, 7]$, the proposed solution required only an average of 2 transmit BSs per user to achieve a slightly higher performance as opposed to the conventional solution ('$M_k = M_{max}$'). Due to the computational complexity involved in obtaining the "optimum CS selection" since relatively high values of K and M_{max} were considered, the proposed heuristic solution could not be benchmarked against the "optimum CS selection" which is a combinatorial optimisation problem known to be NP-hard. So in this chapter, the proposed joint and adaptive CS selection would be improved and compared to the performance using the "optimum CS selection" for a relatively small number of M_{max}. This comparison is important since the "optimum CS selection" is the global solution to obtaining Δ, but is not scalable and attractive for implementation due to its complexity.

The contributions of this chapter are as follows: Firstly, an improved joint solution to obtain the CSs and corresponding solutions to the beamforming design and power allocation are presented. Secondly, while taking into account the different factors that may affect the CS size such as the QoS requirements and the power constraints, the CS selection is obtained by optimising one of the two criteria, i.e., either a) minimisation of the total transmit power with given target rate or b) the maximisation of the minimum SINR (max-min SINR). For each optimisation problem, three different power constraints are considered: total power constraint (TPC), per base station power constraint (PBPC) and per antenna power constraint (PAPC). Thirdly, based on simulation results, the achieved performance using the proposed CS selection algorithm is compared to the "optimum CS selection" and the conventional solution.

The remaining parts of this chapter are organised as follows. The system model is shown in Section 4.2. The main idea behind the "optimum CS selection" is presented in Section 4.3 and the proposed joint CS selection is presented in Section 4.4 using two different optimisation strategies under three different power constraints. The solution to the total power minimisation optimisation problems and the max-min SINR optimisation problems are presented in Sections 4.5 and 4.6 respectively. Finally the conclusion is presented in Section 4.7.

4.2 System Model

Fig. 4.1 illustrates CoMP transmission to multiple users on a shared RB, in a multi-cell network with $K = 10$ BS-UE pairs. Each BS and UE are equipped with M_t and N_r transmit and receive antennas respectively. The number of BSs scheduled to transmit to user k is denoted by M_k and $1 \leq M_k \leq M_{max}$, where M_{max} is the maximum number of serving BSs allowed per user. Let $\mathbf{H}_k = [\mathbf{H}_{k,1}, \mathbf{H}_{k,2}, ..., \mathbf{H}_{k,K}]$ be the flat-fading channel matrix between the user k and all K transmit BSs. The coefficients of $\mathbf{H}_{k,m}, m = 1, \cdots K, \in \mathbb{C}^{N_r \times M_t}$ are complex random variables, with zero-mean Gaussian real and imaginary parts. The

channel links experience large scale fading, with path loss exponent (α) and log-normal shadowing having zero-mean and variance η_s^2. And the CSI are assumed to be known at the transmitter. Let $\mathbf{U} = [\mathbf{u}_1, ..., \mathbf{u}_K]$, be the matrix containing all the receive beamforming column vectors ($\mathbf{u}_k$) of user k. Let $\mathbf{V} = [\mathbf{v}_1, \mathbf{v}_2, ..., \mathbf{v}_K]$, be the matrix containing all the unit norm precoding vector for user k's data, where $\mathbf{v}_k = [\mathbf{v}_{1,k}^T, \mathbf{v}_{2,k}^T, ..., \mathbf{v}_{K,k}^T]^T$ and column vector $\mathbf{v}_{m,k}$ is used to precode the data of the k-th user from the m-th BS.

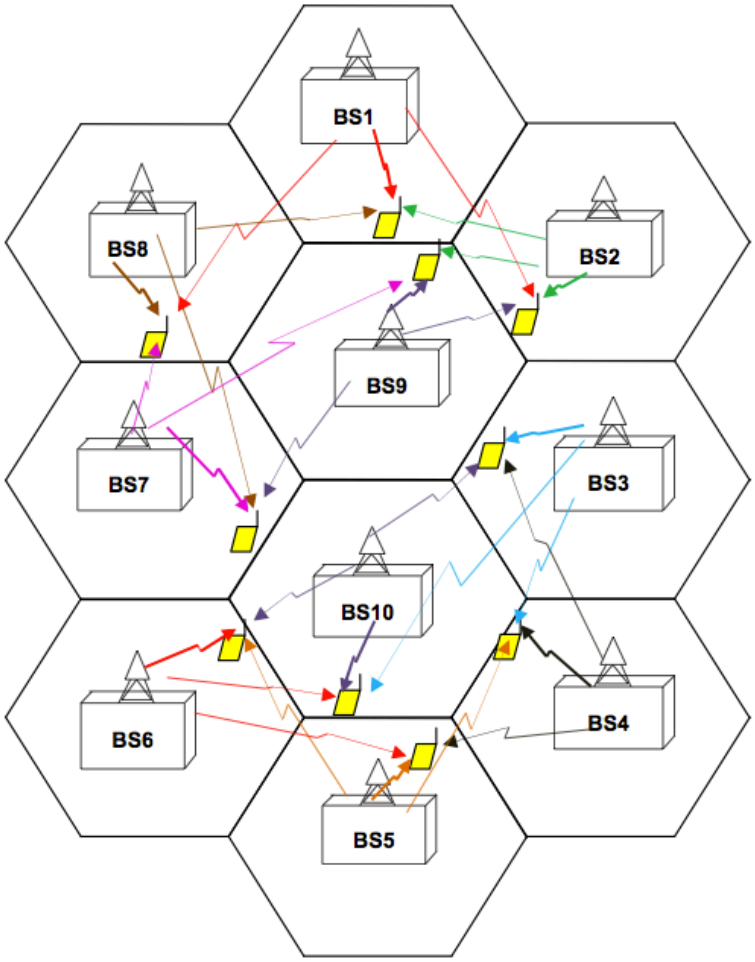

Figure 4.1: CoMP transmission in a multi-cell multi-user network on a shared RB, K = 10 BS-UE pairs, M_{max} = 3 BSs/user.

In addition, $\mathbf{p} = [\rho_1, \rho_2, \ldots, \rho_K]^T$ and ρ_k is the power allocated to the k-th user's data

at each selected m-th BS in the k-th CS. The complex (scalar) data signal destined for the k-th user is represented by s_k ($\mathrm{E}\{|s_k|^2\} = 1$) and $\mathbf{n}_k$ is an additive, zero-mean, white, complex Gaussian noise vector where each element has a variance of σ_k^2.

In providing wireless communication to the user, certain health risks associated with radio frequency electromagnetic energy (EME) should be taken into account. For each BS, it is necessary to regulate the BS transmit power, to ensure the health and safety of the environment and users. Another factor is the practical power implementation on each transmit antenna. Since each antenna is equipped with its own power amplifier, the power rating of each antenna must also be taken into account during power allocation. Based on the aforementioned factors, this chapter aims to determine the CSs jointly (defined by the matrix $\mathbf{\Delta}$), the corresponding receive beam-formers ($\mathbf{U}$), transmit pre-coders ($\mathbf{V}$) and the transmit antenna power allocation ($\mathbf{p}$) that solves either of the given optimisation problems, subject to either the TPC, the PBPC or the PAPC as shown in (4.2.1), (4.2.2) or (4.2.3) respectively.

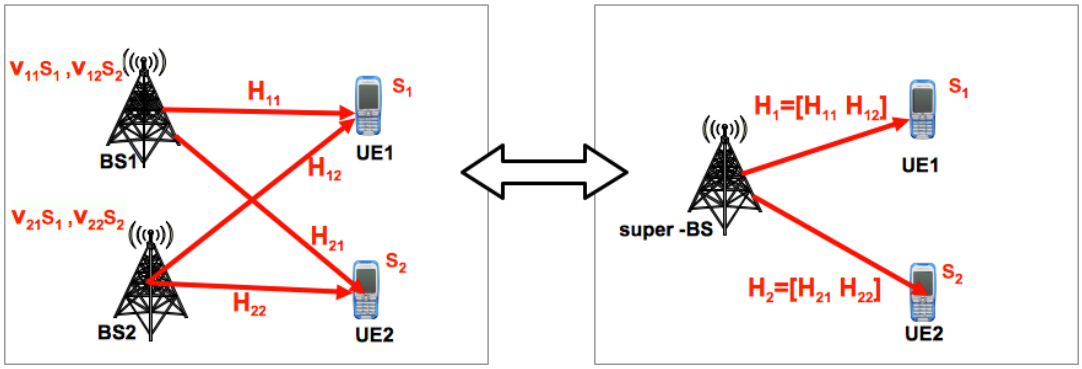

Figure 4.2: Transformation of multi-cell BSs into single cell BSs with distributed antennas $K = 2$ BS-UE pairs.

The total power consumed in the network (P_T) and at the m-th BS (P_m) are given in (4.2.1) and (4.2.2) respectively where p^{TOT}, p_m^{PBPC} (for the $m-th$ transmit BS) and $p_{m,i}^{PAPC}$ (for the $i-th$ antenna on the $m-th$ transmit BS) are the respective power

constraints under the TPC, PBPC and PAPC strategies. The power constraints are given as:

$$C1 : P_T = \sum_{k=1}^{K} \rho_k \leq p^{TOT}, \tag{4.2.1}$$

$$C2 : P_m = \sum_{\substack{k=1 \\ \delta_{m,k}=1}}^{K} \mathbf{v}_{m,k}^H \mathbf{v}_{m,k} \rho_k \leq p_m^{PBPC}, \ \forall m \in [1, 2, \cdots, K], \tag{4.2.2}$$

$$C3 : \left[\sum_{\substack{k=1 \\ \delta_{m,k}=1}}^{K} \rho_k \mathbf{v}_{m,k} \mathbf{v}_{m,k}^H \right]_{i,i} \leq p_{m,i}^{PAPC}, \ \forall m \in [1, 2, \cdots, K], \ \forall i \in [1, 2, \cdots, M_t], \tag{4.2.3}$$

where $[.]_{i,i}$ denotes a (i, i)-th entry of a matrix. The power constraint on a system can affect the CS selection of the users. For instance, under a given BS power constraint, a non-CoMP transmission can utilise the total BS power to transmit data to its given user while ensuring interference cancellation to other users. But with CoMP transmission, under the same BS power constraint, the power has to be shared between the data signals of all the users supported by that BS. This means that the signal strength from a given BS to its desired or paired user would be reduced. Now, if the desired user is still able to achieve its QoS constraint, with a reduced power allocation, then there is no need to assign a supporting BS to that user.

The subsets of BSs scheduled to simultaneously transmit data to the users are represented by the "CS selection matrix" (Δ) (see 3.2.4) and the "BS serving factor" ($\delta_{m,k}$) (see 3.2.5).

The received signal ($\mathbf{y}_k$) for the k-th UE is post-processed by the receive beamforming vector ($\mathbf{u}_k$) as in (4.2.4):

$$\mathbf{u}_k^H \mathbf{y}_k = \mathbf{u}_k^H \mathbf{H}_k^{(k)} \bar{\mathbf{v}}_k \sqrt{\rho_k} s_k + \mathbf{u}_k^H \sum_{\substack{p=1 \\ p \neq k}}^{K} \mathbf{H}_k^{(p)} \bar{\mathbf{v}}_p \sqrt{\rho_p} s_p + \mathbf{u}_k^H \mathbf{n}_k, \forall \ k \in [1, 2, \cdots, K], \tag{4.2.4}$$

where $\mathbf{H}_k^{(i)}$ is the flat-fading channel from the i-th CS to the k-th user and $\bar{\mathbf{v}}_i$ is the precoding vector on the i-th CS for user data i, $\mathbf{H}_k^{(i)} \in \mathbb{C}^{N_r \times \sum_j \delta_{j,i} M_t}$, $\bar{\mathbf{v}}_i \in \mathbb{C}^{\sum_j \delta_{j,i} M_t \times 1}$, $\mathbf{H}_k^{(i)} = [\mathbf{H}_{k,j}; \ \delta_{j,i} = 1, \forall j \in [1, 2, \cdots, K]]$ and $\bar{\mathbf{v}}_i = [\mathbf{v}_{j,i}^T; \ \delta_{j,i} = 1, \forall j \in [1, 2, \cdots, K]]^T$. So

the SINR at the k-th UE ($\text{SINR}_k^{(dl)}$), also denoted as $\gamma_k^{(dl)}$ in this chapter, is expressed as:

$$\gamma_k^{(dl)} = \frac{\left|\mathbf{u}_k^H \mathbf{H}_k^{(k)} \bar{\mathbf{v}}_k\right|^2 \rho_k}{\sum_{\substack{p=1 \\ p \neq k}}^{K} \left|\mathbf{u}_k^H \mathbf{H}_k^{(p)} \bar{\mathbf{v}}_p\right|^2 \rho_p + \sigma_k^2}. \tag{4.2.5}$$

Note that the rate of user k (R_k) and the sum-rate (R_T) can be obtained by (2.3.13).

4.3 The "Optimum CS Selection"

For LTE CoMP JT to be successful, one of the key requirements is very low latency. When a large number of transmit BSs are used for CoMP transmission, a corresponding high processing and transfer time is needed to obtain the required data and precoding information at the BSs. Minimising the number of transmit BSs per user, whilst still achieving the target performance would lead to better latency and reduced data overhead on the backhaul link. It is important to note that obtaining the best CS for each user's CoMP transmission is dependent on the CS of other users, the channel conditions, the QoS constraints and the system constraints. To obtain the optimum CS solution, means selecting the CSs of the users simultaneously based on the system conditions. This problem is computationally complex, especially for a very large network and can be solved using a hard search through all possible combination of solutions.

The "optimum CS selection" to find Δ is a combinatorial optimisation problem, which would require using a search algorithm over the total number of (potentially very large) possible solutions given by N_{TS} (see (3.4.18)). This problem is NP-hard but it is solvable for smaller values of M_{max} and K, so there is a need to develop a solution strategy with low complexity that can obtain Δ jointly, while still ensuring meeting the objective of the optimum CS solution. For example, considering K = 2 BS-UE pairs and M_{max} = 2, then the number of possible CS solutions using the equation in (3.4.18) is 9 and the possible CS solutions for both users is given in Table 4.1. Now consider K = 4 BS-UE pairs and

M_{max} = 4, the number of possible CS solutions is 50625. Also if K = 5 BS-UE pairs and M_{max} = 4, the number of possible CS solutions is 24.3×10^6.

Table 4.1: List of possible CSs solution for K = 2 BS-UE pairs.

	Users	
CSs	**User 1**	**User 2**
1	{BS 1}	{BS 1}
2	{BS 1}	{BS 2}
3	{BS 1}	{BS 1, BS 2}
4	{BS 2}	{BS 1}
5	{BS 2}	{BS 2}
6	{BS 2}	{BS 1, BS2 }
7	{BS 1, BS 2}	{BS 1}
8	{BS 1, BS 2}	{BS 2}
9	{BS 1, BS 2}	{BS 1, BS 2}

For this reason, a sub-optimum CS selection is presented in the next section, using different optimisation problems to validate the advantages of the joint and adaptive proposed solution as opposed to the conventional CoMP transmission strategy.

4.4 The "Sub-optimum CS Selection"

As seen from the joint and adaptive CS selection algorithm presented earlier in Chapter 3, further reductions in the data overhead and energy consumption was achieved, when variable numbers of transmit BSs were allowed for each user's data transmission. The joint and adaptive solution to the optimisation problem required to obtain the CS selection ($\mathbf{\Delta}$), the corresponding receive beam-formers ($\mathbf{U}$), transmit pre-coders ($\mathbf{V}$) and the transmit antenna power allocation ($\mathbf{p}$) is very complex. In Chapter 3, the proposed

iterative algorithm for the CS selection was based on maximising the "effective gain" of the users while using a simple power allocation problem to solve the given optimisation problems. However in this chapter, the proposed iterative algorithm is based on the SINR of the users and a better power optimisation solution is used.

The proposed solution is considered for small values of K and M_{max}, to enable the performance of the proposed CS selection algorithm to be compared to the performance of the "optimal CS selection" using the hard search, while still comparing both solutions to the conventional full CoMP transmission. The proposed algorithm aims to achieve the objectives of the "optimum solution", which is obtaining a joint CS selection for the given users and achieve a significant percentage of the gain expected with the "optimum CS selection".

The two optimisation strategies considered in this chapter are: i) the total power minimisation with given target rates as in (4.4.6) and ii) the max-min SINR problem as in (4.4.7):

$$\min_{\mathbf{\Delta},\mathbf{U},\mathbf{V},\mathbf{p}} \sum_{k=1}^{K} \rho_k \text{ s.t., } R_k \geq \phi_k, \ \forall k \in [1, 2, \cdots, K], \quad \text{conditions C1 or C2 or C3}, \tag{4.4.6}$$

$$\max_{\mathbf{\Delta},\mathbf{U},\mathbf{V},\mathbf{p}} \min_{1 \leq k \leq K} \gamma_k^{(dl)} \text{ s.t., conditions C1 or C2 or C3}, \tag{4.4.7}$$

These optimisation problems would be considered based on three separate power constraint models: i.) C1 as shown in (4.2.1) (TPC), ii.) C2 as shown in (4.2.2) (PBPC) and iii.) C3 as shown in (4.2.3) (PAPC). The CS selection, receive beam-former design, transmit pre-coder design and power allocation will be carried out separately on the six different scenarios. The problems in (4.4.6) and (4.4.7) are joint complex problems of $\mathbf{\Delta}$, **U, V** and **p** which can be transformed into simpler problems that allow $\mathbf{\Delta}$, **U, V** and **p** to be solved separately in an iterative manner. The CS selection matrix ($\mathbf{\Delta}$), can be found by searching through a significantly reduced set of possible solutions using the algorithm proposed in Tables 4.2 and 4.3. For each $\mathbf{\Delta}$ obtained, the corresponding solutions to **U, V** and **p** are then determined as shown in the following sections. The joint corresponding solutions to **U, V** and **p** are computationally complex to solve. To simplify the problem

further, the multi-cell BSs are transformed into a super BS with distributed antennas as seen in Fig. 4.2. This assumption is valid since the CoMP transmission from the BSs to the user are done simultaneously.

4.4.1 System Output-to-Cost-Ratio (OCR)

For the purpose of this thesis, the output-to-cost ratio (OCR) of the system is measured. The OCR is defined as the measure of the system performance, efficiency or productivity based on a given cost factor. This is given as the ratio of the desired output to the cost of production or performance. The cost can refer to either the overhead, CS allocation time (CAT), BS power consumption or CS search complexity (N_{TS}), while the output refers to the obtained sum-rate. The CAT is the time taken to allocate CSs to all the users. The different types of OCR measurements are given below:

$$\text{OCR}_O = \frac{\text{sum-rate}}{\text{Overhead factor}} \text{ bps/Hz}, \tag{4.4.8}$$

$$\text{OCR}_P = \frac{\text{sum-rate}}{\text{Avg. BS Power}} \text{ bits/JHz}. \tag{4.4.9}$$

The proposed OCR would be used in the simulation result analysis to measure the performance achieved in the network, under the given optimisation problems and power constraints defined earlier.

4.5 Total Power Minimisation Problem

Here the total power minimisation optimisation problem with given user target rate (see 4.4.6) is considered under three different power strategies: TPC (4.2.1), PBPC (4.2.2) and PAPC (4.2.3). Before presenting the CS selection algorithm, the beamforming and power optimisation strategies used to obtain the solutions to **U, V** and **p** are presented. For a given solution to $\Delta^{(i+1)}$, the corresponding solutions to $\mathbf{U}^{(i+1)}$, $\mathbf{V}^{(i+1)}$ and $\mathbf{p}^{(i+1)}$ are found iteratively. Begin the iteration by setting $j = 1$ and randomly choosing $\mathbf{V}^{(j)}$ and $\mathbf{p}^{(j)}$,

then using the beamforming and power allocation solutions presented in Sections 4.5.1 and 4.5.2, $\mathbf{U}^{(j+1)}$, $\mathbf{V}^{(j+1)}$ and $\mathbf{p}^{(j+1)}$ are obtained iteratively till $\max|\mathbf{p}^{(j)} - \mathbf{p}^{(j+1)}| < \varpi$, and ϖ is the convergence constraint. So the solutions to $\mathbf{U}^{(i+1)}$, $\mathbf{V}^{(i+1)}$ and $\mathbf{p}^{(i+1)}$ are given by $\mathbf{U}^{(j+1)}$, $\mathbf{V}^{(j+1)}$ and $\mathbf{p}^{(j+1)}$ respectively.

4.5.1 Beamforming Design

To solve the given optimisation problem, the respective solutions to $\mathbf{U}$ and $\mathbf{V}$ can be found by maximising the SINR and the SLNR of the *k*-th user's data. Now considering the downlink SINR expression in (4.2.5) as the optimisation criteria in finding $\{\mathbf{u}_k\}_{k=1}^{K}$, the downlink SINR ($\gamma_k^{(dl)}$) expression in (4.2.5) can be re-written as:

$$\gamma_k^{(dl)} = \frac{\mathbf{u}_k^H \left[\mathbf{H}_k^{(k)} \bar{\mathbf{v}}_k \bar{\mathbf{v}}_k^H \mathbf{H}_k^{(k)H} \rho_k\right] \mathbf{u}_k}{\mathbf{u}_k^H \left[\sum_{\substack{p=1 \\ p \neq k}}^{K} \mathbf{H}_k^{(p)} \bar{\mathbf{v}}_p \bar{\mathbf{v}}_p^H \mathbf{H}_k^{(p)H} \rho_p + \mathbf{I}\sigma_k^2\right] \mathbf{u}_k}, \ \forall\, k \in [1, 2, \cdots, K], \tag{4.5.10}$$

where $\mathbf{I}$ is the identity matrix. From (4.5.10), it is easy to show that if $\{\bar{\mathbf{v}}_k\}_{k=1}^{K}$ and $\mathbf{p}$ are fixed and given, then $\mathbf{u}_k$ can be found as the eigenvector corresponding to the maximum eigenvalue of:

$$\left((\sum_{\substack{p=1 \\ p \neq k}}^{K} \mathbf{H}_k^{(p)} \bar{\mathbf{v}}_p \bar{\mathbf{v}}_p^H \mathbf{H}_k^{(p)H} \rho_p + \mathbf{I}\sigma_k^2)^{-1} (\mathbf{H}_k^{(k)} \bar{\mathbf{v}}_k \bar{\mathbf{v}}_k^H \mathbf{H}_k^{(k)H} \rho_k) \right), \ \forall\, k \in [1, 2, \cdots, K], \tag{4.5.11}$$

and $\|\mathbf{u}_k\| = 1$.

The SLNR of the k-th user's data is expressed as:

$$\begin{aligned}\text{SLNR}_k =& \frac{|\mathbf{u}_k^H \mathbf{H}_k^{(k)} \bar{\mathbf{v}}_k|^2 \rho_k}{\sum\limits_{\substack{p=1 \\ p \neq k}}^{K} |\mathbf{u}_p^H \mathbf{H}_p^{(k)} \bar{\mathbf{v}}_k|^2 \rho_k + \sigma^2}, \\ =& \frac{\bar{\mathbf{v}}_k^H \left[\mathbf{H}_k^{(k)H} \mathbf{u}_k \mathbf{u}_k^H \mathbf{H}_k^{(k)} \rho_k \right] \bar{\mathbf{v}}_k}{\bar{\mathbf{v}}_k^H \left[\sum\limits_{\substack{p=1 \\ p \neq k}}^{K} \mathbf{H}_p^{(k)H} \mathbf{u}_p \mathbf{u}_p^H \mathbf{H}_p^{(k)} \rho_k + \mathbf{I}\sigma^2 \right] \bar{\mathbf{v}}_k}, \ \forall\, k \in [1, 2, \cdots, K]. \end{aligned} \tag{4.5.12}$$

If $\mathbf{U}$ and $\mathbf{p}$ are fixed and given, then from (4.5.12), $\bar{\mathbf{v}}_k$ can be found as the eigenvector corresponding to the maximum eigenvalue of:

$$\left((\sum_{\substack{p=1 \\ p \neq k}}^{K} \mathbf{H}_p^{(k)H} \mathbf{u}_p \mathbf{u}_p^H \mathbf{H}_p^{(k)} + \mathbf{I}(\sigma^2/\rho_k))^{-1} (\mathbf{H}_k^{(k)H} \mathbf{u}_k \mathbf{u}_k^H \mathbf{H}_k^{(k)}) \right), \ \forall\, k \in [1, 2, \cdots, K], \tag{4.5.13}$$

where σ^2 is the noise power and $\|\bar{\mathbf{v}}_k\| = 1$.

4.5.2 Power Optimisation

The disjoint power optimisation problem to (4.2.5), based on the power constraints in (4.2.1), (4.2.2) or (4.2.3) respectively is given in (4.5.14), (4.5.15) and (4.5.16). The power allocation solution ($\mathbf{p}$) can be found by solving the following power optimisation problems:

$$\min_{\mathbf{p}} \sum_{k=1}^{K} \rho_k$$

$$\text{s.t., } \{R_k \geq \phi_k\}_{k=1}^{K}, \sum_{k=1}^{K} \rho_k \leq p^{TOT}, \mathbf{p} \succeq 0, \tag{4.5.14}$$

$$\text{or s.t., } \{R_k \geq \phi_k\}_{k=1}^{K}, \sum_{\substack{k=1 \\ \delta_{m,k}=1}}^{K} \mathbf{v}_{m,k}^H \mathbf{v}_{m,k} \rho_k \leq p_m^{PBPC}, m \in [1, 2, \cdots, K], \mathbf{p} \succeq 0, \tag{4.5.15}$$

$$\text{or s.t., } \{R_k \geq \phi_k\}_{k=1}^{K}, \left[\sum_{\substack{k=1 \\ \delta_{m,k}=1}}^{K} \rho_k \mathbf{v}_{m,k}\mathbf{v}_{m,k}^H\right]_{i,i} \leq p_{m,i}^{PAPC}, \ \forall m \in [1,2,\cdots,K],$$

$$\forall i \in [1,2,\cdots,M_t], \mathbf{p} \succeq 0, \quad (4.5.16)$$

where ϕ_k is the target rate of user k. The user-rate constraint (R_k) in (4.2.5), (4.5.14), (4.5.15) and (4.5.16) can be re-written in its equivalent SINR constraint function as:

$$\frac{g_{k,k}\rho_k}{\sum_{\substack{p=1 \\ p\neq k}}^{K} g_{k,p}\rho_p + \sigma_k^2} \geq \bar{\gamma_k}, \forall k \in [1,2,\cdots,K] \quad (4.5.17)$$

where $g_{i,j} = \left|\mathbf{u}_i^H \mathbf{H}_i^{(j)} \bar{\mathbf{v}}_j\right|^2$, σ_k^2 = 1 and $\bar{\gamma}_k = (2^{\phi_k} - 1)$ is the target SINR for user k. The solutions to **U** and **V** can be found from (4.5.11) and (4.5.13) respectively. Now let

$$\mathbf{B}_{i,j} = \begin{cases} g_{i,j}, & \forall i,j \in [1,2,\cdots,K] \\ 0, & i = j, \end{cases} \quad (4.5.18)$$

$$\mathbf{A}_{i,i} = \begin{cases} g_{i,i}, & \forall i \in [1,2,\cdots,K] \\ 0, & i \neq j, \end{cases} \quad (4.5.19)$$

$$\mathbf{C} = diag\left([\bar{\gamma}_1, \bar{\gamma}_2, \cdots, \bar{\gamma}_K]\right). \quad (4.5.20)$$

The closed form expression of the power allocation problem based on the TPC, PBPC and PAPC can now be expressed respectively as:

$$\min_{\mathbf{p}} \mathbf{1}^T\mathbf{p} \ \text{ s.t.} (\mathbf{A} - \mathbf{CB})\mathbf{p} \succeq \mathbf{C1}, \ \mathbf{1}^T\mathbf{p} \leq p^{TOT} \text{ and } \mathbf{p} \succeq 0, \quad (4.5.21)$$

$$\min_{\mathbf{p}} \mathbf{1}^T\mathbf{p} \ \text{ s.t.} (\mathbf{A} - \mathbf{CB})\mathbf{p} \succeq \mathbf{C1}, \ \mathbf{Xp} \preceq \mathbf{p}^{PBPC} \text{ and } \mathbf{p} \succeq 0, \quad (4.5.22)$$

$$\min_{\mathbf{p}} \mathbf{1}^T\mathbf{p} \ \text{ s.t.} (\mathbf{A} - \mathbf{CB})\mathbf{p} \succeq \mathbf{C1}, \ \mathbf{Wp} \preceq \mathbf{p}^{PAPC} \text{ and } \mathbf{p} \succeq 0, \quad (4.5.23)$$

where $\mathbf{1}^T$ is a row vector having all elements set as 1,

$$\mathbf{X} = \begin{bmatrix} \|\mathbf{v}_{1,1}\|^2 & \|\mathbf{v}_{1,2}\|^2 & \cdots & \|\mathbf{v}_{1,K}\|^2 \\ \|\mathbf{v}_{2,1}\|^2 & \|\mathbf{v}_{2,2}\|^2 & \cdots & \|\mathbf{v}_{2,K}\|^2 \\ \vdots & \vdots & \cdots & \vdots \\ \|\mathbf{v}_{K,1}\|^2 & \|\mathbf{v}_{K,2}\|^2 & \cdots & \|\mathbf{v}_{K,K}\|^2 \end{bmatrix}, \mathbf{p}^{PBPC} = \left[p_1^{PBPC}, p_2^{PBPC}, \cdots, p_K^{PBPC}\right]^T,$$

$$\mathbf{W} = \begin{bmatrix} |\mathbf{v}_1|^2 & |\mathbf{v}_2|^2 & \cdots & |\mathbf{v}_K|^2 \end{bmatrix},$$

and $\mathbf{p}^{PAPC} = \left[p_{1,1}^{PAPC}, \cdots, p_{1,M_t}^{PAPC}, \cdots, p_{K,1}^{PAPC}, \cdots, p_{K,M_t}^{PAPC}\right]^T$.

The power optimisation problems above can be easily solved as a constrained linear least square optimisation problem.

4.5.3 CS Selection Algorithm under Total Power Minimisation Optimisation Problem

In this section, the proposed algorithm in Section 3.4.1, Table 3.1 is improved by considering the SINR (which is the global metric required to optimise any capacity-based optimisation problem) as opposed to the "effective channlel". This is because the rate of the user is directly dependent on the SINR, so the SINR which is a standard metric should be considered when optimising the network capacity. The sub-optimal joint CS selection (Δ), that achieves the given target rate for each user (i.e., satisfying the QoS constraint of the users) with minimum total power, while complying with the power constraint C1 or C2 or C3 (i.e., the network constraint), is obtained by searching through a significantly reduced set of possible solutions. The proposed algorithm begins the search by assigning a single transmit BS with the best channel quality to each user. Then the algorithm aims to improve the obtained performance by assigning more BSs to the users with lower performance than the given QoS constraint or network set threshold. The achievable user rate at the cell edge, R_k, is limited by factors such as the power constraints, channel conditions, number of antennas and other network conditions. Hence, the required target rate, ϕ_k, may not be achieved at every given time. In such cases, the algorithm chooses

the Δ that achieves the best rate (i.e. closest performance to the target rate), which is associated with the lowest error, η, as defined in Table 4.2(4).

Initialise the variables as shown in Table 4.2, where i is the iteration count, $x^{(i)}$ is the convergence variable of the algorithm, f_k is the number of assigned BSs to user k and γ_{avg} is the SINR threshold. Then assign the BS with the best channel quality to each user to obtain $\Delta^{(i+1)}$ and find the corresponding solutions $\mathbf{U}^{(i+1)}, \mathbf{V}^{(i+1)}$ and $\mathbf{p}^{(i+1)}$ iteratively. At each iteration, using the proposed scheduling algorithm, the minimum SINR is maximised. This is achieved by finding the downlink SINR at user k ($\text{SINR}_k^{dl(i+1)}$ - i.e. $\gamma_k^{dl(i+1)}$ as shown in (4.4.7)), the user rate ($R_k^{(i+1)}$), total power ($P_T^{(i+1)}$), error ($\eta^{(i+1)}$) and the average SINR ($\gamma_{avg}^{(i+1)} = \frac{1}{K}(\sum_{k=1}^{K} \gamma_k^{dl(i+1)})$), which is the SINR threshold for the next iteration. The SINR of each user k is maximised by assigning another BS to user k when $\gamma_k^{(dl)} < \gamma_{avg}$. This process is done iteratively until the maximum number of transmit BSs per user is reached and no BS assignment is possible. The Δ and corresponding **U, V** and **p** that best satisfy the target rate of each user with minimum total power is selected as the CS for the users required for CoMP transmission.

Table 4.2: Proposed CS selection algorithm based on total power (P_T) minimisation

---

Initialization: $i = 0$, $P_T^{(i)} = \infty$, $\left\{f_k^{(i)}\right\}_{k=1}^{K} = 0, \eta^{(i)} = \infty$,
$\left\{\text{SINR}_k^{dl(i)}\right\}_{k=1}^{K} = 0$, $\gamma_{avg}^{(i)} = 1$, $x^{(i)} = 1$, $\Delta^{(i)} = \mathbf{0}$.
while any ($\text{SINR}_k^{dl(i)} < \gamma_{avg}^{(i)}$)
if $x^{(i)} \neq 0$
1. From (3.2.5), find $\Delta^{(i+1)}$
for $k = 1 : K$
if $\text{SINR}_k^{dl(i)} < \gamma_{avg}^{(i)}$ and $f_k^{(i)} < M_{max}$
$f_k^{(i+1)} = f_k^{(i)} + 1$ and $\delta_{m,k}^{(i+1)} = 1$
(if BS m has the best channel quality to user k and $\delta_{m,k}^{(i)} = 0$).
end if, **end for**
2. Find $\mathbf{U}^{(i+1)}$, $\mathbf{V}^{(i+1)}$ and $\mathbf{p}^{(i+1)}$ as shown in Sections 4.5.1 and 4.5.2.
3. Find $\text{SINR}_k^{dl(i+1)}$, $R_k^{(i+1)}$ and $P_T^{(i+1)}$ from (4.2.5), (2.3.13) and (4.2.2) respectively.

4. Find $\eta^{(i+1)} = \sum_{\substack{k=1 \\ R_k<\phi_k}}^{K} \left|\phi_k - R_k^{(i+1)}\right|^2$.

if $R_k^{(i+1)} \geq \phi_k,\ \forall\ k \in [1, 2, \cdots, K]$

if $P_T^{(i+1)} < P_T^{(i)}$

$\Delta \leftarrow \Delta^{(i+1)}$, $\mathbf{U} \leftarrow \mathbf{U}^{(i+1)}$, $\mathbf{V} \leftarrow \mathbf{V}^{(i+1)}$ and $\mathbf{p} \leftarrow \mathbf{p}^{(i+1)}$

else $P_T^{(i+1)} = P_T^{(i)}$

end if $\eta^{(i+1)} = \eta^{(i)}$

else

if $\eta^{(i+1)} < \eta^{(i)}$

$\Delta \leftarrow \Delta^{(i+1)}$, $\mathbf{U} \leftarrow \mathbf{U}^{(i+1)}$, $\mathbf{V} \leftarrow \mathbf{V}^{(i+1)}$ and $\mathbf{p} \leftarrow \mathbf{p}^{(i+1)}$

else $\eta^{(i+1)} = \eta^{(i)}$

end if $P_T^{(i+1)} = P_T^{(i)}$

$\gamma_{avg}^{(i+1)} = \frac{1}{K}(\sum_{k=1}^{K} \text{SINR}_k^{dl(i+1)})$, $x^{(i+1)} = \sum_{k=1}^{K}(f_k^{(i+1)} - f_k^{(i)})$, *i*++.

end if, **end while**.

5. **repeat** steps 1 - 4 **until** $x^{(i+1)} = 0$ or $f_k^{(i+1)} = f_k^{(i)}$, $\forall k$.

4.5.4 Simulation Results and Evaluation

Table 4.3: Summary of simulation parameters [3, 4, 5].

Parameters	**Value**
Antenna type, Cell layout (K)	Omnidirectional, 3 cell sites.
Time slot per RB, $[\alpha, \eta_s]$	0.5msecs, [2, 8dB]
Inter site distance (ISD)	500m
cell-edge user distance	$\geq$ 260m
Number of antennas (M_t, N_r)	(4, 2)

$p^{TOT}, p_m^{PBPC}, p_{m,i}^{PAPC}$	[120W, 40W, 100W]
Note: PBPC annd PAPC parameter is selected as in [46], set $p^{TOT} = Kp_m^{PBPC}$.	

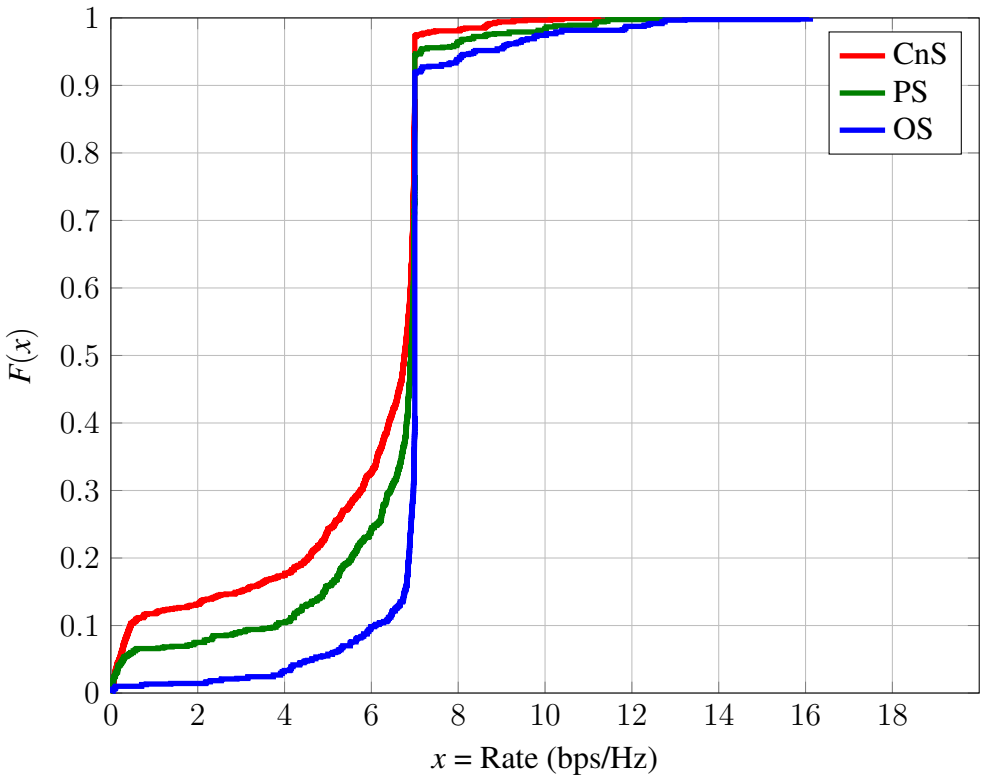

Figure 4.3: CDF plot showing the probability of achieving the target rate under TPC.

For ease of implementation, perfect CSI, synchronization and no latency constraints are assumed as well as the system parameters given in Table 4.3. For the given simulation set-up, different values of M_{max} are considered in a step-wise manner, i.e. $M_{max} = 2, 3, \cdots, K$ and the results obtained are presented in Table 4.4 and analysed, for K = 4, M_{max} = 2, 3 and 4. The given parameters for the power constraints are: $p_{m,i}^{PAPC}(\forall m, i)$ = 100 W, $p_m^{PBPC}(\forall m)$ = 40 W, p^{TOT} = 160 W [46] and a target rate of 7 bps/Hz for all users on the given RB. The following definitions are used for the purpose of this work:

1.) The "optimum solution" (OS): The CS selection is determined using a hard search through all possible combinations of transmitting BSs for all users, however **U, V** and **p** are solved disjointly.

2.) The "proposed solution" (PS): The CS selection is obtained using the proposed algorithm to obtain the CS for all users (i.e. $M_k \leq M_{max}, \forall k$). 3.) The "conventional solution" (CnS): In this case, all users are served with M_{max} BSs at any given time (i.e. $M_k = M_{max}$). It selects the best transmitting BSs to each user at every given time. Both the OS and CnS will be used as a reference when comparing with the proposed solution. Also note that the average BS power consumption is given by P_{ABS}.

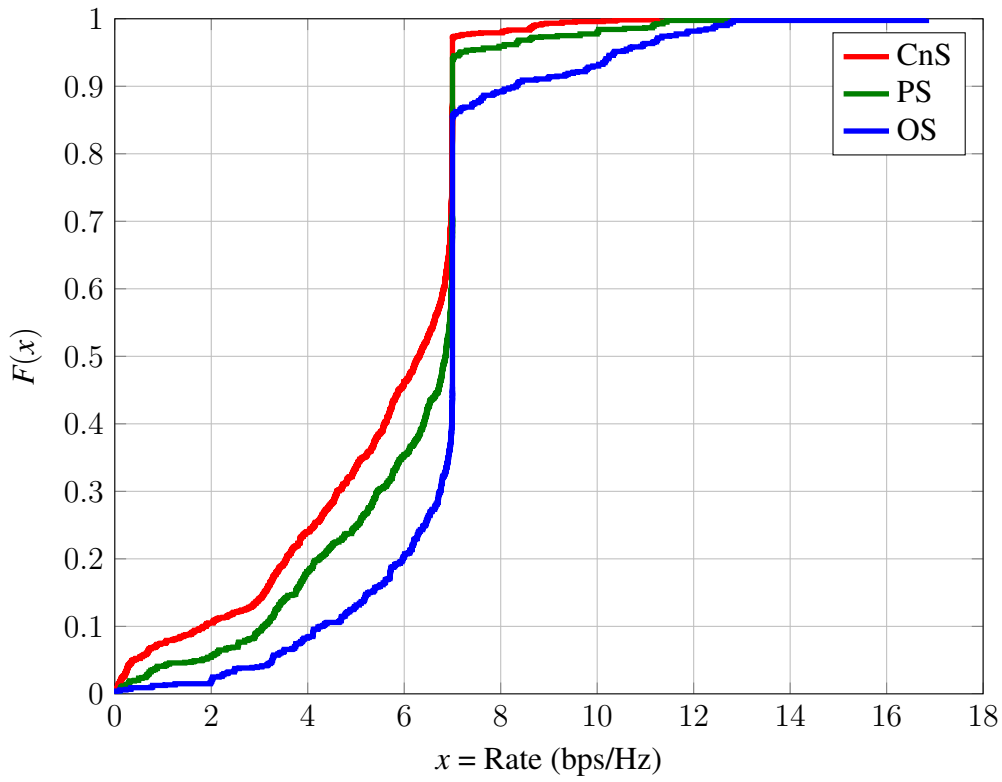

Figure 4.4: CDF plot showing the probability of achieving the target rate under PBPC.

As shown in Figs. 4.3, 4.4 and 4.5, the CDF plot for the obtained user rate is shown. The expected target rate is 7 bps/Hz for each user on each RB. It can be observed that the probability of achieving the required QoS contraint (i.e. 7 bps/Hz) on a given RB

for each user is 0.3, 0.5 and 0.71 using CnS, PS and OS respectively under TPC, while under the PBPC the probability of achieving the given QoS constraint is 0.3, 0.43 and 0.62 respectively and under PAPC is 0.58, 0.7 and 0.88 respectively. It can be seen that the OS and PS using the joint CS selection strategy has a higher chance of achieving the QoS constraint under the same conditions as opposed to CnS.

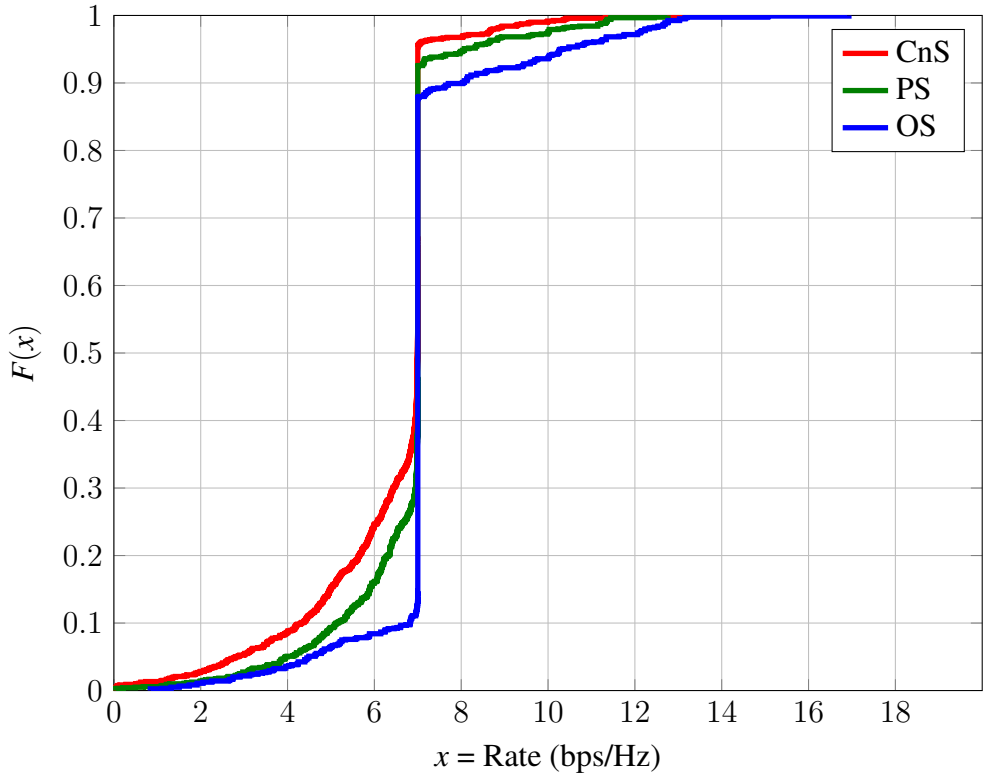

Figure 4.5: CDF plot showing the probability of achieving the target rate under PAPC.

The sum-rate attained under the given set-up and system conditions can be seen in Table 4.4. Generally across the three solution types (i.e., CnS, PS and OS) and under the three different power strategies, one can observe that the sum-rate increases only slightly as the value of M_{max} is increased. This proves that allowing a large number of transmit BSs per user for CoMP transmission, especially for the cell-edge users, does not achieve a significant increase in the sum-rate, especially under constrained power conditions.

In Table 4.4 under the PBPC for M_{max} = 2, one can observe that CnS, PS and OS

respectively achieve a sum-rate of 42.70 kbps/Hz, 46.33 kbps/Hz and 53.63 kbps/Hz with an overhead factor of 2, 1.57 and 1.55. From the results, it is obvious that OS which selects the CSs jointly is able to achieve the best sum-rate performance with minimum overhead, using the hard search which is highly complex. CnS achieves the lowest sum-rate and requires a 29% increase in overhead when compared to the OS. The proposed approach (PS) achieves a better sum-rate performance and reduces the demanded backhaul overhead by 21.5%, when compared to CnS.

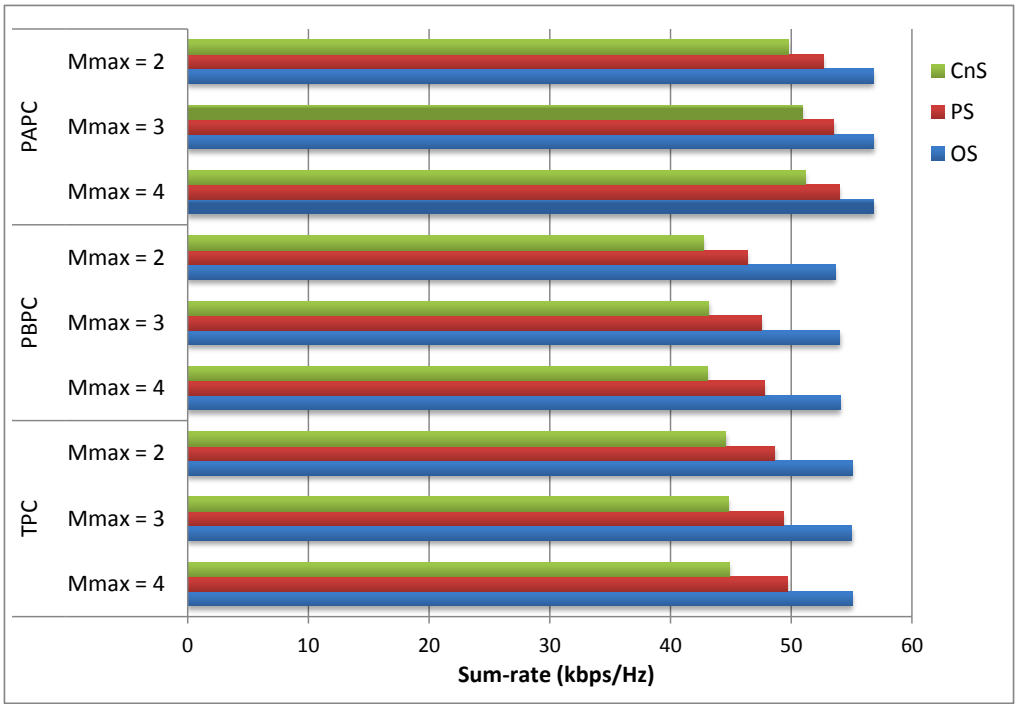

Figure 4.6: The achieved sum-rate per RB using CnS, PS and OS for different power constraints and M_{max} = 2, 3 and 4.

From Table 4.4 under the PAPC for M_{max} = 3, the sum-rate achieved by CnS, PS and OS are 50.91 kbps/Hz, 53.53 kbps/Hz and 56.82 kbps/Hz with a corresponding overhead factor of 3, 1.97 and 1.66. Again, one can observe a reduction of 45% and 34% respectively in the data overhead achieved by the OS and PS compared to CnS. This

validates again that a joint selection of the CSs is necessary to further reduce the data overhead in the backhaul. Now considering the CAT required to obtain the CSs of the users, it can be seen that PS requires only 0.071 secs compared to 437 secs required by the OS. Under PAPC when M_{max} = 4, PS obtains the CSs in 0.094 secs compared to 625 secs required using the OS. The PS is shown to reduce the CAT by over 99 %. It is very important to have a low CAT time to prevent very high latency and poor synchronisation within the system. Even though OS is seen to achieve a better sum-rate than PS, the CAT is very high even for a relatively small number of K and M_{max}, making it very unattractive for deployment in a network system. Note that the CAT in this simulation was computed by a desktop computer (4GB RAM, Interl(R) Core(TM)2 Duo CPU E8400 @3GHz processor).

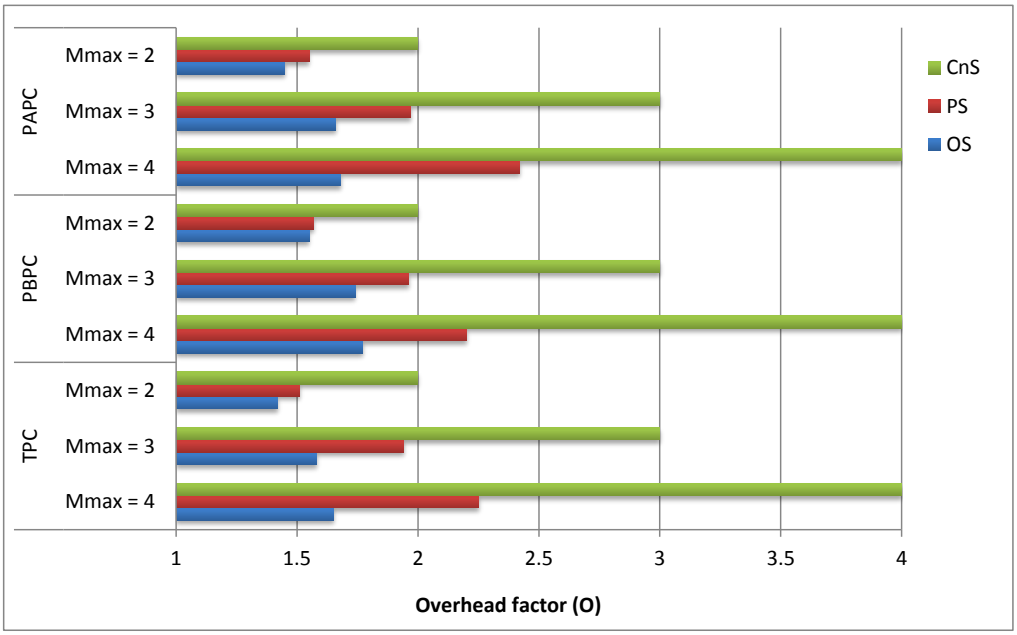

Figure 4.7: Overhead of the given system under CnS, PS and OS for different power constraints and M_{max} = 2, 3 and 4.

From (3.4.18), the search complexity to obtain the CSs for OS when M_{max} = 2, 3 and 4 respectively is N_{TS} = 10000, 38416 and 50625. This is the number of hard searches through all possible CS solutions. From simulations the complexity obtained with PS is given respectively as N_{TS} = 4, 5 and 7 for M_{max} = 2, 3 and 4, while the search complexity for CnS is given by N_{TS} = 1 for all values of M_{max}. CnS has a complexity of 1 because the system chooses M_{max} BSs with the best channel quality, for CoMP transmission to each user. However from previous observations the performance and data overhead obtained is poor compared to the performance obtained with PS and OS.

Table 4.4: Simulation results under the total power minimization optimisation problem given the user target rate and different power constraints.

Sum-rate (kbps/Hz)									
	TPC			PBPC			PAPC		
M_{max}	2	3	4	2	3	4	2	3	4
OS	55.06	55.02	55.06	53.63	54.02	54.04	56.79	56.84	56.82
PS	48.46	49.34	49.69	46.33	47.53	47.77	52.63	53.53	53.98
CnS	44.59	44.79	44.86	42.70	43.16	43.06	49.74	50.91	51.18
Overhead factor (O)									
	TPC			PBPC			PAPC		
M_{max}	2	3	4	2	3	4	2	3	4
OS	1.42	1.58	1.65	1.55	1.74	1.77	1.45	1.66	1.68
PS	1.51	1.94	2.25	1.57	1.96	2.20	1.55	1.97	2.42
CnS	2.00	3.00	4.00	2.00	3.00	4.00	2.00	3.00	4.00

CAT (secs)									
	TPC			PBPC			PAPC		
M_{max}	2	3	4	2	3	4	2	3	4
OS	68.12	300.29	412.02	71.92	322.99	448.43	88.49	437.37	625.82
PS	0.032	0.045	0.057	0.030	0.049	0.060	0.044	0.071	0.094
CnS	0.011	0.012	0.013	0.011	0.013	0.013	0.017	0.021	0.027
Average BS Power (W)									
	TPC			PBPC			PAPC		
M_{max}	2	3	4	2	3	4	2	3	4
OS	31.85	35.98	35.86	25.62	25.44	25.24	54.41	51.16	50.70
PS	37.60	37.58	37.73	28.81	31.60	32.43	90.98	106.23	119.20
CnS	40	39.82	40	33.95	38.65	40	115.96	148.60	168.25
Output-Cost Ratio based on Overhead (OCR_O (bps/Hz))									
	TPC			PBPC			PAPC		
M_{max}	2	3	4	2	3	4	2	3	4
OS	19.39	17.41	16.68	17.30	15.52	15.27	19.58	17.12	16.91
PS	16.05	12.72	11.04	14.75	12.13	10.85	16.98	13.59	11.15
CnS	11.15	7.47	5.61	10.68	7.19	5.38	12.43	8.49	6.40
Output-Cost Ratio based on P_{ABS} (OCR_P (bits/JHz))									
	TPC			PBPC			PAPC		
M_{max}	2	3	4	2	3	4	2	3	4
OS	1.73	1.53	1.54	2.09	2.12	2.14	1.04	1.11	1.12
PS	1.29	1.31	1.32	1.61	1.50	1.47	0.58	0.50	0.45
CnS	1.11	1.12	1.12	1.26	1.12	1.08	0.43	0.34	0.30

4.6 Max-Min SINR Optimisation Problem

The max-min SINR optimisation problem is considered under three different power strategies: TPC (4.2.1), PBPC (4.2.2) and PAPC (4.2.3). The CSs of the users are chosen such that the minimum SINR is maximised. The joint optimisation problem presented in (4.4.7) is very complex, but can be solved iteratively as a series of simpler sub-problems. By exploiting the uplink and downlink SINR duality, the solutions to **U, V** and **p** can be obtained for any given Δ.

SINR duality was introduced in [47] for single-cell MISO downlink channel, the authors showed that the minimum sum power required to achieve a set of SINR values in the downlink is equal to the minimum power required to achieve the same set of SINR values in the uplink. In [48] and [49], the authors analysed the duality between the downlink broadcast channel and the uplink multi access channel (MAC), and showed that the downlink problem could be solved in the dual uplink since the analytical structure of the uplink problem was simpler. The SINR duality theorem has been proven for single-cell multi-user systems [47]. Since the BSs are cooperating, the BSs can be said to be transmitting as a single unit, (i.e. a "super BS") with distributed antennas and that the power allocation per user data is same across all BSs. Hence for the purpose of this work, the multi-cell multi-user system is converted to a single-cell multi-user system and the SINR duality theorem can be directly applied.

Consider the reciprocal uplink model, the received signal ($\mathbf{r}$) at the super-BS after post-processing by the receive beamforming vector ($\bar{\mathbf{v}}_k^H$) is given by:

$$\bar{\mathbf{v}}_k^H \mathbf{r} = \bar{\mathbf{v}}_k^H \mathbf{H}_k^{(k)H} \mathbf{u}_k \sqrt{q_k} s_k + \sum_{\substack{p=1 \\ p \neq k}}^{K} \bar{\mathbf{v}}_k^H \mathbf{H}_p^{(k)H} \mathbf{u}_p \sqrt{q_p} s_p + \bar{\mathbf{v}}_k^H \mathbf{n}, \ \forall\, k \in [1, 2, \cdots, K], \quad (4.6.24)$$

where $\mathbf{q} = [q_1,\, q_2, \cdots, q_K]^T$, q_k is the uplink power allocated to the k-th user data, $\mathbf{u}_k$ is the transmit pre-coder at the k-th user, $\bar{\mathbf{v}}_k$ is the receive beam-former at the super-BS

used to obtain the *k*-th user data and **n** is an additive, zero-mean, white, complex Gaussian noise vector where each element has a variance of σ^2. The uplink SINR ($\gamma_k^{(ul)}$) of the *k*-th user data can be derived as:

$$\gamma_k^{ul} = \frac{\left|\bar{\mathbf{v}}_k^H \mathbf{H}_k^{(k)H} \mathbf{u}_k\right|^2 q_k}{\sum\limits_{\substack{p=1 \\ p \neq k}}^{K} \left|\bar{\mathbf{v}}_k^H \mathbf{H}_p^{(k)H} \mathbf{u}_p\right|^2 q_p + \sigma^2}, \ \forall\, k \in [1, 2, \cdots, K]. \tag{4.6.25}$$

Given $\Delta^{(i+1)}$, the general approach in obtaining the corresponding solutions to $\mathbf{U}^{(i+1)}$, $\mathbf{V}^{(i+1)}$ and $\mathbf{p}^{(i+1)}$ in (4.4.7) is presented as follows.

1. Begin the iteration by setting *j* = 1 and randomly choosing $\mathbf{V}^{(j)}$ and $\mathbf{p}^{(j)}$.

2. Using the beamforming solution given in (4.6.26) obtain $\mathbf{U}^{(j+1)}$. Then find the downlink SINR ($\gamma_k^{dl(j+1)}, \forall k$) using (4.2.5). Set $\bar{\gamma}_k^{ul} = \min(\gamma_k^{dl(j+1)}, \forall k)$, $\bar{\gamma}_k^{ul}$ is equal for all *k*.

3. Find the uplink power allocation $\mathbf{q}^{(j+1)}$ by solving the optimisation problem in (4.6.28).

4. Find the precoding vector $\mathbf{V}^{(j+1)}$ using the general precoding solution given in (4.6.27). Then find the uplink SINR ($\gamma_k^{ul(j+1)}$) using (4.6.25). Set $\bar{\gamma}_k^{dl} = \min(\gamma_k^{dl(j+1)}, \forall k)$, $\bar{\gamma}_k^{dl}$ is equal for all *k*.

5. Find the power allocation $\mathbf{p}^{(j+1)}$ by solving the optimisation problem in (4.6.29).

6. Calculate $\max|\mathbf{p}^{(j)} - \mathbf{p}^{(j+1)}| < \varpi$, where ϖ is the convergence constraint. If the convergence constraint is satisfied then the solutions to $\mathbf{U}^{(i+1)}$, $\mathbf{V}^{(i+1)}$ and $\mathbf{p}^{(i+1)}$ are given by $\mathbf{U}^{(j+1)}$, $\mathbf{V}^{(j+1)}$ and $\mathbf{p}^{(j+1)}$ respectively. Otherwise set $j = j + 1$ and proceed to number 2.

   Note that the iterative method based on the virtual uplink and downlink is a virtual technique and requires no communication between the BS and the users as the iteration algorithm takes place at only the BS controller.

4.6.1 Beamforming Design

The following lemmas are useful in finding the solution to $\mathbf{U}$ and $\mathbf{V}$ in (4.4.7) using the well-known linear minimum mean square error (LMMSE) receiver [50]. Also the proof to the solutions obtained below are shown in Appendix A.

Proposition 1

Consider the downlink channel in (4.2.4) where $\Delta, \mathbf{V}$ and $\mathbf{p}$ are fixed and given. The normalised set of beamformers $\mathbf{U} = [\mathbf{u}_1, \mathbf{u}_2, \cdots, \mathbf{u}_K]$ that solves the optimisation problem in (4.4.7) is given in (4.6.26):

$$\begin{aligned} \mathbf{u}_k &= \hat{\mathbf{u}}_k / \left\|\hat{\mathbf{u}}_k\right\|_2, \quad \text{where} \\ \hat{\mathbf{u}}_k^H &= (\sum_{\substack{p=1 \\ p \neq k}}^{K} \mathbf{H}_k^{(p)} \bar{\mathbf{v}}_p \bar{\mathbf{v}}_p^H \mathbf{H}_k^{(p)H} \rho_p + \mathbf{I}\sigma_k^2)^{-1} \sqrt{\rho_k} \bar{\mathbf{v}}_k^H \mathbf{H}_k^{(k)H}. \end{aligned} \tag{4.6.26}$$

Proposition 2

Consider the virtual reciprocal (uplink) channel in (4.6.24) where $\Delta, \mathbf{U}$ and $\mathbf{q}$ are fixed and given. The normalised set of beam-formers $\{\bar{\mathbf{v}}_k\}_{k=1}^K$ that solves the optimisation problem in (4.4.7) is given in (4.6.27):

$$\begin{aligned} \bar{\mathbf{v}}_k &= \hat{\mathbf{v}}_k / \left\|\hat{\mathbf{v}}_k\right\|_2, \quad \text{where} \\ \hat{\mathbf{v}}_k^H &= (\sum_{\substack{p=1 \\ p \neq k}}^{K} \mathbf{H}_p^{(k)H} \mathbf{u}_p \mathbf{u}_p^H \mathbf{H}_p^{(k)} q_p + \mathbf{I}\sigma^2)^{-1} \sqrt{q_k} \mathbf{u}_k^H \mathbf{H}_k^{(k)}. \end{aligned} \tag{4.6.27}$$

4.6.2 Power Optimisation

Proposition 3

Considering the virtual reciprocal (uplink) channel in (4.6.24) where $\Delta, \mathbf{U}$ and $\mathbf{V}$ are fixed and given. The power optimisation problem in the virtual uplink needed to find $\mathbf{q}$

can be expressed as function of $\Delta, \mathbf{U}$ and $\mathbf{V}$ as shown in (4.6.28). The linear program is formulated as:

$$\begin{aligned}
&\max_{\mathbf{q}} \quad \min_{1\leq k\leq K} \frac{\left|\bar{\mathbf{v}}_k^H \mathbf{H}_k^{(k)H} \mathbf{u}_k\right|^2 q_k}{\sum\limits_{\substack{p=1\\p\neq k}}^{K} \left|\bar{\mathbf{v}}_k^H \mathbf{H}_p^{(k)H} \mathbf{u}_p\right|^2 q_p + \sigma^2}, \\
&\text{s.t.,} \frac{\left|\bar{\mathbf{v}}_k^H \mathbf{H}_k^{(k)H} \mathbf{u}_k\right|^2 q_k}{\sum\limits_{\substack{p=1\\p\neq k}}^{K} \left|\bar{\mathbf{v}}_k^H \mathbf{H}_p^{(k)H} \mathbf{u}_p\right|^2 q_p + \sigma^2} \geq \bar{\gamma}_k^{ul}, \\
&\sum_{k=1}^{K} q_k \leq p^{TOT} \text{ and } \mathbf{q} \succeq 0, \ \forall k \in [1, 2, \cdots, K].
\end{aligned} \tag{4.6.28}$$

Also considering the downlink in (4.2.4) where $\Delta, \mathbf{U}$ and $\mathbf{V}$ are fixed and given. The power optimisation problems required to find the transmit power $\mathbf{p}$, under TPC or PBPC or PAPC can be expressed as:

$$\begin{aligned}
&\max_{\mathbf{p}} \quad \min_{1\leq k\leq K} \frac{\left|\mathbf{u}_k^H \mathbf{H}_k^{(k)} \bar{\mathbf{v}}_k\right|^2 \rho_k}{\sum\limits_{\substack{p=1\\p\neq k}}^{K} \left|\mathbf{u}_k^H \mathbf{H}_k^{(p)} \bar{\mathbf{v}}_p\right|^2 \rho_p + \sigma_k^2}, \\
&\text{s.t.,} \frac{\left|\mathbf{u}_k^H \mathbf{H}_k^{(k)} \bar{\mathbf{v}}_k\right|^2 \rho_k}{\sum\limits_{\substack{p=1\\p\neq k}}^{K} \left|\mathbf{u}_k^H \mathbf{H}_k^{(p)} \bar{\mathbf{v}}_p\right|^2 \rho_p + \sigma_k^2} \geq \bar{\gamma}_k^{dl}, \ \forall k \in [1, 2, \cdots, K] \text{ and}
\end{aligned} \tag{4.6.29}$$

$$\mathbf{1}^T \mathbf{p} \leq p^{TOT}, \ \mathbf{p} \succeq 0, \text{ under TPC} \tag{4.6.30}$$

$$\text{or} \sum_{\substack{k=1\\\delta_{m,k}=1}}^{K} \mathbf{v}_{m,k}^H \mathbf{v}_{m,k} \rho_k \leq p_m^{PBPC}, m \in [1, 2, \cdots, K], \ \mathbf{p} \succeq 0, \text{ under PBPC} \tag{4.6.31}$$

$$\text{or} \left[\sum_{\substack{k=1\\\delta_{m,k}=1}}^{K} \rho_k \mathbf{v}_{m,k} \mathbf{v}_{m,k}^H\right]_{i,i} \leq p_{m,i}^{PAPC}, \ \forall m \in [1, 2, \cdots, K],$$

$$\forall i \in [1, 2, \cdots, M_t],\ \mathbf{p} \succeq 0,\ \text{under PAPC} \qquad (4.6.32)$$

where σ_k^2 and σ^2 are assumed to be 1, $\bar{\gamma}_k^{ul}$ and $\bar{\gamma}_k^{dl}$ are the minimum required SINR in the uplink and downlink respectively for the *k* user's data stream. The general approach used to approximate the problems in (4.6.28) and (4.6.29) into a convex optimisation problem is presented in [51], and can be solved by an optimisation solver. In the simulations, the Yalmip solver is used to obtain the power optimisation solutions [52].

4.6.3 CS Selection Algorithm for Max-Min SINR Optimisation Problem

The Δ that maximises the minimum SINR optimisation problem in (4.4.7) subject to C1 or C2 or C3, is obtained using the algorithm below. The iterative solution is obtained by searching through a significantly reduced set of possible solutions. First initialise the variables, where *i* is the iteration count, $x^{(i)}$ is the convergence variable of the algorithm, f_k is the number of assigned BSs to user *k* and $\bar{\gamma} = \min(\{\gamma_k^{dl}\}_{k=1}^{K})$ is the minimum SINR. At each iteration, the minimum SINR is maximised among the users by assigning another BS to user *k* when $\gamma_k^{dl} < \bar{\gamma}$. The iteration continues until the maximum number of allowed transmit BSs per user (M_{max}) is reached and BS assignment is no longer possible. The Δ and corresponding **U, V** and **p** that achieves the highest minimum SINR, is selected for CoMP transmission. The pseudo-code of the CS selection algorithm is given in Table 4.5).

Table 4.5: Proposed CS selection algorithm based on maximising the minimum SINR

Initialization: $i = 0,\ \left\{f_k^{(i)}\right\}_{k=1}^{K} = 0,\ \left\{\text{SINR}_k^{dl(i)}\right\}_{k=1}^{K} = 0,\ \bar{\gamma}^{(i)} = 1,\ x^{(i)} = 1,\ \Delta^{(i)} = \mathbf{0}$.

while any ($\text{SINR}_k^{dl(i)} < \bar{\gamma}^{(i)}$)

if $x^{(i)} \neq 0$

1. From (3.2.5), find $\Delta^{(i+1)}$.

for $k = 1 : K$

if $\text{SINR}_k^{dl(i)} < \bar{\gamma}^{(i)}$ and $f_k^{(i)} < M_{max}$

$f_k^{(i+1)} = f_k^{(i)} + 1$ and $\delta_{m,k}^{(i+1)} = 1$

(if BS m has the best channel quality to user k and $\delta_{m,k}^{(i)} = 0$).

end if, **end for**

2. Find $\mathbf{U}^{(i+1)}$, $\mathbf{V}^{(i+1)}$ and $\mathbf{p}^{(i+1)}$ as shown in Section 4.6.

3. Find $\text{SINR}_k^{dl(i+1)}$ ($\gamma_k^{dl(i+1)}$), $\forall k$ from (4.2.5).

if $\bar{\gamma}^{(i+1)} > \bar{\gamma}^{(i)}$

$\Delta \leftarrow \Delta^{(i+1)}$, $\mathbf{U} \leftarrow \mathbf{U}^{(i+1)}$, $\mathbf{V} \leftarrow \mathbf{V}^{(i+1)}$ and $\mathbf{p} \leftarrow \mathbf{p}^{(i+1)}$.

else $\bar{\gamma}^{(i+1)} = \bar{\gamma}^{(i)}$

end if

$x^{(i+1)} = \sum_{k=1}^{K} (f_k^{(i+1)} - f_k^{(i)})$, i++.

end if, **end while**.

4. **repeat** steps 1-3 **until** $x^{(i+1)} = 0$ or $f_k^{(i+1)} = f_k^{(i)}$, $\forall k$.

4.6.4 Simulation Results and Evaluation

Table 4.6: Summary of simulation parameters [3, 4, 5].

Parameters	**Value**
Antenna type, Cell layout (K)	Omnidirectional, 3 cell sites.
Time slot per RB, $[\alpha, \eta_s]$	0.5msecs, [2, 8dB]
Inter site distance (ISD)	500m
cell-edge user distance	$\geq$ 260m
Number of antennas (M_t, N_r)	(4, 2)
P^{TOT}, P_m^{PBPC}, $P_{m,i}^{PAPC}$	[120W, 40W, 10W]

Note: PBPC parameter is selected as in [46], set $p^{TOT} = Kp_m^{PBPC}$ and $p_{m,i}^{PAPC} = p_m^{PBPC}/M_t$.

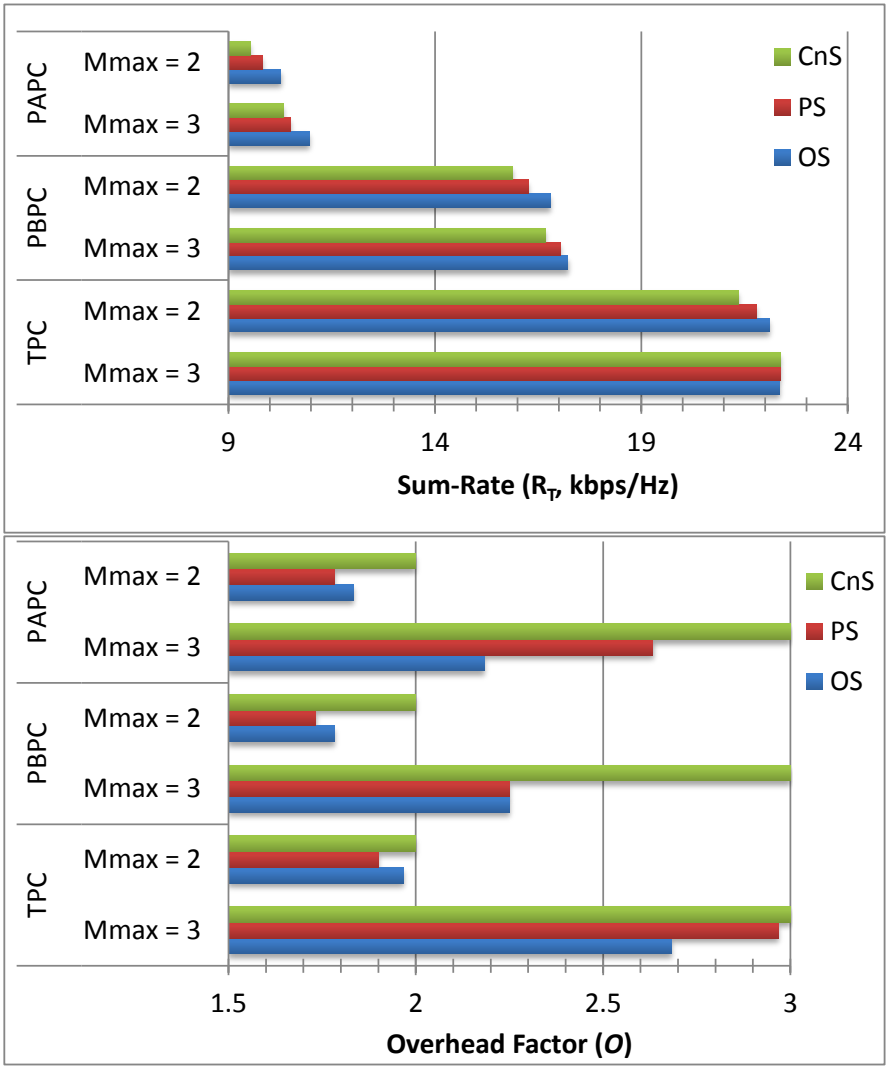

Figure 4.8: The achieved sum-rate (R_T) (top) and overhead factor (O) (bottom), for the max-min SINR problem according to three different power constraints (TPC, PBPC and PAPC), and three different approaches (CnS, PS and OS) to a solution.

For different values of M_{max}, under the given simulation parameters in Table 4.6, the simulation results for the max-min SINR optimisation problem is obtained while

considering different power constraints. In this section, "CnS" (i.e. $M_k = M_{max}, \forall k$) refers to the *conventional solution* with equal number of BSs per CS, "OS" refers to the *optimum CS solution* based on the hard search and "PS" (i.e. $M_k \leq M_{max}, \forall k$) refers to the CS solution using the *proposed solution*.

From Table 4.7 and Fig. 4.8, the minimum SINR achieved under the PBPC using the OS, PS and CnS is 11.70 dB, 11.58 dB and 11.55 dB respectively for M_{max} = 2 and 11.78 dB, 11.68 dB and 11.64 dB for M_{max} = 3. The resulting sum-rate performance is given by 16.80 kbps/Hz, 16.27 kbps/Hz and 15.88 kbps/Hz. The corresponding overhead factor (O) of the backhaul demand is 1.78, 1.73 and 2 respectively when M_{max} = 2, and 2.25, 2.25 and 3 when M_{max} = 3.

From the results, one can see that the OS achieves the highest minimum SINR and sum-rate, but its backhaul demand is 10.85% and 25% less for M_{max} = 2 and 3 respectively, when compared to the conventional solution. Also PS achieves almost similar output performance to the OS, but with a 13.35% and 25% reduction in the backhaul overhead for M_{max} = 2 and 3 respectively, when compared to the CnS. Note that in this case PS is sub-optimum and even though the data overhead reduction is more but the min-SINR achieved is less than that achieved with the OS.

These results show that a joint and adaptive solution of the CSs is necessary to reduce the backhaul demand required during CoMP transmission, while still achieving a better system performance. As a result of this, an OCR of 9.42 bps/Hz, 9.39 bps/Hz and 7.94 bps/Hz is obtained for M_{max} = 2 using OS, PS and CnS and 7.65 bps/Hz, 7.57 bps/Hz and 5.56 bps/Hz for M_{max} = 3. It is clear that the OS and PS solutions achieve the best productivity with almost similar performance, while the CnS approach achieves the lowest. The achieved sum-rates and overhead factor under PAPC when M_{max} = 2 is 10.27 kbps/Hz and 1.83 with OS. The CnS achieves an almost similar sum-rate of 10.33 kbps/Hz when M_{max} = 3 but with an overhead factor of 3. Again without the complexity of OS, the joint selection of the CSs is capable of achieving a given QoS constraint, while reducing the data overhead by 64%.

Table 4.7: Optimisation results

		TPC		PBPC		PAPC	
	Sol. Type	$M_{max}=2$	$M_{max}=3$	$M_{max}=2$	$M_{max}=3$	$M_{max}=2$	$M_{max}=3$
Sum-rate (kbps/Hz)	OS	25.21	27.81	20.70	22.65	16.58	18.58
	PS	25.05	27.68	20.27	22.27	14.92	17.39
	CnS	25.05	27.68	20.18	22.20	14.80	16.68
Overhead factor (O)	OS	1.98	2.79	1.83	2.47	1.88	2.27
	PS	1.96	3.00	1.78	2.88	1.84	2.46
	CnS	2.00	3.00	2.00	3.00	2.00	3.00
min SINR (dB)	OS	15.40	15.45	11.70	11.78	6.43	6.58
	PS	15.32	15.45	11.58	11.68	6.17	6.30
	CnS	15.26	15.45	11.55	11.64	6.11	6.18
CAT (secs)	OS	1022	2760	805	1765	468	1102
	PS	16.0	25.7	12.6	18.5	5.6	9.3
	CnS	1.8	2.0	3.9	3.9	5.4	7.0
OCR_O (bps/Hz)	OS	11.24	8.33	9.42	7.65	5.60	5.02
	PS	11.47	7.54	9.39	7.57	5.51	3.99
	CnS	10.67	7.46	7.94	5.56	4.76	3.44

The results in Fig. 4.8 and Table 4.7 under the given power strategies, show that CnS achieves the lowest sum-rate performance and CS allocation time (CAT), but has the highest demand as regards to the backhaul load. The OS approach is seen to generally achieve the best sum-rate and the lowest backhaul demand but requires a much longer CAT. In Table 4.7 it can be seen that the CAT for OS is extremely high, ranging from 468

- 1022 secs and 1102 - 2760 secs respectively for M_{max} = 2 and 3, while for PS the CAT ranges from 5.6 - 16 secs and 9.3 - 25.7 secs respectively.

Also the search complexity, N_{TS}, for OS is 216 and 343, when M_{max} = 2 and 3 respectively, and from simulations a corresponding search complexity of N_{TS} = 4 and 5 respectively for PS is obtained. The advantage of an optimum joint CS selection for users is undeniable. However, the complexity involved using hard-search and the CAT taken to achieve this is very high and can lead to poor synchronisation and high latency. The PS significantly reduces both the OS complexity and CAT by at least 98%, while still maintaining the advantage offered by OS, and exceeding the CnS performance.

Intuitively, as the number of supporting BSs per user increases (i.e $M_{max} > 3$), the percentage increase in data rate diminishes while the data overhead increases. This happens because the BSs with poorer signal strength will contribute no significant improvement to the user's performance but the inclusion of such BSs in the CSs will increase the overhead. Hence for this optimisation problem, higher values of M_{max} are not considered for data overhead reduction.

Now to obtain the effective M_{max} for this system, the OCR performance based on the data overhead is considered. When M_{max} = 3 the OCR performance with OS, under TPC, PBPC and PAPC respectively, is 26%, 19% and 10% lower than when M_{max} = 2 as seen in Table 4.7. This shows that when M_{max} = 3, the productivity based on the overhead demanded is significantly reduced. For instance, a 47% increase in the backhaul data overhead is needed to obtain a 7% increase in sum-rate performance using PS under PAPC. So in this case, M_{max} = 2 is the system condition that achieves the best productivity.

4.7 Summary

This chapter analysed the challenges faced in CoMP transmission while improving the system performance of cell-edge users. It also analysed previous proposed strategies like the fixed cluster size or fixed number of BSs per user pre-set by the network for

CoMP transmission. This strategy limits the data overhead in the backhaul, but further improvement was required to obtain more reduction in the network costs and better system performance. The improved CS selection introduced in this chapter shows that a further reduction can be obtained in the backhaul data overhead while improving the system performance, if the CSs of the users are chosen jointly. Using two different optimisation strategies under three different power constraints, the proposed solution was presented and compared to the optimum CS solution and the conventional "fixed" size solution. It was shown that the proposed solution outperformed the conventional solution by achieving a higher sum-rate performance as well as greatly reducing the required backhaul data overhead demand. Also the proposed solution was shown to achieve the advantage of the optimum solution but with reduced complexity and CS allocation time. This advantage means that a joint CS selection is achievable and necessary to obtain a reduction in the data overhead and energy consumption, in order to achieve low latency and better synchronisation in the system during CoMP transmission.

Chapter 5

Radio Resource Management for Interference Coordination

5.1 Introduction

In this chapter, the challenges faced by existing RRM strategies for interference avoidance in homogeneous and heterogeneous networks are analysed. One of the major forms of RRM is the RBA of frequency and time slots to the users within the cellular network, such that the interference is avoided. However, issues such as high data overhead, poor synchronisation, high latency, poor channel utilisation, poor spectral efficiency, high interference, and limited resources available for existing and future demands need to be addressed in order to improve the existing system performance.

Several works have been proposed in the past to deal with interference in the homogeneous network. Different RBA modes and metrics have been used to allocate RBs to users, but several challenges are still to be solved. For instance most proposed works have been based on the centralised RBA, semi-centralised RBA and very few on distributed RBA. Also the RBA metric used is mostly based on the location of the user, the SNR of each user and the path loss from the BSs to the user. So far no known technique has been proposed which directly uses the SINR as a RBA metric to assign RBs in a

centralised, semi-centralised or distributed approach. RBA metrics based on interference estimation such as the SINR, have been avoided by most authors in the past since the pre-knowledge of existing users on the RBs are required to obtain the SINR for each user on all available RBs prior to resource allocation. The authors in [53, 54] stated that obtaining the SINR is impossible, hence their preferred strategy is an approach which removes the direct dependency on the SINR of the users during RBA.

The HetNet system model has been developed to cope with the ever increasing traffic, but the multi-layers of the network leads to very high interference. An intelligent RRM strategy is needed to limit the interference within the system. Considering both the homogeneous and heterogeneous network model, this chapter aims to provide a solution that achieves a distributed RBA such that each macro cell or small cell is responsible for assigning RBs to its users and the overall system performance is improved.

The contributions of this chapter are as follows: Firstly, the RBA techniques used for interference avoidance for the homogeneous network are considered. A distributed RBA technique based on limiting the interference received by the users is proposed. The proposed method under the homogeneous network, shows a distributed strategy that assigns the RBs in a manner that allows the interference to be estimated and avoided while maximising the sum-SINR within each cell. Note that this distributed RBA approach using the sum-SINR as a RBA metric, can also be applied to HetNets.

Secondly, the proposed distributed technique using the SINR as a RBA metric is compared to the traditional distributed RBA using SNR as a RBA metric. Also the proposed distributed RBA strategy will be compared to other modes of RBA and the advantage of the distributed strategy will be presented and analysed using simulation results.

Thirdly, another distributed RBA technique is proposed for the HetNets, such that a further reduction in the interference within the system is achieved, thereby improving the attainable system performance even in a high interference network. The proposed distributed technique uses the signal to leakage plus interference and noise ratio (SLINR) as a RBA metric.

Fourthly, through obtained simulation results the proposed technique is analysed for the HetNet system model and compared to other RBA metrics such as the proposed sum-SINR maximisation strategy and the already existing sum-SNR maximisation strategy.

The rest of this chapter is organised as follows: Section 5.2 presents different forms of RBA, Section 5.3 presents the associated costs on the network needed for RBA which would be used to analyse the simulation results. The proposed interference avoidance technique for the homogeneous network is presented in Section 5.4, and the interference avoidance technique for the HetNet is proposed in Section 5.5. Finally the conclusion of this chapter is found in Section 5.6.

5.2 Different Modes of RBA

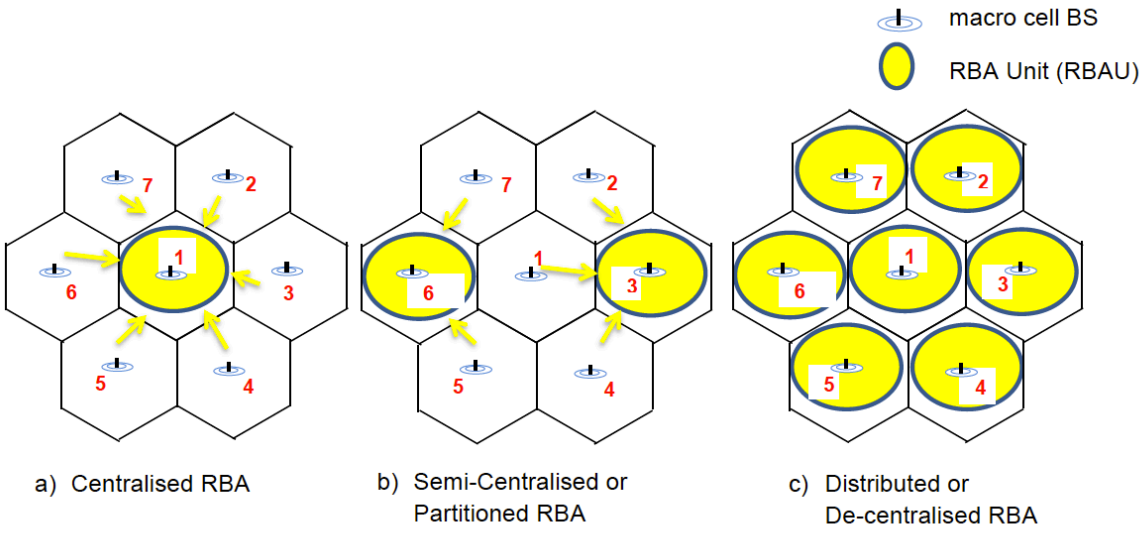

Figure 5.1: Different modes of resource block allocation.

Several resource management techniques for ICIC have been investigated for the cellular network, especially traditional homogeneous networks. Most works proposed in this

area fall into static, semi-static and dynamic ICIC techniques, with different advantages and challenges. The well known static ICIC is based on hard frequency partitioning [55, 56, 57, 58], which is used for interference avoidance within a network. This includes fractional frequency re-use (FFR), soft-frequency reuse (SFR) and partial frequency reuse (PFR). In [59, 60], Alcatel proposed an ICIC technique that aggressively assigned resources to the cell-edge users, thereby causing poor utilisation of resources at the cell-centre area. Under semi-static frequency partition, signalling exchange is done periodically, while taking the network load changes into consideration. In [61, 62, 63], several semi-static frequency partition schemes such as semi-static fractional frequency re-use (FFR), whispering approach, softer frequency re-use (SerFR) and adaptive FFR were proposed. These proposed schemes faced setbacks such as poor frequency utilisation at the cell-edge and/or cell-centre area. The frequency partition was partially adaptive, so the varying traffic load and channel conditions were not fully taken into consideration.

Dynamic ICIC (D-ICIC) adapts to the changing network conditions and traffic loads, hence frequency allocation can be more complex and challenging. D-ICIC techniques require more frequent exchange of channel information, which comes with a high cost of backhaul overhead especially for the centralised D-ICIC. Other types of D-ICIC are: semi-centralised/partitioned coordination and de-centralised/distributed coordination [64]. D-ICIC schemes offer better system performance, gain, spectral efficiency, user diversity and frequency diversity compared to the static or semi-static methods. Although, the challenges faced include very high backhaul overhead, frequent exchange of CSI and user information, high latency, poor synchronisation and increased RBA time.

The following sections will present the advantages and drawback of the different modes of RBA such as centralised RBA, semi-centralised/partitioned RBA, de-centralised/ distributed RBA under dynamic ICIC and frequency partitioned RBA under static ICIC. The proposed RBA technique is based on the distributed RBA, which is now the main strategy sought for current and future generation cellular network. The proposed distributed RBA strategy will be compared with results obtained using the centralised RBA, semi-centralised/partitioned RBA and frequency partitioned RBA to analyse and

evaluate the advantages of the preferred and proposed approach to other forms of RBA.

5.2.1 Dynamic ICIC

Centralised RBA

As can be seen in Fig. 5.1(a), the centralised D-ICIC, requires all CSI and user information to be fed from all BSs or eNodeBs (eNBs) in the network to the radio network controller (RNC) which is situated with a BS. The Resource Block Allocation Unit (RBAU) performs the RBA using the information gathered and then transmits the assigned RBs back to the serving BSs for each user's data transmission. The major problem associated with the centralised approach is the high data load exchanged in the backhaul network. This puts a strain on the network and increases the RBA time and required overhead. The control function of the RNC is now embeded into the NodeB to form the eNodeB in LTE-A. This makes the centralised D-ICIC technique impractical for LTE-A as it has no RNC which is needed for the centralised RBA. However in [65, 66, 67], the authors proposed the mobility management entity (MME) to enable the centralised coordination and management of the radio resources.

Some authors have investigated this mode of resource allocation in [53, 54], where the RBA was carried out centrally. The main challenge for the authors was performing the RBA centrally based on the SINR of the users, so the RBA problem was approached and solved in two steps. First, the interference level was managed using graph theory to match users into clusters such that the interference seen by the users are minimised. Then the resource allocation is performed on the clusters to leverage the CSI quality based on the SNR values of the users in the clusters.

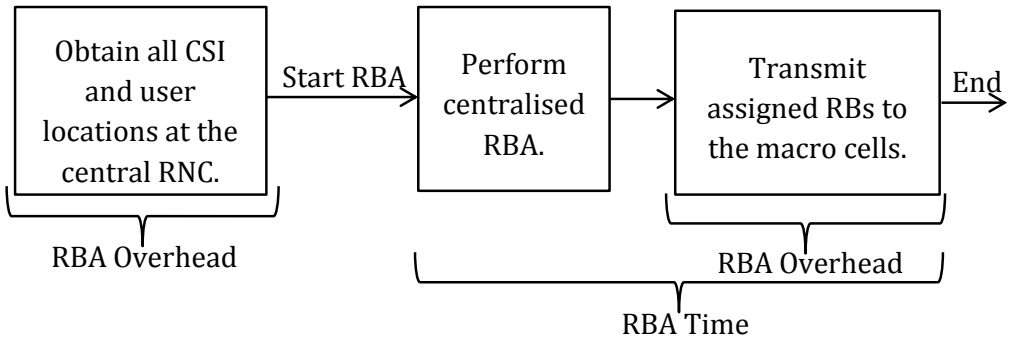

Figure 5.2: Centralised RBA performed by the RNC.

In Fig. 5.2 the diagram shows the RBA overhead experienced in the backhaul in order to obtain the CSI at the central RNC and also when transmitting allocated RBs to the macro cell sectors. The RBA time is the time used to allocate resources and transmit the information back to the BSs/eNBs for data transmission.

Semi-Centralised or Partitioned RBA

The semi-centralised or partitioned RBA approach divides the macro-cells within the network into sub-groups or clusters as shown in Fig. 5.1(b). Each cluster is delegated a RBAU, which is geographically located with a serving cell-site. In Table 5.1, different possible partition types are proposed with different numbers and sizes of clusters, for W = 19 macro cell sites. The macro cell site index number in the box is where the RBAU is located, and other cell sites within the cluster transmit information to the RBAU for resource management. This method is similar to the centralised D-ICIC but with smaller groups of BSs. The smaller the number of partitions, the lower the interference and vice versa. This is because as the number of partitions increase, possible interference from less number of neighbouring cells are considered during RBA which results in an increased interference within the network. In the simulation results, it can be observed that as the number of partitions within the network increases, a corresponding decrease is observed in the backhaul overhead and RBA time required to assign RBs to users within the network.

However, since the other clusters are not taken into account during the resource allocation, an increase in the sum-interference power is expected within the network. Another form of semi-centralised and frequency partitioned based RBA requires the RBs to be assigned centrally to different macro cells, and then the macro cells assign RBs to their users based on the allocation of RBs received [68].

Table 5.1: Proposed cell partition types.

Type	Number of Partitions	Partition Sets
Group A	2	$\{1, 2, \boxed{3}, 4, 8, 9, 10, 11, 12, 19\}$, $\{5, \boxed{6}, 7, 13, 14, 15, 16, 17, 18\}$
Group B	3	$\{1, \boxed{2}, 3, 8, 9, 10\}$,$\{4, 5, 11, 12, \boxed{13}, 14\}$, $\{6, 7, \boxed{15}, 16, 17, 18, 19\}$
Group C	4	$\{1, \boxed{4}, 11, 12, 13\}$,$\{2, 3, 8, \boxed{9}, 10\}$, $\{7, 17, \boxed{18}, 19\}$, $\{5, 6, 14, \boxed{15}, 16\}$
Group D	5	$\{\boxed{1}, 4, 6\}$,$\{2, \boxed{8}, 9, 19\}$,$\{3, 10, \boxed{11}, 12\}$, $\{5, 13, \boxed{14}, 15\}$, $\{7, 16, \boxed{17}, 18\}$
Group E	6	$\{1\boxed{2}, 8, 9\}$,$\{3, 10, \boxed{11}\}$,$\{4, 12, \boxed{13}\}$, $\{5, 14, \boxed{15}\}$,$\{6, 16, \boxed{17}\}$,$\{7, 18, \boxed{19}\}$

Intuitively, one can see that this approach is repetitive as the RBs need to be re-assigned or re-evaluated at the RNC to minimise the interference. This could result in large overhead, poor synchronisation, high latency and poor interference avoidance. These methods are hybrids of centralised and distributed strategies, with the aim of trading off performance with high data backhaul and complexity. The problem of high data overhead and latency associated with RBA for interference management within the network is still a huge challenge. The cell partition shown in "Group B" and "Group E" will be used later in this chapter with the proposed RBA metric and compared to the proposed distributed RBA strategy.

In Fig. 5.3 the diagram shows the CSI information collected centrally at each cell

partition. The larger the number of partitions the lower the CSI overhead and RBA time. The trade-off for lower RBA time and overhead in the system is a higher interference level. Since the BSs in each cell partition does not communicate with the BSs in other partitions, the interference is partially mitigated.

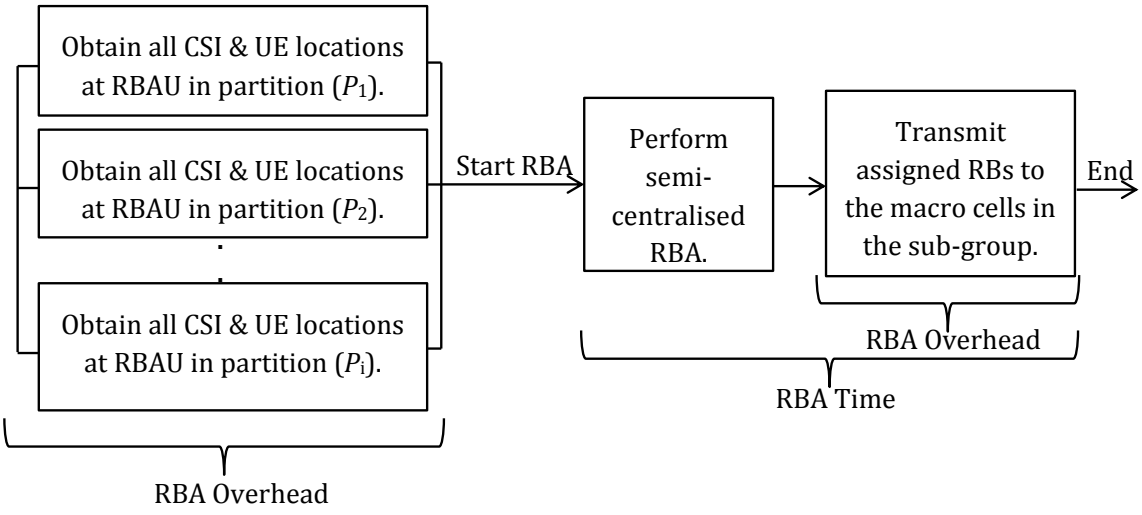

Figure 5.3: Semi-centralised or partitioned RBA performed by the RBAU in each partition.

Distributed or De-centralised RBA

The distributed or de-centralised RBA under D-ICIC, aims to reduce the backhaul overhead by allowing the resource management techniques to be performed independently by the macro cells for its users as shown in Fig. 5.1(c). This method is most suitable for the LTE-A standard, since there is no provision for a central control unit (CCU) in the LTE-A standards for 4G networks. Also this method is needed to ensure that current and future cellular wireless networks are self-organising networks (SON). However, this approach faces several challenges especially interference, since the allocation on each cell is expected to be done simultaneously, hence the BSs have no prior information of possible interference transmitted or received from neighbouring cells.

To exploit the achievable rates, it became necessary to develop radio resource management techniques that tend towards an adaptive and dynamic coordination, taking into account the channel and user diversity in the time spectrum, frequency spectrum or both. In [69], a non-cooperative distributed RB allocation strategy was proposed to minimise the total transmit power in each cell, in order to achieve an efficient network. The solution did not fully exploit the achievable throughput in each cell, since the effect of interference was not taken into account. In [70], each BS was made to assign transmit powers and RBs independently, while minimising the total transmit power with a given minimum QoS constraint. The allocated RBs for the cell-edge users are then exchanged so that the neighbouring BSs do not use high transmit powers on those selected RBs. In reducing the transmit powers on the selected RBs, the user's previous attainable rates are reduced and may not meet the QoS requirements previously attained during the RBA. Also in [62], the proposed distributed RBA approach is based on a limited feedback of SNRs of the "best M-RBs" for each user, and the users are then assigned RBs on a first-come, first-serve basis based on the available RBs and information on the best M-RBs for that user. This method only reduces the feedback of information and is ineffective since the effect of interference from neighbouring cells are not considered. The distributed RBA approach proposed by other authors in the past, avoids using any RBA metric that requires computing the interference for any user as this is very complex to achieve especially for the distributed mode of RBA. This has resulted in methods that avoid the interference entirely. But since the HomoNet is limited by high interference, and the achievable rates are dependent on the SINR of the users, it is important to take the interference into consideration during RBA for interference avoidance. The proposed work in Section 5.4 shows that this can be achieved in a distributed approach.

5.2.2 Static ICIC - Fractional Frequency Reuse

Earlier, the static and semi-static frequency partition techniques for ICIC were presented for homogeneous networks. In Fig. 5.4, the FFR is shown using the cell sectors, m = [1,

2, 3, 5, 6, 7, 8, 9, 10, 20]. The different areas of the cells are allowed some portions of the available spectrum, thereby reducing the spectral efficiency and gains obtained from frequency diversity. The frequency partitioning in 'Type B' achieves a better channel diversity than 'Type A', since the channel may experience deep fading in some parts of the frequency spectrum. The FFR has been shown using different strategies in order to maximise the frequency utilisation and restrict any possible interference, but this strategy still experiences poor spectral efficiency.

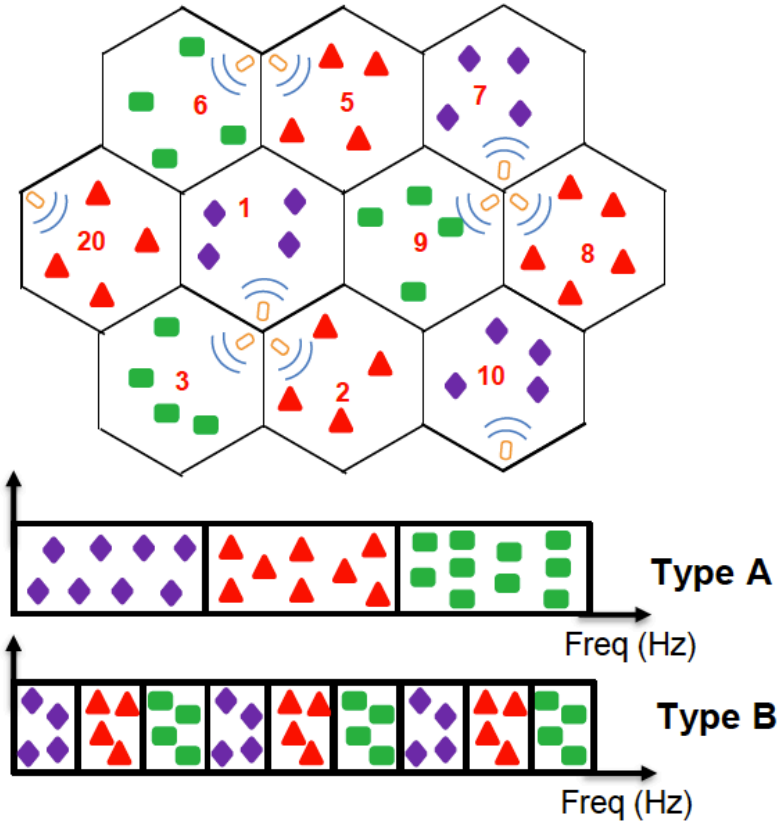

Figure 5.4: Frequency partitioned RBA.

For instance, as shown in Fig. 5.4, the macro cell sectors have access to only one-third of the available spectrum. However, this approach has some advantages such as very low RBA time, no overhead and less complexity. But the obtained rate does not meet the huge

capacity demands especially as the traffic load of the network increases.

5.3 RBA Costs

The RBA costs analysed in this chapter include the time taken to allocate the RBs to the users and the overhead required to obtain the RBs for each user based on the mode of allocating the RBs such as centralised, semi-centralised (or partitioned) and distributed (or de-centralised) RBA. The following definitions are defined: the macro cell site considered are $w = [1, 2, \cdots, W]$, where w is the macro cell site index and W is the number of macro cell sites. Each macro cell site uses δ-sectored macro cell directional antennas resulting in $m = [1, 2, \cdots, M]$ macro cell sectors and $M = W\delta$, $l = [1, 2, \cdots, \delta]$ where l is the macro cell sector antenna index and δ is the number of directional antennas per macro cell site.

5.3.1 RBA Time

The RBA time is defined as the total time taken to perform the RBA centrally, semi-centrally or de-centrally and then transmit the information back to the cells. The total RBA time (t_{TRBA}) for the centralised and semi-centralised RBA is given by (5.3.1) and (5.3.2) respectively, while the distributed total RBA time is given by (5.3.3):

$$t_{TRBA}^{cent} = 2t_{prop} + \sum_{w=1}^{W} t_w + t_{tran}^{CSI} + t_{tran}^{pos} + t_{tran}^{RB}. \tag{5.3.1}$$

$$t_{TRBA}^{s-cent(i)} = \max\{2t_{prop} + \sum_{w=1, w\in P_i}^{W} t_w + t_{tran}^{CSI} + t_{tran}^{pos} + t_{tran}^{RB},\ i = [1, 2, \cdots, N_i]\}. \tag{5.3.2}$$

$$t_{TRBA}^{dist} = \sum_{l=1}^{\delta} (t_l + e_l). \tag{5.3.3}$$

where t_{prop} is the propagation delay time, t_w is the RBA processing time for the w-th macro cell site w, t_{tran}^{CSI} is the time taken to transmit the CSI to the MME or RBAU, t_{tran}^{pos}

is the time taken to transmit the user's position to the RBAU, and t_{tran}^{RB} is the time taken to transmit the allocated RB information back to the macro cell BSs. N_i is the number of clusters or partitions, P_i is the i-th cluster/partition in the network. Also, t_l is the maximum time taken to simultaneously assign RBs to all the users in all the macro cell sectors with antenna index l and e_l is the maximum time taken to exchange RB information assigned at time t_l to neighbouring macro cell sites.

$$e_l = \max\{t_{prop} + \frac{\varphi_m}{\zeta}, \forall w = [1, 2, \cdots, W], m = (w-1)\delta + l\}, \ \forall l = [1, 2, \cdots, \delta], \tag{5.3.4}$$

where $\varphi_m = \alpha\bar{K}_m$ is the RB information data size from the m-th macro cell sector, $\bar{K}_m$ is the number of users in the m-th macro cell sector, α is the number of bits required to transmit each RB information and ζ is the data rate through the backhaul link.

5.3.2 Overhead

The backhaul overhead is defined as the associated data or backhaul load required in the backhaul network when performing RBA within a given network at a given time. This includes the data load required when sharing users' data CSI from the macro cell to the central unit (MME or RBAU) for RBA. Assuming β, ϕ and α bits are required to transmit the channel quality information (CQI), the user's location to the MME (for the case of centralised and semi-centralised RBA) and the allocated RB information from the MME/RBAU to the macro cells respectively. So the total number of bits transmitted in the backhaul under the centralised, semi-centralised and distributed RBA, per unit time, is given by (5.3.5), (5.3.6) and (5.3.7) respectively:

$$O_{cent} = \sum_{w=2}^{W} \sum_{l=1}^{\delta} \bar{K}_m(\beta N_{RB}(\theta_m + 1) + \phi + \alpha), m = (w-1)\delta + l, \tag{5.3.5}$$

$$O_{semi-cent} = \sum_{i=1}^{N_i} \sum_{\substack{w=1, w\in P_i \\ w\neq x_i}}^{W} \sum_{l=1}^{\delta} \bar{K}_m(\beta N_{RB}(\theta_m + 1) + \phi + \alpha), m = (w-1)\delta + l, \tag{5.3.6}$$

$$O_{dist} = \sum_{l=1}^{\delta} \sum_{w=1}^{W} \alpha \bar{K}_m \theta_m, \; m = (w-1)\delta + l. \tag{5.3.7}$$

where x_i is the macro cell site hosting the RBAU in each cell partition P_i, N_{RB} is the number of available RBs per time slot and θ_m is the number of macro cell sectors receiving RB information from the m-th macro cell sector.

5.4 Interference Management in Homogeneous Network

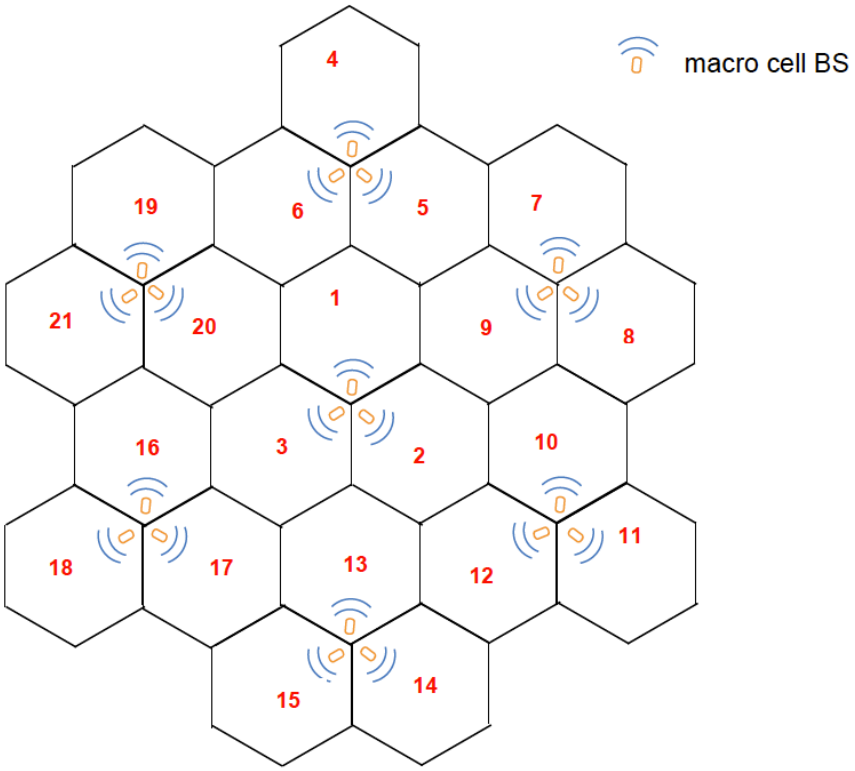

Figure 5.5: Homogeneous network with $W = 7$ macro cell sites and $\delta = 3$ sectors per site.

For several decades, the HomoNet has been the traditional approach for network deployment. The HomoNet comprises of macro cell BSs which cover wide areas and serve several users. The macro cell locations are carefully planned and located, so

that maximum coverage and capacity is achieved. Each macro cell BS has the same antenna patterns, transmit power capacity and backhaul connectivity. As the network user demand increased, more BS deployment was needed. However, the cost of acquisition and deployment of macro cell sites in dense urban areas became more difficult [71].

5.4.1 HomoNet System Model

For the homogeneous model, most of the variables used to present the work are defined in Table 5.2. The HomoNet in Fig. 5.5 shows the deployment of $W = 7$ macro cell sites and $\delta = 3$ sectors for each macro cell site within the network. Each macro cell sector transmits data on allocated RBs to the users within the macro cell sector. The homogeneous network is OFDMA based and has a frequency reuse of 1. Based on the system in Fig. 5.5, the signal received by the *k*-th user from the *m*-th macro cell BS on the *r*-th RB, is given by:

$$\mathbf{y}_{k,r}^{(m)} = \mathbf{H}_{k,r}^{(m)} \sqrt{\rho_{k,r}^{(m)}} s_{k,r}^{(m)} + \sum_{\substack{d=1,\, d\neq m \\ j\in[1,2,\cdots,\bar{K}_d] \\ a_{j,r}^{(d)}=1}}^{M} \mathbf{H}_{k,r}^{(d)} \sqrt{\rho_{j,r}^{(d)}} s_{j,r}^{(d)} + \mathbf{n}_{k,r}^{(m)}, \text{ if } a_{k,r}^{(m)} = 1,$$

$$\forall\, k \in [1, 2, \cdots, \bar{K}_m],\ \forall m \in [1, 2, \cdots, M],\ \forall r \in [1, 2, \cdots, N_{RB}]. \tag{5.4.8}$$

The coefficients of $\mathbf{H}_{k,r}^{(m)}$ are complex random variables, with zero-mean Gaussian real and imaginary parts. The channel links experience large scale fading, with path loss exponent (α) and log-normal shadowing having zero-mean and variance σ_s^2. $s_{j,r}^{(d)}$ is the complex (scalar) data signal destined for the *j*-th user on the *r*-th RB in the *d*-th macro cell (E $\left\{|s_{j,r}^{(d)}|^2\right\} = 1$), and $\mathbf{n}_{k,r}^{(m)}$ is an additive, zero-mean, white, complex Gaussian noise vector with a variance of $(\sigma_{k,r}^{(m)})^2$. The downlink SINR of the *k*-th UE on the *r*-th RB, served by the *m*-th macro cell, is given below in (5.4.9):

$$\gamma_{k,r}^{(m)} = \frac{g_{k,r}^{(m)} \rho_{k,r}^{(m)}}{\sum_{\substack{d=1,\, d\in T_m \\ j\in[1,2,\cdots,\bar{K}_d],\, a_{j,r}^{(d)}=1}}^{M} g_{k,r}^{(d)} \rho_{j,r}^{(d)} + (\sigma_{k,r}^{(m)})^2}, \text{ if } a_{k,r}^{(m)} = 1,$$

$$\forall\, k \in [1, 2, \cdots, \bar{K}_m],\ \forall m \in [1, 2, \cdots, M],\ \forall r \in [1, 2, \cdots, N_{RB}], \tag{5.4.9}$$

where $g_{k,r}^{(m)} = \|\mathbf{H}_{k,r}^{(m)}\|_F^2$. The user-rate at the k-th UE on the r-th RB, served by the m-th macro cell, is given by $R_{k,r}^{(m)}$, while the sum-rate for the m-th macro cell sector is given by $R_T^{(m)}$, and the total rate in the network is given below (5.4.10) as:

$$R_T = \underbrace{\sum_{m=1}^{M} \sum_{k=1}^{\bar{K}_m} \sum_{r=1}^{N_{RB}} \underbrace{a_{k,r}^{(m)} \log_2\left(1+\gamma_{k,r}^{(m)}\right)}_{R_{k,r}^{(m)}}}_{\mathrm{R}_T^{(m)}}. \tag{5.4.10}$$

where $a_{k,r}^{(m)}$ = 1, if user k is served by macro cell m (i.e., the m-th macro cell BS) on the r-th RB, otherwise $a_{k,r}^{(m)}$ = 0 and each RB is allocated to only one user in a macro cell sector:

$$\sum_{k=1}^{\bar{K}_m} a_{k,r}^{(m)} \leq 1,\ a_{k,r}^{(m)} \in \{0,1\},\ \forall r \in [1,2,\cdots,N_{RB}]\,,\ \forall m \in [1,2,\cdots,M]\,. \tag{5.4.11}$$

Table 5.2: Summary of notations.

Notation	**Definition**
δ	Number of macro cell sectors and macro cell sector antennas in each macro cell site.
N_{RB}	Number of available RBs at each time slot.
$\bar{K}_m$	Number of users in a macro cell sector, m = 1: M.
W, M	Number of macro cell sites and macro cell sectors respectively, $w = 1:W$ and $m = 1:M$
T_m	Set of interfering macro cell sectors to the m-th macro cell sector.
$a_{k,r}^{(m)}$	The bit-wise element that indicates if the r-th RB is assigned to the k-th UE in the m-th macro cell sector, $a_{k,r}^{(m)} \in \{0,1\}$.
$s_{k,r}^{(m)}$	The k-th user data transmitted on the r-th RB from the m-th macro cell sector BS, $k \in [1,2,\cdots,K]$.
$\mathbf{H}_{k,r}^{(m)}$	The flat-fading channel on the r-th RB, from the m-th macro cell sector BS to the k-th UE.

$g_{k,r}^{(m)}$	The channel gain on the *r*-th RB, from the *m*-th macro cell sector BS to the *k*-th UE.
$\rho_{k,r}^{(m)}$	The power allocation to the *k*-th user on the *r*-th RB in the *m*-th macro cell sector.
$\mathbf{n}_{k,r}^{(m)}$	The noise vector received by the *k*-th user on the *r*-th RB in the *m*-th macro cell sector.
$\mathbf{y}_{k,r}^{(m)}$	The received signal vector of the *k*-th user on the *r*-th RB in the *m*-th macro cell sector.
$\gamma_{k,r}^{(m)}$	The SINR of the *k*-th user on the *r*-th RB in the *m*-th macro cell sector.
$R_{k,r}^{(m)}$	The rate of the *k*-th user on the *r*-th RB in the *m*-th macro cell sector.
$R_T^{(m)}$	The sum-rate of the users in the *m*-th macro cell sector.

5.4.2 Proposed Distributed RBA for HomoNets

Problem Formulation

The proposed RBA optimisation problem is based on maximising the sum-SINR of the users within each macro cell, while ensuring the effective interference experienced is at its minimum. The optimisation problem can be formulated as:

$$\max_{\mathbf{a}} \sum_{r=1}^{N_{RB}} \sum_{k}^{\bar{K}_m} a_{k,r}^{(m)} \gamma_{k,r}^{(m)}, \quad \forall m \in [1, 2, \cdots, M],$$

$$\text{s.t.} \quad \gamma_{k,r}^{(m)} = \frac{g_{k,r}^{(m)} \rho_{k,r}^{(m)}}{\sum\limits_{\substack{d=1,\, d\in T_m \\ j\in[1,2,\cdots,\bar{K}_d],\, a_{j,r}^{(d)}=1}}^{M} g_{k,r}^{(d)} \rho_{j,r}^{(d)} + (\sigma_{k,r}^{(m)})^2},$$

$$\sum_{k=1}^{K_m} a_{k,r}^{(m)} \leq 1, \;\; \forall r, m, \; a_{k,r}^{(m)} \in \{0,1\}, \;\; \rho_{k,r}^{(m)} \geq 0, \; \textit{if } a_{k,r}^{(m)} = 1, \forall m, k, \tag{5.4.12}$$

where **a** is the RBA solution to the given optimisation problem, and **a** = $[a_{k,r}^{(m)}, \forall\, m, k, r]$.

The problem above is a constrained non-linear optimisation problem, which is very complex to solve. The authors in [53, 54] stated that the calculation of the SINR values of each user is not possible, since the SINR cannot be calculated without first allocating RBs. The authors sought another approach that eliminated the use of interference estimation for the users on each RB. A centralised strategy that assigned the users into different clusters using interference weights was proposed, and each cluster was assigned a RB to maximise the throughput. Although the strategy aims to avoid interference, the clusterisation strategy does not take into account the full interference from the neighbouring cells on individual users simultaneously. Subsequently, the RBs are allocated to each cluster to maximise the sum-SNR of the users in the cluster. The centralised clustering approach using interference weights and the maximisation of the sum-SNR over the clusters does not effectively mitigate the interference in the network, it also does not seek to maximise the sum-SINR in each macro cell sector and does not solve the challenges of the centralised approach as explained in Section 5.2.1. For this reason, a step-by-step algorithm under the distributed RBA approach that maximises the SINR of the users in each macro cell sector, is proposed to solve the problem in (5.4.12).

Problem Solution

The first and foremost objective of the proposed distributed RBA solution based on maximising the sum-SINR within each macro cell, is obtained using a distributed approach to allocate RBs within a cellular system, that would significantly reduce the overhead resources and time required for jointly allocating RBs to the users. Secondly, the proposed distributed RBA strategy aims to choose the RBs that maximise the sum-SINR of the users within the given macro cell sector, while avoiding the reception of high interference from neighbouring macro cells on the same RB. In order to achieve a distributed RBA based on interference avoidance, and obtain the perceived SINR of each user on every given RB in each macro cell, it is important to have pre-knowledge of the RBs already allocated in the neighbouring cells.

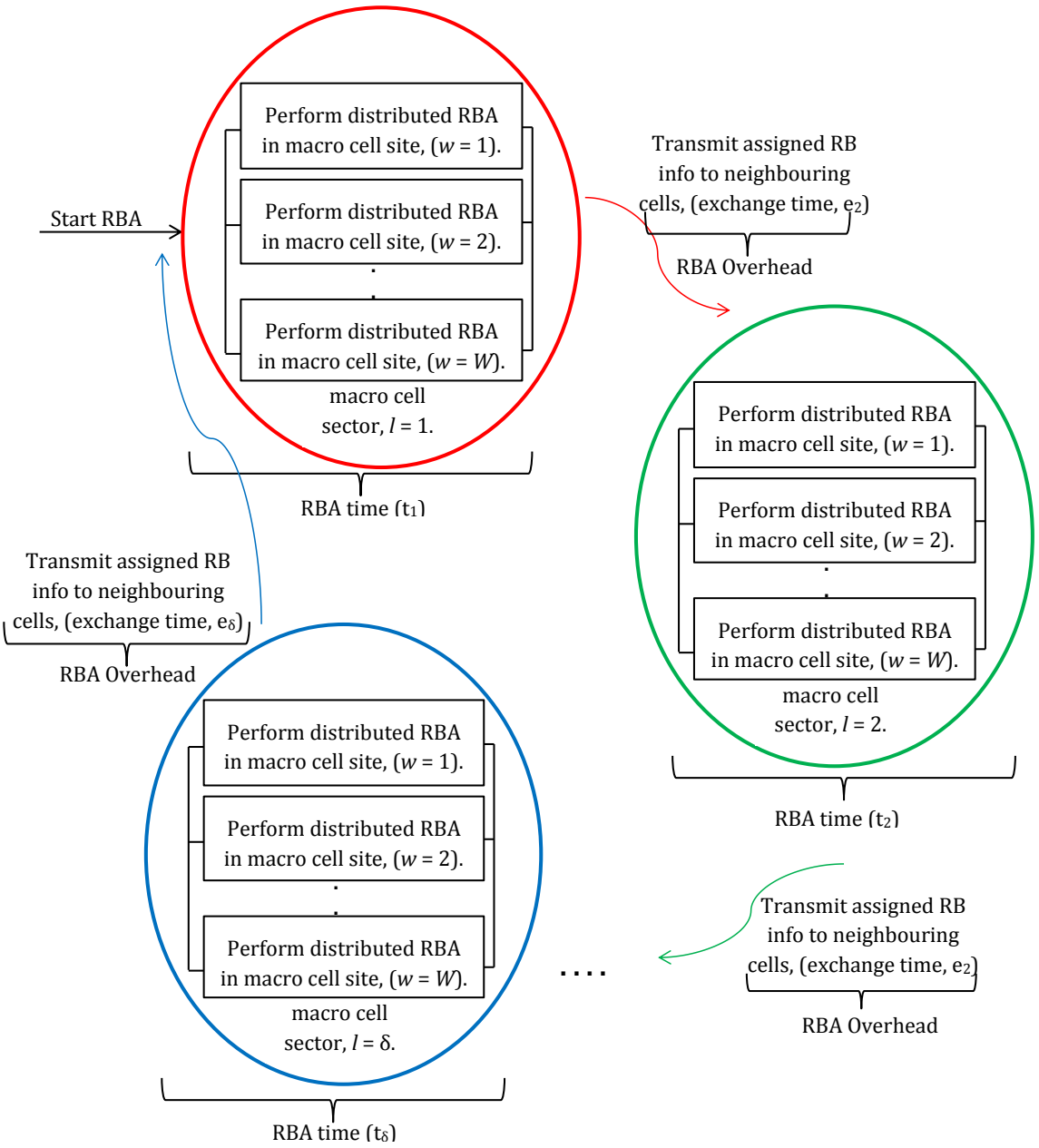

Figure 5.6: Proposed distributed or de-centralised RBA strategy for HomoNets.

Without this knowledge, the interference to each user cannot be properly taken into consideration during the RBA process. It is easy to see why this metric for RBA proves

to be a challenge and is almost impossible to achieve, if the interfered RBs are not yet known. The definition of the variables used in the flow charts and algorithms can be found in Table 5.2.

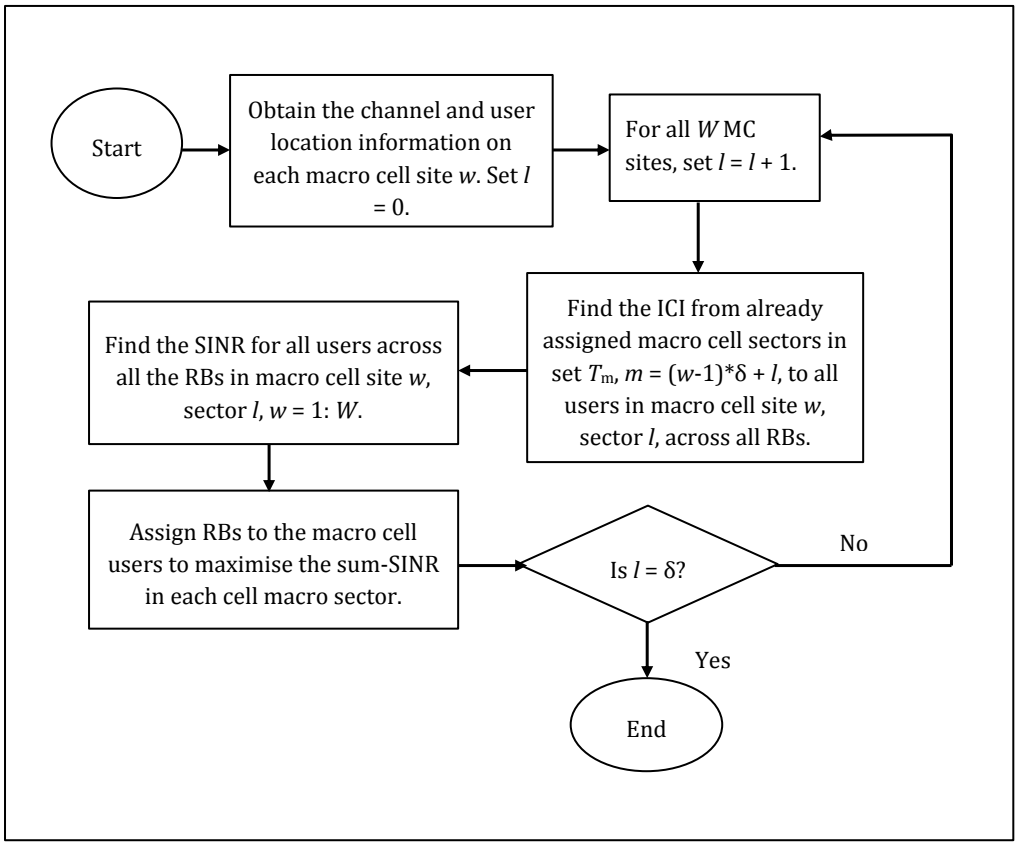

Figure 5.7: Flow chart of the proposed distributed RBA strategy for W macro cell (MC) sites and δ sectors per cell site.

Algorithm 1

Figs. 5.6 and 5.7 present the proposed distributed RBA strategy using a round robin, sector-by-sector approach, as described below:

Step 1: As shown in 'Block A' in Fig. 5.8, the RBA begins with the macro cell sectors

with antenna index $l = 1$, for all macro cell sites $w = 1, 2, \cdots, W$. The perceived SINR for the users on each RB is estimated while the interference received is considered as zero, since the users in other neighbouring cell sectors with macro cell sector index $l = 2$ and 3 have not been assigned RBs. Then using the well-known Hungarian method [72], the RBs are assigned to all the users to maximise the sum-SINR within the macro cell sector.

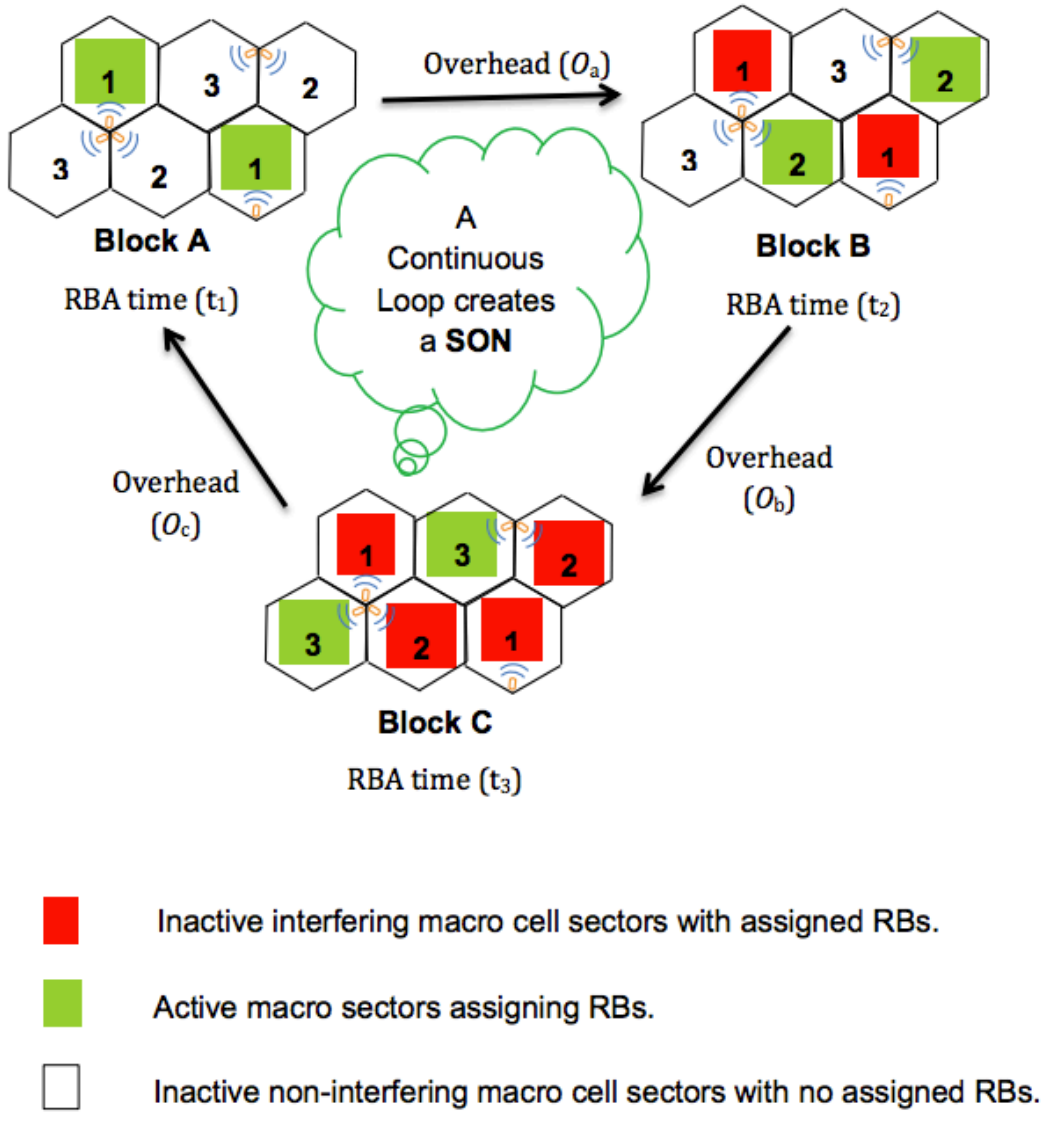

Figure 5.8: RBA based on sum-SINR maximisation

Step 2: The assigned RB information are then passed to the neighbouring macro cell sites of neighbouring and interfering BSs in the set T_m, where T_m is the set of neighbouring and interfering BSs to the m-th macro cell sector.

Step 3: Now the macro cell sectors with antenna index $l = 2$ finds the SINR at each user on each RB, while considering the interferers on the already assigned RBs in neighbouring macro cell sectors with sector index $l = 1$, as shown in 'Block B' in Fig. 5.8. The Hungarian method is used to assign the RBs to all users to maximise the sum-SINR within each macro cell sector.

Step 4: The assigned RBs information are then passed to the neighbouring macro cell sites of neighbouring and interfering BSs in the set T_m.

Step 5: Now the macro cell sites with macro cell sectors with antenna index $l = 3$ finds the SINR at each user on each RB, while considering the interferers on the already assigned RBs in neighbouring macro cell sectors with sector index $l = 1$ and 2, as shown in 'Block C' in Fig. 5.8. The Hungarian method is used to assign the RBs to all the users to maximise the sum-SINR within the macro cell sector.

Step 6: The assigned RBs information are then passed to the neighbouring macro cell sites of neighbouring and interfering BSs in the set T_m.

Note that as the users enter and leave the network, the proposed RBA strategy enables RBs to be assigned to new entrants while ensuring that the interference within the network is managed. This continuous process leads to a distributed RBA strategy fit for a SON.

5.4.3 Performance Evaluation in HomoNet

Using the simulation parameters in Table 5.3, the following results are obtained and analysed. In Fig. 5.9 and Fig. 5.10 respectively, the average sum-rate and average sum-interference per macro cell is shown using the proposed distributed RBA based on maximising the sum-SINR (represented by 'dist-SINR') and compared to the traditional approach based on maximising the sum-SNR (represented by 'dist-SNR'). The traditional

RBA using SNR as the RBA metric is distributed since each macro cell can estimate the SNR of all users within the cell and then allocate RBs to maximise the sum-SNR. Note that the conventional distributed approach for 'dist-SNR' is not similar to the proposed distributed RBA strategy using the SINR as a RBA metric.

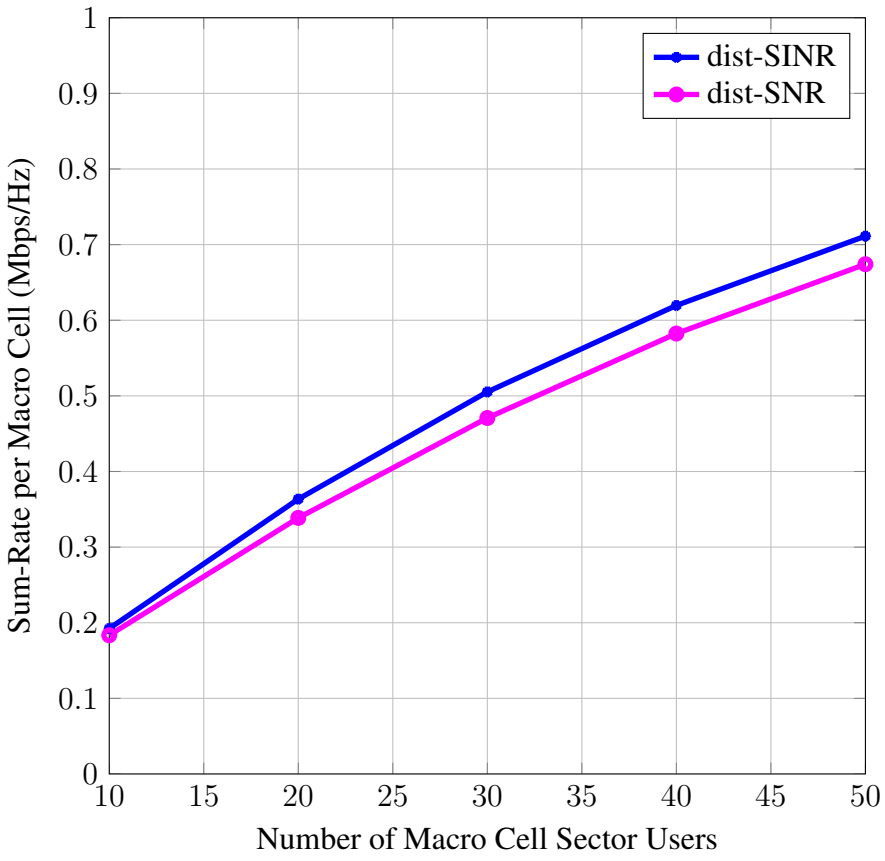

Figure 5.9: Sum-rate per macro cell using the proposed distributed RBA based on sum-SINR maximisation.

However, for this simulation the RBs are allocated to maximise the sum-SINR in each macro cell sector, using the proposed distributed RBA technique. While varying the number of macro cell users (nMCUs) in the macro cell sector, the proposed 'dist-SINR' achieves a better performance than 'dist-SNR'. For instance an increase of 0.03 Mbps/Hz is achieved with the proposed 'dist-SINR' strategy as the number of users increases and the interference within the cell increases. Also in Fig. 5.10, the proposed 'dist-SINR'

strategy achieves up to 50% reduction in the total interference power within the system. For instance the total interference power experienced with 'dist-SINR' and 'dist-SNR' respectively, when the number of MCU is 40 are 0.31 kW and 0.58 kW respectively. The interference is seen to be reduced by approximately 50%.

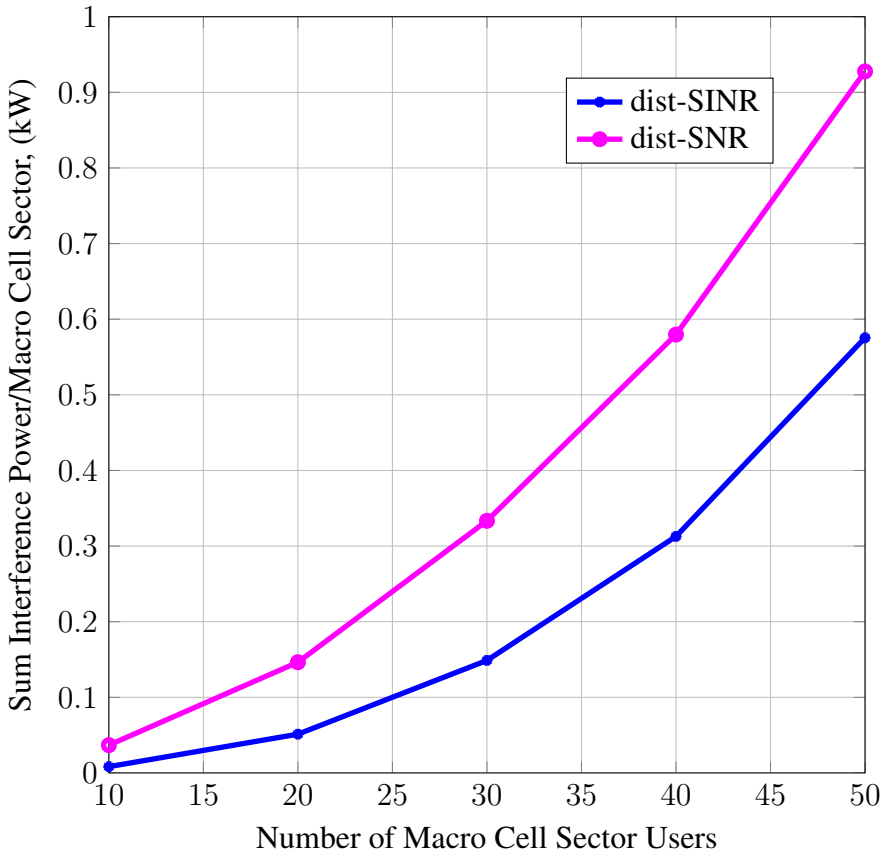

Figure 5.10: Sum interference power per macro cell using the proposed distributed sum-SINR maximisation.

Table 5.3: Summary of simulation parameters.

Parameter	**Value**
Cell Type	HomoNet
Number of macro cell sites	19
Number of sectors per macro cell site	3
Channel frequency	2.0 GHz

Carrier bandwidth	10 MHz
Number of RBs	50
Bandwidth of RB	180 kHz
Sub-carrier spacing	15kHz
Bandwidth per RB	180kHz
Shadowing standard deviation, σ_s	8dB
Pathloss coefficient, α	2
Macro cell BS power	43 dBm
[Inter site distance (ISD), D_o]	[750m, 100m]
Macro cell radius	250m
Macro cell antenna type	directional antennas
Number of antennas (M_t, N_r)	(4, 2)
Backhaul link rate (ζ)	1 Gbps
(β, ϕ, α)	(8, 8, 8) bits

To further evaluate the proposed distributed RBA strategy based on maximising the sum-SINR, other forms of RBA such as the centralised, semi-centralised and frequency-partitioned solutions are shown. For fair comparison, the centralised and semi-centralised are implemented using the RBA metric based on the SINR and the SNR. The different forms of RBA used for comparison are:

- The centralised RBA mode assigns the RBs centrally at the chosen RBAU. The RBs are selected using the proposed sum-SINR maximisation strategy and the existing sum-SNR maximisation approach, represented by 'cent-SINR' and 'cent-SNR' respectively as shown in Fig. 5.11 and Fig. 5.12.

  For the centralised approach, the RBAU begins with the first macro cell site *w* = 1, the macro cell sectors with antenna index $l = [1, 2, \cdots \delta]$ simultaneously

assigns RBs to the users. This is valid with the assumption of no interference between the macro cell sectors of the same macro cell site. The round-robin approach subsequently assigns RBs in the same manner to the other macro cell sites $w = [2, \cdots, W]$, while avoiding the interference from previously assigned macro cell sites on assigned RBs.

- The semi-centralised or partitioned RBA mode uses the partition types 'Group B' and 'Group E' as shown in Table. 5.1 to assign the RBs semi-centrally at the chosen RBAUs. The RBs are selected using the proposed sum-SINR maximisation strategy and the existing sum-SNR maximisation approach, which are represented by 'part-SINR Gp B' and 'part-SNR Gp B' respectively for 'Group B' and 'part-SINR Gp E' and 'part-SNR Gp E' respectively for 'Group E', as shown in Figs. 5.11 and 5.12.

  The semi-centralised approach is similar to the centralised approach since the RBs are assigned in the same manner within each sub-group. However, the partitions or sub-groups assign the RBs independently without taking into consideration the interference from the macro cell BSs in other sub-groups or partitions.

- The frequency partitioned RBA mode uses the sum-SINR maximisation strategy and sum-SNR maximisation approach as a metric to schedule resources in each macro cell sector and are represented by 'freq-SINR' and 'freq-SNR' as shown in Figs. 5.11 and 5.12 respectively.

  Note that the macro cells are already allocated subsets of the frequency resources and for each time slot the macro cell is allowed to allocate only a single user to a given RB. Considering N_{RB} = 50 and δ = 3, each macro cell sector with antenna index l = 1, 2 and 3 respectively are allotted 16 RBs, 17 RBs and 17 RBs respectively using frequency partitioning 'Type A' as shown in Fig. 5.4 for the simulations.

As seen in Fig. 5.11 for different density of users per macro cell sector using the centralised, semi-centralised and distributed mode of allocation, the proposed RBA metric

based on the sum-SINR of the users achieves a better system performance than the RBA metric based on sum-SNR of the users, except for the frequency partitioned RBA strategy. The RBA based on the proposed sum-SINR maximisation strategy and the existing sum-SNR maximisation approach would yield the same result since the interference is zero. The interference is zero because parts of the available RBs have been allotted and reserved for certain macro cell sectors, hence interference is avoided completely. However, the 'freq-SINR' and 'freq-SNR' achieve poor performance due to unavailable RBs when the density of users is high in each macro cell sector. Remember that multiple users in a given macro cell sector cannot be assigned to the same RB.

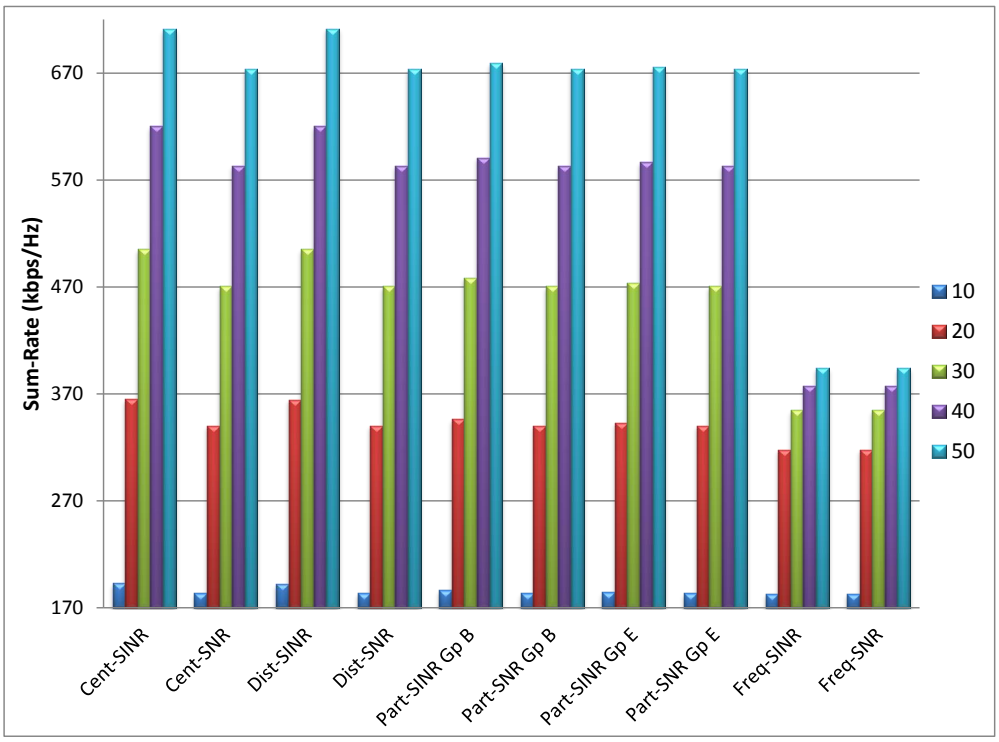

Figure 5.11: Sum-rate per macro cell on different modes of RBA based on the proposed sum-SINR and existing sum-SNR maximisation when nMCUs = 10, 20, 30, 40 and 50.

Also it can be seen that the distributed approach 'dist-SINR' achieves very similar sum-

rate performance with the centralised approach 'cent-SINR'. Both strategies achieve the best sum-rate performance compared to other strategies. The sum-rate performance under the semi-centralised RBA reduces as the number of sub-groups or partition increases. This is a result of an increase in the interference within the system, since the interference from other clusters/sub-groups was not considered during RBA. The performance under the frequency partition RBA strategy is seen to achieve the worst sum-rate performance especially as the density of users in the cell increases. It shows that hard frequency partition diminishes the available frequency spectrum, which can cause very poor system efficiency within the network during peak times or in a high user density area.

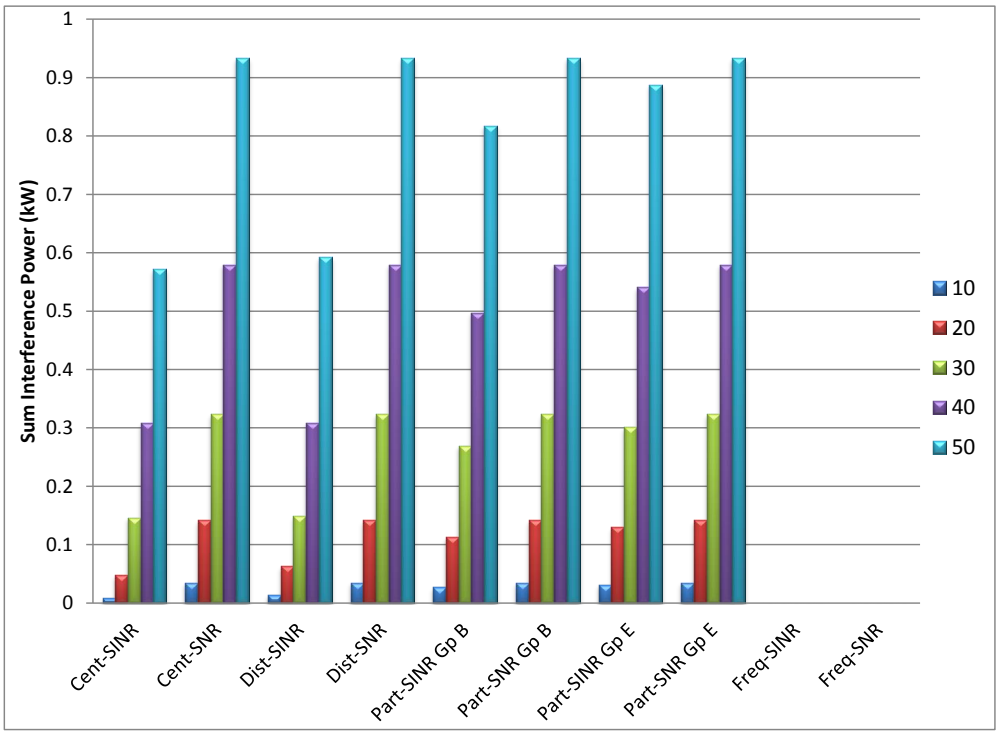

Figure 5.12: Sum interference power per macro cell on different modes of RBA based on the proposed sum-SINR and existing sum-SNR maximisation when nMCUs = 10, 20, 30, 40 and 50.

Fig. 5.12 shows the interference power within the system under the different RBA

strategies. It can be seen that the centralised and distributed approach based on maximising the sum-SINR results in better interference management compared to other strategies. Also the 'part-SINR Gp B' is seen to have less interference than 'part-SINR Gp E', which has more sub-groups within the network. The benefits of the fractional frequency re-use strategy as mentioned earlier is the ease of interference control, fast RBA time and no overheads. It can be observed that no interference is experienced under the frequency partition RBA strategy, since each macro cell only assigns the RBs allocated to it and only one user is assigned to any RB at any time.

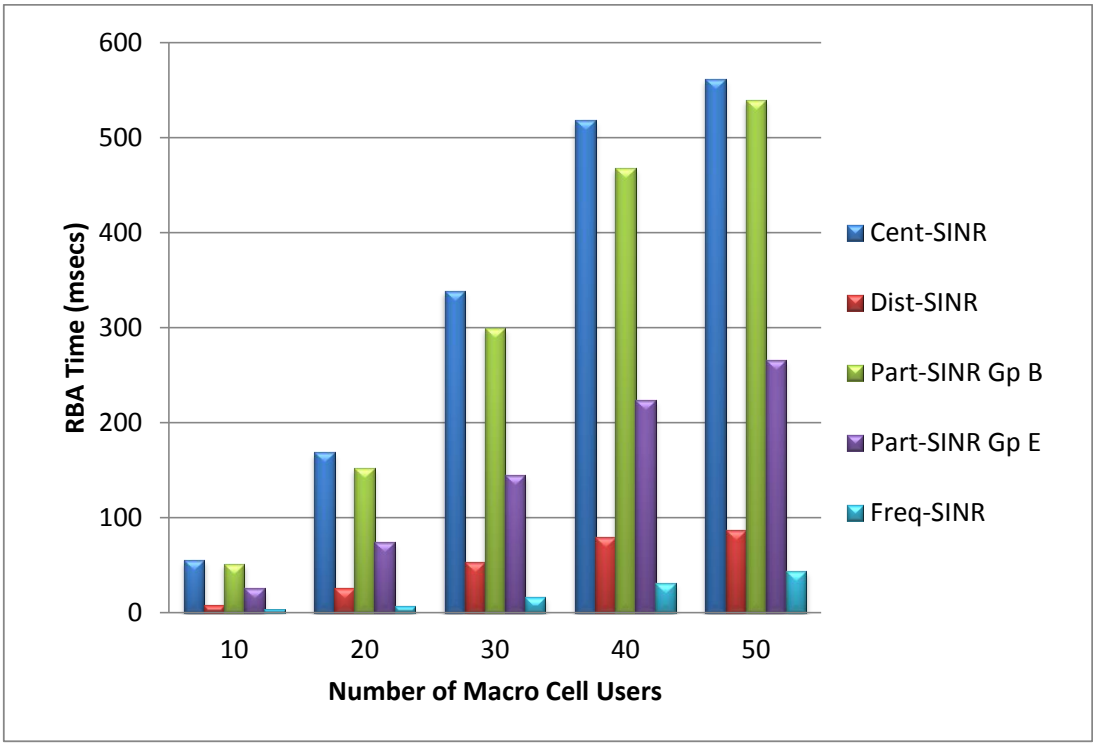

Figure 5.13: RBA time obtained for different modes of RBA based on the proposed sum-SINR maximisation when nMCUs = 10, 20, 30, 40 and 50.

In Figs. 5.13 and 5.14 respectively, the RBA time and RBA overhead for different modes of RBA using the proposed RBA metric based on the sum-SINR maximisation are shown. From Figs. 5.13 and 5.14, it can be observed that as the density of the users within

the macro cell increases, the 'cent-SINR' requires the longest time for its RBA and also demands the highest overhead resources compared to other strategies. For example, when the number of users $\bar{K}_m = 50$, $\forall m$, the 'cent-SINR' requires an overhead of 3.46 Mbits compared to the 'dist-SINR', 'part-SINR Gp B' and 'part-SINR Gp E' which requires 0.05 Mbits, 2.98 Mbits and 2.25 Mbits respectively. Also, the RBA time used under the 'cent-SINR' is 561 msecs compared to the 'dist-SINR', 'part-SINR Gp B', 'part-SINR Gp E' and 'freq-SINR' which requires 87 msecs, 540 msecs, 266 msecs and 44 msecs respectively. It can be observed that the frequency partitioned strategy has no overhead and has the quickest RBA time. From these results, it can be concluded that the proposed distributed strategy based on the sum-SINR maximisation, obtains the overall best performance compared to other strategies.

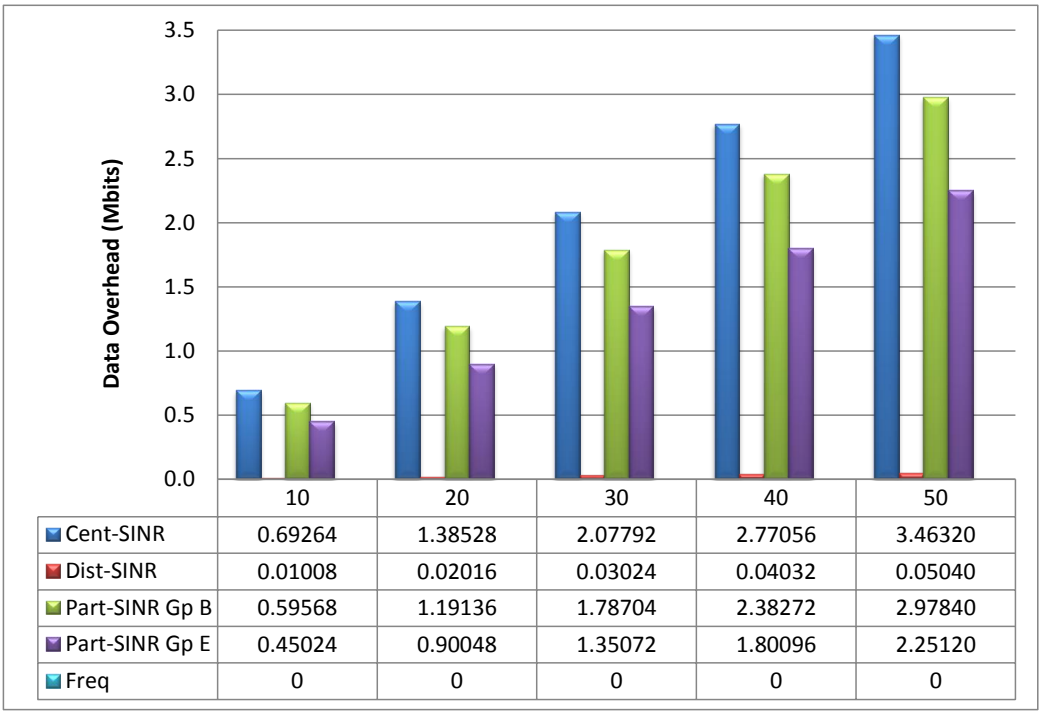

	10	20	30	40	50
Cent-SINR	0.69264	1.38528	2.07792	2.77056	3.46320
Dist-SINR	0.01008	0.02016	0.03024	0.04032	0.05040
Part-SINR Gp B	0.59568	1.19136	1.78704	2.38272	2.97840
Part-SINR Gp E	0.45024	0.90048	1.35072	1.80096	2.25120
Freq	0	0	0	0	0

Figure 5.14: Data overhead obtained for different modes of RBA based on the proposed sum-SINR maximisation.

5.5 Interference Management in Heterogeneous Network

Previously, cellular network system were mainly homogeneous and macro cells having the same transmit power were deployed for network coverage. But over the years massive reductions occurred in costs and improvements in micro-chips technology, semi-conductor devices and advanced digital signal processing. This resulted in an explosion of user equipments and programs that require real-time applications and high data speeds. Over the past few years, more user devices have been introduced into the network, resulting in competition for network resources in a frequency limited cellular network. Other major challenges faced in HomoNets are poor cell coverage and performance at the macro cell edge area, high call drops and network resource contention in densely populated areas. These challenges were the drivers to evolve the existing homogeneous networks into heterogeneous networks, popularly called HetNets [73].

To achieve better coverage and improve capacity, small cells with low transmission power were deployed over existing macro cells [74]. The type of heterogeneous network considered in this chapter is the macro cell and pico cell network operating over the same frequency band. The major challenge for the HetNet is the intra-cell interference (IaCI) and the ICI. The IaCI is the interference within the same macro cell sector area, from the macro cell BS to the pico cell UE or from the pico cell BS to the macro cell UE. While the ICI is the interference from a macro cell BS to the pico cell and macro cell UEs in another macro cell sector area. The interference experienced in HetNets limits the predicted performance in HetNets. Another challenge seen in the HetNet is the loading of users to the small cells, such that the small cells are not under utilised since the UEs would mostly prefer service from the high power macro cell eNB [74], but this is not the focus for the work. For this work, the users are assumed to be already associated to a given macro or pico cell area.

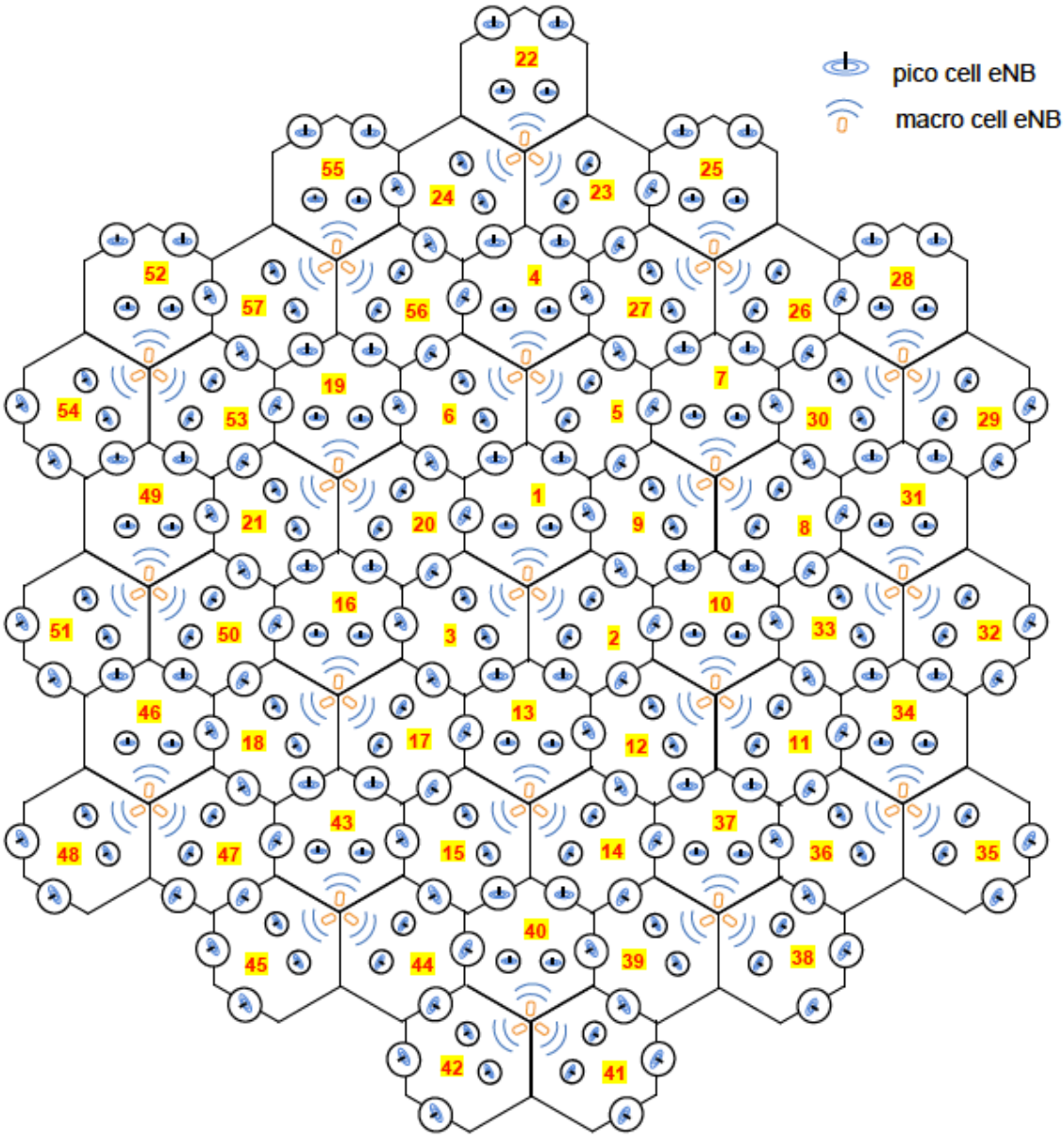

Figure 5.15: HetNet with $W = 19$ macro cell sites, $\delta = 3$ macro cell sector per cell site, $nPC = 4$ pico cells per macro cell sector.

3GPP LTE HetNet systems are based on OFDMA and both macro and small cells have access to the same frequency band. As discussed previously, more focus is on D-ICIC techniques, since it has been shown to achieve more performance gain and improved spectral efficiency as opposed to the traditional static and semi-static approach used in 2G system for frequency partitions between cells. HetNets are more complex systems and interference management techniques are more challenging. So it is important to have an effective D-ICIC strategy that associates RBs to users such that each user is allocated a RB with good SINR. Some techniques such as almost blank sub-frames (ABS) which uses time domain ICIC have been proposed, to allow subframes on the macro cell sectors to be reserved for small cell users prone to high interference, especially the cell-edge users. Depending on the number of cell-edge users, this resource reservation can cause low spectral efficiency for the macro cells especially in a dense network [74]. For this reason, the proposed distributed RBA strategy allows both macro and small cells detect and avoid RBs with high interference without pre-allotting RBs for specific users. This allows the available subframes and RBs both in the time and frequency domain to be available to all cell-types.

5.5.1 HetNet System Model

The HetNet system model in Fig. 5.15 shows the deployment of pico and macro cells within the network. The system model shown has $W = 19$ macro cell-sites and $M = 57$ macro cell sectors. There exist 5 cells within each macro cell sector, i.e., 1 macro cell and 4 pico cells. The macro cell sector BSs use directional antennas while the pico cell BSs use omni-directional antennas. Each macro cell sector consists of: a macro cell denoted by $c = 1$; two (2) cell-edge pico cells (CEPCs) strategically positioned to improve the coverage at the macro cell-edge, denoted by $c = 2$ and 3 respectively; and two (2) hotspot pico cells (HSPCs) strategically placed to cover the hotspot areas in the cell-centre, denoted by $c = 4$ and 5 respectively. The variables used in this section and subsequent sections are defined in Table 5.4.

Table 5.4: Summary of notations.

Notation	Definition
δ	Number of macro cell sectors in each macro cell site.
N_{RB}	Number of available RBs at each time slot.
$\bar{K}_{(m,c)}$	Number of users served by the c-th eNB in the m-th macro cell sector, $m = 1: M$.
$\bar{K}_m$	Total number of users in the m-th macro cell sector, $m = 1: M$.
$\tilde{K}_w$	Total number of users in the w-th macro cell site, $w = 1: W$.
W, M	Number of macro cell sites and macro cell sectors respectively, $w = 1 : W$ and $m = 1 : M$
C	Number of transmitting eNBs in each macro cell sector, $c = 1 : C$, $c = 1$ indicates a macro cell, otherwise a pico cell.
T_m	Set of interfering macro cell sectors on the m-th macro cell sector.
(m,c)	The c-th cell in the m-th macro cell sector.
$a_{k,r}^{(m,c)}$	The bit-wise element that indicates if the r-th RB is assigned to the k-th UE on (m, c), $a_{k,r}^{(m,c)} \in \{0, 1\}$.
$s_{k,r}^{(m,c)}$	The k-th user data transmitted on the r-th RB from the eNB in *(m,c)*.
$\mathbf{H}_{k,r}^{(m,c)}$	The flat-fading channel on the r-th RB, from the eNB in *(m,c)* to the k-th UE.
$\bar{\mathbf{H}}_{k,r}^{(m,c,o)}$	The flat-fading channel on the r-th RB, from the o-th interfering macro cell sector eNB to the k-th UE in *(m,c)*.
$g_{k,r}^{(m,c)}$	The channel gain on the r-th RB, from the eNB in *(m,c)* to the k-th UE.
$\bar{g}_{k,r}^{(m,c,o)}$	The channel gain on the r-th RB, from the o-th interfering macro cell sector eNB to the k-th UE in *(m,c)*.
$\rho_{k,r}^{(m,c)}$	The power allocation from eNB in *(m,c)* to the k-th user on the r-th RB.
$\mathbf{n}_{k,r}^{(m,c)}$	The noise vector received by the k-th user on the r-th RB in *(m,c)*.
$\mathbf{y}_{k,r}^{(m,c)}$	The received signal vector of the k-th user on the r-th RB in *(m,c)*.
$\gamma_{k,r}^{(m,c)}$	The SINR of the k-th user on the r-th RB in *(m,c)*.

$R_{k,r}^{(m,c)}$	The rate of the *k*-th user on the *r*-th RB in *(m,c)*.
$R_T^{(m)}$, $R_T^{(m,c)}$	The sum-rate of the users in the *m*-th macro cell sector and in *(m,c)* respectively.

Based on the system in Fig. 5.15, the *k*-th user in the *m*-th macro cell-sector, served by the *c*-th BS on the *r*-th RB, is given by:

$$\mathbf{y}_{k,r}^{(m,c)} = \mathbf{H}_{k,r}^{(m,c)} \sqrt{\rho_{k,r}^{(m,c)}} s_{k,r}^{(m,c)} + \sum_{\substack{d=1,\, d\neq c,\\ j\in[1,2,\cdots,\bar{K}_{(m,d)}],\\ a_{j,r}^{(m,d)}=1.}}^{C} \mathbf{H}_{k,r}^{(m,d)} \sqrt{\rho_{j,r}^{(m,d)}} s_{j,r}^{(m,d)}$$

$$+ \sum_{\substack{o=1,\, o\in T_m,\\ q\in[1,2,\cdots,\bar{K}_{(o,1)}],\\ a_{q,r}^{(o,1)}=1.}}^{M} \bar{\mathbf{H}}_{k,r}^{(m,c,o)} \sqrt{\rho_{q,r}^{(o,1)}} s_{q,r}^{(o,1)} + \mathbf{n}_{k,r}^{(m,c)}, \text{ if } a_{k,r}^{(m,c)} = 1, \ \forall\, k \in [1,2,\cdots,\bar{K}_{(m,c)}],$$

$$\forall c \in [1,2,\cdots,C], \ \forall m \in [1,2,\cdots,M], \ \forall r \in [1,2,\cdots,N_{RB}]. \tag{5.5.13}$$

The coefficients of $\mathbf{H}_{k,r}^{(m,c)}$ are complex random variables, with zero-mean Gaussian real and imaginary parts. The channel links experience large scale fading, with path loss exponent (α) and log-normal shadowing having zero-mean and variance σ_s^2. $s_{k,r}^{(m,c)}$ is the complex (scalar) data signal on the *r*-th RB, destined for the *k*-th user in *(m,c)*, (E $\left\{|s_{k,r}^{(m,c)}|^2\right\}$ = 1) and $\mathbf{n}_{k,r}^{(m,c)}$ is an additive, zero-mean, white, complex Gaussian noise vector with a variance of $(\sigma_{k,r}^{(m,c)})^2$. The downlink SINR of the *k*-th UE on the *r*-th RB, served by the *c*-th BS in the *m*-th macro cell, is given below in (5.5.14):

$$\gamma_{k,r}^{(m,c)} = \frac{g_{k,r}^{(m,c)} \rho_{k,r}^{(m,c)}}{\sum\limits_{\substack{d=1,\, d\neq c,\\ j\in[1,2,\cdots,\bar{K}_{(m,d)}],\\ a_{j,r}^{(m,d)}=1.}}^{C} g_{k,r}^{(m,d)} \rho_{j,r}^{(m,d)} + \sum\limits_{\substack{o=1,\, o\in T_m,\\ q\in[1,2,\cdots,\bar{K}_{(o,1)}],\\ a_{q,r}^{(o,1)}=1.}}^{M} \bar{g}_{k,r}^{(m,c,o)} \rho_{q,r}^{(o,1)} + (\sigma_{k,r}^{(m,c)})^2}, \text{ if } a_{k,r}^{(m,c)} = 1,$$

$$\forall\, k \in [1, 2, \cdots, \bar{K}_{(m,c)}],\ \forall c \in [1, 2, \cdots, C],\ \forall m \in [1, 2, \cdots, M],\ \forall r \in [1, 2, \cdots, N_{RB}]. \tag{5.5.14}$$

where $g_{k,r}^{(m,c)} = \|\mathbf{H}_{k,r}^{(m,c)}\|_F^2$. The sum-rate ($R_T^{(m)}$) of all the users in the m-th macro cell sector is given in (5.5.15):

$$R_T = \underbrace{\sum_{m=1}^{M} \underbrace{\sum_{c=1}^{C} \underbrace{\sum_{k=1}^{\bar{K}_{(m,c)}} \sum_{r=1}^{\bar{N}_{RB}} \underbrace{a_{k,r}^{(m,c)} \log_2\left(1 + \gamma_{k,r}^{(m,c)}\right)}_{R_{k,r}^{(m,c)}}}_{\mathrm{R}_T^{(m,c)}}}_{\mathrm{R}_T^{(m)}}}, \tag{5.5.15}$$

where $a_{k,r}^{(m,c)}$ = 1, if user k is served by the eNB in *(m,c)* (i.e., the c-th eNB in the m-th macro cell sector) using the r-th RB, otherwise $a_{k,r}^{(m,c)}$ = 0. Each RB is assumed to be allocated to only one user in a given pico or macro cell sector and

$$\sum_{k=1}^{\bar{K}_{(m,c)}} a_{k,r}^{(m,c)} \leq 1,\ a_{k,r}^{(m,c)} \in \{0, 1\},\ \forall c \in [1, 2, \cdots, C],\ \forall m \in [1, 2, \cdots, M],$$
$$\forall r \in [1, 2, \cdots, N_{RB}]. \tag{5.5.16}$$

The Shannon capacity is used as a measure of the achievable rate by user k on RB r from the c-th eNB in the m-th macro cell in (5.5.15). The user-rate at the k-th UE on the r-th RB, served by the c-th eNB in the m-th macro cell is $R_{k,r}^{(m,c)}$, $R_T^{(m,c)}$ is the sum-rate of all the users in the m-th macro cell sector served by the c-th eNB.

5.5.2 Proposed Distributed RBA for Heterogeneous Networks

One important factor required in 4G LTE-A and beyond is the ability for HetNets to be SONs. SONs need to be able to manage self-discovery, self-configuration, self-healing, dynamic interference management and so on. Also perfect synchronisation, low latency, fast RBA time, and very limited overhead are all important factors in the RBA strategy used in HetNets for interference management. In Section 5.4.2, the proposed distributed

RBA strategy was shown to obtain the best performance in terms of RBA time, overhead and performance compared to other D-ICIC modes of RBA. For this reason the proposed distributed method shown in Section 5.4.2 would be used in obtaining the RB assignment de-centrally for the HetNets.

The proposed strategy under LTE-A for HetNets is based on interference avoidance. As can be seen in Fig. 5.15, the network supports different cell types: pico cells and macro cells. The different cell types cover different distance ranges and also use different BS transmit powers for data transmission. However, in this case we assume that the entire channel bandwidth is available to both cell types. This creates a complete overlap of the cells which causes greater interference within the HetNet as opposed to the homogeneous networks. In LTE-A, coordination between the pico cells and macro cells are achieved through the X2 interface. ABS was proposed to limit the severe interference for the cell-edge users in the small cell, by reserving blank subframes in the macro cell, to allow the cell-edge users utilise the in-active subframes [75]. This makes the macro cell spectrally inefficient over the time domain, especially in a very dense network. The proposed RBA strategy is based on assigning RBs in each cell to maximise the SINR of the users in each cell type, while ensuring that the interference is avoided and each cell maximises its potential throughput, by having access to all available frequency channels. The proposed strategy aims to achieve the following objectives:

- Ensure that the utilisation efficiency of the available channels in every cell type is maximised.

- Develop a novel interference management strategy that aggressively minimises the interference within the HetNet especially during peak times.

- Obtain a further interference reduction within the HetNets, which in turn allows the total system capacity to be maximised.

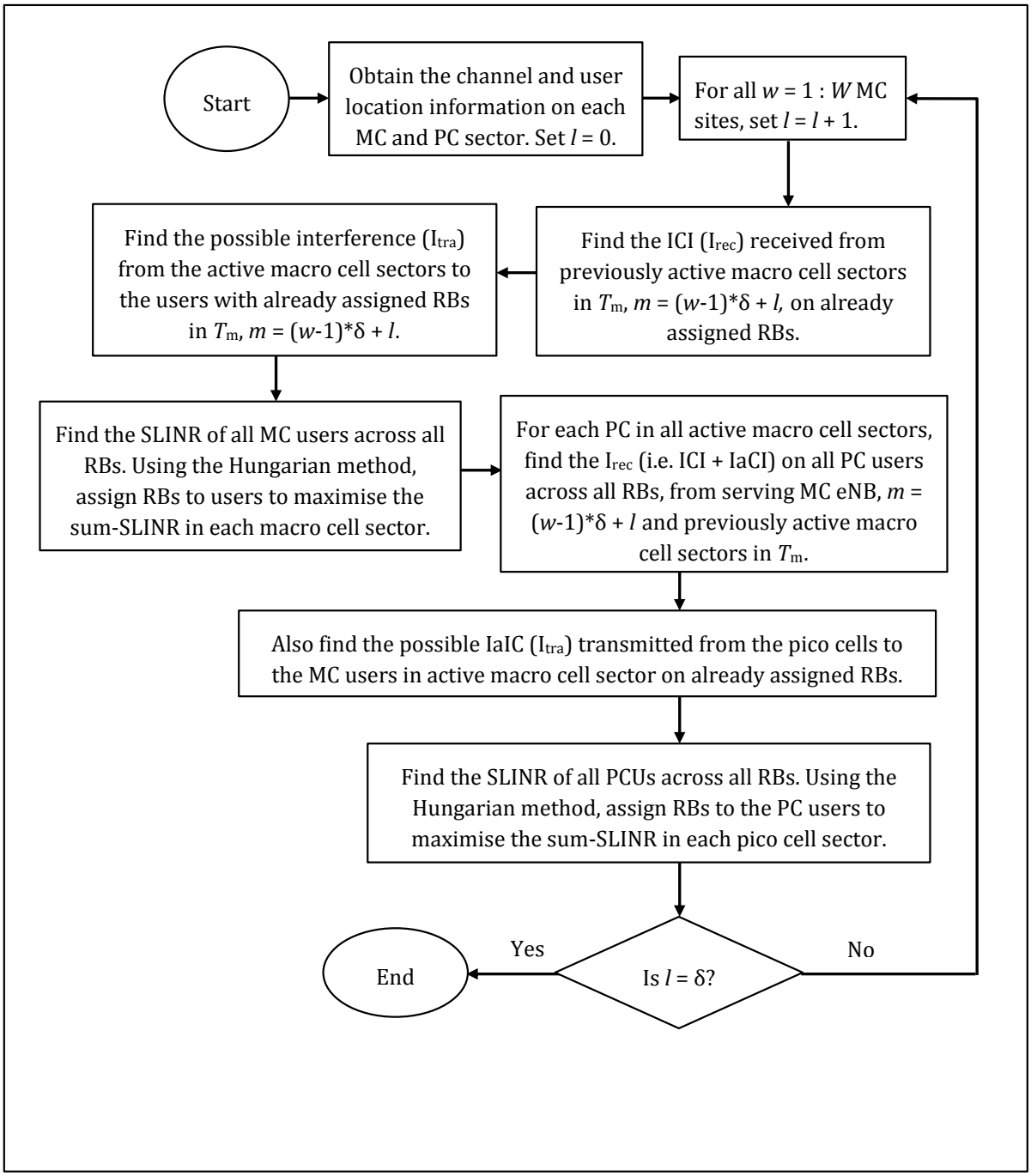

Figure 5.16: Proposed distributed RBA based on maximisation of the sum-SLINR for each cell type.

Assumptions

The following assumptions are considered for the purpose of this study:

1.) Interference between a macro cell sector to the macro cell and pico cell users of neighbouring macro cell sectors. No pico cell to pico cell user interference. No macro cell sector to macro cell sector interference within the same macro cell site.

2.) For each macro cell sector, intra-cell interference is assumed (i.e. macro cell BS to pico cell user interference and pico cell BS to macro cell user interference within the same macro cell sector).

3.) Every user (i.e. the pico cell and macro cell user) within a macro cell sector is susceptible to interference from 4 (four) neighbouring macro cell sectors namely the left-side macro cell sector (LSMCS), left-top macro cell sector (LTMCS), right-top macro cell sector (RTMCS) and right-side macro cell sector (RSMCS) as shown in Fig. 5.15. For instance, users in the macro cell sector $m = 1$ receives interference from cell sectors $m = 20$ (LSMCS), $m = 6$ (LTMCS), $m = 5$ (RTMCS) and $m = 9$ (RSMCS).

4.) No adjacent co-channel interference between any two physcial resource blocks (PRBs).

5.) Full frequency reuse of 1 in both macro and pico cells. This means the whole spectrum is available to all cell types.

6.) The HetNet has pico cells deployed for coverage at macro cell-edge areas and for hot spot areas.

7.) All the pico cells in each macro cell are connected to the macro cell through optical fibre or a dedicated super-fast wireless link. The macro cell serves as a controller and gateway for the pico cells, to the cellular network.

8.) For the purpose of this work, each user requires a single RB allocation, in the frequency domain at every transmission time, to meet its QoS constraint. Note that this

solution can be extended to assign multiple RBs in the time and frequency domain, to meet each user's QoS constraints.

9.) Each pico-cell and macro-cell maintains a neighbour list of all interfering BSs and exchanges information updates at a fixed interval, to ensure a SON.

10.) Equal power allocation on each RB is assumed. Note that this work can be extended to consider power optimisation to enhanced network performance. But this is not the main focus of this chapter.

To tackle the interference problem in HetNets, as well as obtaining a distributed resource management strategy, the solution to this problem is presented in two parts. The first part is based on obtaining a distributed RBA strategy for the HetNet, using a similar strategy of the round robin sector-by-sector strategy presented earlier in Figs. 5.7 and 5.8. This strategy however also considers the RBA to the pico cell users. Since the pico cells are associated with their serving macro cell sector, the round robin sector-by-sector approach shown earlier can be easily applied to the HetNet system as shown in Fig. 5.16.

The second part of the proposed work is creating the RBA metric used in developing the qualification matrix needed for matching the RBs to the users. For this case the proposed RBA metric is based on the signal to leakage and interference plus noise ratio (SLINR). The transmitted interference is the leaked interference from the active BSs to the users already assigned RBs. The received interference (I_{rec}) is the interference received from previously active macro cell sectors to the users currently being assigned RBs by the active macro cell sectors and the noise power is given by σ^2. The proposed RBA metric is given by:

$$\text{SLINR} = \frac{\text{Received Signal Power}(P_s)}{\text{Trans. Int Power}(I_{tra}) + \text{Recvd Int Power}(I_{rec}) + \sigma^2}. \tag{5.5.17}$$

The RBA optimisation problem is based on maximising the sum-SLINR of the users in each cell type within each macro cell sector, while avoiding high transmitted and received interference. The optimisation problem can be expressed as:

$$\max_{\mathbf{a}} \sum_{k}^{\bar{K}_{(m,c)}} \sum_{r}^{N_r} a_{k,r}^{(m,c)} \gamma_{k,r}^{(m,c)},\ \forall c \in [1,2,\cdots,C],\ \forall m \in [1,2,\cdots,M],$$

$$\text{s.t.}\quad \gamma_{k,r}^{(m,c)} = \frac{g_{k,r}^{(m,c)} \rho_{k,r}^{(m,c)}}{\sum\limits_{\substack{d=1,\, d\neq c,\\ j\in\left[1,2,\cdots,\bar{K}_{(m,d)}\right],\\ a_{j,r}^{(m,d)}=1.}}^{C} g_{k,r}^{(m,d)} \rho_{j,r}^{(m,d)} + \sum\limits_{\substack{o=1,\, o\in T_m,\\ q\in\left[1,2,\cdots,\bar{K}_{(o,1)}\right],\\ a_{q,r}^{(m,o)}=1.}}^{M} \bar{g}_{q,r}^{(m,o)} \rho_{q,r}^{(m,o)} + (\sigma_{k,r}^{(m,c)})^2},$$

$$\sum_{k=1}^{\bar{K}_{m,c}} a_{k,r}^{(m,c)} \leq 1,\ \forall r, m, c,\ a_{k,r}^{(m,c)} \in \{0,1\}, \rho_{k,r}^{(m,c)} \geq 0,\ \textit{if}\ a_{k,r}^{(m,c)} = 1, \forall m, c, k, \quad (5.5.18)$$

where $\mathbf{a}$ is the RBA solution to the given optimisation problem, and $\mathbf{a} = [a_{k,r}^{(m,c)}, \forall\, m, c, k, r]$. The constrained non-linear optimisation problem in (5.5.18) is very complex to solve. However, the step-by-step algorithm in Fig. 5.16 is proposed to solve the optimisation problem using a distributed approach and based on the sum-SLINR maximisation in each cell. Based on the same distributed RBA strategy proposed for the HomoNet, RBs are assigned to the macro cell sectors with sector index $l = [1, 2, \cdots, \delta]$ in a round-robin approach. For each macro cell sector index, the macro cell sectors assign RBs to its users while taking into account the transmitted and received interference on each given RB for each user. The SLINR is obtained for all users on every RB and using the Hungarian method the RBs are allocated to the users to maximise the sum-SLINR of the macro cell sector. Subsequently the pico cells allocate RBs to their users while taking into account the interference received from the neighbouring macro cell sectors including its serving macro cell sector and the interference transmitted to the macro cell users within its serving macro cell sector. The SLINR for the pico cell users are obtained and the RBA chooses RBs for all users to maximise the sum-SLINR of the cell.

To further explain the concept of interference avoidance behind the proposed algorithm based on maximising the sum-SLINR for each cell, the given cell set-up in Fig. 5.17 is considered, with two macro cells (MC 1 and MC 2) and two users per cell, using all available channels (i.e. RBs (a) - (e)) across all time slots.

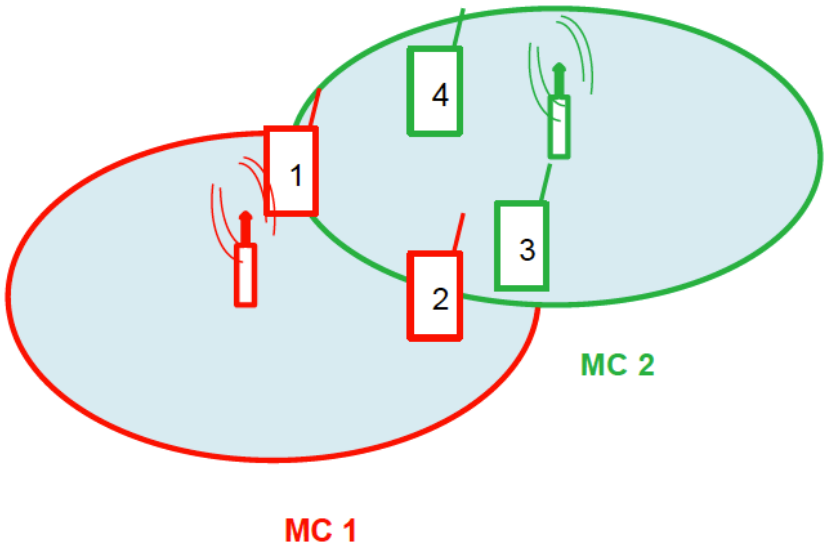

Figure 5.17: Cell set-up with two macro cells and 4 macro cell users.

In Fig. 5.18, the values of the signal power and interference power (transmitted and received interference) across all RBs are given for each user in each cell. Using the round-robin sector-by-sector distributed approach, the users in MC 1 are assigned RBs first. Since there has been no previously, active macro cells, the interference received and transmitted is zero (i.e., $I_{rec} = 0$ and $I_{tra} = 0$). Assuming a unit noise power, the RBs (a) and (b) are assigned to users 1 and 2 respectively, to maximise the sum-SLINR. The information on the assigned RBs and the MC 1 users is made known to MC 2. At MC 2, the interference transmitted and received to the users on RBs (a) and (b) can be estimated. The SLINR for users 3 and 4 can be obtained across all RBs as shown in Table E. RBs (d) and (e) are assigned to users 3 and 4 respectively, to maximise the sum-SLINR. The RB allocation based on sum-SINR (proposed earlier for the homogeneous network in section 5.5.1) and sum-SNR are shown in Tables F and G respectively. Both strategies assign RBs (a) and (e) to users 3 and 4 respectively.

Table A: Received Signal Power (W) in MC 1

	a	**b**	**c**	**d**	**e**
User 1	4.1	1.8	1.9	2.8	3.5
User 2	5.7	5.2	0.9	2.5	4.1

Table B: Received Signal Power (W) in MC 2

	a	**b**	**c**	**d**	**e**
User 3	4.1	1.8	1.2	3.0	3.0
User 4	3.5	2.5	3.5	3.5	4.9

Table C: Interference (I_{rec}) power (W) from MC 1 to UEs in MC 2 on assigned RBs

	a	**b**	**c**	**d**	**e**
User 3	0.3	0.1	0.0	0.0	0.0
User 4	0.4	0.2	0.0	0.0	0.0

Table D: Interference (I_{tra}) power (W) from MC 2 to UEs on occupied RBs in MC 1.

	a	**b**	**c**	**d**	**e**
User 3	0.7	0.1	0	0	0
User 4	0.4	0.6	0	0	0

Table E: RBA based on biased SLINR = $P_s/(I_{rec} + I_{tra} + \sigma^2)$, $\sigma^2 = 1$.

	a	**b**	**c**	**d**	**e**
User 3	2.05	1.5	1.2	3.0	3.0
User 4	1.94	1.38	3.5	3.5	4.9

Firstly, find the SLINR for all users on RBs (a) - (e) in MC1, using the proposed SLINR as a RBA metric. $I_{rec} = 0$, $I_{tra} = 0$ and let the noise power, $\sigma^2 = 1$. RBs (a) and (b) are chosen for users 1 and 2 respectively to maximise the sum-SLINR in MC1.

Secondly, find the SLINR for all users on RBs (a) - (e) in MC2, using the proposed SLINR as a RBA metric. Obtain I_{rec} and I_{tra} on already occupied RBs (i.e. RBs (a) and (b)). Calculate the SLINR for each user on each RB. The RBs (d) and (e) are chosen for users 3 and 4 respectively to maximise the sum-SLINR in MC2.

To compare with the sum-SINR and sum-SNR maximisation approach. The RBs chosen for MC1 remains the same. Find the RBs that maximise the sum-SINR and sum-SNR in MC2 as shown in Table F and G respectively.

Table F: RBA based on SINR = P_s / ($I_{rec} + \sigma^2$).

	a	**b**	**c**	**d**	**e**
User 3	3.15	1.63	1.2	3.0	3.0
User 4	2.5	2.08	3.5	3.5	4.9

Table G: RBA based on SNR = P_s / σ^2.

	a	**b**	**c**	**d**	**e**
User 3	4.1	1.8	1.2	3.0	3.0
User 4	3.5	2.5	3.5	3.5	4.9

Figure 5.18: Illustration to compare the performance of the proposed distributed RBA based on sum-SLINR to the sum-SINR and sum-SNR maximisation approach.

Finally in Table H, based on the allocated RBs for each user, the resulting SINR, total SINR and total interference are obtained for all users within the network, using the proposed distributed RBA that maximises the sum-SLINR, sum-SINR and the distributed

approach using sum-SNR maximisation. From Table H, it can be seen that the sum-SINR obtained under the proposed SLINR RBA metric achieved a better system performance than the proposed SINR RBA metric and the already known SNR RBA metric. From Table F, the proposed RBA metric based on the SINR is seen to result in a different qualification matrix after taking into account the received interference on RBs (a) and (b) as opposed to using the SNR as a RBA metric. However since the I_{rec} at user 3 (RB (a)) is small compared to the signal power received at user 3 (RB (a)), the resulting SINR for user 3 (RB (a)) is still good compared to the other RBs, so RB (a) is assigned to user 3. Now considering the proposed SLINR RBA metric, the obtained qualification matrix in Table E shows that after taking I_{rec} and I_{tra} into account, the resulting SLINR for users 3 and 4 under RBs (a) and (b) is much lower than the SLINR obtained in other RBs. Hence, RBs (d) and (e) are allocated to users 3 and 4 respectively and the interfered RBs are avoided, resulting in less interference within the system.

For each user, find the SINR using the three RBA types based on maximising the sum-SLINR, sum-SINR and sum-SNR respectively, as shown in Table H.

Table H

	(RB allocated) Received SINR after RBA based on:		
	SLINR	**SINR**	**SNR**
User 1	(a) 4.1	(a) 2.41	(a) 2.41
User 2	(b) 5.2	(b) 5.2	(b) 5.2
User 3	(d) 3.0	(a) 3.15	(a) 3.15
User 4	(e) 4.9	(e) 4.9	(e) 4.9
total-SINR(dB)	24.96	22.87	22.87
total-interference (W)	0	1.0	1.0

Figure 5.19: SINR performance obtained after RBA using the proposed sum-SLINR, proposed sum-SINR and sum-SNR maximisation.

5.5.3 Performance Evaluation in HetNet

Table 5.5: Summary of simulation parameters.

Parameters	**Value**
Cell layout	HetNet
Number of macro cell sites	19
Number of sectors per macro cell site	3
Number of pico cells per macro cell sector	4
Channel frequency	2.0 GHz
Carrier bandwidth	10 MHz
Number of RBs	50
Bandwidth of RB	180 kHz
Sub-carrier spacing	15kHz
Bandwidth per RB	180kHz
Shadowing standard deviation, σ_s	8dB
Pathloss coefficient, α	2
Macro cell BS power	43 dBm
Pico cell BS power	30dBm
[Inter site distance (ISD), D_o]	[750m, 100m]
Macro cell radius	250m
CEPC, HSPC radius	[70m, 50m]
Pico cell antenna type	omnidirectional
Macro cell antenna type	directional antennas
Number of transmit and receive antennas (M_t, N_r)	(4, 2)

In this section, the proposed distributed RBA strategy based on maximising the sum-SLINR of the users within a cell is evaluated using the obtained simulation results. The

simulation considers the cell set-up in Fig. 5.15 with $W = 19$ macro cell sites and $\delta = 3$ cell sectors per cell site giving a total of $M = 57$ macro cell sectors. Each macro cell sector has two CEPC and two HSPC at the cell center and 20 MCUs are considered. The following definitions are used in analysing the results: number of macro cell users (nMCUs), number of pico cell users (nPCUs), macro cell users (MCUs), pico cell users (PCUs), cell-edge pico cell users (CEPCUs), hotspot pico cell users (HSPCUs). 'd-SLINR MCU', 'd-SINR MCU' and 'd-SNR MCU' respectively are used to represent the proposed distributed RBA based on the proposed sum-SLINR, the proposed sum-SINR and the existing sum-SNR maximisation within the macro cell. 'd-SLINR PCU', 'd-SINR PCU' and 'd-SNR PCU' respectively are used to represent the proposed distributed RBA based on the proposed sum-SLINR, the proposed sum-SINR and the existing sum-SNR maximisation within the pico cell.

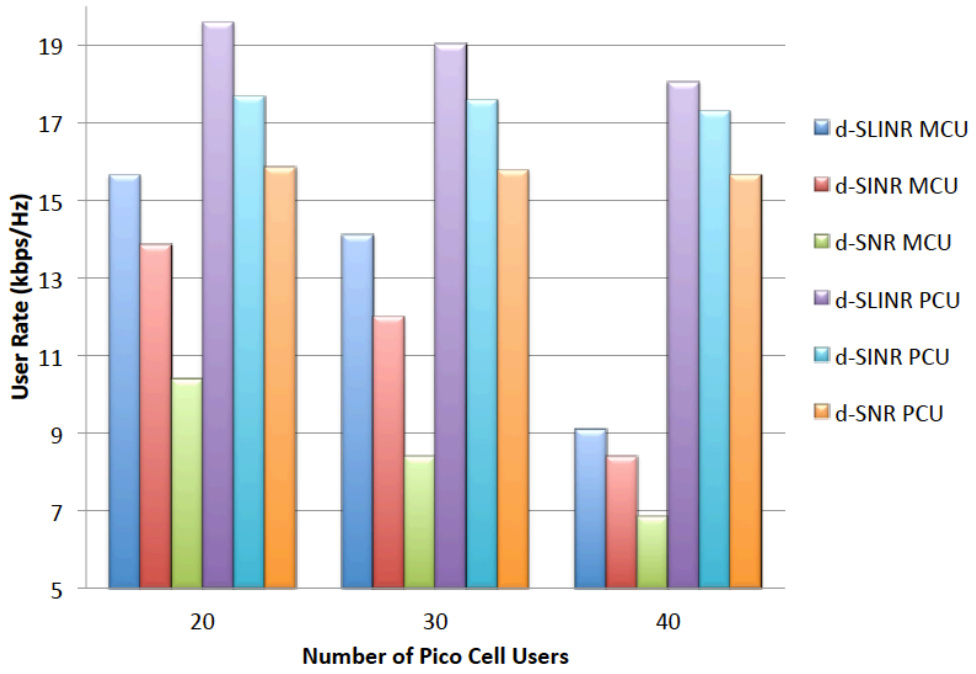

Figure 5.20: Average user rate per cell, with RBA based on sum-SLINR, sum-SINR and sum-SNR maximisation when nMCU = 20.

The average user rate for pico and macro cells can be observed in Fig. 5.20 using different RBA metrics when nMCU = 20. As the number of PCUs increases the obtained rates for the PCU and the MCU are seen to decrease due to increased level of interference within the system. Using the proposed strategy, it can be observed that 'd-SLINR MCU' achieves a user rate of 15.65 kbps/Hz, 14.1 kbps/Hz and 9.1 kbps/Hz respectively when the nPCUs = 20, 30 and 40. The achieved performance shows a significant improvement compared to 13.85 kbps/Hz, 12 kbps/Hz and 8.4 kbps/Hz achieved by 'd-SINR MCU' and 10.4 kbps/Hz, 8.4 kbps/Hz and 6.85 kbps/Hz achieved by 'd-SNR MCU'. This shows that the proposed distributed strategy for the HetNet ('d-SLINR MCU') is capable of obtaining a better user performance when compared to the proposed 'd-SINR MCU' and the 'd-SNR MCU' strategy.

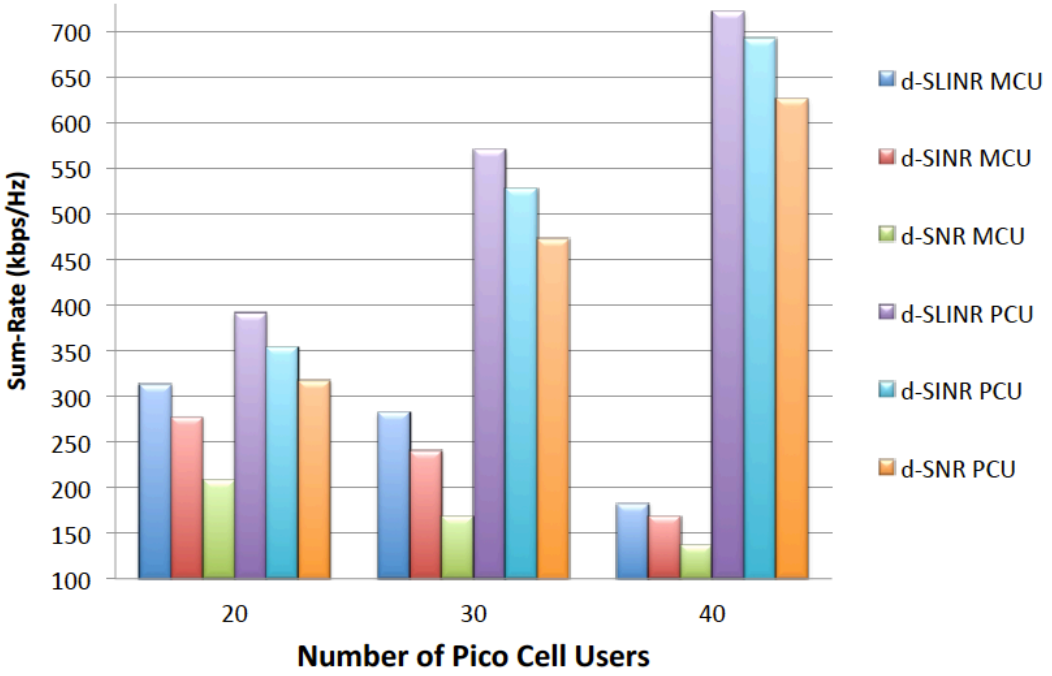

Figure 5.21: Average sum-rate per cell, with RBA based on sum-SLINR, sum-SINR and sum-SNR maximisation when nMCU = 20.

As expected, the average rate of the macro cell users decreases as the number of pico

cell users increase. This is due to a reduced number of interference-free RBs for the pico cell users, as the pico cell users begin utilising interfered RBs occupied by the macro cell users. However, the proposed strategy is still able to achieve exceptional performance compared to other strategies, as it aims to reduce the total interference introduced into the network, by considering the possible interference transmitted to already assigned users if the same RB is occupied.

Now consider the average-user rate and sum-rate performance for the pico cell, as shown Figs. 5.20 and 5.21. The obtained result shows that 'd-SLINR PCU' achieves a user rate of 19.58 kbps/Hz, 19.01 kbps/Hz and 18.03 kbps/Hz respectively when the nPCUs = 20, 30 and 40. This performance is significantly higher than 17.68 kbps/Hz, 17.58 kbps/Hz and 17.30 kbps/Hz achieved by 'd-SINR PCU' and 15.85 kbps/Hz, 15.77 kbps/Hz and 15.66 kbps/Hz achieved by 'd-SNR PCU'. As can be observed the MC and PC user rate performance obtained under sum-SLINR exceeds the performance obtained under sum-SINR and sum-SNR as the number of pico cell users increase. It also can be seen that the pico cell user rate performance obtained using the proposed sum-SLINR strategy when nPCUs is 40 (high interference) exceeds the performance obtained using the sum-SINR and sum-SNR strategy when nPCUs = 20, 30 and 40 (low to high interference). This shows that the strategy based on 'dist-SLINR' avoids more interference within the network thereby achieving better MC and PC user rates. The obtained results are achieved since for each RB, the leakage from the MC or PC BS and the interference from neighbouring MCs and PCs are considered during RBA. The sum-rate obtained in Fig. 5.21 also shows that the proposed RBA based on sum-SLINR exceeds the performance of the RBA based on sum-SINR and sum-SNR. When nPCUs = 30, 'd-SLINR PCU', 'd-SINR PCU' and 'd-SNR PCU' achieves a sum-rate of 570.5 kbps/Hz 527.5 kbps/Hz and 473 kbps/Hz respectively.

Based on the results obtained in Fig. 5.22, the level of interference can be observed for different RBA strategies. For instance, the sum-interference power per macro and pico cell under the sum-SNR appraoch is very high, with a power of 2.9 kW, 4.3 kW and 5.7 kW in the macro cell and 7.8 kW 11.8 kW and 15.8 kW in the pico cell when nPCUs

are 20, 30 and 40 respectively. The RBA based on the sum-SINR achieves a significant reduction of the interference power to 1.4 kW, 2.3 kW and 4.3 kW respectively in the macro cell and 3 kW, 4.1 kW and 4.7 kW respectively in the the pico cell when nPCUs are 20, 30 and 40 respectively. However, using the proposed RBA strategy based on maximising the sum-SLINR, the interference power is further reduced to 0.25 kW, 0.74 kW, 3.5 kW respectively in the macro cell and 0.3 kW, 0.6 kW and 1.4 kW respectively in the pico cell. The proposed strategy based on SLINR achieves an interference reduction of 82% and 90% respectively in the macro cell and pico cell, compared to the RBA based on SINR when nPCUs is 20.

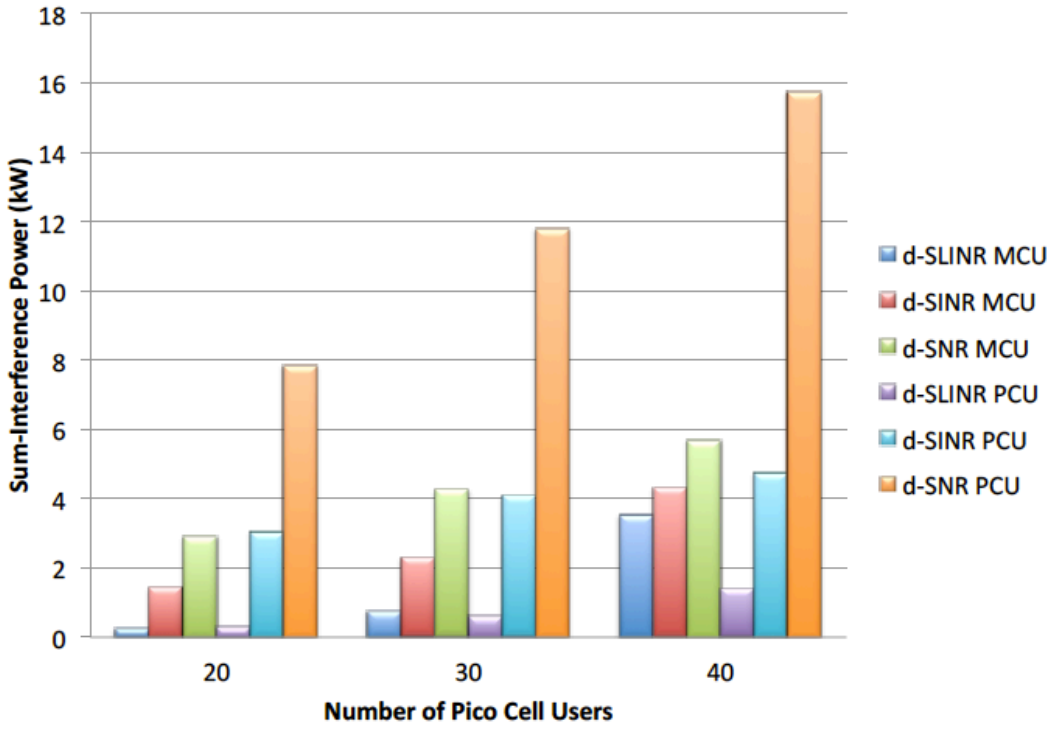

Figure 5.22: Sum interference power per cell, with RBA based on sum-SLINR, sum-SINR and sum-SNR maximisation when nMCU = 20.

From the results obtained, it is clear that the distributed proposed RBA metric based on the SLINR is able to address the problem of high interference in the HetNet system, through strategically avoiding both the transmitted and received interference within the network,

the resources are allocated in a more effective way compared to the other strategies, which results in increased system performance even in dense network traffic. Another significant advantage is derived from using the distributed round robin sector-by-sector approach. The proposed method allows the macro and pico cells to take responsibility for their RB allocation while still ensuring low RBA time and overhead when compared to other forms of RBA. This assumption can be said to be true since the proposed distributed RBA mode was shown for HomoNets to achieve the lowest RBA time and overhead, as opposed to other D-ICIC RBA modes presented earlier. The same underlying technique from the proposed distributed RBA was applied to the HetNet.

5.6 Summary

This chapter has considered the challenges faced with RRM for both homogeneous and heterogeneous networks. A novel, distributed RBA mode based on a round-robin sector-by-sector approach was proposed. This approach allowed the macro cell sectors of a given sector index, on every macro cell site, to allocate RBs to their users simultaneously, while considering the interference conditions within the network at that given time. In this way the interference within the network can be avoided and the total SINR of each macro cell sector can be maximised.

A self organising network is easily achieved using the proposed distributed mode of RBA, since the loop is continuous and periodically updates itself to adapt to the channel changes, entry of new users and terminated session of existing users. Apart from achieving a self organising network, it is important to avoid single points of failure in a system. Unlike the distributed mode of RBA, the centralised and semi-centralised approach have a high risk of single point of failure within a network, which can have huge sections of the network down at a given period of time. This means that if the RBAU fails the entire network would be down.

The proposed distributed mode of RBA enabled the proposed RBA metrics based on the

SINR and SLINR, to be used to solve the RBA optimisation problem and maximise the capacity of the HomoNet and HetNet since estimating the interference within the given network is now possible. The proposed SINR RBA metric was shown to also improve the system performance in the HomoNet as opposed to the SNR RBA metric. The proposed distributed RBA mode coupled with the proposed SLINR RBA metric was shown to increase the system performance in the HetNet as opposed to the proposed SINR RBA metric.

The proposed distributed RBA strategy was shown to give the best overall performance when compared to other modes of RBA. The proposed distributed RBA scheme solves the challenges faced with the centralised, semi-centralised and frequency partitioned RBA approach by reducing the high backhaul overhead, latency and poor synchronisation experienced during resource management, without affecting the maximum obtainable performance. Both the centralised and semi-centralised RBA strategies are not scalable in the LTE network, since the RNC is not part of the standardised network. However, the proposed distributed round robin sector-by-sector approach achieves a localised RBA strategy, since the LTE network has no provision for a central control unit.

Chapter 6

Interference Avoidance and Cancellation in Heterogeneous Network

6.1 Introduction

In this chapter, the interference problem faced in HetNet is further investigated. As mentioned earlier, the HetNet model was proposed to meet the continuous increase in capacity demand and obtain a better coverage especially for the cell-edge users. To achieve this objective, the HomoNet was transformed into the HetNet by introducing smaller cells within the macro cells to meet the high demands in hot spot areas and also improve coverage at the cell edge. This scheme is known to be one of the important drivers of LTE-A. However the HetNet suffers from very high interference which limits the expected gains of this system [76].

The ICI between a macro cell BS and the macro cell users in a nearby macro cell has been considered and several strategies to cancel and mitigate the interference has been proposed. This includes coordinated scheduling or beamforming, CoMP transmission and DCS. Also for cellular systems with a frequency reuse of 1, D-ICIC techniques such as RBA has been proposed for RRM. Static ICIC techniques such as FFR, SFR and adaptive frequency reuse have been proposed to tackle the problem of interference in

HomoNets and HetNets by assigning RBs to users in order to avoid the interference within the network. After the introduction of HetNets, some of the above mentioned technologies and techniques have been applied to HetNets to achieve an interference reduction within the system. RRM techniques such as RBA, power control, cell expansion, ABS have been introduced for interference management [76, 77]. Interference management techniques for HetNet such as cognitive sensing, cognitive beamforming, enhanced-ICIC (e-ICIC), small cell beamforming, adaptive beamforming and CoMP, have been proposed to combat the high level of interference in HetNets [78, 75].

The contributions of this chapter are as follows: Firstly, a joint interference avoidance and interference mitigation strategy is proposed, the effect of using both strategies to combat interference and improve the attainable capacity in the HetNet is investigated. Secondly, the interference avoidance technique used for the required analysis is the proposed distributed RBA technique presented in Chapter 5 based on maximising the sum-SLINR for HetNets. This technique is used jointly with an interference mitigation technique to achieve a further reduction in the interference, thereby improving the overall system. The interference mitigation techniques considered with the proposed distributed RBA strategy are: (i.) beamforming and (ii.) CoMP transmission. Thirdly, through obtained simulation results the two proposed joint interference management systems are analysed (i.e., (i.) the proposed distributed RBA and beamforming, (ii.) the proposed distributed RBA and CoMP transmission and compared to the results obtained using only the proposed distributed RBA strategy proposed in Chapter 5.

The rest of this chapter is presented as follows. The interference mitigation technique using beamformers for a single-cell multi-user system is presented in Section 6.2. Section 6.3 presents the proposed joint interference management system. The proposed joint RBA with beamforming is presented in Section 6.4 and the proposed joint RBA with CoMP transmission is proposed in Section 6.5. The simulation results are presented in Section 6.6. Finally the conclusion to this chapter is reached in Section 6.7.

6.2 Interference Mitigation for Single-Cell Multi-User MIMO System

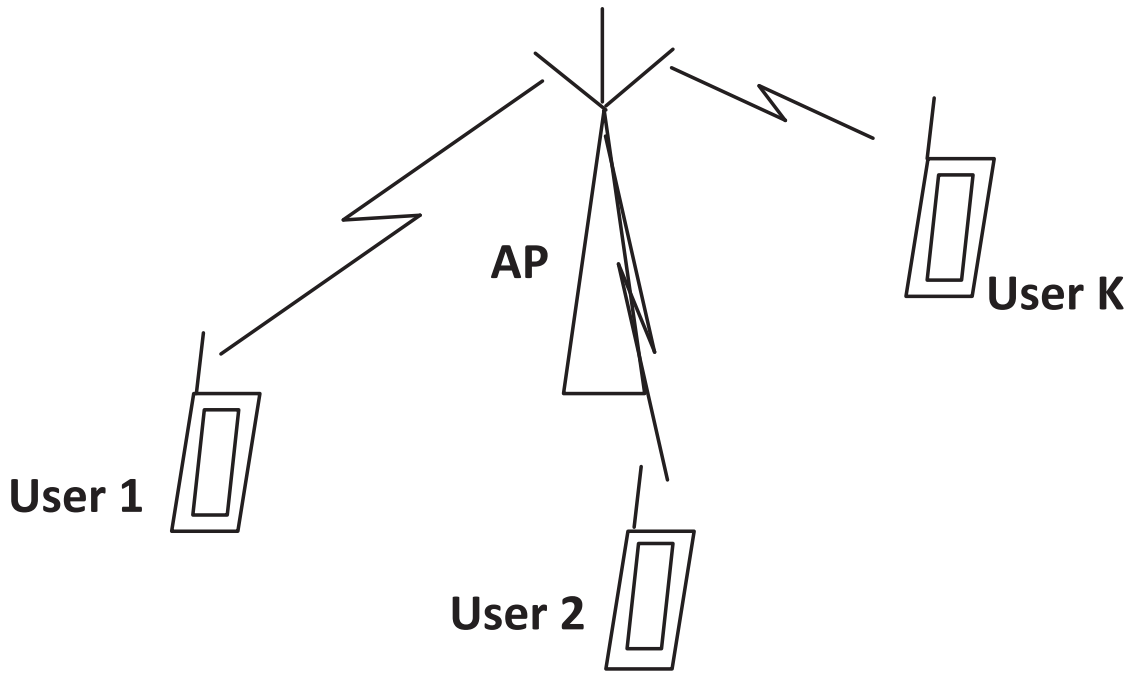

Figure 6.1: A single-cell multi-user system.

A single-cell multi-user MIMO system is shown in Fig. 6.1 with M_t antennas on the access point (AP) and K UEs, each having N_r antennas. The AP transmits data signals simultaneously to all users. Assuming a flat fading channel between the k-th user and the AP is given by $\mathbf{H}_k$, the coefficients of $\mathbf{H}_k$ are complex random variables, with zero-mean Gaussian real and imaginary parts. The BS finds the precoding matrix for each user's data transmission and combines the precoding matrices and signals of each user as a single signal before transmitting it to all K users.

The main aim is to choose the precoding matrix for each user's data signal such that the IUI is cancelled at the undesired UEs. IUI is the interference experienced at a desired user caused by transmitting other user's data signal simultaneously from the same AP at the same time.

Assuming perfect CSIT, the interference at each user can be minimized by designing the precoding vectors at the transmitter that cancels the leakage interference to each user. The leakage is the unwanted data signal or interference transmitted from a given AP or BS to the users in the network [23]. In [79], the authors proposed a precoding technique that chooses the precoding vectors to maximise the signal-to-leakage ratio (SLR) simultaneously for all users. Several research in [80], [81], [82], [83] has been shown to cancel ICI and IUI interference which resulted in an improved performance, however antenna conditions at the transmitter need to be met for this gain to be achieved. For instance, based on the use of only transmit precoders for interference cancellation and a single data stream for each user, the number of transmit antennas (M_t) must be greater than or equal to the sum of all the receive antennas (N_r) at the users. The constraint on the number of antennas is required to provide enough degrees of freedom for CCI cancellation at the receiver [84], [85].

The AP multiplies each precoding vector ($\mathbf{v}_k$) with dimension $M_t \times 1$ and $\|\mathbf{v}_k\|^2 = 1$, with a complex (scalar) data signal (s_k) corresponding to the user k, $\mathrm{E}\{\|s_k\|^2\} = 1$. The overall transmitted data is given by:

$$\mathbf{x} = \sum_{k=1}^{K} \mathbf{v}_k s_k \tag{6.2.1}$$

The vector $\mathbf{x}$ with dimensions $M_t \times 1$ is transmitted to all the users in the cell. The received signal $\mathbf{y}_k$ with dimension $N_r \times 1$ at any user k is given by:

$$\mathbf{y}_k = \mathbf{H}_k \mathbf{v}_k \sqrt{\rho_k} s_k + \sum_{m=1,\, m\neq k}^{K} \mathbf{H}_k \mathbf{v}_m \sqrt{\rho_m} s_m + \mathbf{n}_k,\ k \in [1, 2, ..., K], \tag{6.2.2}$$

where ρ_k is the power assigned to the k-th user's data, the noise received at the k-th user is given by $\mathbf{n}_k$, an additive, zero-mean, white, complex Gaussian noise vector with variance σ_k^2 and the second term in equation (6.2.2) is the IUI. To find the $\mathbf{v}_k$ for each user k, that cancels the interference caused to other users, the constraint in equation (6.2.3) must be met:

$$M_t \geq \sum_{m=1;m\neq k}^{K} N_r \tag{6.2.3}$$

The SLNR at the *k*-th user is given by:

$$\begin{aligned}\text{SLNR}_k =& \frac{\left\|\mathbf{H}_k\mathbf{v}_k\right\|^2\rho_k}{\sum_{m=1,m\neq k}^{K}\left\|\mathbf{H}_m\mathbf{v}_k\right\|^2\rho_k+\sigma_k^2},\\ =& \frac{\mathbf{v}_k^H\mathbf{H}_k^H\mathbf{H}_k\mathbf{v}_k\rho_k}{\mathbf{v}_k^H\widehat{\mathbf{H}}_k^H\widehat{\mathbf{H}}_k\mathbf{v}_k\rho_k+\sigma_k^2}, \quad k\in[1,2,...,K],\\ \text{where} \quad & \widehat{\mathbf{H}}_k=[\mathbf{H}_1^H,\cdots,\mathbf{H}_{k-1}^H,\mathbf{H}_{k+1}^H,\cdots,\mathbf{H}_K^H]^H.\end{aligned} \tag{6.2.4}$$

The denominator in (6.2.4) contains both the received noise power and the leakage power of other user's data signal when transmitting simultaneously to the *k*-th user. The beamforming vector $\mathbf{v}_k$ for each user *k* can be obtained as there are K decoupled optimization problems. The precoding vector $\mathbf{v}_k$ for each user is obtained such that the SLNR of each user can be maximized, using the Rayleigh-Ritz quotient result [86]. The equations in (6.2.5) and (6.2.6) have been proven in [38]:

$$\mathbf{v}_k \propto \max \text{ gen eigenvector}(\mathbf{H}_k^H\mathbf{H}_k,(\widehat{\mathbf{H}}_k^H\widehat{\mathbf{H}}_k+(\sigma_k^2/\rho_k)\mathbf{I}_{M_t})). \tag{6.2.5}$$

Since $(\widehat{\mathbf{H}}_k^H\widehat{\mathbf{H}}_k+\sigma_k^2\mathbf{I}_{M_t})$ is invertible, then the generalised eigenvector problem in (6.2.5) reduces to a standard eigenvector problem and $\mathbf{v}_k$ is chosen as the eigenvector associated with the maximum eigenvalue of:

$$((\widehat{\mathbf{H}}_k^H\widehat{\mathbf{H}}_k+(\sigma_k^2/\rho_k)\mathbf{I}_{M_t})^{-1}\mathbf{H}_k^H\mathbf{H}_k) \tag{6.2.6}$$

where $\mathbf{I}_{M_t}$ is the identity matrix of dimension M_t.

6.3 RBA and Interference Mitigation Techniques

Cross-tier interference is defined as the interference between two different cell types, while co-tier interference is defined as the interference between two similar cell types.

In [87], the authors proposed a 2-step strategy to address the cross-tier and co-tier downlink interference in the HetNet. To tackle this problem the interference alignment (IA) strategy was used to mitigate the interference so that more small cells can transmit data using the same time slot on a given channel. Then a link scheduling algorithm was used to reschedule small cells to another time slot when the interference could not be avoided. Also in [88], the authors proposed a radio resource management strategy to avoid interference within the HetNet and a decision algorithm to determine whether CoMP transmission was required for the user's data transmission.

In Chapter 2, 3 and 4, CoMP transmission has been considered for interference mitigation in interference limited networks, as a strategy to improve the performance of the users, especially at the cell edge. CoMP transmission was shown to improve the overall system performance (especially for the cell-edge users) by transmitting data signals from neighbouring BSs to the users. Other forms of interference mitigation techniques like adaptive beamforming were highlighted in Chapter 2. This form of interference mitigation is used to cancel or minimise the unwanted interference to other users, by designing precoders and/or receive beamformers. In Chapter 5, the RBA was analysed as a technique for radio resource management based on an interference avoidance strategy within the network, where RBs are assigned to users while avoiding the allocation of RBs with high interference to the users, thereby improving the overall system capacity and user data rate. Two distributed RBA techniques were proposed based on maximising the sum-SINR and maximising the sum-SLINR and they were shown to improve the system performance compared to other known strategies.

In this chapter, both forms of ICIC, i.e. interference mitigation or cancellation and interference avoidance will be applied jointly to further reduce the high interference observed in the HetNet especially during peak times, thereby improving the user's performance. Using the distributed RBA techniques based on maximising the sum-SLINR as proposed in Chapter 5, the qualification matrix is obtained by estimating the SLINR of each user's data transmission and then allocating RBs to all users to maximise the sum-SLINR within the macro cell or pico cell. Subsequently, using an interference

mitigation scheme, the unavoidable interference is cancelled to obtain a further reduction in the interference and an improved system performance. The two interference mitigation techniques considered in this chapter are: Beamforming and CoMP transmission.

For the purpose of this work, cross-tier interference will be mitigated between the macro cell sector and pico cell sector and co-tier interference will be mitigated between interfering macro cell sectors. The cross-tier interference considered for each macro cell sector includes: macro cell BS to pico cell user interference and pico cell BS to macro cell user interference both within the same cell sector. It also includes the macro BS of another cell sector to pico cell users in another macro cell sector. The co-tier interference considered is the ICI from a macro cell sector to the macro cell users in a different cell sector.

Table 6.1: Summary of variable notations and definitions

Notation	**Definition**
δ	Number of macro cell sectors in each macro cell site.
N_{RB}	Number of available RBs at each time slot.
$\bar{K}_{(m,c)}$	Number of users served by the c-th eNB in the m-th macro cell sector, $m = [1, 2, \cdots, M]$.
$\bar{K}_m$	Total number of users in the m-th macro cell sector, $m = [1, 2, \cdots, M]$.
$\tilde{K}_w$	Total number of users in the w-th macro cell site, $w = 1: W$.
W, M	Number of macro cell sites and macro cell sectors respectively, $w = [1, 2, \cdots, W]$ and $m = [1, 2, \cdots, M]$, $M = \delta W$
C	Number of transmitting eNBs in each macro cell sector, $c = 1$ indicates a macro cell, otherwise a pico cell, $c = [2, 3, \cdots, C]$.
T_m	Set of interfering macro cell sectors on the m-th macro cell sector.
(m,c)	The c-th cell in the m-th macro cell sector.
$a_{k,r}^{(m,c)}$	The bit-wise element that indicates if the r-th RB is assigned to the k-th UE in (m, c).

$s_{k,r}^{(m,c)}$	The *k*-th user data transmitted on the *r*-th RB from the eNB in *(m,c)*, $\mathrm{E}\{\|\|s_{k,r}^{(m,c)}\|\|^2\} = 1$.
$\mathbf{v}_{k,r}^{(m,c)}$	The precoder used to transmit the *k*-th user's data on the *r*-th RB from the eNB in *(m,c)*, $\|\|\mathbf{v}_{k,r}^{(m,c)}\|\|^2 = 1$.
$\bar{\mathbf{v}}_{k,r}^{(m,d)}$	The precoder used to transmit the data to the *k*-th user in *(m,d)* on the *r*-th RB from the eNB in $(m,1)$ (i.e. the *m*-th macro cell eNB), $\|\|\bar{\mathbf{v}}_{k,r}^{(m,d)}\|\|^2 = 1$.
$\mathbf{u}_{k,r}^{(m,c)}$	The receiver beamformer used at the *k*-th user on the *r*-th RB in *(m,c)* to cancel the received interference, $\|\|\mathbf{u}_{k,r}^{(m,c)}\|\|^2 = 1$.
$\mathbf{H}_{k,r}^{(m,c)}$	The flat-fading channel on the *r*-th RB, from the eNB in *(m,c)* to the *k*-th UE.
$\bar{\mathbf{H}}_{k,r}^{(m,c,o)}$	The flat-fading channel on the *r*-th RB, from the *o*-th interfering macro cell sector eNB to the *k*-th UE in *(m,c)*.
$g_{k,r}^{(m,c)}$	The channel gain on the *r*-th RB, from the eNB in *(m,c)* to the *k*-th UE.
$\bar{g}_{k,r}^{(m,c,o)}$	The channel gain on the *r*-th RB, from the *o*-th interfering macro cell sector eNB to the *k*-th UE in *(m,c)*.
$\rho_{k,r}^{(m,c)}$	The power allocation from eNB in *(m,c)* to the *k*-th user on the *r*-th RB.
$\bar{\rho}_{k,r}^{(m,d)}$	The power allocated to transmit data from the eNB in $(m,1)$ (i.e. the *m*-th macro cell eNB) to the *k*-th user in *(m,d)* on the *r*-th RB.
$\mathbf{n}_{k,r}^{(m,c)}$	The noise vector received by the *k*-th user on the *r*-th RB in *(m,c)*, elements are complex random Gaussian variable with zero mean and variance $(\sigma_{k,r}^{(m,c)})^2$.
$\mathbf{y}_{k,r}^{(m,c)}$	The received signal vector of the *k*-th user on the *r*-th RB in *(m,c)*.
$\gamma_{k,r}^{(m,c)}$	The SINR of the *k*-th user on the *r*-th RB in *(m,c)*.
$R_{k,r}^{(m,c)}$	The rate of the *k*-th user on the *r*-th RB in *(m,c)*.
$R_T^{(m)}$, $R_T^{(m,c)}$	The sum-rate of the users in the *m*-th macro cell sector and in *(m,c)* respectively.

6.4 RBA with Beamforming

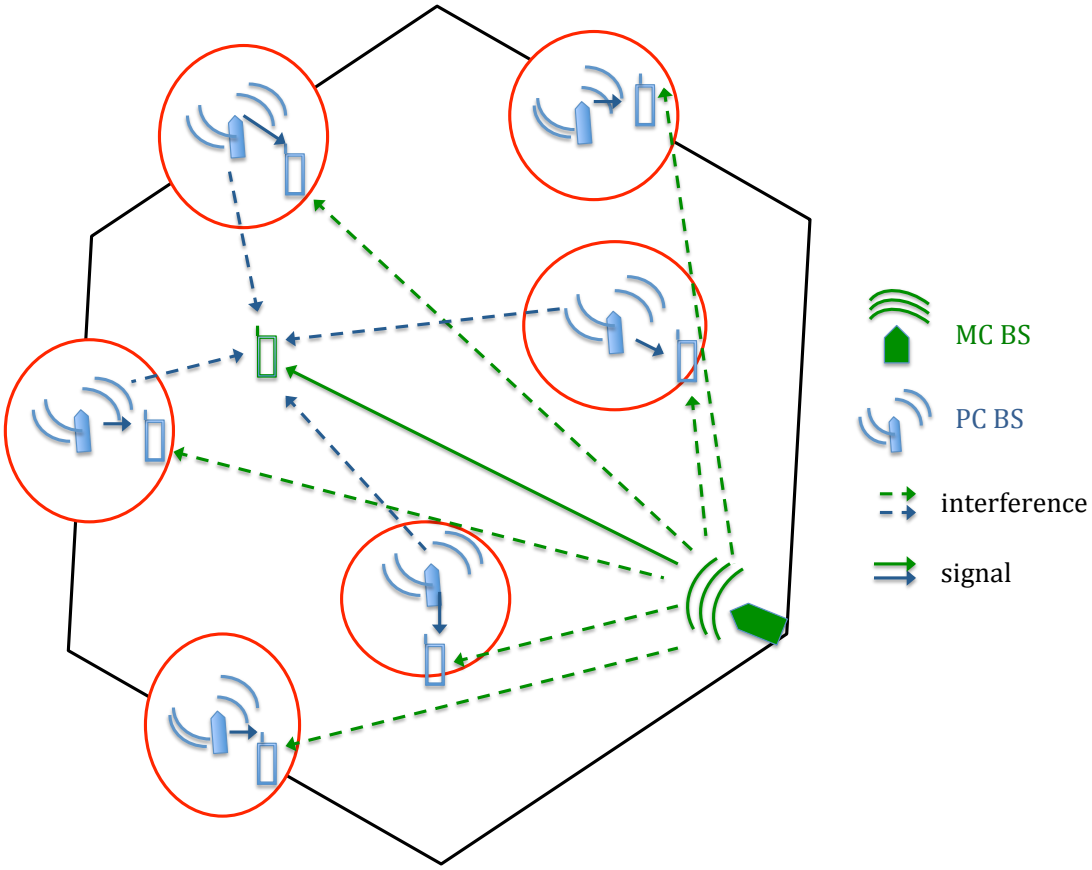

Figure 6.2: Interference cancellation from a macro cell (MC) BS to the pico cell (PC) users.

The joint RBA with beamforming uses the proposed distributed RBA strategy for HetNets (proposed in Chapter 5) to assign the RBs. For the r-th RB assigned, transmit and receive beam-formers are designed to further mitigate the interference within each cell type. The HetNet system model in Fig. 5.15 is considered and each variable used subsequently is defined in Table. 6.1.

6.4.1 System Model

The received signal ($\mathbf{y}_{k,r}^{(m,c)}$) at the *k*-th UE in (m,c) assigned to the *r*-th RB, is post-processed by the receive beamforming vector ($\mathbf{u}_{k,r}^{(m,c)}$) is shown in (6.4.7):

$$\mathbf{u}_{k,r}^{(m,c)H}\mathbf{y}_{k,r}^{(m,c)} = \mathbf{u}_{k,r}^{(m,c)H}\mathbf{H}_{k,r}^{(m,c)}\mathbf{v}_{k,r}^{(m,c)}\sqrt{\rho_{k,r}^{(m,c)}}s_{k,r}^{(m,c)} \tag{6.4.7a}$$

$$+ \sum_{\substack{d=1,\, d\neq c,\\ j\in[1,2,\cdots,\bar{K}_{(m,d)}],\\ a_{j,r}^{(m,d)}=1.}}^{C} \mathbf{u}_{k,r}^{(m,c)H}\mathbf{H}_{k,r}^{(m,d)}\mathbf{v}_{j,r}^{(m,d)}\sqrt{\rho_{j,r}^{(m,d)}}s_{j,r}^{(m,d)} \tag{6.4.7b}$$

$$+ \sum_{\substack{o=1,\, o\in T_m,\\ q\in[1,2,\cdots,\bar{K}_{(o,1)}],\\ a_{q,r}^{(o,1)}=1.}}^{M} \mathbf{u}_{k,r}^{(m,c)H}\bar{\mathbf{H}}_{k,r}^{(m,c,o)}\mathbf{v}_{q,r}^{(o,1)}\sqrt{\rho_{q,r}^{(o,1)}}s_{q,r}^{(o,1)} + \mathbf{u}_{k,r}^{(m,c)H}\mathbf{n}_{k,r}^{(m,c)}, \tag{6.4.7c}$$

$$\text{if } a_{k,r}^{(m,c)} = 1, \forall\, k \in [1,2,\cdots,\bar{K}_{(m,c)}], \forall c \in [1,2,\cdots,C],\ \forall m \in [1,2,\cdots,M],$$

$$\forall r \in [1,2,\cdots,N_{RB}]. \tag{6.4.7d}$$

The coefficients of $\mathbf{H}_{k,r}^{(m,c)}$ are complex random variables, with zero-mean Gaussian real and imaginary parts. The channel links experience large scale fading, with path loss exponent (α) and log-normal shadowing having zero-mean and variance σ_s^2. The signal received in (6.4.7a) is the desired signal from the associated pico cell or macro cell. The interference received from the other cell type within the same macro cell sector is given in (6.4.7b) while the interference from neighbouring macro cell sectors in T_m plus the received noise is given in (6.4.7c). The SINR at the *k*-th UE in (m,c) on the *r*-th RB, $\forall r \in [1,2,\cdots,N_{RB}]$, is given by($\gamma_{k,r}^{(m,c)}$):

$$\gamma_{k,r}^{(m,c)} = \frac{|\mathbf{u}_{k,r}^{(m,c)H}\mathbf{H}_{k,r}^{(m,c)}\mathbf{v}_{k,r}^{(m,c)}|^2\rho_{k,r}^{(m,c)}}{\sum\limits_{\substack{d=1,\, d\neq c,\\ j\in[1,2,\cdots,\bar{K}_{(m,d)}],\\ a_{j,r}^{(m,d)}=1.}}^{C} g_{k,r}^{(m,d)}\rho_{j,r}^{(m,d)} + \sum\limits_{\substack{o=1,\, o\in T_m,\\ q\in[1,2,\cdots,\bar{K}_{(o,1)}],\\ a_{q,r}^{(o,1)}=1.}}^{M} \bar{g}_{k,r}^{(m,c,o)}\rho_{q,r}^{(o,1)} + (\sigma_{k,r}^{(m,c)})^2},$$

$$\text{if } a_{k,r}^{(m,c)} = 1, \forall\, k \in [1,2,\cdots,\bar{K}_{(m,c)}], \forall c \in [1,2,\cdots,C],\ \forall m \in [1,2,\cdots,M]. \tag{6.4.8}$$

where $g_{k,r}^{(m,d)} = |\mathbf{u}_{k,r}^{(m,c)H}\mathbf{H}_{k,r}^{(m,d)}\mathbf{v}_{j,r}^{(m,d)}|^2$ and $\bar{g}_{k,r}^{(m,c,o)} = |\mathbf{u}_{k,r}^{(m,c)H}\bar{\mathbf{H}}_{k,r}^{(m,c,o)}\mathbf{v}_{q,r}^{(o,1)}|^2, \forall k, m, c, r.$ The user-rate ($R_{k,r}^{(m,c)}$), cell sum-rate ($R_T^{(m,c)}$), macro cell sum-rate ($R_T^{(m)}$), and the network sum-rate (R_T) is given in (5.4.10).

6.4.2 Beamforming Design

The macro cell sectors are autonomous since the RBA is distributed on each macro cell sector and pico cells. The macro cell sector also acts as the gateway of the pico cells to the core network, and is responsible for providing the data from the core network to the pico cell BS. The RNC for LTE-A does not exist and since the RBA is distributed, it is safe to assume that the beamforming design should also be distributed. First assuming the receive beam-formers are designed for the users in each cell type using only the channel information available. The receive beam-former for each user on each cell type is designed to minimise the ICI from neighbouring macro cell sectors in T_m on each RB r. So $\mathbf{u}_{k,r}^{(m,c)}$ is chosen as the eigenvector of the minimum eigenvalue of:

$$\sum_{o=1,\, o\in T_m}^{M} (\bar{\mathbf{H}}_{k,r}^{(m,c,o)H}\bar{\mathbf{H}}_{(k,r)}^{(m,c,o)}),\ \text{if } a_{k,r}^{(m,c)} = 1,\ k = [1, 2, \cdots, \bar{K}_{(m,c)}],$$
$$m = [1, 2, \cdots, M], c = [1, 2, \cdots, C],\ r = [1, 2, \cdots, N_{RB}]. \tag{6.4.9}$$

Precoder Design based on max-SLNR

Assuming that the receive beam-former information is made available to the neighbouring cells, the transmit pre-coders for each user's data are designed to maximise the SLNR using the known channel information and the obtained receive beam-former information. For the r-th RB ($r \in [1, 2, \cdots, N_{RB}]$), the transmit precoders for the pico cell users are designed to minimise the leakage to the macro cell user in the same macro cell sector, while maximising the desired signal to the pico cell user, $\mathbf{v}_{k,r}^{(m,c)}$ is chosen as the eigenvector corresponding to the maximum eigenvalue of (6.4.10a):

$$(\vartheta_{k,r}^{(m,c)}\mathbf{I}_{M_t} + (\mathbf{H}_{j,r}^{(m,c)H}\mathbf{u}_{j,r}^{(m,1)}\mathbf{u}_{j,r}^{(m,1)H}\mathbf{H}_{j,r}^{(m,c)}))^{-1}(\mathbf{H}_{k,r}^{(m,c)H}\mathbf{u}_{k,r}^{(m,c)}\mathbf{u}_{k,r}^{(m,c)H}\mathbf{H}_{k,r}^{(m,c)}), \quad (6.4.10a)$$

$$\text{if } a_{k,r}^{(m,c)} = 1, k = [1, 2, \cdots, \bar{K}_{(m,c)}],\ m = [1, 2, \cdots, M], c = [2, \cdots, C], \quad (6.4.10b)$$

$$r = [1, 2, \cdots, N_{RB}], \vartheta_{k,r}^{(m,c)} = ((\sigma_{k,r}^{(m,c)})^2/\rho_{k,r}^{(m,c)}),\ j \in [1, 2, \cdots, \bar{K}_{(m,1)}]. \quad (6.4.10c)$$

The transmit precoder needed to transmit data to the macro cell sector user on each RB ($r = [1, 2, \cdots, N_{RB}]$), is designed to minimise the leakage to (i.) the macro cell users in the neighbouring macro cell sectors in T_m, (see (6.4.11c)) (ii.) the pico cell served by the left-side macro cell sector (LSMCS) and the other pico cell served by the right-side macro cell sector (RSMCS) (see (6.4.11d)) (iii.) the four pico cell users in the same macro cell sector (see (6.4.11e)). The leakage in (ii.) and (iii.) are shown in Fig. 6.2 and $\mathbf{v}_{k,r}^{(m,c)}$ is chosen as the eigenvector corresponding to the maximum eigenvalue of (6.4.11a):

$$(\vartheta_{k,r}^{(m,c)}\mathbf{I}_{M_t} + (\mathbf{Z}_{k,r}^{(m,c)H}\mathbf{Z}_{k,r}^{(m,c)})^{-1}(\mathbf{H}_{k,r}^{(m,1)H}\mathbf{u}_{k,r}^{(m,c)}\mathbf{u}_{k,r}^{(m,c)H}\mathbf{H}_{k,r}^{(m,1)}),\ \text{if } a_{k,r}^{(m,1)} = 1,$$
$$c = 1, k = [1, 2, \cdots, \bar{K}_{(m,c)}],\ m = [1, 2, \cdots, M], r = [1, 2, \cdots, N_{RB}],$$
$$\vartheta_{k,r}^{(m,c)} = ((\sigma_{k,r}^{(m,c)})^2/\rho_{k,r}^{(m,c)}). \quad (6.4.11a)$$

$$\mathbf{Z}_{k,r}^{(m,c)} = \begin{bmatrix} \bar{\mathbf{Z}}_{k,r}^{(m,c)} \\ \hat{\mathbf{Z}}_{k,r}^{(m,c)} \\ \tilde{\mathbf{Z}}_{k,r}^{(m,c)} \end{bmatrix}, \quad \text{if } a_{k,r}^{(m,1)} = 1, \quad (6.4.11b)$$

$$\bar{\mathbf{Z}}_{k,r}^{(m,c)} = [[\mathbf{u}_{q,r}^{(o,1)H}\bar{\mathbf{H}}_{q,r}^{(o,1,m)}]^T, a_{q,r}^{(o,1)} = 1, o = [1, 2, \cdots, M]]^T,$$
$$q \in [1, 2, \cdots, \bar{K}_{(o,1)}],\ o \in T_m, \quad (6.4.11c)$$

$$\hat{\mathbf{Z}}_{k,r}^{(m,c)} = \begin{bmatrix} \mathbf{u}_{q,r}^{(T_m(1),2)H}\bar{\mathbf{H}}_{q,r}^{(T_m(1),2,m)}, a_{q,r}^{(T_m(1),2)} = 1,\ q \in [1, 2, \cdots, \bar{K}_{(T_m(1),2)}] \\ \mathbf{u}_{q,r}^{(T_m(4),3)H}\bar{\mathbf{H}}_{q,r}^{(T_m(4),3,m)}, a_{q,r}^{(T_m(4),3)} = 1,\ q \in [1, 2, \cdots, \bar{K}_{(T_m(4),3)}] \end{bmatrix}, \quad (6.4.11d)$$

$$\tilde{\mathbf{Z}}_{k,r}^{(m,c)} = [[\mathbf{u}_{j,r}^{(m,d)H}\mathbf{H}_{j,r}^{(m,1)}]^T,\ a_{j,r}^{(m,d)} = 1,\ d = [1, 2, \cdots, C]]^T,$$
$$j \in [1, 2, \cdots, \bar{K}_{(m,d)}], d \neq c, \quad (6.4.11e)$$

$\mathbf{Z}_{k,r}^{(m,c)}, \bar{\mathbf{Z}}_{k,r}^{(m,c)}, \hat{\mathbf{Z}}_{k,r}^{(m,c)}$ and $\tilde{\mathbf{Z}}_{k,r}^{(m,c)}$ all have M_t columns.

6.4.3 Power Allocation

For the IC technique using transmit and receive beamformers, the power allocation problem is based on the per-BS power constraint (PBPC). The PBPC for the pico cell BS and macro cell BS is given by p_{pico}^{PBPC} and p_{macro}^{PBPC} respectively. On the r-th RB, the power allocation is assigned to satisfy the constraint in (6.4.12):

$$\begin{cases} \|\mathbf{v}_{k,r}^{(m,c)}\|^2 \rho_{k,r}^{(m,c)} = p_{macro}^{PBPC}, & \text{if } a_{k,r}^{(m,c)} = 1, c = 1 \\ \|\mathbf{v}_{k,r}^{(m,c)}\|^2 \rho_{k,r}^{(m,c)} = p_{pico}^{PBPC}, & \text{if } a_{k,r}^{(m,c)} = 1, c \in [2, 3, \cdots, C\} \end{cases}, \\ k = [1, 2, \cdots, \bar{K}_{(m,c)}],\ m = [1, 2, \cdots, M],\ c = [1, 2, \cdots, C]. \tag{6.4.12}$$

Assuming the full power transmission for all BSs types, then the macro and pico cell BS transmits the user information such that the power constraints in (6.4.12) are met. It is easy to see that for the macro and pico cell users, since $\|\mathbf{v}_{k,r}^{(m,c)}\|^2 = 1$, the power allocated for data transmission is given by:

$$\rho_{k,r}^{(m,c)} = \begin{cases} p_{macro}^{PBPC} & c = 1 \\ p_{pico}^{PBPC} & c = [2, 3, \cdots, C] \end{cases}, \tag{6.4.13}$$
$$k = [1, 2, \cdots, \bar{K}_{(m,c)}],\ m = [1, 2, \cdots, M].$$

6.5 RBA with CoMP

In this section, the proposed joint distributed RBA with CoMP transmission is investigated as a tool to improve the capacity of the HetNet system in very high interference during peak times. The CoMP transmission will be considered from only the macro cell sector BSs (or eNBs) to the PC users within each macro cell sector. Beam-formers will be used to mitigate interference from the pico cell BSs. The technique and idea behind CoMP transmission has been investigated in Chapters 2, 3 and 4. The definition of variables used subsequently can be found in Table 6.1

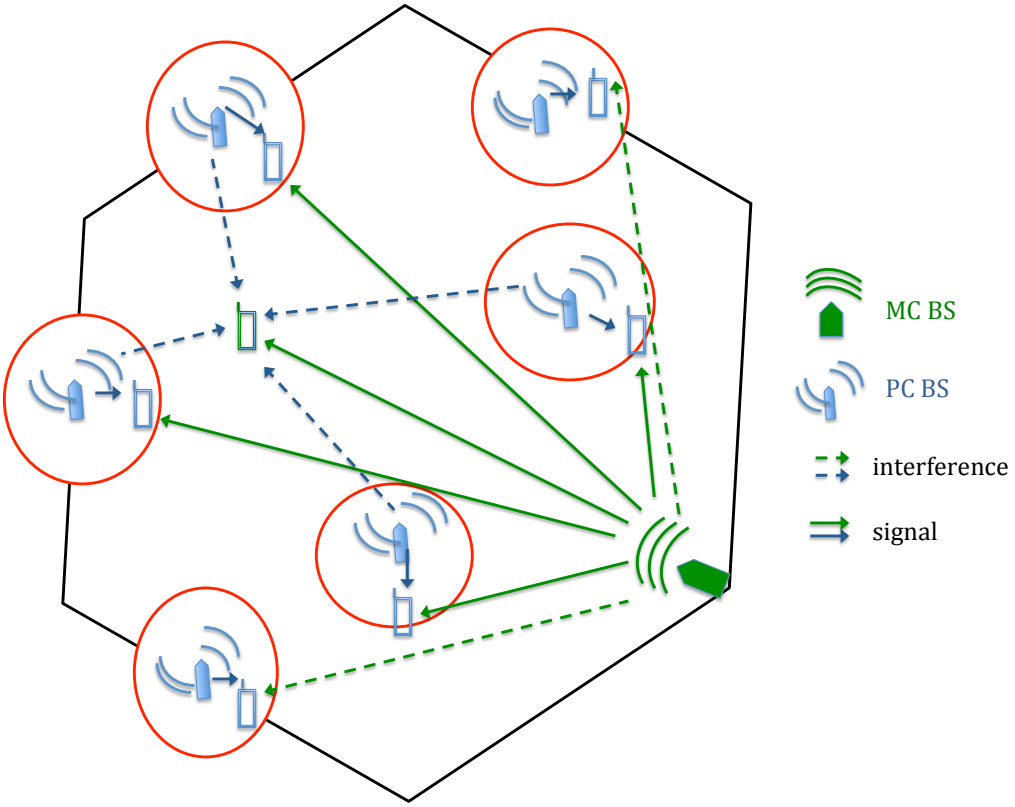

Figure 6.3: CoMP transmission from the MC BS to the PC users.

6.5.1 Assumption

The following assumptions are made for this section:

1. CoMP transmission is only considered in each macro cell sector, from the macro cell BS to the pico cell users on the same RB.
2. On each RB, each macro cell sector can only perform CoMP transmission to other pico cells within the same macro cell sector if a macro cell user is assigned to that RB.
3. No pico cell to pico cell user interference.
4. No interference between macro cell sectors of the same macro cell site.

6.5.2 System Model

The received signal ($\mathbf{y}_{k,r}^{(m,c)}$) at the k-th UE in (m,c) assigned to the r-th RB is post-processed by the receive beamforming vector ($\mathbf{u}_{k,r}^{(m,c)}$) as in (6.5.14). The desired signal is shown in (6.5.14a), where $\varpi_{k,r}^{(m,c)}$ is the received signal from the pico cell BS to the pico cell user (see (6.5.14g)). The IUI (in the case of the macro cell user) and the cross-tier interference (in the case of the pico cell user) within the same macro cell sector is seen in (6.5.14b). The co-tier interference from neighbouring interfering macro cell sectors to macro cell and pico cell users in a given macro cell sector is given by (6.5.14c). The cross-tier interference received from the pico cell BSs to the macro cell user is given by $\xi_{k,r}^{(m,c)}$ as seen in (6.5.14d) and (6.5.14f).

$$\mathbf{u}_{k,r}^{(m,c)H}\mathbf{y}_{k,r}^{(m,c)} = \varpi_{k,r}^{(m,c)} + \mathbf{u}_{k,r}^{(m,c)H}\mathbf{H}_{k,r}^{(m,1)}\bar{\mathbf{v}}_{k,r}^{(m,c)}\sqrt{\bar{\rho}_{k,r}^{(m,c)}}s_{k,r}^{(m,c)} \tag{6.5.14a}$$

$$+ \sum_{\substack{d=1,\, d\neq c,\\ j\in[1,2,\cdots,\bar{K}_{(m,d)}],\\ a_{j,r}^{(m,d)}=1.}}^{C} \mathbf{u}_{k,r}^{(m,c)H}\mathbf{H}_{k,r}^{(m,1)}\bar{\mathbf{v}}_{j,r}^{(m,d)}\sqrt{\bar{\rho}_{j,r}^{(m,d)}}s_{j,r}^{(m,d)} \tag{6.5.14b}$$

$$+ \sum_{o=1,\, o\in T_m}^{M} \mathbf{u}_{k,r}^{(m,c)H}\bar{\mathbf{H}}_{k,r}^{(m,c,o)} \sum_{\substack{d=1,\, a_{q,r}^{(o,d)}=1,\\ q\in[1,2,\cdots,\bar{K}_{(o,d)}].}}^{C} \bar{\mathbf{v}}_{q,r}^{(o,d)}\sqrt{\bar{\rho}_{q,r}^{(o,d)}}s_{q,r}^{(o,d)} \tag{6.5.14c}$$

$$+ \xi_{k,r}^{(m,c)} + \mathbf{u}_{k,r}^{(m,c)H}\mathbf{n}_{k,r}^{(m,c)}, \forall\, k = [1,2,\cdots,\bar{K}_{(m,c)}], \tag{6.5.14d}$$

$$\forall\, r = [1,2,\cdots,N_{RB}],\ \forall m = [1,2,\cdots,M], \forall c = [1,2,\cdots,C]. \tag{6.5.14e}$$

$$\xi_{k,r}^{(m,c)} = \begin{cases} \sum_{\substack{d=2,\, d\neq c,\\ j\in[1,2,\cdots,\bar{K}_{(m,d)}],\\ a_{j,r}^{(m,d)}=1.}}^{C} \mathbf{u}_{k,r}^{(m,c)H}\mathbf{H}_{k,r}^{(m,d)}\mathbf{v}_{j,r}^{(m,d)}\sqrt{\rho_{j,r}^{(m,d)}}s_{j,r}^{(m,d)}, & c=1 \ \&\ a_{k,r}^{(m,c)}=1 \\ 0, & c\neq 1 \end{cases}. \tag{6.5.14f}$$

$$\varpi_{k,r}^{(m,c)} = \begin{cases} \mathbf{u}_{k,r}^{(m,c)H}\mathbf{H}_{k,r}^{(m,c)}\mathbf{v}_{k,r}^{(m,c)}\sqrt{\rho_{k,r}^{(m,c)}}s_{k,r}^{(m,c)}, & \text{if } c\neq 1 \text{ and } a_{k,r}^{(m,c)}=1 \\ 0, & \text{if } c=1 \text{ and } a_{k,r}^{(m,c)}=1 \end{cases}, \tag{6.5.14g}$$

The SINR at the k-th UE in (m,c) on the r-th RB, is given by ($\gamma_{k,r}^{(m,c)}$) :

$$\gamma_{k,r}^{(m,c)} = \frac{|\varpi_{k,r}^{(m,c)}|^2 + |\mathbf{u}_{k,r}^{(m,c)H}\mathbf{H}_{k,r}^{(m,1)}\bar{\mathbf{v}}_{k,r}^{(m,c)}|^2\bar{\rho}_{k,r}^{(m,c)}}{\eta_{k,r}^{(m,c)} + \tau_{k,r}^{(m,c)} + \mu_{k,r}^{(m,c)} + (\sigma_{k,r}^{(m,c)})^2}, \text{ if } a_{k,r}^{(m,c)} = 1, \tag{6.5.15a}$$

$$\forall\, k \in [1,2,\cdots,\bar{K}_{(m,c)}], \forall c \in [1,2,\cdots,C],\ \forall m \in [1,2,\cdots,M],\ \forall r \in [1,2,\cdots,N_{RB}], \tag{6.5.15b}$$

$$\eta_{k,r}^{(m,c)} = \sum_{\substack{d=1,d\neq c,\\ j\in[1,2,\cdots,\bar{K}_{(m,d)}],\\ a_{j,r}^{(m,d)}=1.}}^{C} |\mathbf{u}_{k,r}^{(m,c)H}\mathbf{H}_{k,r}^{(m,1)}\bar{\mathbf{v}}_{j,r}^{(m,d)}|^2\bar{\rho}_{j,r}^{(m,d)}, \tag{6.5.15c}$$

$$\tau_{k,r}^{(m,c)} = \sum_{o=1,o\in T_m}^{M} \sum_{\substack{d=1,\ a_{q,r}^{(o,d)}=1\\ q\in[1,2,\cdots,\bar{K}_{(o,d)}]}}^{C} |\mathbf{u}_{k,r}^{(m,c)H}\bar{\mathbf{H}}_{k,r}^{(m,c,o)}\bar{\mathbf{v}}_{q,r}^{(o,d)}|^2\bar{\rho}_{q,r}^{(o,d)}, \tag{6.5.15d}$$

$$\mu_{k,r}^{(m,c)} = \begin{cases} \sum\limits_{\substack{d=2,d\neq c\\ j\in[1,2,\cdots,\bar{K}_{(m,d)}]\\ a_{j,r}^{(m,d)}=1}}^{C} |\mathbf{u}_{k,r}^{(m,c)H}\mathbf{H}_{k,r}^{(m,d)}\mathbf{v}_{j,r}^{(m,d)}|^2\rho_{j,r}^{(m,d)}, & \text{if } c=1 \text{ and } a_{k,r}^{(m,c)}=1 \\ 0, & \text{if } c\neq 1 \end{cases}. \tag{6.5.15e}$$

6.5.3 Beamforming Design

The receive beam-former is designed to minimise the inter-cell interference from neighbouring macro cell sectors on each RB r (see (6.4.9)).

Precoder Design based on max-SLNR

The transmit precoders for each user's data are designed to maximise the SLNR. For the r-th RB ($r \in [1,2,\cdots,N_{RB}]$), the transmit precoders for the pico cell users are designed to minimise the leakage to the macro cell user in the same macro cell sector, while maximising the desired signal to the pico cell user, $\mathbf{v}_{k,r}^{(m,c)}$ is chosen as the eigenvector

corresponding to the maximum eigenvalue of (6.5.16a):

$$(\vartheta_{k,r}^{(m,c)}\mathbf{I}_{M_t} + (\mathbf{H}_{k,r}^{(m,1)H}\mathbf{u}_{j,r}^{(m,1)}\mathbf{u}_{j,r}^{(m,1)H}\mathbf{H}_{k,r}^{(m,1)}))^{-1}(\mathbf{H}_{k,r}^{(m,c)H}\mathbf{u}_{k,r}^{(m,c)}\mathbf{u}_{k,r}^{(m,c)H}\mathbf{H}_{k,r}^{(m,c)}), \quad (6.5.16a)$$

$$\text{if } a_{k,r}^{(m,c)} = 1, k = [1, 2, \cdots, \bar{K}_{(m,c)}],\ m = [1, 2, \cdots, M], c = [2, \cdots, C], \quad (6.5.16b)$$

$$,\ r = [1, 2, \cdots, N_{RB}], \vartheta_{k,r}^{(m,c)} = ((\sigma_{k,r}^{(m,c)})^2/\rho_{k,r}^{(m,c)}). \quad (6.5.16c)$$

The transmit pre-coder needed for CoMP transmission to the macro cell sector user and other pico cell users on each RB ($r = [1, 2, \cdots, N_{RB}]$), is designed to minimise the leakage to (i.) the macro cell users in the neighbouring macro cell sectors in T_m, (see (6.5.17c)) (ii.) the pico cell served by the LSMCS and the other pico cell served by the RSMCS (see (6.5.17d)) (iii.) the undesired pico cell and macro cell users in the same macro cell sector (i.e. the IUI, see (6.5.17e)). The leakage in (ii.) and (iii.) are shown in Fig. 6.2 and $\bar{\mathbf{v}}_{k,r}^{(m,c)}$ is chosen as the eigenvector corresponding to the maximum eigenvalue of (6.5.17a):

$$(\vartheta_{k,r}^{(m,c)}\mathbf{I}_{M_t} + (\mathbf{Z}_{k,r}^{(m,c)H}\mathbf{Z}_{k,r}^{(m,c)})^{-1}(\mathbf{H}_{k,r}^{(m,1)H}\mathbf{u}_{k,r}^{(m,c)}\mathbf{u}_{k,r}^{(m,c)H}\mathbf{H}_{k,r}^{(m,1)}),\ \text{if } a_{k,r}^{(m,1)} = 1,$$
$$c = [1, 2, \cdots, C], k = [1, 2, \cdots, \bar{K}_{(m,c)}],\ m = [1, 2, \cdots, M],\ r = [1, 2, \cdots, N_{RB}],$$
$$\vartheta_{k,r}^{(m,c)} = ((\sigma_{k,r}^{(m,c)})^2/\bar{\rho}_{k,r}^{(m,c)}). \quad (6.5.17a)$$

$$\mathbf{Z}_{k,r}^{(m,c)} = \begin{bmatrix} \bar{\mathbf{Z}}_{k,r}^{(m,c)} \\ \hat{\mathbf{Z}}_{k,r}^{(m,c)} \\ \tilde{\mathbf{Z}}_{k,r}^{(m,c)} \end{bmatrix},\ \text{if } a_{k,r}^{(m,1)} = 1, \quad (6.5.17b)$$

$$\bar{\mathbf{Z}}_{k,r}^{(m,c)} = [[\mathbf{u}_{q,r}^{(o,1)H}\bar{\mathbf{H}}_{q,r}^{(o,1,m)}]^T, a_{q,r}^{(o,1)} = 1, o = [1, 2, \cdots, M]]^T,$$
$$q \in [1, 2, \cdots, \bar{K}_{(o,1)}],\ o \in T_m, \quad (6.5.17c)$$

$$\hat{\mathbf{Z}}_{k,r}^{(m,c)} = \begin{bmatrix} \mathbf{u}_{q,r}^{(T_m(1),2)H}\bar{\mathbf{H}}_{q,r}^{(T_m(1),2,m)}, a_{q,r}^{(T_m(1),2)} = 1,\ q \in [1, 2, \cdots, \bar{K}_{(T_m(1),2)}] \\ \mathbf{u}_{q,r}^{(T_m(4),3)H}\bar{\mathbf{H}}_{q,r}^{(T_m(4),3,m)}, a_{q,r}^{(T_m(4),3)} = 1,\ q \in [1, 2, \cdots, \bar{K}_{(T_m(4),3)}] \end{bmatrix}, \quad (6.5.17d)$$

$$\tilde{\mathbf{Z}}_{k,r}^{(m,c)} = [[\mathbf{u}_{j,r}^{(m,d)H}\mathbf{H}_{j,r}^{(m,1)}]^T,\ a_{j,r}^{(m,d)} = 1,\ d = [1, 2, \cdots, C]]^T,$$
$$j \in [1, 2, \cdots, \bar{K}_{(m,d)}], d \neq c, \quad (6.5.17e)$$

$\mathbf{Z}_{k,r}^{(m,c)}, \bar{\mathbf{Z}}_{k,r}^{(m,c)}, \hat{\mathbf{Z}}_{k,r}^{(m,c)}$ and $\tilde{\mathbf{Z}}_{k,r}^{(m,c)}$ all have M_t columns.

6.5.4 Power Allocation

The HetNet system model considered is Fig. 5.15 in Chapter 5 which has a multi-layer of the pico cells and macro cells and different transmit power for each cell type. For the purpose of this study, the per base station power constraint is considered for the power optimisation problem. The PBPC power constraint is given below in (6.5.18):

$$\begin{cases} \sum\limits_{\substack{d=1, a_{j,r}^{(m,d)}=1 \\ j\in[1,2,\cdots,\bar{K}_{(m,d)}]}}^{C} \|\bar{\mathbf{v}}_{j,r}^{(m,d)}\|^2 \bar{\rho}_{j,r}^{(m,d)} = p_{macro}^{PBPC}, & \text{if } a_{k,r}^{(m,c)} = 1, c = 1 \\ \|\mathbf{v}_{k,r}^{(m,c)}\|^2 \rho_{k,r}^{(m,c)} = p_{pico}^{PBPC}, & \text{if } a_{k,r}^{(m,c)} = 1, c = [2,3,\cdots,C\} \end{cases},$$

$$k = [1,2,\cdots,\bar{K}_{(m,c)}],\ m = [1,2,\cdots,M],\ r = [1,2,\cdots,N_{RB}]. \quad (6.5.18)$$

This section considers CoMP transmission for only the macro cell BS to pico cell users. Assuming the full power transmission for all BSs types, then the pico cell BS transmit power is given in (6.4.13) such that the pico cell power constraint in (6.5.18) is met. Now for the macro cell BS, power allocation for each data transmission is required since the BS transmits data to multiple users, however the macro cell power constraint in (6.5.18) needs to be satisfied. Given a QoS constraint, in this case a target user rate for both pico and macro cell user in the macro cell sector as $\phi_{k,r}^{(m,c)}, \forall\, k, m, c, r$. The optimisation problem considered aims to achieve the target rate while ensuring the macro cell PBPC is met.

Next generation systems (i.e, HetNets) need to have the capabilities of a SON and the latency time before data transmission needs to be limited as much as possible. Hence for this reason, the macro cell sector obtains the power allocation while considering only the macro cell and pico cell users within the macro cell sector. The power optimisation

problem can be expressed as:

$$\frac{|\varpi_{k,r}^{(m,c)}|^2 + g_{c,c}\bar{\rho}_{k,r}^{(m,c)}}{\sum\limits_{\substack{d=1,\, d\neq c \\ a_{k,r}^{(m,d)}=1}}^{K} g_{c,d}\bar{\rho}_{k,r}^{(m,d)} + 1} \geq \bar{\gamma}_{k,r}^{(m,c)}, \quad g_{c,d} = |\mathbf{u}_{k,r}^{(m,c)H}\mathbf{H}_{k,r}^{(m,1)}\bar{\mathbf{v}}_{k,r}^{(m,d)}|^2, \tag{6.5.19a}$$

$$\text{s.t.} \sum_{\substack{d=1,\, a_{j,r}^{(m,d)}=1 \\ j\in[1,2,\cdots,K_{(m,d)}]}}^{C} \|\bar{\mathbf{v}}_{j,r}^{(m,d)}\|^2 \bar{\rho}_{j,r}^{(m,d)} = p_{macro}^{PBPC},\ \bar{\rho}_{j,r}^{(m,d)} \geq 0, \tag{6.5.19b}$$

$$\text{if } a_{k,r}^{(m,1)} = 1,\ \forall k = [1,2,\cdots,\bar{K}_{(m,c)}],\ m = [1,2,\cdots,M],\ c = [1,2,\cdots,C,$$
$$r = [1,2,\cdots,N_{RB}] \text{ and } \bar{\gamma}_{k,r}^{(m,c)} = 2^{\phi_{k,r}^{(m,c)}} - 1, \tag{6.5.19c}$$

where $\bar{\gamma}_{k,r}^{(m,c)}$ is the SINR constraint for the k user's data on the r-th RB in (m,c). The problem in (6.5.19) can easily be solved as a constrained linear least square optimisation problem.

6.6 Performance Evaluation

In this section, the performance obtained using a joint interference avoidance and mitigation technique is evaluated using Fig. 6.4 and Fig. 6.5. The proposed distributed RBA strategy based on maximising the sum-SLINR of the users within a cell is jointly used with two separate interference mitigation techniques: beamforming and CoMP transmission. The simulation considers the cell set-up in Fig. 5.15 with W = 7 macro cell sites and δ = 3 cell sectors per cell site giving a total of M = 21 macro cell sectors and the simulation parameters given in Table 6.2. Each macro cell sector has two CEPC and two HSPC at the cell center and 40 MCU are considered in each macro cell sector.

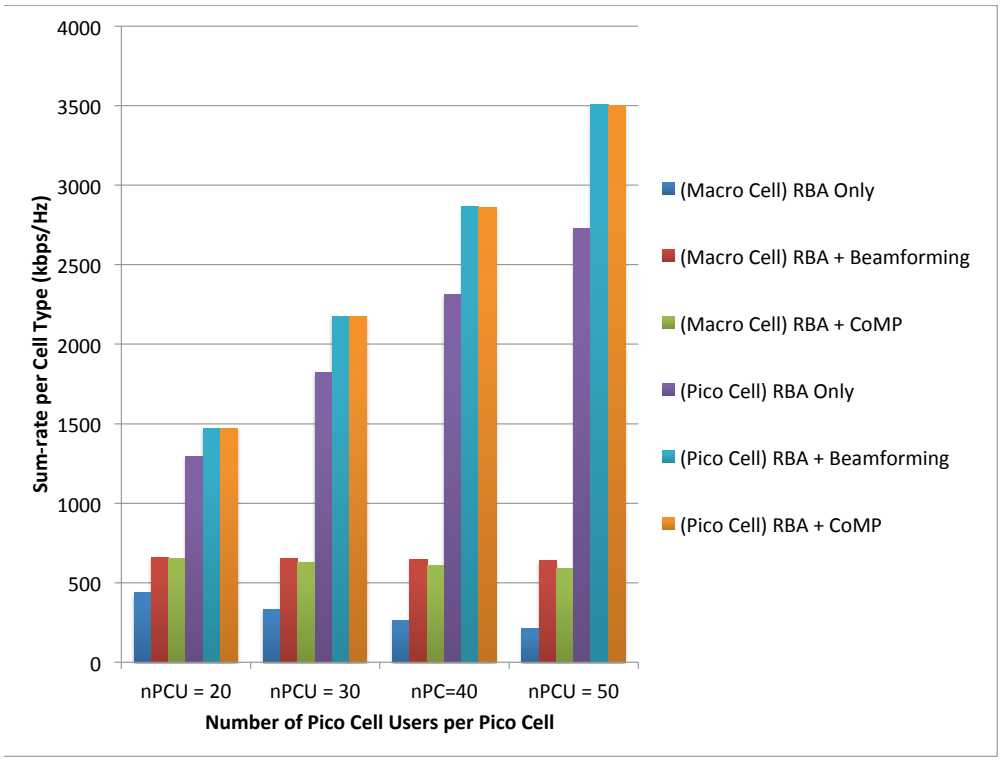

Figure 6.4: The sum-rate performance using the proposed joint interference management scheme, nMCU = 40.

The sum-rate for the pico and macro cells can be observed in Fig. 6.4 when nMCU = 40. As nPCU increases the obtained sum-rate for the macro cell is seen to decrease as expected when using only the proposed distributed RBA solution. But when used in conjunction with beamforming and CoMP transmission, the system performance is seen to improve significantly. For instance using only the RBA when nPCU = 20, 30 and 40 respectively, the sum-rate per macro cell sector is 435 kbps/Hz, 334 kbps/Hz and 262 kbps/Hz. But when using the RBA with beamforming, the sum-rate increases to 658 kbps/Hz, 653 kbps/Hz and 647 kbps/Hz. Also for RBA with CoMP transmission the sum-rate performance increases to 649 kbps/Hz, 628 kbps/Hz and 605 kbps/Hz. The reduced sum-rate performance for the macro cell using CoMP transmission as opposed to beamforming is a result of the reduced power allocation to the macro cell user's data transmission during CoMP transmission. The sum-rate of the pico cells when nPCU =

Table 6.2: Network set-up and simulation parameters

Parameters	**Value**
Cell layout	HetNet
Number of macro cell sites	7
Number of sectors per macro cell site	3
Number of pico cells per macro cell sector	4
Channel frequency	2.0 GHz
Carrier bandwidth	10 MHz
Number of RBs	50
Bandwidth of RB	180 kHz
Sub-carrier spacing	15kHz
Bandwidth per RB	180kHz
Shadowing standard deviation, σ_s	8dB
Pathloss coefficient, α	2
Macro cell BS power	43 dBm
Pico cell BS power	30dBm
[Inter site distance (ISD), D_o]	[750m, 100m]
Macro cell radius	250m
CEPC, HSPC radius	[70m, 50m]
Pico cell antenna type	omnidirectional
Macro cell antenna type	directional antennas
Number of transmit and receive antennas (M_t, N_r)	(8, 4)
Target rate for pico cell and macro cell users respectively	(16 kps/Hz, 20 kbps/Hz)

20, 30 and 40 respectively using only the RBA solution are 1291 kbps/Hz, 1824 kbps/Hz and 2311 kbps/Hz respectively while the proposed joint solution using both the RBA and beamforming achieves a greater performance of 1471 kbps/Hz, 2173 kbps/Hz and 2863 kbps/Hz respectively and 1471 kbps/Hz, 2171 kbps/Hz and 2859 kbps/Hz respectively when using the proposed joint RBA and CoMP transmission technique. The proposed solutions clearly obtain a significant improved performance to both the pico cell users and macro cell users even with high density of users in the HetNet.

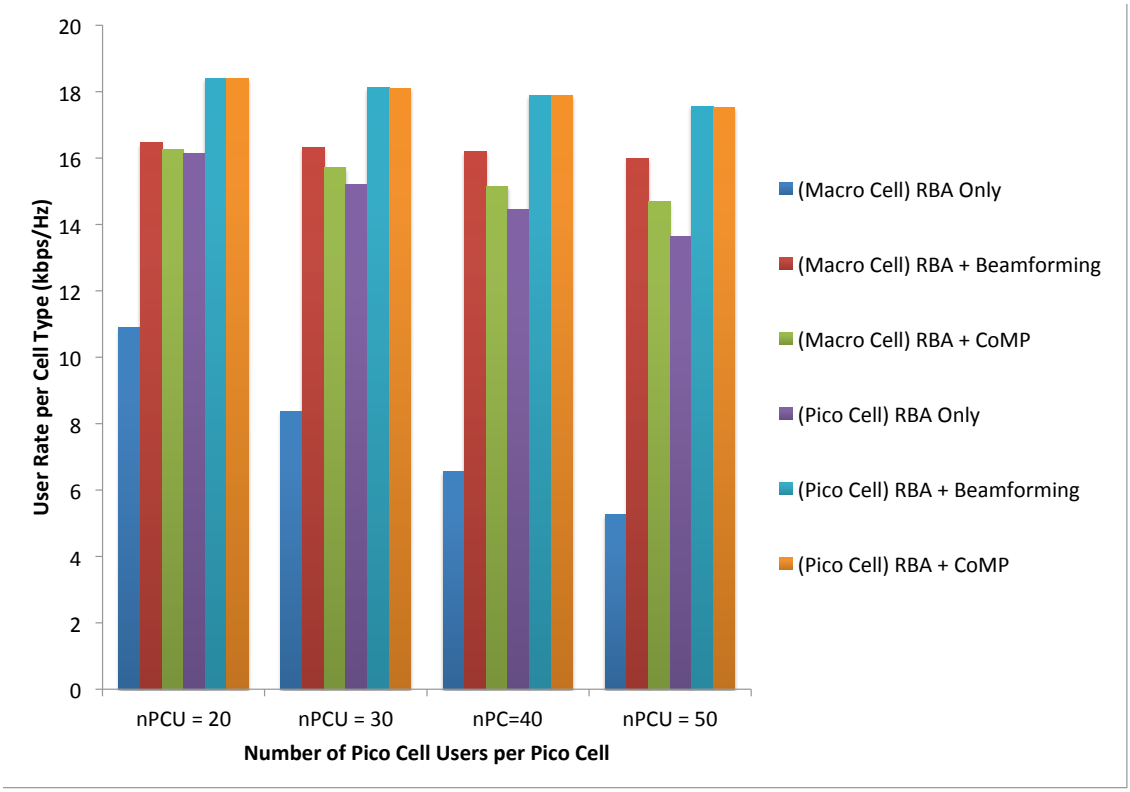

Figure 6.5: The CoMP model under a given macro cell sector showing CoMP transmission from the MC BS to PC user.

The user-rate for the pico and macro cells can also be observed in Fig. 6.5 when nMCU = 40. The target user rate considered for the simulation is 16 kbps/Hz and 20 kbps/Hz

respectively for the pico cell and macro cell user. It can be clearly seen that as nPCU increases, the obtained user-rate for the macro cell and pico cell users decreases. This is expected as the RBs available for the user's data transmission become prone to high interference. When nMCU = 40 and nPCU = 40, the user rate for the pico cell and macro cell respectively is 6.55 kbps/Hz and 14.44 kbps/Hz using only the proposed RBA solution. However using a joint solution with beamforming the user rate increases to 16.2 kbps/Hz and 17.8 kbps/Hz and with CoMP transmission the achieved user rate is 15.1 kbps/Hz and 17.8 kbps/Hz. The target rate for the pico cell users was achieved using both joint solutions but the target rate for the macro cell users was not achieved. This is as a result of the power constraint of the BS and also a high QoS constraint. However, the performance achieved was significantly improved compared to the performance using only the RBA. Again the performance obtained by the macro cell users using RBA and CoMP transmission is slightly lower when compared to the performance obtained using RBA and beamforming. This is due to the decrease in the transmit power used for the macro cell user's data transmission under the given PBPC. The results in Figs. 6.4 and 6.5 evidently show that a significant improvement in performance can be obtained for highly dense networks with high interference using the proposed joint solution of interference avoidance and cancellation.

6.7 Summary

This chapter has considered the high interference expected in HetNets which have multiple layers of different cell types and capabilities, but having access to the same frequency channels, thereby increasing the interference within the system as opposed to a homogeneous network. A joint interference management solution was proposed using the proposed distributed RBA strategy with a round-robin sector-by-sector approach based on maximising the sum-SLINR within each macro cell and pico cell in the HetNet downlink cellular OFDMA systems, as a tool for interference avoidance. The proposed RBA strategy was successively followed by an interference mitigation technique: beamforming

or CoMP transmission. From Chapter 5, the proposed distributed RBA was seen to offer the best performance compared to other interference avoidance strategy for HetNets. However this chapter investigated and analysed the effect of coupling the RBA with an interference mitigation technique. In this way the interference within the network can be avoided and unavoidable interference can be further mitigated using beamforming or CoMP transmission.

The proposed joint solution was compared with the interference avoidance using the proposed RBA strategy. The results showed a significant improvement when using a joint interference avoidance and mitigation technique. The RBA plus beamforming and RBA plus CoMP transmission techniques showed that greater throughput can be achieved especially in a high-density network where resources are in high demand especially during peak times. This result is of great importance as it allows both small and macro cells to have access to the full channel spectrum, thereby improving the frequency utilisation efficiency as opposed to other solutions like almost blank subframe, carrier aggregation, and other forms of resource partitioning that limits the available resources to each cell type.

Chapter 7

Conclusion and Future Work

7.1 Conclusion

In this thesis, the CoMP transmission technique has been investigated as an interference management system in multi-cell multi-user MIMO systems. The setbacks associated with this technique are the high data overhead demand on the backhaul network architecture which results in huge costs to the network provider. In Section 2.3 and 2.4, the network centric and user centric approach to CoMP transmission was presented and investigations which would reduce the data overhead for a trade-off in system performance were carried out.

The network centric clustering approach was investigated to analyse the system performance of the cell-edge users under CoMP transmission. The standard proposed method required the network to form clusters of BSs and then allow multiple transmission the BSs within each cluster to improve the overall system performance. The results obtained showed that the linear increase in transmit BSs per user resulted in a linear increase in the data overhead but the obtained increase in performance was not linear. It was shown that reducing the data overhead significantly only resulted in very slight loss in system performance under certain system conditions.

The user centric approach was investigated as well and was shown to attain a better performance when compared to the network centric clusterisation method. This is because under the network centric approach the clusters are selected based on the quality of the sum-interference channels to each user. Since this solution is not based on the individual requirements of the users, this means that the users may be assigned very poor channels for CoMP transmission which would not provide any significant improvement to the cell-edge user's performance. The user centric approach was studied in Section 2.4 and the obtained performance was shown to outperform the network centric performance. The chapter proposed a direct reduction of the data overhead by using a lesser number of transmit BSs per user but allowing the transmit BSs to be chosen in such a way to maximise the gain achieved by the user. The simulation results in Figs. 2.12 - 2.15 showed that a significant reduction in the data overhead was attainable without sacrificing the BER and sum-rate performance. Also in some scenario where complete interference cancellation was unobtainable, CoMP transmission with a reduced number of BSs outperformed CoMP transmission with a larger number of transmit BSs. This is the result of choosing the best channels for CoMP transmission and assigning the maximum allowed transmit powers to these channels.

In Chapter 3, a proposed joint and adaptive selection of the BSs for each user's data transmission based on the user centric approach was investigated. The selected BSs for each user's data transmission form a CS. Since the QoS constraints, channel condition, number of antennas, interference, amongst other factors affect the performance of the user, it is important to avoid a network pre-set size of CSs for the users. Also some users may achieve the QoS constraints using only a single BS, so it is important to avoid increasing the ICI or IUI within the system by using CoMP transmission from multiple BSs. To further improve the overall system performance with reduced data overhead, a heuristic approach to obtaining the CS size and given BSs for each user's CS was proposed. The proposed joint and adaptive CS selection was shown to attain a further reduction in the data overhead and energy consumption of the system with a slight increase in the sum-rate.

Chapter 4 proposed an improved joint and adaptive CS selection under the max-min SINR optimisation problem and the total power minimisation problem using three different power constraint types. Also in Chapter 4, the "optimum CS selection" based on a hard search is shown using a limited number of cells. This was necessary in order to evaluate and compare the obtained performance using the proposed joint CS selection algorithm against both the "optimum CS selection" and the traditional pre-set number of BSs per user (standard solution). The optimum performance is known to be NP-hard and unachievable for a relatively small number of cells due to the very high computational complexity involved but this can be achieved and shown with a very small number of BS-user pairs. The advantages of the proposed method includes achieving a joint selection of all CSs, a reduction in complexity and time as opposed to the "optimum solution" and better overall system performance (i.e., data overhead, energy, OCR) when compared to the conventional method.

The RBA techniques used for radio resource management have been investigated in Chapter 5. Two distributed RBA techniques were proposed to manage the interference in the HomoNet and HetNet. Studies showed that the RBA metric used in the past avoided the direct estimation of interference in the network. Other techniques were proposed to associate RBs to the users to maximise the sum-rate performance of the system. The interference on each RB for the users cannot be obtained without pre-knowledge of RB utilisation by the neighbouring BSs. Another important factor in RBA is the mode of allocation. Several strategies have been proposed under static and dynamic ICIC for RRM. The centralised or semi-centralised mode of RBA under the dynamic ICIC is not scalable with the standards for LTE-A in 4G networks and static ICIC is set back by poor frequency utilisation. However in Chapter 5, the RBA problem was solved in two dimensions. Firstly, the proposed RBA mode is distributed and allows each cell to allocate RBs to the users in a round-robin approach thereby making the proposed RBA metrics based on interference estimation (i.e. the SINR and the SLINR) possible to obtain. Secondly, based on the proposed RBA metric, an appropriate qualification matrix is obtained for RB allocation to each user. The simulation result show the significant

advantage compared to other modes of RBA and RBA metrics proposed in the past.

Finally in Chapter 6, a joint interference management strategy was proposed to further improve the system performance of the HetNets. Using interference avoidance and interference cancellation techniques, an additional gain was shown to be achievable especially with a high density of users in each cell (during peak times). The interference avoidance technique was based on the proposed distributed strategy based on maximising the sum-SLINR shown in Chapter 5, Section 5.5.2 for the HetNet. This was coupled separately with two interference mitigation techniques: Beamforming and CoMP transmission. The simulation results showed that a joint interference management scheme using an effective RBA technique coupled with beamforming or CoMP transmission is capable of achieving an increased gain in the system performance, especially for very high interference limited systems such as the HetNet with a frequency reuse factor of 1.

7.2 Future Work

Interference management techniques are very important features for current and future wireless network technologies in order to attain the maximum possible performance and meet the high demand of the users. Due to the continuous and exponential demand in faster data rate and increased capacity, today's techniques would need to be further improved to meet the demands of tomorrow.

The following suggestions and investigations are proposed for future work, that could lead to an improvement in the management of interference for both homogeneous and heterogeneous networks.

1. A joint CS selection for CoMP transmission was proposed in Chapter 3 and improved in Chapter 4. The heuristic solution was shown to achieve about 90% of the performance using the "optimal CS selection", while reducing the complexity and computation time by over 98%. A less complex, joint and adaptive

solution capable of achieving a much closer performance to that obtained under the "optimum CS selection" could be investigated. This would boost the possible gains achieved with CoMP transmission without the setbacks of high data overhead and energy consumption.

2. In Chapter 5 the RBA technique was considered for both HomoNets and HetNets. The distributed RBA strategy and the proposed metric based on the sum-SINR and sum-SLINR was considered with certain assumptions. Pico cell to pico cell interference (under HetNets) can be considered and inter macro cell sector interference within the same macro cell site can also be considered for future study. The distributed RBA strategy can be improved to reduce the RBA time, overhead and also satisfy additional criteria of the SON.

3. In Chapter 6, the joint interference avoidance and cancellation technique was proposed to further reduce the effect of interference in the HetNet. The work in Chapter 6 only considered a given portion of the interference model. Interference avoidance using the proposed distributed RBA strategy was jointly used with beamforming and CoMP transmission. CoMP transmission was considered only for the macro cell to pico cell users in each macro cell sector. Future works should consider CoMP transmission from the pico cell to the macro cell user. The HetNet, especially high-density HetNet, is a more complex network and research is still limited in this area. Investigations should be carried out to analyse the effect of co-tier CoMP transmission, i.e. using neighbouring macro cells to support the macro cell users, while comparing this to cross-tier CoMP transmission using pico cells to support macro cells users in HetNets.

Appendices

A Proof of Lemma 1 & 2

The linear least mean-square error (LLMSE) estimation is used to determine the solutions obtained in (4.6.26) and (4.6.27) as shown below [50]:

Consider the received signal obtained in the downlink channel as shown in (4.4.7), which can be written as:

$$\hat{s}_k = \mathbf{u}_k^H \mathbf{H}_k^{(k)} \bar{\mathbf{v}}_k \sqrt{\rho_k} s_k + \mathbf{u}_k^H \sum_{\substack{p=1 \\ p \neq k}}^{K} \mathbf{H}_k^{(p)} \bar{\mathbf{v}}_p \sqrt{\rho_p} s_p + \mathbf{u}_k^H \mathbf{n}_k, \forall\, k \in [1, 2, \cdots, K], \tag{A.1}$$

The MSE is given by:

$$\begin{aligned} \mathbf{J} &\triangleq \mathbb{E}[|s_k - \hat{s}_k|^2] \triangleq \mathbb{E}\{(s_k - \hat{s}_k)(s_k - \hat{s}_k)^H\} \\ &\triangleq \mathbb{E}[|s_k - \mathbf{u}_k^H \sum_{p=1}^{K} \mathbf{H}_k^{(p)} \bar{\mathbf{v}}_p \sqrt{\rho_p} s_p - \mathbf{u}_k^H \mathbf{n}_k|^2] \\ &\triangleq \mathbb{E}\{(s_k - \mathbf{u}_k^H \sum_{p=1}^{K} \mathbf{H}_k^{(p)} \bar{\mathbf{v}}_p \sqrt{\rho_p} s_p - \mathbf{u}_k^H \mathbf{n}_k)(s_k^H - \sum_{p=1}^{K} s_p^H \sqrt{\rho_p} \bar{\mathbf{v}}_p^H \mathbf{H}_k^{(p)H} \mathbf{u}_k - \mathbf{n}_k^H \mathbf{u}_k)\} \end{aligned} \tag{A.2}$$

Note that $\mathbb{E}[s_k s_k^H] = 1$, $\mathbb{E}[s_k s_p^H] = 0$, $p \neq k$, $\mathbb{E}[s_p] = 0$, $\mathbb{E}[\mathbf{n}_k \mathbf{n}_k^H] = \sigma_k^2 \mathbf{I}$. So from (A.2), J is obtained as:

$$\mathrm{J} \triangleq 1 - \sqrt{\rho_k}\bar{\mathbf{v}}_k\mathbf{H}_k^{(k)H}\mathbf{u}_k - \mathbf{u}_k^H\mathbf{H}_k^{(k)}\bar{\mathbf{v}}_k\sqrt{\rho_k} + \mathbf{u}_k^H(\sum_{p=1}^{K}\mathbf{H}_k^{(p)}\bar{\mathbf{v}}_p\rho_p\bar{\mathbf{v}}_p^H\mathbf{H}_k^{(p)H})\mathbf{u}_k + \sigma_k^2\mathbf{I} \quad \text{(A.3)}$$

Given $\mathbf{V}$, the receive beam-former $\mathbf{U}$ is found by obtaining the gradient of the MSE w.r.t $\mathbf{u}_k$ and setting it to zero. The normalised linear beam-former is obtained by normalising the resulting solution as shown below:

$$\begin{aligned}
&\mathbf{u}_k = \hat{\mathbf{u}}_k / \left\|\hat{\mathbf{u}}_k\right\|_2, \quad \text{where} \\
&\hat{\mathbf{u}}_k^H = (\sum_{\substack{p=1 \\ p\neq k}}^{K}\mathbf{H}_k^{(p)}\bar{\mathbf{v}}_p\bar{\mathbf{v}}_p^H\mathbf{H}_k^{(p)H}\rho_p + \mathbf{I}\sigma_k^2)^{-1}\sqrt{\rho_k}\mathbf{v}_k^H\bar{\mathbf{H}}_k^{(k)H}, \forall\ k \in [1, 2, \cdots, K]. \qquad \text{(A.4)}
\end{aligned}$$

To obtain the beamforming vector ($\mathbf{V}$) at the transmitter, the virtual reciprocal (uplink) channel as shown in (4.5.12) is considered. This can be written as

$$\hat{s}_k = \bar{\mathbf{v}}_k^H\mathbf{H}_k^{(k)H}\mathbf{u}_k\sqrt{q_k}s_k + \sum_{\substack{p=1 \\ p\neq k}}^{K}\bar{\mathbf{v}}_k^H\mathbf{H}_p^{(k)H}\mathbf{u}_p\sqrt{q_p}s_p + \bar{\mathbf{v}}_k^H\mathbf{n}_k,\ \forall\ k \in [1, 2, \cdots, K], \quad \text{(A.5)}$$

The MSE is given by:

$$\begin{aligned}
\mathrm{J} &\triangleq \mathbb{E}[|s_k - \hat{s}_k|^2] \triangleq \mathrm{E}\{(s_k - \hat{s}_k)(s_k - \hat{s}_k)^H\} \qquad \text{(A.6)} \\
&\triangleq \mathbb{E}[|s_k - \bar{\mathbf{v}}_k^H\sum_{p=1}^{K}\mathbf{H}_p^{(k)H}\mathbf{u}_p\sqrt{q_p}s_p - \bar{\mathbf{v}}_k^H\mathbf{n}_k|^2] \\
&\triangleq \mathbb{E}\{(s_k - \bar{\mathbf{v}}_k^H\sum_{p=1}^{K}\mathbf{H}_p^{(k)H}\mathbf{u}_p\sqrt{q_p}s_p - \bar{\mathbf{v}}_k^H\mathbf{n}_k)(s_k^H - \sum_{p=1}^{K}s_p^H\sqrt{q_p}\mathbf{u}_p^H\mathbf{H}_k^{(p)}\bar{\mathbf{v}}_k - \mathbf{n}_k^H\bar{\mathbf{v}}_k)\}
\end{aligned}$$

Note that $\mathbb{E}[s_k s_k^H] = 1$, $\mathbb{E}[s_k s_p^H] = 0$, $p \neq k$, $\mathbb{E}[s_p] = 0$, $\mathbb{E}[\mathbf{n}_k\mathbf{n}_k^H] = \sigma_k^2\mathrm{I}$. So from (A.6), we obtain

$$\mathrm{J} \triangleq 1 - \sqrt{q_k}\mathbf{u}_k\mathbf{H}_k^{(k)}\bar{\mathbf{v}}_k - \mathbf{v}_k^H\mathbf{H}_k^{(k)H}\mathbf{u}_k\sqrt{q_k} + \bar{\mathbf{v}}_k^H(\sum_{p=1}^{K}\mathbf{H}_k^{(p)H}\mathbf{u}_p q_p\mathbf{u}_p^H\mathbf{H}_k^{(p)})\bar{\mathbf{v}}_k + \sigma^2\mathbf{I} \quad \text{(A.7)}$$

Given $\mathbf{U}$, the receive beam-former $\mathbf{V}$ is found by obtaining the gradient of the MSE w.r.t $\bar{\mathbf{v}}_k$ and setting it to zero. The normalised linear beam-former is obtained by normalising the resulting solution as shown below:

$$\begin{aligned}
&\bar{\mathbf{v}}_k = \hat{\mathbf{v}}_k / \left\|\hat{\mathbf{v}}_k\right\|_2, \quad \text{where} \\
&\hat{\mathbf{v}}_k^H = (\sum_{\substack{p=1 \\ p\neq k}}^{K} \mathbf{H}_p^{(k)H} \mathbf{u}_p \mathbf{u}_p^H \mathbf{H}_p^{(k)} q_p + \mathbf{I}\sigma^2)^{-1} \sqrt{q_k} \mathbf{u}_k^H \mathbf{H}_k^{(k)}.
\end{aligned} \tag{A.8}$$

Bibliography

[1] X. Zhang and X. Zhou, "LTE-Advanced air interface technology." CRC Press, 2012.

[2] K. Du and M. N. S. Swamy, "Wireless Communication Systems - From RF Subsystems to 4G Enabling Technologies." Cambridge University Press, 2010.

[3] "Radio Planning Capacity, RA41207EN20GLA0," in *Nokia Siemens Networks*.

[4] K. Herring, J. Holloway, D. Staelin, and D. Bliss, "Path-Loss Characteristics of Urban Wireless Channels ," *IEEE Transactions on Information Theory*, vol. 58, no. 1, pp. 171 – 177, Jan. 2010.

[5] A. Kumar, D. Manjunath, and J. Kuri, *Wireless Networking*. Morgan Kaufmann, 2008.

[6] "Technical Specifications and Technical Reports for a UTRAN-based 3GPP system," in *3GPP, TS 21.101*.

[7] I. Cavdar, G. Dinc, and K. Erdogdu, "Propagation modelling of cellular mobile communication on non-Rayleigh and non-Rician fading channels," in *Proceedings of 1997 International Conference on Information, Communications and Signal Processing (ICICS)*, vol. 3, Sep. 1997, pp. 1705 – 1708.

[8] A. Paulraj, R. Nabar, and D. Gore, "Introduction to space-time wireless communications." Cambridge University Press, 2008, pp. 86–92.

[9] "Overhead reduction of best-M based CQI reporting," in *3GPP, R1-063086*.

[10] "Physical layer aspects for evolved UTRA," in *3GPP TR 25.814*.

[11] R. Irmer, H. Droste, P. Marsch, M. Grieger, G. Fettweis, S. Brueck, H. Mayer, L. Thiele, and V. Jungnickel, "Coordinated multipoint: concepts, performance, and field trial results," *IEEE Communication Magazine*, vol. 49, pp. 102 – 111, Feb. 2011.

[12] K. Son, H. Kim, Y. Yi, and B. Krishnamachari, "Base station operation and user association mechanisms for energy-delay tradeoffs in green cellular networks," *IEEE Journal on Selected Areas in Communications*, vol. 29, no. 8, pp. 1525 – 1536, Sept. 2011.

[13] E. Pateromichelakis, M. Shariat, A. ul Quddus, and R. Tafazolli, "On the evolution of multi-cell scheduling in 3GPP LTE/LTE-A," *IEEE Communications Surveys and Tutorials*, vol. 15, no. 2, pp. 701 – 717, May 2013.

[14] "Mobile broadband innovation path to 4G: release 9,10 and beyond," in *3GPP TR*, Feb. 2010.

[15] E. Pateromichelakis, M. Shariat, A. ul Quddus, and R. Tafazolli, "On the evolution of multi-cell scheduling in 3GPP LTE/LTE-A," *IEEE Int'l Symposium on Personal Indoor and Mobile Radio Communications (PIMRC)*, Sept. 2011.

[16] "3rd Generation Partnership Project; Technical Specification Group Radio Access Network; Evolved Universal Terrestrial Radio Access Network (E-UTRAN); X2 general aspecs and principles (Release 11)," in *3GPP, TS 36.420 V11.0.0 (2012-09)*.

[17] "Backhauling X2," in *Cambridge Broadband Networks*.

[18] A. Papadogiannis, D. Gesbert, and E. Hardouin, "A dynamic clustering approach in wireless networks with multi-cell cooperative processing," in *IEEE International Conference on Communications*, May 2008.

[19] J. Zhang, R. Chen, J. Andrews, A. Ghosh, and R. Heath, "Networked MIMO with clustered linear precoding," *IEEE Transactions on Communications*, vol. 8, no. 4, pp. 1910–1921, Apr 2009.

[20] M. Amin, M. Nafie, M. Fikri, and M. Abdallah, "An interference mitigation scheme for multi-user multi-cell MIMO systems," in *IEEE International Conference on Computer Engineering Conference*, Dec. 2010, pp. 40 – 43.

[21] J. Lee, S. Kim, S. Jin, and D. Park, "A multi-user beamforming scheme in MIMO downlink channels for multi-cell networks," in *IEEE International Conference on Consumer Electronics*, Jan. 2011, pp. 587 – 588.

[22] M. Ku and D. Kim, "Tx-Rx beamforming with multiuser MIMO channels in multi-cell systems," in *Proc. Int'l Conf. on Advanced Communication Technology, 2008*, 2008.

[23] M. Sadek, A. Tarighat, and A. Sayed, "A leakage-based precoding scheme for downlink multi-user MIMO channels," *IEEE Transactions on Wireless Communications*, vol. 6, no. 5, pp. 1711 – 1714, May 2007.

[24] D. Wei, L. Youjian, B. Rider, and V. Lau, "On the Information Rate of MIMO Systems With Finite Rate Channel State Feedback Using Beamforming and Power On/Off Strategy," *IEEE Transactions on Information Theory*, vol. 55, no. 11, pp. 5032 – 5047, Nov. 2009.

[25] A. Goldsmith, S. Jafar, N. Jindal, and S. Vishwanath, "Capacity limits of MIMO channels," *IEEE Journal on Selected Areas in Communications*, vol. 21, no. 5, pp. 684 – 702, Nov. 2003.

[26] R. Weber, A. Garavaglia, M. Schulist, S. Brueck, and A. Dekorsy, "Self-organizing adaptive clustering for cooperative multipoint transmission," May 2011.

[27] V. Cadambe and S. Jafar, "Degrees of Freedom of Wireless Networks - What a Difference Delay Makes," in *Conference Record of the Forty-First Asilomar*

Conference on Signals, Systems and Computers (ACSSC 2007), Nov. 2007, pp. 133 – 137.

[28] J. Proakis and M. Salehi, *Digital Communications*. McGraw-Hill Education, 2007.

[29] "Text proposal for RAN1 TR on LTE-Advanced," in *3GPP R1-083410, NTT DOCOMO*, Aug. 2008.

[30] G. J. Foschini, K. Karakayali, and R. A. Valenzuela, "Coordinating multiple antenna cellular networks to achieve enormous spectral efficiency," *IEE Proceedings on Communications*, vol. 153, no. 4, pp. 548 – 555, Feb. 2006.

[31] M. K. Karakayali, G. J. Foschini, and R. A. Valenzuela, "Network coordination for spectrally efficient communication in cellular systems," *IEEE Wireless Communications Magazine*, vol. 13, no. 4, pp. 56 – 61, Aug. 2006.

[32] "Further discussion on inter-cell interference mitigation through limited coordination," in *3GPP R1-083569, Samsung*, Oct. 2008.

[33] K. T. Kim and S. K. Oh, "Multi-cell coordinated radio resource management scheme using a cell-specific sequence in OFDMA cellular systems," in *IEEE Wireless and Microwave Technology Conference*, Dec. 2006.

[34] M.Trivellato, F. Boccardi, and F. Tosato, "User selection schemes for mimo broadcast channels with limited feedback," in *IEEE Vehicular Technology Conference*, April 2007.

[35] L. Thiele, T. Wirth, T. Haustein, V. Jungnickel, E. Schulz, and W. Zirwas, "A unified feedback scheme for distributed interference management in cellular systems: Benefits and challenges for real-time implementation," in *European Signal Processing Conference*, Aug. 2009.

[36] C. Unachukwu, L. Zhang, D. McLernon, and M. Ghogho, " Downlink CoMP transmission with multiple cooperating sets," in *IEEE International Symposium for Wireless Communication Systems*, Aug. 2012.

[37] ——, "Cooperating set selection for reduced power consumption and data overhead in downlink CoMP transmission," in *IEEE International Symposium for Wireless Communication Systems*, Aug. 2013.

[38] M. Sadek, A. Tarighat, and A. H. Sayed, "Active antenna selection in multiuser MIMO communications," *IEEE Transactions on Signal Processing*, vol. 55, no. 4, pp. 1498–1510, April 2007.

[39] F. Boccardi and H. Huang, "A near-optimum technique using linear precoding for the mimo broadcast channel," in *IEEE International Conference on Acoustics, Speech and Signal Processing*, April 2007.

[40] Y.-H. Yang, S.-C. Lin, and H.-J. Su, "Multiuser MIMO downlink beamforming based on group maximum SINR filtering with per stream power allocation," in *IEEE International Conference on Communications*, June 2009.

[41] W. Cao, Z. Teng, and J. Wu, "A Power Allocation Scheme Using Updated SLNR Value Based on Perturbation Theory*," in *Communications and Network, http://dx.doi.org/10.4236/cn.2013.53B2035 Published Online (http://www.scirp.org/journal/cn)*, Sep. 2013, pp. 181 – 186.

[42] "MATLAB and Statistics Toolbox Release 2013b," in *The MathWorks, Inc.*

[43] S. Tombaz, P. Monti, K. Wang, A. Vastberg, M. Forzati, and J. Zander, "Impact of backhauling power consumption on the deployment of heterogeneous mobile networks," *IEEE Global Telecommunications Conference*, Dec. 2011.

[44] "Further advancements for E-UTRA, physical layer aspects," in *3rd Generation Partnership Project (3GPP), TR 36.814 V9. 0. 0*, March 2010.

[45] "Coordinated multi-point operation for LTE physical layer aspects," in *3rd Generation Partnership Project (3GPP), TR 36.819 V11.1.0*, Dec. 2011.

[46] "AN-1433 base station closed-loop RF power control with LMV232 crest-factor invariant detector," in *SNWA003A Texas Instruments*, Apr. 2013.

[47] E. Visotsky and H. Huang, "Optimum beamforming using transmit antenna arrays," in *IEEE 49th Vehicular Technology Conference, 1999*, May 1997.

[48] H. Boche and M. Schubert, "A general duality theory for uplink and downlink beamforming," in *IEEE Vehicular Technology Conference*, Sept 2002, pp. 87–91.

[49] P. Viswanath and D. N. C. Tse, "Sum capacity of the vector Gaussian broadcast channel and uplink-downlink duality," *IEEE Transactions on Communications*, vol. 49, no. 8, pp. 1912 – 1921, Aug 2003.

[50] D. Palomar, "A unified framework for communications through MIMO channels," in *Ph.D. Dissertation. Signal Theory and Communications Dept., Tech. Uni. Catalonia, Barcelona, Spain.*, May 2003.

[51] M. Codreanu, A. Tolli, A. M. Juntti, and M. Latva-aho, "Joint design of Tx-Rx beamformers in MIMO downlink channel," *IEEE Transactions on Signal Processing*, vol. 55, no. 9, pp. 4639 – 4655, Sept. 2007.

[52] J. Lfberg, "YALMIP: A toolbox for modeling and optimization in MATLAB," in *Proceedings of the CACSD Conference, Taipei, Taiwan*, 2004.

[53] R. Chang, Z. Tao, J. Zhang, and C.-C. Kuo, "Multicell OFDMA downlink resource allocation using a graphic framework," *IEEE Transactions on Vehicular Technology*, vol. 58, no. 7, pp. 3494 – 3507, Sept. 2009.

[54] N. Forouzan and S. Ghorashi, "Inter-cell interference coordination in downlink orthogonal frequency division multiple access systems using Hungarian method," *IET Communications*, vol. 7, no. 1, pp. 23 – 31, Nov. 2012.

[55] M. Sternad, T. Ottosson, A. Ahlen, and A. Svensson, "Attaining both coverage and high spectral efficiency with adaptive OFDM downlinks," in *IEEE 58th Vehicular Technology Conference, VTC 2003-Fall*, Oct. 2003, pp. 2486 – 2490.

[56] "OFDMA downlink inter-cell interference mitigation," in *3rd Partnership Project (3GPP), Project Document, R1-060291*, Feb. 2006.

[57] "Soft frequency reuse scheme for UTRAN LTE," in *3rd Partnership Project (3GPP), Project Document, R1-050507*, May 2005.

[58] "Downlink inter-cell interference coordination/avoidance evaluation of frequency reuse," in *3rd Partnership Project (3GPP), Project Document, Ericsson R1-061374*, May 2006.

[59] "Multi-cell simulation results for interference coordination in new OFDM DL," in *3rd Partnership Project (3GPP), Project Document, Alcatel R1-050694*, Aug. 2005.

[60] "System simulation results for downlink interference coordination," in *3rd Partnership Project (3GPP), Project Document, Alcatel R1-060209*, Jan 2006.

[61] "Aspects of interference mitigation by coordination," in *3rd Partnership Project (3GPP), Project Document, Siemens R1-051366*, Nov. 2005.

[62] S. Kim, K. Cho, D. Yoon, K. Young-Jo, and J. K. Kwon, "Performance analysis of downlink Inter cell interference coordination in the LTE-Advanced system," in *Fourth International Conference on Digital Telecommunications, 2009 (ICDT '09)*, July 2009, pp. 30 – 33.

[63] G. D. Gonzalez, M. Garcia-Lozano, S. Ruiz, J. Olmos, and V. Corvino, "Performance evaluation of downlink interference coordination techniques in LTE networks," *IEEE 72nd Vehicular Technology Conference Fall (VTC 2010-Fall)*, Sept. 2010.

[64] A. S. Hamza, S. S. Khalifa, H. S. Hamza, and K. Elsayed, "A survey on inter-cell interference coordination techniques in OFDMA-based cellular networks," *IEEE Communications Survey and Tutorial*, vol. 15, no. 4, pp. 1642 – 1670, Mar. 2013.

[65] F. Khan, "LTE for 4G mobile broadband: Air interface technologies and performance," in *Cambridge University Press*, Apr. 2009.

[66] R. Madan, J. Borran, A. Sampath, N. Bhushan, A. Khandekar, and T. Ji, "Cell association and interference coordination in heterogeneous LTE-A cellular

networks," *IEEE Journal in Selected Areas Communications*, vol. 28, no. 9, pp. 1479 – 1489, Dec. 2010.

[67] M. Rahman and H. Yanikomeroglu, "Enhancing cell-edge performance: A downlink dynamic interference avoidance scheme with inter-cell coordination," *IEEE Transaction in Wireless Communications*, vol. 9, no. 4, pp. 1414 – 1425, Apr. 2010.

[68] S. Ali and V. Leung, "Dynamic frequency allocation in fractional frequency reused OFDMA networks," *IEEE Transaction in Wireless Communications*, vol. 8, no. 8, pp. 4286 – 4295, Aug. 2009.

[69] A. Stoylar and H. Viswanathan, "Self-organizing dynamic fractional frequency reuse in OFDMA systems," *IEEE INFOCOM 2008. The 27th Conference on Computer Communications*, Apr. 2008.

[70] D. Lopez-Perez, A. Vasilakos, and H. Claussen, "On distributed and coordinated resource allocation for interference mitigation in self-organizing LTE networks," in *IEEE Transaction in Wireless Communications*, Aug. 2013, pp. 1145 – 1158.

[71] "LTE Advanced: Heterogeneous network." Qualcomm Incorporated, Jan. 2011.

[72] J. Munkres, "Algorithms for the assignment and transportation problems," *Journal of the Society for Industrial and Applied Mathematics*, vol. 5, no. 1, pp. 32 – 38, May 1957.

[73] S. Yeh, S. Talwar, G. Wu, N. Himayat, and K. Johnsson, "Capacity and coverage enhancement in heterogeneous networks," *IEEE Wireless Communications*, vol. 18, no. 3, pp. 32 – 138, 2011.

[74] A. Damnjanovic, J. Montojo, J. Cho, H. Ji, J. Yang, and P. Zong, "UE's role in LTE advanced heterogeneous networks," *IEEE Communications Magazine*, vol. 50, no. 2, pp. 164 – 176, 2012.

[75] B. Soret, H. Wang, K. I. Pedersen, and C. Rosa, "Multicell cooperation for LTE-Advanced heterogeneous network scenarios," *IEEE Wireless Communications*, vol. 20, no. 1, pp. 27 – 34, Feb. 2013.

[76] A. Ghosh, N. Mangalvedhe, R. Ratasuk, B. Mondal, M. Cudak, E. Visotsky, T. A. Thomas, J. G. Andrews, P. Xia, H. S. Jo, H. S. Dhillon, and T. D. Novlan, "Heterogeneous cellular networks: From theory to practice," *IEEE Communications Magazine*, vol. 50, no. 6, pp. 54 – 64, June 2012.

[77] N. Himayat, S. Talwar, A. Rao, and R. Soni, "Interference management for 4G cellular standards," *IEEE Communications Magazine.*, vol. 48, no. 8, pp. 86 – 92, Aug 2010.

[78] G. Bartoli, R. Fantacci, K. B. Letaief, D. Marabissi, N. Privitera, M. Pucci, and J. Zhang, "Beamforming for small cell deployment in LTE-Advanced and beyond," *IEEE Wireless Communications*, vol. 21, no. 2, pp. 50 – 56, Apr 2014.

[79] M. Tarighat, A. Sadek and A. H. Sayed, "A multi-user beamforming scheme for downlink MIMO channels based on maximizing signal-to-leakage ratios," in *IEEE International Conference on Acoustics, Speech and Signal Processing*, vol. 3, March 2011, pp. 1129 – 1132.

[80] Q. H. Spencer, A. Swindlehurst, and M. Haardt, "Zeroforcing methods for downlink spatial multiplexing in multiuser MIMO channels," *IEEE Transactions on Signal Processing*, vol. 52, pp. 461 – 471, Feb. 2004.

[81] M. Bengtsson, "A pragmatic approach to multi-user spatial multiplexing," in *Proc. IEEE Sensor Array and Multichannel Signal Processing Workshop*, Aug. 2002, pp. 130 – 134.

[82] R. Chen, J. Andrews, and R. Heath, "Multiuser space time block coded MIMO system with unitary downlink precoding," in *Proc. IEEE International Conf. on Communications*, 2004.

[83] K. Wong, R. Murch, and K. Letaief, "Performance enhancement of multiuser MIMO wireless communication systems," *IEEE Transactions on Communications*, vol. 50, pp. 1960 – 1970, Feb. 2002.

[84] R. Heath, M. Airy, and A. Paulraj, "Multiuser diversity for MIMO wireless systems with linear receivers," in *Proc. IEEE International Conference on Signals, Systems, and Computers*, Nov. 2001, pp. 1194 – 1199.

[85] T. Yoo and A. Goldsmith, "Optimality of zero-forcing beamforming with multi-user diversity," in *Proc. IEEE International Conf. on Communications*, 2005.

[86] G. Golub and V. C. Koan, "Matrix Computations," in *The Johns Hopkins University Press*, 1996.

[87] G. Liu, M. Sheng, X. Wang, Y. Li, and J. Li, "Joint interference alignment and avoidance for downlink," *IEEE Communications Letters*, vol. 18, no. 8, pp. 1431 – 1434, Aug 2010.

[88] Q. Li, R. Q. Hu, Y. Qian, and G. Wu, "Intracell cooperation and resource allocation in a heterogeneous network With relays," *IEEE Transactions on Vehicular Technology*, vol. 62, no. 4, pp. 1770 – 1784, May 2013.